Leachability of Radioactive Constituents from Uranium Mine Tailings

Final Report

Report EPS 3 MM 2
April 1987

Environment CANADA Environnement
2039102F VOL 3MM 198 2 670400
EXC # 001
TD 182 R46
REPORT (CANADA. ENVIRONMENT CANADA)
OCFF

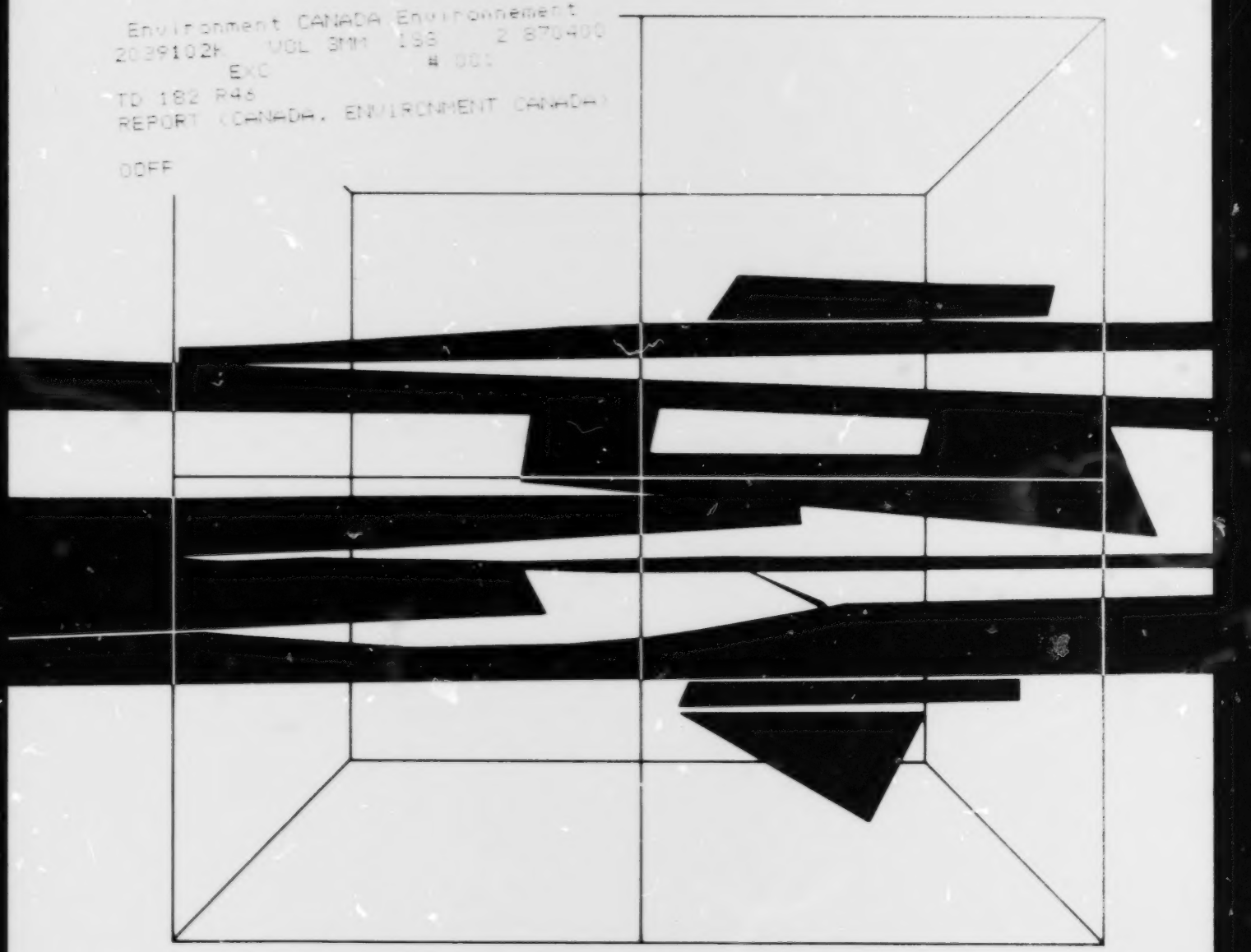

Environment Canada Environnement Canada

Canada

87-05112/

ENVIRONMENTAL PROTECTION SERIES REPORTS

Sample Number:

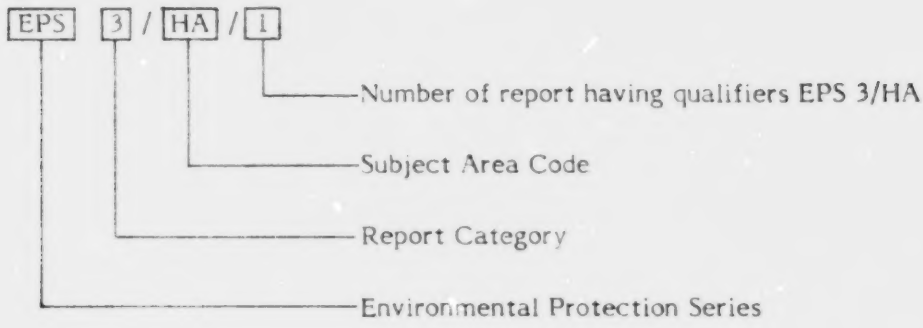
EPS 3 / HA / 1
Number of report having qualifiers EPS 3/HA
Subject Area Code
Report Category
Environmental Protection Series

Categories

1	Regulations/Guidelines/Codes of Practice
2	Public Consultation: Problem Assessment, Control Options
3	Research and Technology Development
4	Literature Reviews
5	Surveys
6	Social, Economic and Environmental Impact Assessments
7	Surveillance
8	Policy Proposals & Statements
9	Manuals

Subject Areas

AG	Agriculture
AP	Airborne Pollutants
AT	Aquatic Toxicity
CC	Commercial Chemicals
CE	Consumers and the Environment
CI	Chemical Industries
FA	Federal Activities
FP	Food Processing
HA	Hazardous Wastes
IC	Inorganic Chemicals
MA	Marine Pollution
MM	Mining & Ore Processing
NR	Northern & Rural Regions
PF	Paper and Fibres
PG	Power Generation
PN	Petroleum and Natural Gas
SF	Surface Finishing
SP	Oil & Chemical Spills
SRM	Standard Reference Methods
TS	Transportation Systems
UP	Urban Pollution

New subject areas and codes are introduced as they become necessary. A list of EPS reports may be obtained from Environmental Protection Publications, Conservation and Protection, Environment Canada, Ottawa, Ontario, Canada, K1A 0E7.

LEACHABILITY OF RADIOACTIVE CONSTITUENTS FROM URANIUM MINE TAILINGS - FINAL REPORT

by

T.W. Constable
Environment Canada
Environmental Protection
Wastewater Technology Centre

and

W.J. Snodgrass
IEC Beak Consultants Ltd.

Report EPS 3/MM/2
April 1987

REVIEW NOTICE

This report has been reviewed by the Environmental Protection Directorate, Conservation and Protection, and approved for publication. Approval does not necessarily signify that the contents reflect the views and policies of Environment Canada. Mention of trade names or commercial products does not constitute recommendation or endorsement for use.

READERS COMMENTS

Readers who wish to comment on the content of this report should address their comments to:

Mr. T.W. Constable
Environment Canada
Environmental Protection
Wastewater Technology Centre
P.O. Box 5050
Burlington, Ontario
L7R 4A6

© Minister of Supply and Services Canada 1987
Cat. No. En 49-7 3-2E
ISBN 0-662-15345-6
BEAUREGARD PRESS LIMITED

ABSTRACT

A series of long-term studies were conducted both to examine the leachability of major constituents (acidity, TDS) and radioisotopes from uranium mining/milling tailings and settling pond sludges, and to assess the effect of two treatment methods (solidification and vegetation) on leachate characteristics. Four bench-scale experiments were conducted to examine the leachability of (1) old tailings and those containing a large portion of (Ba,Ra)SO_4 sludges, (2) untreated and solidified (Ba,Ra)SO_4 sludges located at the bottom of settling ponds, (3) new tailings that had been vegetated or solidified, and (4) new tailings subject to varying flow rates. A fifth study was conducted to examine the microbiology of Experiments 2 and 3. In addition, the lysimeter solids remaining in the old tailings at the end of Experiment 1 were characterized through chemical and radionuclide analyses and Scanning Electron Microscope-X-ray Emission and Mossbauer Spectroscopy techniques.

This report provides an extensive database of temporal variations in leachate characteristics under both normal and accelerated water application rates. It also presents hypotheses of possible leaching mechanisms in the wastes that could explain the observed data, and a conceptual model of tailings leaching processes which integrates the results of all the tailings experiments.

RÉSUMÉ

Une série d'études à long terme ont été effectuées afin d'examiner les possibilités d'entraînement par lixiviation des principaux constituants (substances acides et solides totaux dissous) et des radioisotopes présents dans les stériles et les boues des étangs de sédimentation résultant de l'extraction et du traitement de l'uranium ainsi que pour évaluer l'effet de deux méthodes de traitement (la solidification et le recouvrement par la végétation) sur les propriétés des lixiviats. En laboratoire, quatre expériences ont été réalisées en vue d'étudier la lixiviation (1) des vieux stériles et de ceux contenant une grande quantité de boues de sulfates de Ba et de Ra, (2) des boues non traitées et solidifiées de sulfates de Ba et de Ra se trouvant au fond des étangs de sédimentation, (3) de nouveaux stériles recouverts de végétation ou solidifiés et (4) et nouveaux stériles, avec un débit variable. Une cinquième étude portait sur les aspects microbiologiques des expériences 2 et 3. En outre, les solides du lysimètre encore présents dans les vieux stériles à la fin de l'expérience 1 ont été identifiés chimiquement et grâce à l'analyse des radionuclides ainsi que par microscopie électronique à balayage et à émission de rayon-X et par spectroscopie Mossbauer.

Le rapport fournit beaucoup de données sur les variations temporelles des propriétés des lixiviats lorsque le débit de l'eau est normal ou accéléré. Il présente aussi des hypothèses concernant les mécanismes possibles de lixiviation des boues qui pourraient expliquer les données obtenues ainsi qu'un modèle conceptuel des processus de lixiviation des stériles qui intègre les résultats de toutes les expériences effectuées.

TABLE OF CONTENTS

		Page
ABSTRACT		iii
RÉSUMÉ		iv
TABLE OF CONTENTS		v
LIST OF FIGURES		vii
LIST OF TABLES		xi
1	INTRODUCTION	1
2	LITERATURE REVIEW	2
2.1	Mill Processes and Tailings Disposal	2
2.2	Environmental Problems	5
3	OBJECTIVES	7
4	EXPERIMENT 1: LEACHABILITY OF OLD TAILINGS AND $(Ba,Ra)SO_4$ SLUDGES	10
4.1	Source of Radioactive Materials	10
4.2	Experimental Program	15
4.3	Results	19
4.3.1	Leachate Characteristics	20
4.3.2	Lysimeter Solids	32
4.4	Discussion	43
4.4.1	Leachate Characteristics	43
4.4.2	Lysimeter Solids	58
4.5	Summary and Conclusions	62
5	EXPERIMENT 2: LEACHABILITY OF $(Ba,Ra)SO_4$ SEDIMENTS FROM THE BOTTOM OF SETTLING PONDS	64
5.1	Experimental Procedure	64
5.2	Results	66
5.3	Discussion	74
5.4	Summary and Conclusions	74
6	EXPERIMENT 3: LEACHABILITY OF NEW TAILINGS SUBJECTED TO VARIOUS TREATMENTS	76
6.1	Experimental Program	77
6.2	Results	79
6.3	Discussion	91
6.4	Summary and Conclusions	94

		Page
7	EXPERIMENT 4: LEACHABILITY OF NEW TAILINGS SUBJECTED TO VARIOUS FLOW RATES	95
7.1	Experimental Program	95
7.2	Results	96
7.2.1	Quirke Mine Tailings	97
7.2.2	Madawaska Mine Tailings	102
7.3	Discussion	109
7.3.1	Quirke Mine Tailings	112
7.3.2	Madawaska Mine Tailings	119
7.3.3	Effect of Sulphate Concentrations on Ra-226 Leaching	121
7.4	Summary and Conclusions	123
8	EXPERIMENT 5: MICROBIOLOGY OF EXPERIMENTS 2 AND 3	125
8.1	Experimental Program	125
8.2	Results and Discussion	127
8.3	Summary and Conclusions	129
9	CONCEPTUAL MODEL OF TAILINGS LEACHING PROCESSES	132
10	SUMMARY	140
REFERENCES		146
ACKNOWLEDGMENTS		150
APPENDIX A:	CHARACTERIZATION OF LEACHATES AND TAILINGS SOLIDS	A-1
A.1	Chemical Characteristics of Leachate from Experiment 1	A-1
A.1.1	TDS Measurements and Electroneutrality Balances	A-4
A.1.2	Cation - Anion Speciation	A-13
A.1.3	Biochemistry of Pyrite Oxidation Reactions	A-45
A.2	Characterization of Lysimeter Solids	A-48
A.2.1	Physical and Chemical Characteristics	A-48
APPENDIX B:	DESCRIPTION OF LYSIMETER SOLIDS USING SEM-XRE AND MOSSBAUER TECHNIQUES	B-1
B.1	Scanning Electron Microscope - X-ray Emission (SEM-XRE)	B-1
B.2	SEM-XRE Analysis of Wash Waters from Gypsum Chemical Analyses	B-27
B.3	Mossbauer Spectra of Uranium Tailings Samples	B-29

LIST OF FIGURES

Figure		Page
1	TREATMENT SYSTEM FOR URANIUM MILL TAILINGS	4
2	PROJECT PHASING AND CHRONOLOGY	8
3	SOURCES OF RADIOACTIVE MATERIAL - ELLIOT LAKE AREA	11
4	LOCATION MAP OF ABANDONED TAILINGS AND $(Ba,Ra)SO_4$ SEDIMENTS COLLECTION SITES AT NORDIC LAKE TAILINGS AREA	11
5	TYPICAL LYSIMETERS USED IN EXPERIMENT 1	16
6	EXPERIMENT 1: TEMPORAL VARIATIONS IN LEACHATE pH	23
7	EXPERIMENT 1: PORE-VOLUMETRIC VARIATIONS IN LEACHATE pH	24
8	EXPERIMENT 1: TEMPORAL VARIATIONS IN TOTAL DISSOLVED SOLIDS CONCENTRATIONS	25
9	EXPERIMENT 1: PORE-VOLUMETRIC VARIATIONS IN TOTAL DISSOLVED SOLIDS CONCENTRATIONS	26
10	EXPERIMENT 1: TEMPORAL VARIATIONS IN LEACHATE CONDUCTIVITY	27
11	EXPERIMENT 1: PORE-VOLUMETRIC VARIATIONS IN LEACHATE CONDUCTIVITY	28
12	EXPERIMENT 1: TEMPORAL VARIATIONS IN DISSOLVED Ra-226	29
13	EXPERIMENT 1: PORE-VOLUMETRIC VARIATIONS IN DISSOLVED Ra-226	30
14	EXPERIMENT 1: CUMULATIVE LEACHED RADIOACTIVITY	31
15	EXPERIMENT 1: TEMPORAL VARIATIONS IN DISSOLVED Pb-210	33
16	EXPERIMENT 1: PORE-VOLUMETRIC VARIATIONS IN DISSOLVED Pb-210	34
17	EXPERIMENT 1: TEMPORAL VARIATIONS IN DISSOLVED Th-228	35
18	EXPERIMENT 1: PORE-VOLUMETRIC VARIATIONS IN DISSOLVED Th-228	36
19	EXPERIMENT 1: TEMPORAL VARIATIONS IN DISSOLVED Th-230	37

Figure		Page
20	EXPERIMENT 1: PORE-VOLUMETRIC VARIATIONS IN DISSOLVED Th-230	38
21	EXPERIMENT 1: TEMPORAL VARIATIONS IN DISSOLVED Th-232	40
22	EXPERIMENT 1: PORE-VOLUMETRIC VARIATIONS IN DISSOLVED Th-232	41
23	EXPERIMENT 1: TEMPORAL VARIATIONS IN TOTAL GROSS α	43
24	EXPERIMENT 1: PORE-VOLUMETRIC VARIATIONS IN TOTAL GROSS α	44
25	EXPERIMENT 1: TEMPORAL VARIATIONS IN TOTAL GROSS β	46
26	EXPERIMENT 1: PORE-VOLUMETRIC VARIATIONS IN TOTAL GROSS β	47
27	EXPERIMENT 1: SCATTERGRAPHS FROM WASHING EXPERIMENT FOR	
	(a) Ra-226 vs. Iron	48
	(b) Ra-226 vs. Lead	48
	(c) Ra-226 vs. Calcium	49
	(d) Ra-226 vs. Barium	49
28	PRINCIPAL DECAY SCHEME OF THE URANIUM SERIES	53
29	TYPICAL SIMULATED SETTLING POND USED IN EXPERIMENT 2	65
30	EXPERIMENT 2: TEMPORAL VARIATIONS IN EFFLUENT pH	68
31	EXPERIMENT 2: TEMPORAL VARIATIONS IN EFFLUENT CONDUCTIVITY	68
32	EXPERIMENT 2: TEMPORAL VARIATIONS IN DISSOLVED AND SUSPENDED SOLIDS	69
33	EXPERIMENT 2: CUMULATIVE MASS OF DISSOLVED AND SUSPENDED SOLIDS vs. TIME	70
34	EXPERIMENT 2: TEMPORAL VARIATIONS IN DISSOLVED Ra-226	71
35	EXPERIMENT 2: CUMULATIVE LEACHED Ra-226 vs. TIME	71
36	TYPICAL LYSIMETER USED IN EXPERIMENT 3	77
37	EXPERIMENT 3: SEASONAL LEACHATE VOLUMES	83
38	EXPERIMENT 3: CUMULATIVE LEACHATE VOLUMES	83

Figure		Page
39	EXPERIMENT 3: AVERAGE SEASONAL LEACHATE pH	84
40	EXPERIMENT 3: AVERAGE SEASONAL LEACHATE CONDUCTIVITY	84
41	EXPERIMENT 3: AVERAGE SEASONAL DISSOLVED Ra-226 IN LEACHATES	85
42	EXPERIMENT 3: CUMULATIVE DISSOLVED Ra-226 IN LEACHATES	85
43	TYPICAL LYSIMETER USED IN EXPERIMENT 4	96
44	EXPERIMENT 4: RIO ALGOM TAILINGS - PORE-VOLUMETRIC VARIATIONS IN LEACHATE pH	98
45	EXPERIMENT 4: RIO ALGOM TAILINGS - PORE-VOLUMETRIC VARIATIONS IN LEACHATE CONDUCTIVITY	99
46	EXPERIMENT 4: RIO ALGOM TAILINGS - PORE-VOLUMETRIC VARIATIONS IN SO_4 CONCENTRATIONS	100
47	EXPERIMENT 4: RIO ALGOM TAILINGS - CUMULATIVE MASS OF TOTAL SOLIDS LEACHED vs. PORE VOLUMES OF LEACHATE	103
48	EXPERIMENT 4: RIO ALGOM TAILINGS - CUMULATIVE MASS OF SO_4 LEACHED vs. PORE VOLUMES OF LEACHATE	104
49	EXPERIMENT 4: RIO ALGOM TAILINGS - CUMULATIVE MASS OF TOTAL SOLIDS LEACHED vs. ELAPSED TIME	105
50	EXPERIMENT 4: RIO ALGOM TAILINGS - CUMULATIVE MASS OF SO_4 LEACHED vs. ELAPSED TIME	106
51	EXPERIMENT 4: RIO ALGOM TAILINGS - PORE-VOLUMETRIC VARIATIONS IN DISSOLVED Ra-226	107
52	EXPERIMENT 4: RIO ALGOM TAILINGS - CUMULATIVE DISSOLVED Ra-226 LEACHED vs. PORE VOLUMES OF LEACHATES	108
53	EXPERIMENT 4: MADAWASKA TAILINGS - PORE-VOLUMETRIC VARIATIONS IN LEACHATE pH	109
54	EXPERIMENT 4: MADAWASKA TAILINGS - PORE-VOLUMETRIC VARIATIONS IN LEACHATE CONDUCTIVITY	110
55	EXPERIMENT 4: MADAWASKA TAILINGS - PORE-VOLUMETRIC VARIATIONS IN SO_4 CONCENTRATIONS	111

Figure		Page
56	EXPERIMENT 4: MADAWASKA TAILINGS - CUMULATIVE MASS OF TOTAL SOLIDS LEACHED vs. PORE VOLUMES OF LEACHATE	112
57	EXPERIMENT 4: MADAWASKA TAILINGS - CUMULATIVE MASS OF SO_4 LEACHED vs. PORE VOLUMES OF LEACHATES	113
58	EXPERIMENT 4: MADAWASKA TAILINGS - PORE-VOLUMETRIC VARIATIONS IN DISSOLVED Ra-226	114
59	EXPERIMENT 4: MADAWASKA TAILINGS - CUMULATIVE DISSOLVED Ra-226 LEACHED vs. PORE VOLUMES OF LEACHATES	115
60	EXPERIMENT 4: RATIO OF RADIUM TO TDS (OR SULPHATE) LEACHED vs. TDS (OR SULPHATE) CONCENTRATION	122
61	EXPERIMENT 5: MICROBIAL RESPIRATION IN VEGETATED AND NON-VEGETATED TAILINGS AND $(Ba,Ra)SO_4$ SEDIMENTS	130
62	CONCEPTUAL MODEL OF THE EVOLUTION OF TAILINGS IN A LYSIMETER	133

LIST OF TABLES

Table		Page
1	CHEMICAL AND RADIOLOGICAL CHARACTERISTICS OF ABANDONED TAILINGS IN THE NORDIC LAKE AREA	14
2	EXAMPLES OF CONTAMINANT LEVELS IN EFFLUENTS FROM TAILING SITES IN THE ELLIOT LAKE AREA	15
3	EXPERIMENT 1: VARIATIONS WITHIN REPLICATED TREATMENTS	21
4	EXPERIMENT 1: VARIATIONS BETWEEN CONTROL LYSIMETERS AND TAILINGS-SEDIMENT LYSIMETERS	22
5	EXPERIMENT 1: RESIDUAL CONCENTRATIONS OF RADIO-ISOTOPES IN LEACHED TAILINGS	32
6	EXPERIMENT 2: VARIATIONS WITHIN AND BETWEEN TREATMENTS	67
7	EXPERIMENT 2: CONCENTRATIONS OF VARIOUS CONSTITUENTS IN LEACHATES	73
8	EXPERIMENT 3: INITIAL RADIONUCLIDE LEVELS	78
9	EXPERIMENT 3: SLUDGE CONSTITUENT CONCENTRATIONS AND LOADING RATES	79
10	EXPERIMENT 3: WITHIN TREATMENT VARIATIONS IN LEACHATE PARAMETERS	80
11	EXPERIMENT 3: BETWEEN TREATMENT VARIATIONS IN LEACHATE PARAMETERS	81
12	EXPERIMENT 3: WITHIN AND BETWEEN TREATMENT VARIATIONS FOR VEGETATION PARAMETERS	82
13	EXPERIMENT 3: PB-210 LEVELS IN LEACHATES	86
14	EXPERIMENT 3: THORIUM LEVELS IN LEACHATES	87
15	EXPERIMENT 3: CONCENTRATIONS OF VARIOUS CONSTITUENTS IN LEACHATES	88
16	EXPERIMENT 3: GRASS YIELDS	90
17	EXPERIMENT 3: AVERAGE RADIONUCLIDE LEVELS IN GRASS CUTTINGS	91
18	EXPERIMENT 4: AVERAGE LEACHATE PRODUCTION RATES	97

Table		Page
19	EXPERIMENT 4: CUMULATIVE Ra-226, SO_4 AND TOTAL SOLIDS MASS LEACHED DURING 136-WEEK STUDY PERIOD	101
20	EXPERIMENT 4: ESTIMATION OF pH CONTROLLING MECHANISM	117
21	EXPERIMENT 4: COMPARISON OF CALCULATED AND OBSERVED pH AND TDS FOR RIO ALGOM TAILINGS (CONTINUOUS FLOW)	118
22	EXPERIMENT 4: TYPICAL PREDICTED COMPOSITION OF LEACHATE FROM RIO ALGOM TAILINGS	120
23	EXPERIMENT 5: MEDIA INOCULATED WITH H_2O SUSPENSION OF SAMPLES TO ISOLATE AND CHARACTERIZE ORGANISMS PRESENT IN THE SAMPLES, AND TO DETERMINE THE SIGNIFICANCE OF THE ORGANISMS	126
24	EXPERIMENT 5: SOME CHEMICAL PROPERTIES OF THE SAMPLES	127
25	EXPERIMENT 5: TOTAL COUNTS OF MICROBIAL POPULATIONS	128
26	EXPERIMENT 5: FINAL MICROBIAL COUNTS FOR RESPIRATION TESTS	131

1 INTRODUCTION

Of all the wastes generated by uranium mining and milling operations, uranium mill tailings present the most significant waste management problem because of their large volume and their radioactivity. Most of the constituents in the tailings are found naturally in soils and bedrock. However, these constituents are much more prevalent in tailings and may reach several hundred times the level normally found in soil. Furthermore, mining and milling operations change the chemical and physical form of these materials so that their potential for mobility is increased. The potential mobility results from the transformation of the tailings from materials well contained by nature to materials more accessible to the environment and the public.

The tailings could adversely affect the public and the environment in several potential ways. The presence of radioactive constituents in the tailings and their possible release to the environment are currently of greatest concern to environmental managers. Release of radioactive constituents can occur by leaching of the radionuclides and discharge to the aqueous environment, erosion of dust from the tailings surface by wind, and release of radon gas to the atmosphere. Environmental degradation can also occur because of increased acidity in receiving waters due to pyrite oxidation, and the release of toxic heavy metals, dissolved solids and environmentally active chemicals into groundwater supplies, lakes, and rivers.

A research program was undertaken at Environment Canada's Wastewater Technology Centre in Burlington, Ontario, to investigate the leachability of radioactive constituents from various mining wastes, and to examine the effects of chemical and biological stabilization techniques on leachate characteristics. The results of the study from September 1974 to January 1977 were presented in a Status Report by Bryant et al. (1979). This report presents the results of the entire experimental program.

2 LITERATURE REVIEW

2.1 Mill Processes and Tailings Disposal

Uranium and other ores are typically associated with reduced minerals in the parent rock. Controversy exists over the exact geological history that resulted in their formation, but the overall formation can be simply described as involving the transport of various metals in a positive oxidation state with hydrothermal or other fluids (e.g., saline) to a location where the groundwater had a lower redox potential. At this site, reactions occurred over time to lower the oxidation state of the metals and induce them to precipitate to form the ore body. The presence of sulphates or arsenates and their reduction to sulphides or arsenides led to the formation of metal sulphides.

The chemistry of milling uranium-bearing ores involves dissolution and oxidation of the uranium, and subsequent uranium extraction from solution. Several steps are carried out in the milling of the ore. The first milling step commonly involves fine grinding to at least 50 percent minus 200 mesh, followed by leaching of uranium from the ore using either an acid leach (sulphuric acid) or an alkaline leach (sodium hydroxide and oxygen). The dissolving agents leach some of the reduced minerals and not others. With pyritic ores, for example, it is thought that only small quantities of pyrite are dissolved by proton attack in a hot sulphuric acid solution. In Canada, only the Eldorado plant at Beaverlodge, Saskatchewan, carried out alkaline leaching. The plant ceased operations in 1982.

The tailings used in this study were produced by mills using an acid-leach process. The process takes place within leaching pachucas (LP). The uranium in the ore is dissolved in hot sulphuric acid. Air, steam, iron balls, or sodium chlorate may be used as oxidants which, with the iron in the ore, ensures that all the dissolved uranium is oxidized to the hexavalent state.

Excess acid from the acid-leach process is neutralized, typically with lime or limestone, in the partial neutralization (PN) tanks. This involves pH adjustment from near 0.5 to 2. The addition of calcium induces precipitation of gypsum and other products from the leach liquor. Little uranium is precipitated during this initial neutralization step.

Mass balance studies suggest that about 90 to 95 percent of the Th-230, Pb-210, and U-238 in the ore are leached in the LP and enter the acid solution. Ra-226 remains in the solid fraction (Skeaff, 1978). Hence, either Ra-226 is not leached, which is improbable, or it is immediately adsorbed or co-precipitated in the leaching pachucas.

Available evidence also suggests that 50 percent of Th-232 minerals (including Th-228) are leached from the parent minerals and enter the leach liquor. These radioisotopes appear to be carried with the leach liquor to the final neutralization (FN) tanks where they precipitate out of solution. After neutralization of the excess acid in the FN tanks, the solution is separated from the solid waste. The solid waste is called tailings. Uranium is then removed from the clarified solution by ion-exchange. Further processing of the uranium produces the final concentrate.

This process extracts more than 93 percent of the uranium from the ores, whereas the heavy metals and most of the radioisotopes (such as Ra-226, Th-230 and Pb-210) are retained in the tailings (Raicevic, 1979). The barren solution, which has been stripped of uranium, is then mixed with the tailings to produce a slurry. About 85 percent of the total radioactivity entering the mill in the ore is discharged in the slurry (Moffett, 1977).

The slurry is neutralized with lime to raise the pH to the 8 to 11 range before being pumped to a tailings basin (impoundment area). This pH neutralization procedure controls acid generation in active tailings impoundments, and maintains the pH in the range of 6.5 to 9.0. In addition, it results in the precipitation of all the dissolved thorium and Pb-210 and of about 90 percent of the dissolved radium contained in the leach liquor (Clark, 1974). It also results in the formation of gypsum ($CaSO_4.2H_2O$), which reportedly contains up to 259 Bq/g of Ra-226 (Kaiman, 1977). This mineral readily dissolves in dilute solutions such as infiltrating rain water.

Jarosite ($KFe_3(SO_4)_2(OH)_6$) precipitates (approximately 0.05 percent of tailings) are also retained in the tailings basin, and have been found to contain up to 2960 Bq/g of Ra-226 (Kaiman, 1977). Jarosite is fairly soluble and redissolves when the concentrations of ferric iron and sulphate fall below initial levels in the tailings basin. Jarosite can thermodynamically form in the leaching pachucas (Beak, 1982). Kaiman (1977) suggests that it forms in the mill and is retained in the tailings basin. Its formation and the coprecipitation of Ra-226 with it in the mill is one possible mechanism for retaining Ra-226 on the solids leaving the LP. The conceptual model presented in Chapter 9, however, argues against mill-formed jarosite and for tailings-formed jarosite.

The system for treating the slurry of mill tailings consists of two separate sections, the tailings basin and the settling pond (Figure 1).

The larger of these is the tailings basin into which the mill tailings slurry is pumped and in which solid residues are then allowed to settle. These basins may cover areas of 200 hectares or more and contain up to 40 x 10^6 tonnes of tailings (Moffett,

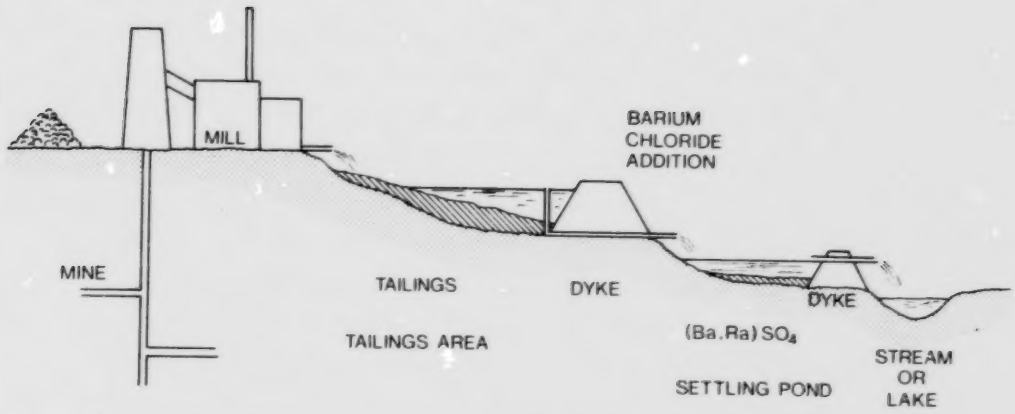

FIGURE 1 TREATMENT SYSTEM FOR URANIUM MILL TAILINGS

1976). For each tonne of ore mined, almost one tonne of tailings and two tonnes of process liquid are produced (AECB, 1978).

The second part of the tailings treatment system consists of a settling or precipitation pond which receives the decanted effluent from the tailings basin. This pond may be a lake, swamp, or man-made basin. Since the decant still contains large amounts of dissolved Ra-226, further treatment with barium chloride ($BaCl_2$) for radium removal is required. The radium co-precipitates with barium sulphate according to a reaction of the type (Moffett, 1976):

$$BaCl_2 + Ra^{2+} + SO_4^{2-} \rightleftarrows 2\,Cl^- + (Ba,Ra)SO_4$$

The resultant barium-radium sulphate ($(Ba,Ra)SO_4$) is a fine, slow-settling precipitate, and requires large settling ponds with long retention times to ensure effective solid-liquid separation. The sediments are stored at the bottom of the treatment pond and the treated effluent is discharged to a local water course.

The insolubility of the precipitated $(Ba,Ra)SO_4$ sediments depends mainly upon the concentration of sulphate in the overlying water. If this concentration falls below a certain level, the dissolution of these sediments may release Ra-226 to the environment (Bland and Gonzalez, 1977).

2.2 Environmental Problems

According to Blakeman (1979), Canadian uranium mills in 1979 generated approximately 14 000 tonnes/day of tailings and 25 000 to 30 000 tonnes (5 to 6 million Imp. gal.)/day of mill process wastewater.

It is estimated that 1 tonne of tailings has a radioactivity of at least 1.85×10^8 Bq (Moffett and Tellier, 1977). About 90 percent of this activity is due to the U-238 series. The most troublesome daughter isotopes of U-238 are Th-230 (half-life: 8.0×10^4 years), Ra-226 (half-life: 1620 years), and Pb-210 (half-life: 22 years). Of these, Ra-226 has been identified as the most radiotoxic (Moffett, 1976).

The environmental problems associated with tailings disposal areas are not limited to the transport of radionuclides into sources of drinking water by seepage and runoff; the transport can also occur through radon emanation and windblown dust. Radon gas, a product of Ra-226 decay, is given off at the surface of tailings and can be picked up by the wind, thus exposing people working or living downwind to its effects and the effects of its short-lived daughters. Wind can also erode and transport fine sand (silica) and radioactive dust from the surface of abandoned tailings areas during dry periods of the year. This problem is compounded because fine particles (slimes) are not only more easily windblown but also more radioactive than the coarser particles. The fine particles contain about 75 percent of the radioactivity in the tailings.

The steps that need to be taken to close out a tailings impoundment are not well defined. Close-out objectives would attempt to ensure that the tailings and sediments would not produce an unacceptable environmental impact after abandonment in the future. It is generally assumed that the tailings surface must at least be stabilized against wind and water erosion. The stabilization procedure may have the added benefit of reducing the amount of water percolating through the tailings. This would reduce the amount of seepage from the tailings and reduce the rate of pyrite oxidation. Pyrite oxidation is undesirable because it causes a decrease in tailings pH and a concomitant solubilization of heavy metals and some radioactive constituents.

Current practice for stabilizing tailings surfaces requires the establishment of a suitable vegetative covering. Revegetation programs have been implemented on several tailings deposits in the Elliot Lake area. The results, according to Schmidt and Moffett (1979), indicate that it is possible to grow grasses and legumes on uranium tailings. However, the acid generating potential and pyrite content of the tailings, in addition to the high concentrations of toxic heavy metals and lack of nutrients, make the success of

the revegetation programs often dependent upon extensive application of lime, organic mulches, and fertilizers.

Other techniques suggested for long-term tailings management include capping with an impervious material, disposal in a deep lake, deep burial in abandoned mines, and solidification (the mixing of chemical additives with tailings to produce a solid matrix analogous to concrete).

3 OBJECTIVES

A Radioactivity Subgroup was formed in 1974 by the Federal Mining Task Force to assist in the development of effluent guidelines and regulations for the uranium mining industry. This subgroup defined knowledge gaps related to the treatment of uranium mining and milling effluents and to the dissolution of various radionuclides from tailings and precipitates (Radioactivity Subgroup, 1974). The current practice of $(Ba,Ra)SO_4$ sediment storage in lagoons was considered to be an unsuitable long-term disposal solution because redissolution might occur after the abandonment and cause contamination of receiving waters.

The Subgroup established that insufficient information was available on concentrations of Th-230, Th-232, and Pb-210 in effluents to set effluent standards, or even to ascertain whether such standards are warranted. As a result, a program was initiated at the Wastewater Technology Centre, Burlington, Ontario, in cooperation with the Abatement and Compliance Branch of Environment Canada. The goals of the program were:

- to investigate the leachability of radioactive constituents from various uranium mining wastes, and
- to assess the effects of solidification and vegetation on the quality of leachate from tailings areas. The approach used was to set up "model tailings areas" in lysimeters, to apply water under controlled experimental conditions, and to monitor the results.

The project was initiated in 1974 (Experiment 1, Phase 1). In 1976, the initial experiment was modified (Experiment 1, Phase 2) and two additional experiments undertaken (Experiments 2 and 3). Experiments 4 and 5 were added in 1978. The phasing and chronology of the project are shown in Figure 2.

The objectives of the experiments were:

1. Experiment 1 - To determine the extent and rate of leaching of radioactive constituents from abandoned uranium mine tailings, from abandoned tailings with a lime-neutralized surface layer (Phase 1 only), and from abandoned tailings containing $(Ba,Ra)SO_4$ sediments.
2. Experiment 2 - To establish the extent and rate of release of radionuclides to surrounding waters from coprecipitated $(Ba,Ra)SO_4$ sediments in bench-scale settling ponds, and to examine the effects of solidification of the sediments on effluent characteristics.

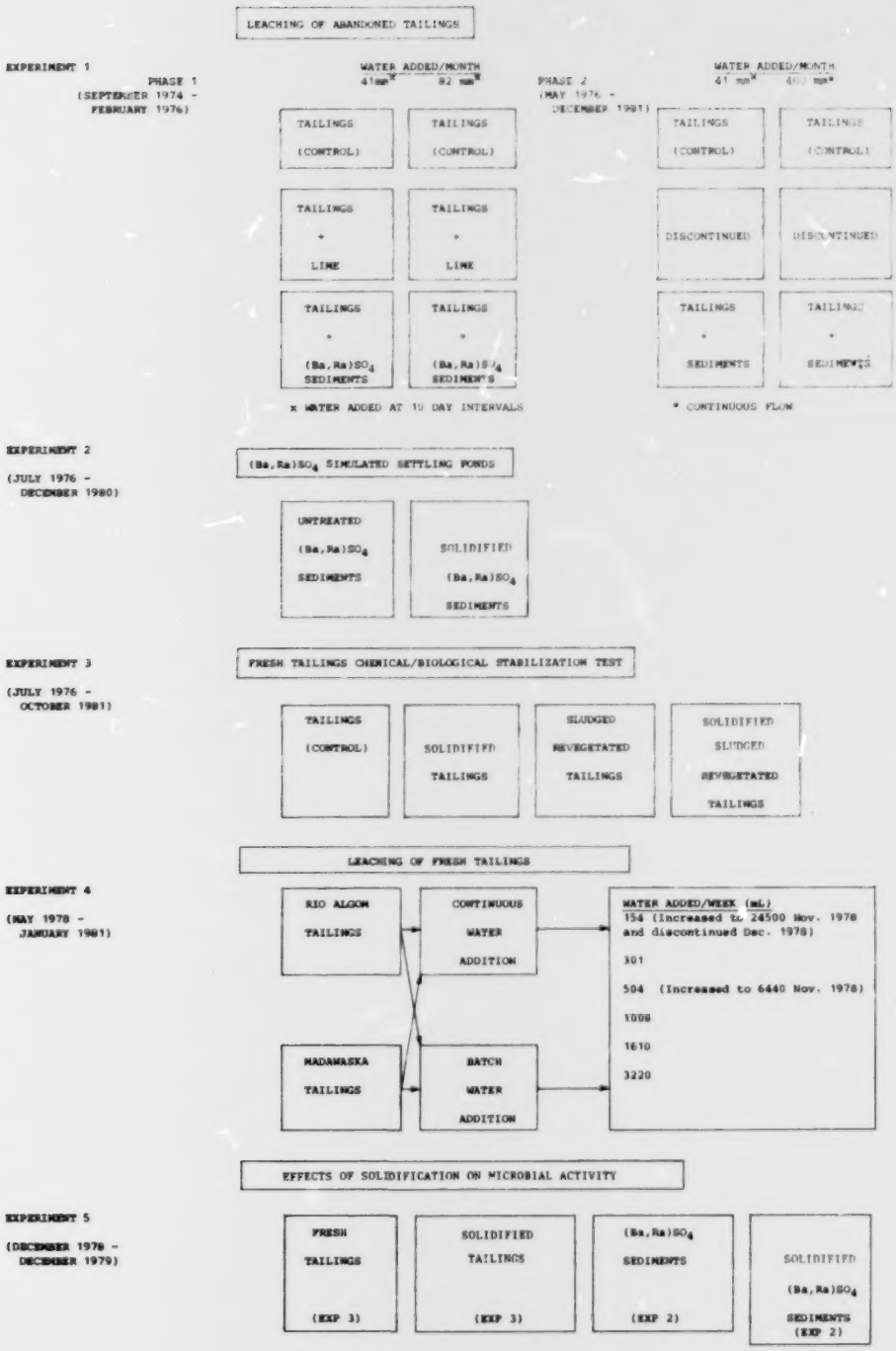

FIGURE 2 PROJECT PHASING AND CHRONOLOGY

3. Experiment 3 - To compare radionuclide leaching rates from freshly milled tailings subjected to the following treatments:

   - solidification of the tailings,
   - the establishment of a vegetative cover aided by the addition of sewage sludge as an organic nutrient supply, and
   - a combination of solidification of the tailings and establishment of vegetative cover.

4. Experiment 4 - To examine the effects of applying water at various flow rates on the leaching characteristics of freshly milled tailings, particularly with respect to sulphate and Ra-226 levels.

5. Experiment 5 - To establish the identity and number of microorganisms in $(Ba,Ra)SO_4$ sediments with and without solidification treatment (from Experiment 2), and in freshly milled tailings with and without solidification treatment (from Experiment 3).

4 EXPERIMENT 1: LEACHABILITY OF OLD TAILINGS AND (Ba,Ra)SO_4 SLUDGES

In response to technology gaps identified by the Radioactivity Subgroup of the Federal Mining Task Force (1974), Experiment 1 was initiated in consultation with the Abatement and Compliance Branch of the Environmental Protection Service. Its objective was to provide information on the rate and extent of leaching of environmentally hazardous radionuclides (Ra-226, Pb-210, Th-228, Th-230, and Th-232) from abandoned uranium tailings under bench-scale experimental conditions, and to examine the effect that applying limestone to the surface of tailings and of mixing (Ba,Ra)SO_4 sediments with tailings has on leaching. Tailings with a limestone-neutralized surface layer was chosen as one of the experimental conditions to simulate conditions similar to those present at the initiation of a revegetation program, where the surface tailings are neutralized before seeding. The tailings-sediment mixture was selected to simulate the dredging and return of sediments to the tailings, which has been suggested as a possible means of disposal of the sediments.

4.1 Source of Radioactive Materials

The tailings and (Ba,Ra)SO_4 sediments were collected from the North Nordic Lake tailings area near Elliot Lake, Ontario (Figures 3 and 4). The Nordic Mine was in continuous production from 1957 to its closure in 1968. The mine operated with a milling capacity ranging from 2 500 to 3 300 tonnes/day, and milled a total of 12.3×10^6 tonnes of ore before closure (Robertson, 1968).

The tailings site consists of two impoundment areas: the Nordic West Arm and the Nordic Main tailings basins (Figure 4). Deposition of tailings in the West Arm impoundment began in 1957 and ceased in 1960. The impoundment was originally created by constructing Dam A. The tailings were discharged so that the clear effluent flowed into Westner Lake. Dam B was then constructed and the flow was altered so that the tailings were discharged through the east end. Tailings were deposited in the middle of the West Arm, and as time progressed the discharge point was moved westward towards Dam B. In 1960, when it was desired to enlarge the tailings area, Dam C was raised to contain the Nordic Main impoundment. The West Arm was abandoned. Dam B was breached to drain the surface water and allow the tailings to dry. The total area of the West Arm is 16 hectares (Moffett and Tellier, 1978).

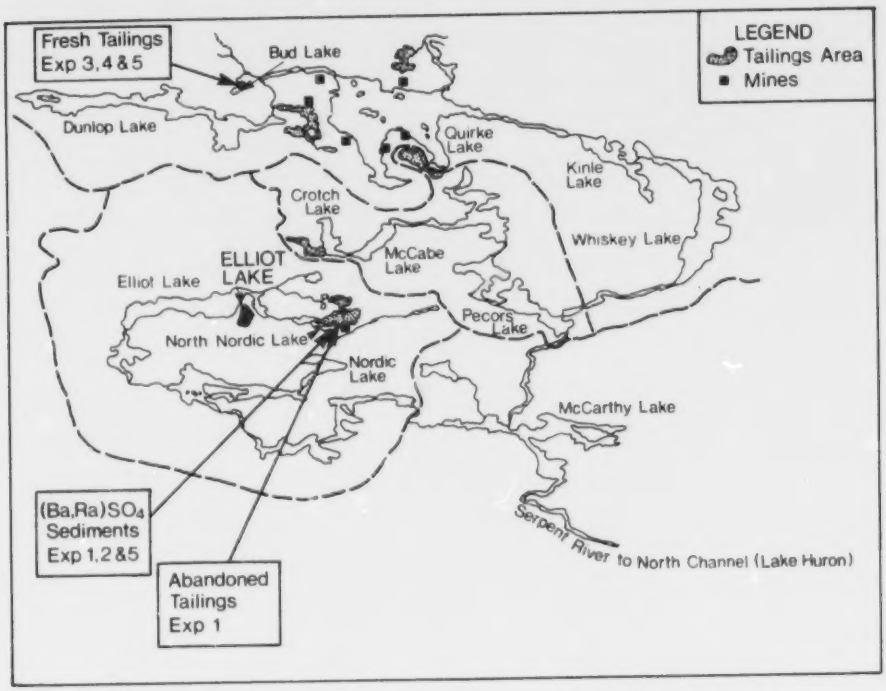

FIGURE 3 SOURCES OF RADIOACTIVE MATERIAL - ELLIOT LAKE AREA

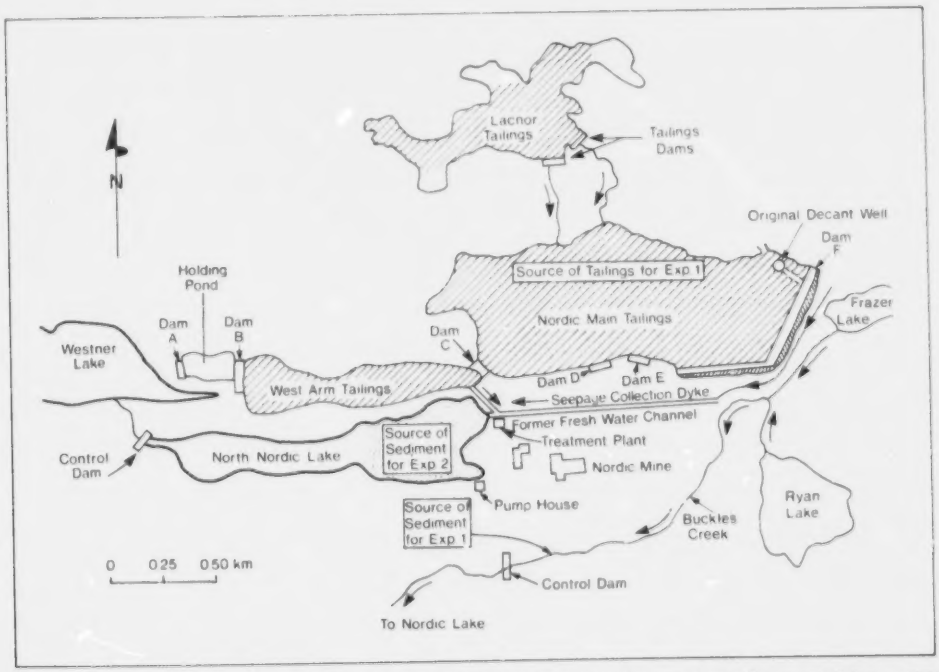

FIGURE 4 LOCATIONS OF ABANDONED TAILINGS AND (Ba, Ra)SO_4 SEDIMENTS COLLECTION SITES AT NORDIC LAKE TAILINGS AREA (after VIVYURKA, 1974)

Deposition in the Nordic Main tailings area began in the southwest corner and extended northward and eastward. The tailings deposit was formed by broad low-level alluvial fans in which the coarser tailings were deposited nearest to the discharge pipe and the finest particles settled farthest away. During the initial deposition period, the east end of the tailings pond was contained by a 3-m berm that impounded process water in the eastern half of the basin. The berm formed the core of the present rockfill tailings dam. During the period of 1960 to 1964, this dam was progressively raised to its current height of 10 to 12 m to contain the eastern and southern perimeters of the basin. The basin is confined along the north and west perimeters by prominent bedrock ridges. Tailings were deposited in the Nordic Main area until the Nordic mine and mill ceased operation in 1968. The Nordic Main tailing deposit occupies an area of approximately 85 hectares measuring 1 460 m east-west and 550 m north-south; its average thickness is 10 m (Blair et al., 1980).

The Lacnor tailings impoundment is located north of the Nordic Main tailings area (Figure 4), and drains into the Nordic Main area. Deposition of tailings in the Lacnor impoundment ceased in 1960 (Cherry et al., 1980).

Prior to 1971, the combined runoff and seepage from Lacnor and Nordic Main tailings areas flowed over Dam F through a decant tower, along the base of Dam F, from where it was piped under the freshwater channel system and discharged into Buckles Creek. Barium chloride treatment was carried out at this point. The treated effluent then overflowed a small settling area and discharged into Nordic Lake. The freshwater channel carried water from Ryan and Fraser Lakes to Nordic and Westner Lakes, and on to Horne and Elliot Lakes. Seepage from Dams D and E was controlled by a lagoon at the base of the dams, to prevent its entering the freshwater system. The solution in the lagoon was periodically pumped back into the tailings area. The drainage and treatment system was revised in the summer of 1971. The revision entailed the following changes (Vivyurka, 1975):

1. The decant well on the Nordic Main tailings impoundment was removed, and the ponded water on the eastern portion of the tailings was drained off.
2. The freshwater drainage from Fraser and Ryan Lakes was diverted to the Buckles Creek system.
3. A small control dam was constructed at Buckles Creek to prevent particulate matter from being carried downstream.
4. The runoff and seepage stream from along the base of Dams D, E, and F was diverted into the previous freshwater channel and towards North Nordic Lake.

5. Drainage ditches and ponds were dug to handle runoff from the easterly portion of the tailings contained by Dam B. This effluent joined the seepage and runoff from Dams D, E, and F before going through the treatment plant and into North Nordic Lake.
6. A lime slurry-barium chloride treatment plant was built at the east end of North Nordic Lake at the point where the combined flows of seepage and runoff could enter the lake. The lake was used as a settling pond. The clarified, treated water was pumped from the lake into Buckles Creek.
7. A dam was constructed on the west end of North Nordic Lake to stop effluent discharging into Westner Lake and subsequently into Elliot Lake.

The effluent water discharged to the Nordic tailings pond was essentially a calcium sulphate solution with a pH of 8 and high concentrations of ammonium and nitrate ions. The concentration of nitrate was approximately 500 mg/L and that of ammonium 100 mg/L. The total dissolved solids concentration of the effluent water was of the order of 2 500 to 3 000 mg/L. The sulphate concentration was approximately 1 500 mg/L and that of calcium 500 mg/L, indicating that the tailings overflow waters were saturated with gypsum ($CaSO_4.2H_2O$). The dissolved heavy metal concentrations, including that of thorium, in the effluent water following lime neutralization were less than 1 mg/L. Upon close out, the concentration of Ra-226 at the tailings discharge point varied from 37 to 185 Bq/L. The Ra-226 concentration in the tailings pore water probably rapidly decreased to the range of 18.5 to 37 Bq/L and then gradually decreased to much lower levels as aging of the deposited tailings occurred (Blair et al., 1980).

Since Elliot Lake ores contain 2 to 7 percent pyrite (FeS_2) by weight, tailings have the potential to become acidic upon the termination of milling, because of the generation of sulphuric acid, mainly by pyrite oxidation. This induces desorption and dissolution of certain radionuclide species and heavy metals from the tailings. The actual metals that are mobilized are described in Section 4.4.

The formation of sulphuric acid and iron sulphates occurs by the following chemical steps (Raicevic, 1979):

$$2FeS_2 + 2H_2O + 7O_2 \rightarrow 2FeSO_4 + 2H_2SO_4$$

pyrite — ferrous sulphate — sulphuric acid

$$4FeSO_4 + O_2 + 2H_2SO_4 \rightarrow 2Fe_2(SO_4)_3 + 2H_2O$$

ferric sulphate

$$Fe_2(SO_4)_3 + 6H_2O \rightarrow \underset{\text{ferric hydroxide}}{2Fe(OH)_{3(s)}} + 3H_2SO_4$$

The subscript(s) denotes a solid.

The chemical and radiological characteristics of abandoned tailings in the Nordic area are given in Table 1 (Zahary et al., 1974). Examples of contaminant levels in effluents from tailings sites in the Elliot Lake area are presented in Table 2 (Vivyurka, 1975).

TABLE 1 CHEMICAL AND RADIOLOGICAL CHARACTERISTICS OF ABANDONED TAILINGS IN THE NORDIC LAKE AREA

Property	Coarse Tailings	Fine Tailings
Chemical Characteristics[1]		
pH	1.9	2.3
Cation exchange capacity (meq/100 g)	0.17	1.75
Si (%)	41.3	37.1
Al (%)	2.0	2.18
S (%)	1.18	4.25
Fe (%)	1.15	3.65
K (%)	1.12	1.14
Ca (%)	0.28	0.87
Mg (%)	0.040	0.043
Mo, Pb (%)	0.05	0.05
Ni, Cu, Zn, Mn, P, Cl (%)	0.01	0.01
Radioisotope Concentrations[2]		
U (µg/g)	15.8	19.1
Th (µg/g)	4.1	6.4
Ra-226 (Bq/kg)	6142	11 618
Pb-210 (Bq/kg)	1332	4810

[1]Zahary et al., 1974
[2]Moffett and Tellier, 1978 - Analyses are reported on oven-dried material

The tailings used in Experiment 1 were collected in 1974 from the Nordic Main tailings area (Figure 4), and shipped to Burlington in 200-L steel drums. The area from which the tailings were taken had not been treated in any way during the revegetation experiments that had been conducted in the area. The tailings were of a coarseness

TABLE 2 EXAMPLES OF CONTAMINANT LEVELS IN EFFLUENTS FROM TAILINGS SITES IN THE ELLIOT LAKE AREA (Vivyurka, 1974)

	Active Tailings Areas	Idle Tailings Areas	
	Decant and Seepage (ppm)	Seepage (ppm)	Runoff (ppm)
pH*	6.5 - 9.0	2.0 - 6.5	3.0 - 4.5
TDS	1000 - 2500	1000 - 6000	300 - 1500
SO_4	600 - 1500	600 - 3200	200 - 1000
NO_3	100 - 200	5 - 10	5 - 10
NH_3	5 - 15	<0.05 - 3	<0.05 - 3
Ca	250 - 450	250 - 600	50 - 350
Fe^{+2}	<0.1	10 - 400	5 - 20
Fe^{+3}	<0.1	10 - 500	5 - 20
Pb	<0.05	<1.0	<0.5
Zn	<0.1	<1.0	<0.5
Cu	<0.1	<1.0	<0.5
Mn	0.01 - 1.0	1 - 3.5	0.5 - 1.5
Ni	<0.1	<1.0	<0.5
Ra-226 (Bq/L)	0.4 - 3.7	0.4 - 11.1	<0.04 - 3.7
U_3O_8	<1.0	<1.0	<1.0

* All analyses in ppm except pH and Radium-226

comparable to medium-fine sand. The particle size distribution of the tailings was not determined at the time of collection. Samples taken from the same area by Murray and Moffett (1977) had a distribution of 64 percent between 2 mm and 50 µm and 36 percent between 50 µm and 2 µm.

The $(Ba,Ra)SO_4$ sediments were dredged from the former settling pond on Buckles Creek in 1974 (Figure 4). The sediments were originally saturated with water. After drying, the texture of the sediments was similar to that of a powder. The sediments also contained some coarser particulates which included creek bed sand and wood chips.

4.2 Experimental Program

Twelve cylindrical acrylic lysimeters, 305 mm in diameter and 120 cm deep (Figure 5), were used to hold four replicates of each of the following tailings compositions:

1. tailings (control),
2. tailings with a limestone-neutralized surface area, and
3. tailings mixed with $(Ba,Ra)SO_4$ sediments in the surface layer.

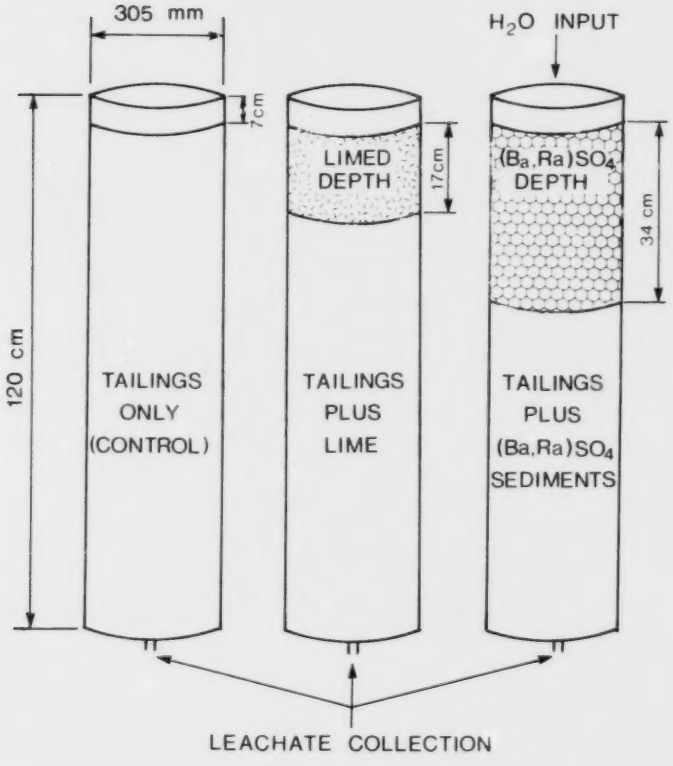

FIGURE 5 TYPICAL LYSIMETERS USED IN EXPERIMENT 1

Before use, the tailings and sediments were air-dried, passed through a 0.64-cm screen, and mixed thoroughly. Each lysimeter was filled in six 15-kg lifts. The sediments and tailings were tamped between each lift. Each control lysimeter received 90 kg of tailings. Each lysimeter dedicated for tailings plus limestone received 80 kg of tailings plus 10 kg of crushed limestone; the limestone was mixed with the top 5 kg of tailings. Each lysimeter dedicated fo. tailings plus sediment received 80 kg of tailings plus 10 kg of sediments; the sediments were mixed with the top 20 kg of tailings.

The sediment-to-tailings ratio of 1:8 used in these lysimeters is much larger than the current sediment-to-tailings mass production ratio of about 1:18000. It was selected so that possible differences in the leaching characteristics of the controls and the tailings-sediment lysimeters would be exaggerated and thus more readily discernable. The tailings-sediment lysimeters were set up to simulate areas in a tailings pile where $(Ba,Ra)SO_4$ sediments overlie mill tailings in an unsaturated groundwater condition.

Each lysimeter contained approximately 73 000 cm^3 of tailings or tailings and sediments. If a particle density of 2.75 g/cm^3 is assumed, the initial bulk density of the contents of each lysimeter was equal to 1.23 g/cm^3 and the porosity equal to 0.55.

During Phase 1 of the study (September 1974 to February 1976), the lysimeters were located outside the Wastewater Technology Centre in Burlington from September to November 1974 and from April to September 1975, and indoors the rest of the time. While outdoors, the only water addition to the lysimeters came from natural precipitation. While indoors, half the lysimeters received 1 L of distilled water every 10 days (equivalent to a precipitation rate of 4.1 cm/month), while the other half received 2 L of distilled water every 10 days (8.2 cm/month).

During Phase 2 of the study (May 1976 to December 1981), the tailings-limestone lysimeters were discontinued, because their leachate characteristics were similar to those of the control leachates. All lysimeters remained indoors. Half of the lysimeters continued to receive 1 L of distilled water every 10 days, but the rate of water addition to the other half (previously loaded at 2 L every 10 days) was increased to 1.12 L of distilled water every day (46 cm/month), and the mode of application was changed from batch to continuous.

Leachate was collected through a perforated drainage pipe installed in the base of each lysimeter, and analyzed periodically for pH, conductivity, total gross alpha and beta, and filtered (0.45 micron) Ra-226, Pb-210, Th-232, Th-230, Th-228, gross alpha, and gross beta.

The radiochemical analyses for leachate samples collected between September 1974 and August 1975 were conducted by the Radiation Protection Laboratory, Ontario Ministry of Labour. Subsequent radiochemical analyses were done at the Radiochemical Laboratory, Canada Centre for Inland Waters.

At the end of the experiment, leachate samples collected from the control lysimeters during the period from December 1979 to December 1981 were analyzed for major anions, major cations, nutrients, and TDS. For several of these leachate samples, measured concentrations were used to describe "model waters" for which chemical

speciation calculations were made. These calculations permitted statements concerning the probable chemical species present and the probable precipitates which would form.

Cores from the control lysimeters were obtained at the end of the experiment and analyzed for chemical composition (sulphide, sulphate, and carbonate) and physical parameters (porosity, moisture content, and bulk density). Measurements of Ra-226, Th-230, Th-232, and Th-228 remaining in the solids were also made. The initial radionuclide contents of the controls were estimated on the basis of these radionuclide analyses and the total mass of each radionuclide leached during the study.

Samples (0.5 g) for Ra-226 and thorium analyses were taken into solution by KF fusion according to Sill (1961). After addition of Ba-133 tracer, the Ra-226 was coprecipitated with Pb^{2+} and Ba^{2+} as a mixed sulphate and subsequently collected on $BaSO_4$ for alpha spectroscopic counting, according to Zimmerman and Armstrong (1976). Thorium nuclides were recovered by solvent extraction and ion exchange according to Durham and Joshi (1979). The purified thorium solution was evaporated to dryness, dissolved in EDTA and coprecipitated with $Ce(OH)_4$ from 3M NaOH according to Sill and Williams (1981) to form the alpha spectroscopy source. The thorium yield was determined by the addition of Th-234 to the sample after fusion. Because lead halides are volatile at fusion temperatures, the samples (0.5 g) were digested with 100 mL of HNO_3 until almost dry. At this point, 10 mL of HCl, 3 mL of HNO_3, 2 mL of H_2O_2, and 1 mL of HF were added and fumed to 1 mL. The contents of the beaker were dissolved in aqua regia, and the amount of Pb-210 determined according to Durham and Joshi (1976). Ra-226 and Th nuclides were counted on a Canberra Alpha Spectrometry System, and Pb-210, Th-234, and Ba-133 were determined on a Canberra 2201 Proportional Counter.

Mineralogical features of solids from some lysimeter sections and of solids from the leaching pachucas, partial neutralization tank and final neutralization tank of the uranium mill at Rio Algom were examined using Scanning Electron Microscope X-ray Emission (SEM-XRE) and Mossbauer Spectroscopy techniques. The mill solids were examined to provide a description of the probable tailings characteristics upon placement. SEM-XRE technology provides the ability to examine the morphology of particles visually, to obtain knowledge of the major elements making up the particles, to identify the probable minerals, and to calculate the mass of these minerals. Mossbauer Spectroscopy can differentiate oxidation states of iron and help to identify both amorphorus (Fe hydroxides) and crystalline minerals (Fe sulphates).

Solids from the Rio Algom leaching pachuca and from the 30 to 40 cm deep section of one high-rate control lysimeter were mixed with KCl and Na EDTA solutions to

determine which constituents would dissolve. The resultant solutions were analyzed for Ra-226 and various cations. Particular attention was paid to minerals which, the literature suggests, may contain Ra-226 (calcium sulphate, lead sulphate, barium sulphate, and jarosite).

4.3 Results

Since the chemical characteristics of leachates from the tailings-limestone lysimeters were similar to those from the controls, only the data from the controls and the tailings-sediment lysimeters are presented.

The objective of the increased rate of water addition in Phase 2 was to accelerate the leaching process and to allow the equivalent of approximately 7 years of rainfall to be applied to the tailings in a year (the average precipitation at Elliot Lake, Ontario is approximately 6.5 cm/month). Increasing the rate of water addition to obtain accelerated leaching data is based on the assumptions that:

- leaching rates depend only on the amount of water passing through the tailings (i.e., dissolution reactions),
- the effects of wetting and drying sequences and of seasonal climatic changes can be ignored, and
- if bacterial activity is important as in pyrite oxidation, it increases with the increased rate of water application.

The dependence of leaching behavior upon hydraulic loading was evaluated by graphing chemical concentrations in the leachates both versus time (days) and versus volume (pore volumes of leachate). If the above assumptions are not correct, then leachate characteristics are not comparable at equivalent pore volumes. The accelerated leaching data could then be used to predict future tailings characteristics only with the formulation of a mechanistic model describing geochemical controls upon the leaching processes occurring in the tailings.

The volumetric results for the leachate characteristics are presented in two graphs, one showing the results during the production of the first four pore volumes (to clarify data presentation), and the other for the entire experimental period up to December 1981. One pore volume in each lysimeter was approximately equal to 40 L. Thus, for the half of the lysimeters receiving 1 L of water every 10 days, it took about 400 days for one pore volume of leachate to be produced. For the other half of the lysimeters, it took about 200 days to achieve one pore volume when water was being

applied at a rate of 2 L every 10 days, and 36 days when the water application rate was 1.12 L/day.

To simplify terminology, the water application rates of 0.1, 0.2, and 1.12 L/day will be referred to as the low, middle, and high flow rates, respectively. The lysimeters receiving water at the low flow rate will be referred to as the low-rate lysimeters, whereas those receiving water initially at the middle flow rate and later at the high flow rate will be referred to as the high-rate lysimeters.

4.3.1 Leachate Characteristics. The results of statistical analyses conducted on the measured leachate characteristics are given in Tables 3 and 4, in the form of coefficients of variation. The coefficient of variation is the standard deviation expressed as a percentage of the mean (Davies and Goldsmith, 1972). It allows comparisons to be made between groups of observations where the means of the groups are different and where the standard deviation increases in proportion to the mean. Relatively large within-treatment coefficients were obtained for many of the parameters, especially for the tailings-sediment lysimeters or those receiving water at the higher rates or both. This indicates that the reproducibility of these parameters in replicated lysimeters was poor. The between-treatment variance for most parameters was significantly greater than the within-treatment variance (as noted by an asterisk in Table 4), indicating that the temporal pattern of those parameters in a tailings-sediment leachate was significantly different from the pattern observed in the corresponding control leachate.

The average leachate production rates for the lysimeters receiving distilled water at a rate of 0.1 L/day were 0.07 L/day during Phase 1 and 0.05 L/day during Phase 2. The average leachate production rates for the high-rate lysimeters were 0.13 L/day during Phase 1 and 0.95 L/day during Phase 2. By the end of the study (i.e., after 7 years of leaching), the average total leachate volumes produced were 152 L (3.8 pore volumes) for each low-rate lysimeter and 1995 L (50 pore volumes) for each high-rate lysimeter.

During Phase 1, leachate pH of all lysimeters followed approximately the same trend, with an initial rapid decrease from between 2.3 and 2.6 to about 1.7 during the first 2 months, followed by a slow decrease to about 1.2 (Figures 5, 6, and 7). During Phase 2, leachate pH for the low-rate lysimeters continued to decrease up to Day 600, generally remained less than 1 up to Day 1900, then increased to 1.5 at the end of the study. Leachate pH for the high-rate lysimeters slowly increased during Phase 2 to about 3.4 for the controls and 3.8 for the tailings-sediment lysimeters. Leachate pH's during the study

TABLE 3 EXPERIMENT 1: VARIATIONS WITHIN REPLICATED TREATMENTS

Coefficient of Variation (Number of Pairs of Replicated Observations)						
	Leachate Produced from Abandoned Tailings			Leachate Produced from Abandoned Tailings +$(Ba,Ra)SO_4$ Sediments		
	Water Application Rate			Water Application Rate		
Parameter	0.1 L/day	0.2 L/day	1.12 L/day	0.1 L/day	0.2 L/day	1.12 L/day
Volume	12.1(34)	4.3(17)	6.3(20)	13.4(34)	5.9(17)	7.4(20)
pH	12.1(22)	8.3(6)	4.1(17)	9.8(22)	6.2(6)	7.7(17)
Conductivity	5.4(18)	7.7(2)	21.9(16)	13.7(18)	89.0(2)	41.1(16)
Dissolved Gross α	33.5(19)	22.8(11)	16.3(8)	28.6(17)	33.4(11)	38.7(9)
Dissolved Gross β	33.6(19)	18.7(11)	20.9(8)	24.2(18)	38.2(11)	40.2(9)
Suspended Gross α	95.6(17)	86.9(12)	21.2(7)	60.5(15)	48.5(10)	104.7(8)
Suspended Gross β	62.2(16)	69.1(12)	42.1(6)	86.5(15)	66.7(10)	59.1(9)
Dissolved Ra-226	53.0(26)	9.1(11)	19.6(15)	65.7(25)	120.4(11)	44.8(15)
Dissolved Pb-210	17.9(27)	14.6(12)	19.2(16)	25.3(26)	32.4(12)	54.7(15)
Dissolved Th-232	56.3(20)	45.1(11)	21.2(5)	49.4(19)	69.1(11)	--
Dissolved Th-230	36.0(19)	49.8(11)	33.3(8)	48.0(19)	59.6(11)	108.1(3)
Dissolved Th-228	24.0(19)	32.3(11)	56.0(9)	29.3(19)	28.8(11)	81.0(8)

The coefficient of variation within replicate treatments for each parameter was calculated from (Davies and Goldsmith, 1972):

$$\text{Coefficient of Variation (\%)} = 100 \left(\frac{\sum_{i=1}^{k} \sum_{j=1}^{2} (\ln y_{ij} - \ln \bar{y}_i)^2}{k} \right)^{1/2}$$

where k = number of pairs of replicated observations within a treatment for each parameter (shown above in brackets)

y_{ij} = jth observation (replicate 1 or 2) of ith pair of replicates (i = 1 to k)

$\bar{y}_i$ = mean of ith pair of replicates

TABLE 4 EXPERIMENT 1: VARIATIONS BETWEEN CONTROL LYSIMETERS AND TAILINGS-SEDIMENT LYSIMETERS

Parameter	Coefficient of Variation (Number of Pairs of Replicated Observations)		
	Water Application Rate		
	0.1 L/day	0.2 L/day	1.12 L/day
Volume	* 32.9(34)	* 14.6(17)	5.6(20)
pH	9.1(26)	* 16.9(11)	* 15.9(17)
Conductivity	* 16.4(21)	37.0(5)	* 77.7(16)
Dissolved Gross α	*367.0(20)	*504.0(11)	40.9(11)
Dissolved Gross β	*221.0(20)	*293.0(11)	25.8(11)
Suspended Gross α	*235.0(17)	*396.0(14)	80.6(8)
Suspended Gross β	*258.0(19)	*479.0(16)	91.0(9)
Dissolved Ra-226	70.4(34)	40.8(16)	*102.0(18)
Dissolved Pb-210	23.5(33)	* 40.8(17)	56.4(18)
Dissolved Th-232	*443.0(29)	*605.0(13)	*142.0(9)
Dissolved Th-230	*495.0(29)	*638.0(13)	*137.0(14)
Dissolved Th-228	*192.0(29)	*252.0(13)	*215.0(17)

1. The coefficient of variation between the two treatments was calculated from (Box et al., 1978):

$$\text{Coefficient of variation (\%)} = 100 \left(\frac{\sum_{i=1}^{m} \sum_{t=1}^{n_t} n_t (\ln \bar{y}_{it} - \ln \bar{y}_i)^2}{m} \right)^{1/2}$$

where m = number of pairs of observations obtained at the same time from the two treatments (shown above in brackets)

n_t = number of observations used in determining $\bar{y}_{it}$ ($n_t = 1$ if leachates from two replicated treatments were composited prior to analysis; $n_t = 2$ if both leachates were analyzed separately)

$\bar{y}_{it}$ = mean of ith set of observations for treatment t (t = 1 for controls; t = 2 for tailings plus sediments lysimeters)

$\bar{y}_i$ = mean of ith set of observations for both treatments

2. A coefficient of variation preceded by an asterisk (*) indicates that the between-treatment variance is significantly greater than the within-treatment variance (F-test, 95-percent level of confidence).

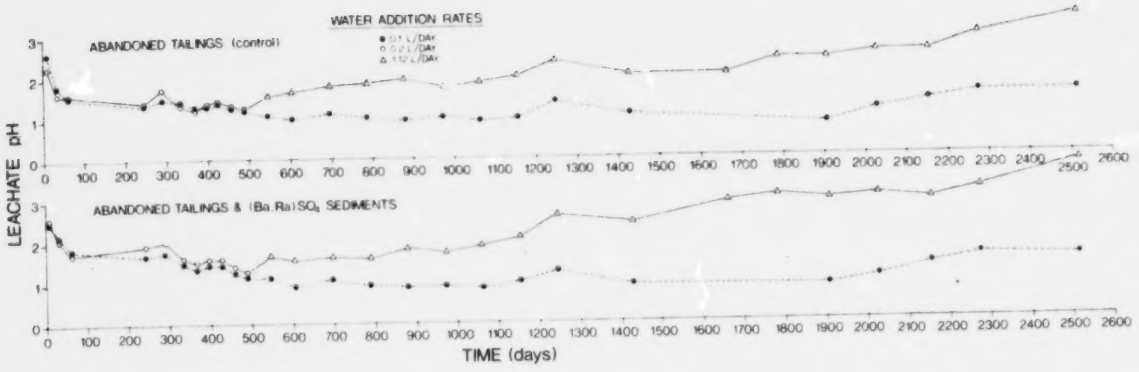

FIGURE 6 EXPERIMENT 1: TEMPORAL VARIATIONS IN LEACHATE pH

are comparable to those of 1.4 to 3.6 observed in the top 1 m of in-situ Nordic tailings in 1979 by Cherry et al. (1980).

Total dissolved solids (TDS) concentrations in all low-rate leachates show four distinct periods. Concentrations increased steadily during the first 1000 days, decreased during the next 200 days, increased to a second peak at 1900 days, then decreased (Figures 8 and 9). TDS concentrations in the high-rate lysimeters increased steadily during Phase 1, then decreased rapidly after the initiation of Phase 2.

Leachate conductivity data are not available for the first year of the study. Conductivities in all low-rate leachates increased during the second year, remained constant until about Day 2000, then decreased (Figures 10 and 11). Conductivities in all high-rate leachates decreased throughout the study. The conductivity values of 250 mS/m achieved in the low-rate leachates near the end of the study are consistent with data collected by Cherry et al. (1980), who measured in-situ conductivities of 30 to 200 mS/m in the Nordic tailings in 1979.

With the exception of Pb-210, radionuclide levels in the tailings-sediment leachates were higher than those in the control leachates. By the end of the study, the ratios of cumulative radioactivity leached from the high-rate tailings-sediment lysimeters to that leached from the controls were:

Ra-226	1.9:1
Th-232	51:1
Th-230	72:1
Th-228	2.3:1

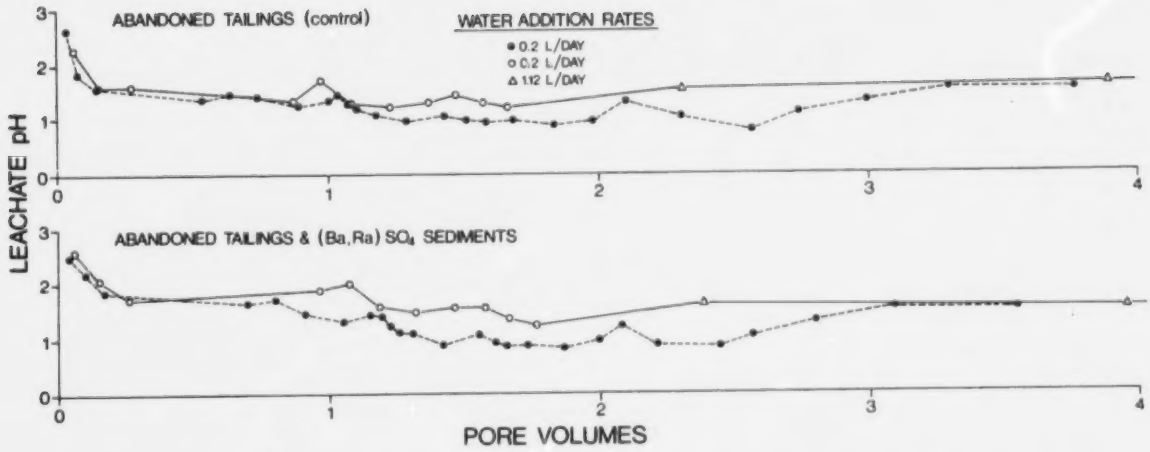

(a) During First Four Pore Volumes

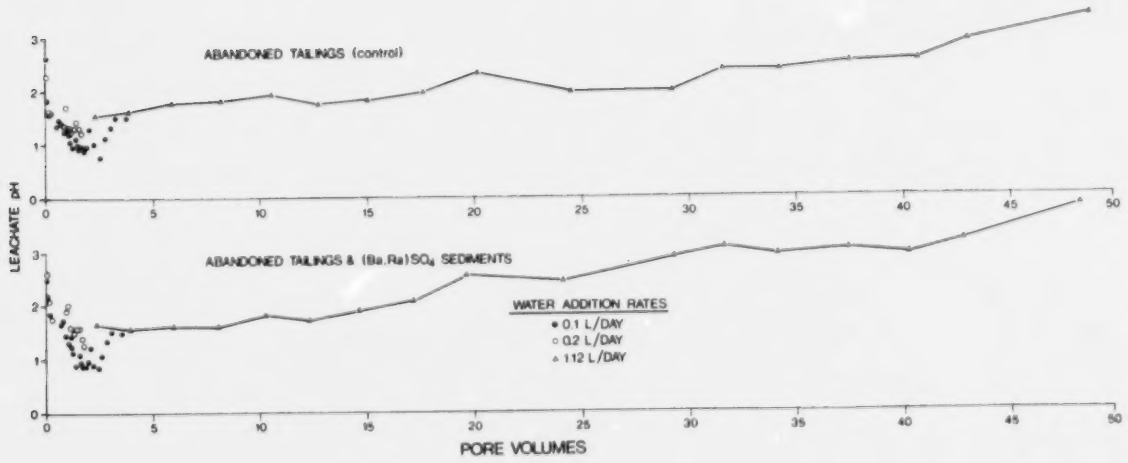

(b) To December 1981

FIGURE 7 EXPERIMENT 1: PORE-VOLUMETRIC VARIATIONS IN LEACHATE pH

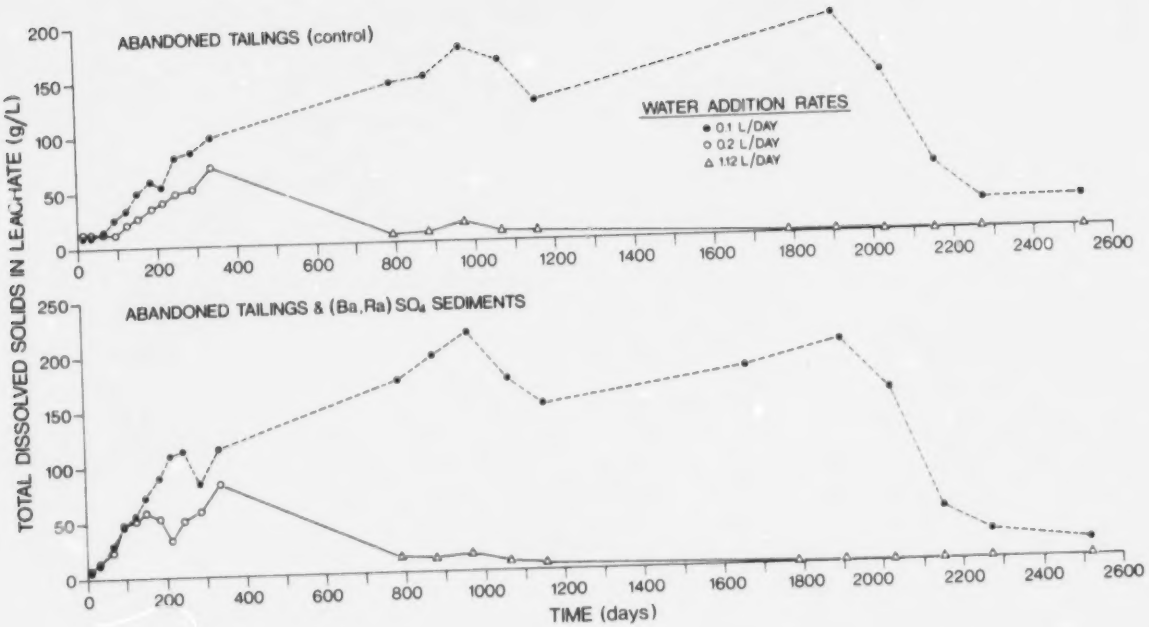

FIGURE 8 EXPERIMENT 1: TEMPORAL VARIATIONS IN TOTAL DISSOLVED SOLIDS CONCENTRATIONS

While only dissolved radionuclide levels were determined, they approach total radionuclide levels because over 99 percent of the measured total gross alpha and beta was in the dissolved state.

The general Ra-226 release pattern for the controls during Phase 1 is almost identical to the pattern displayed by leachate pH. An initial rapid decrease during the first 2 months preceded a slower decrease to the end of Phase 1 (Figures 12 and 13). During Phase 2, Ra-226 levels in the low-rate control leachates remained less than 15 pCi/L (0.56 Bq/L), whereas those in the high-rate control leachates remained relatively constant at about 20 pCi/L (0.74 Bq/L) up to Day 1100 then increased to peak at Day 2275. Radium-226 levels in the control leachates were comparable to in-situ levels of 35 to 100 pCi/L (1.3 to 3.7 Bq/L) measured at the water table in the Nordic tailings in 1979 (Blair et al., 1980).

Radium-226 levels in the tailings-sediment leachates, although fluctuating more than those in the control leachates, showed the same general pattern of decreasing during Phase 1. During Phase 2, levels in the low-rate tailings-sediment leachates

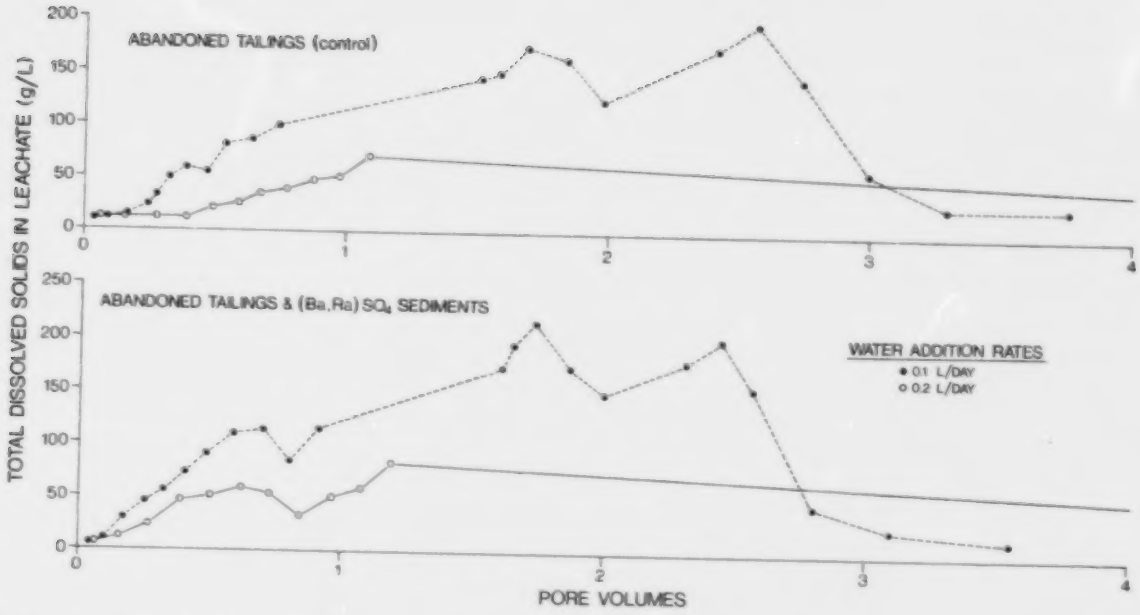

(a) During First Four Pore Volumes

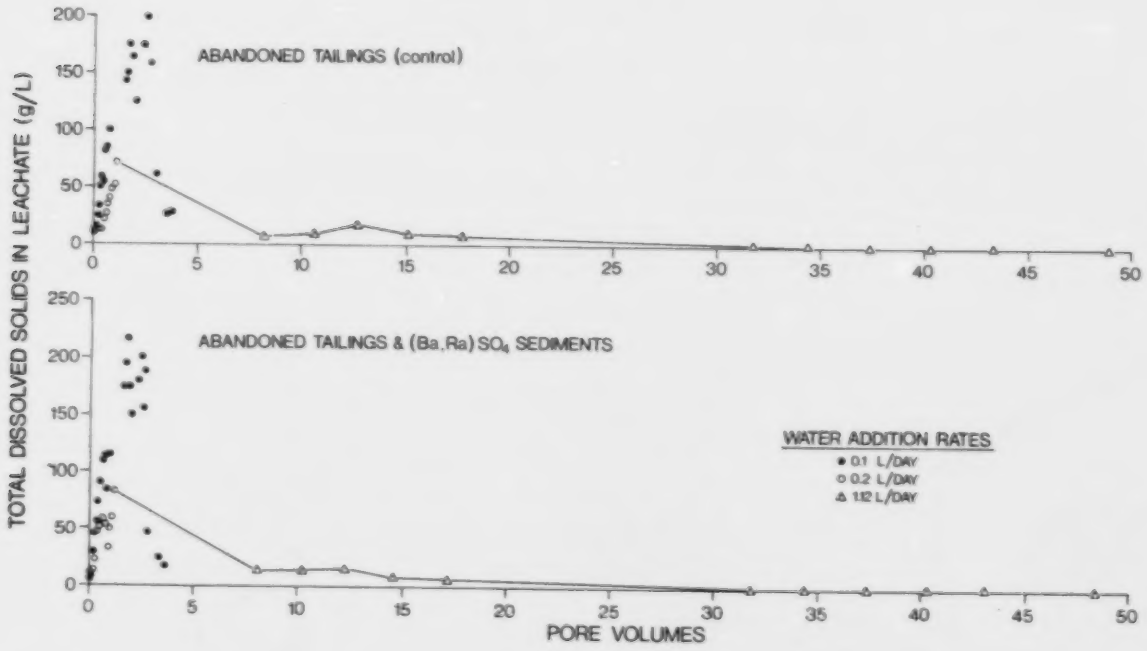

(b) To December 1981

FIGURE 9 EXPERIMENT 1: PORE-VOLUMETRIC VARIATIONS IN TOTAL DISSOLVED SOLIDS CONCENTRATIONS

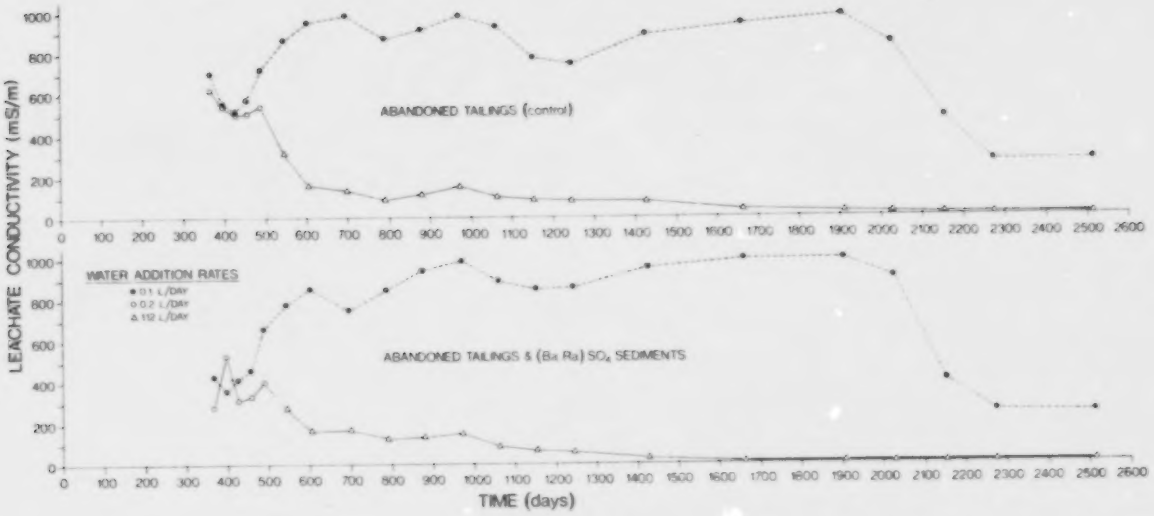

FIGURE 10 EXPERIMENT 1: TEMPORAL VARIATIONS IN LEACHATE CONDUCTIVITY

decreased to less than 20 pCi/L (0.74 Bq/L), whereas those in the high-rate leachates remained at about 40 pCi/L (1.5 Bq/L) for 1 000 days (12 pore volumes), then increased to a peak of 830 pCi/L (30.7 Bq/L) at 1 900 days (34 pore volumes).

The cumulative amounts of Ra-226 leached from the high-rate lysimeters are plotted against pore volumes of leachate in Figure 14. Initial Ra-226 radioactivity in the control lysimeters was about 1 uCi (4.1×10^5 Bq). The high-rate controls had leached 0.8 percent of the estimated initial Ra-226 content after 50 pore volumes, whereas the low-rate controls had leached approximately 0.02 percent after four pore volumes (Table 5).

Lead-210 levels in both the low-rate and high-rate control leachates were almost identical during Phase 1 (Figures 15 and 16). This similarity in control lysimeter leachate characteristics during Phase 1 has already been noted for pH and Ra-226. However, in Phase 2, whereas pH and Ra-226 levels increased in the high-rate leachates and decreased in the low-rate leachates, Pb-210 levels did exactly the opposite. The same amounts of Pb-210 were released from the high-rate tailings-sediment lysimeters and the controls over 50 pore volumes (Figure 14), even though the high-rate lysimeters initially contained more Pb-210.

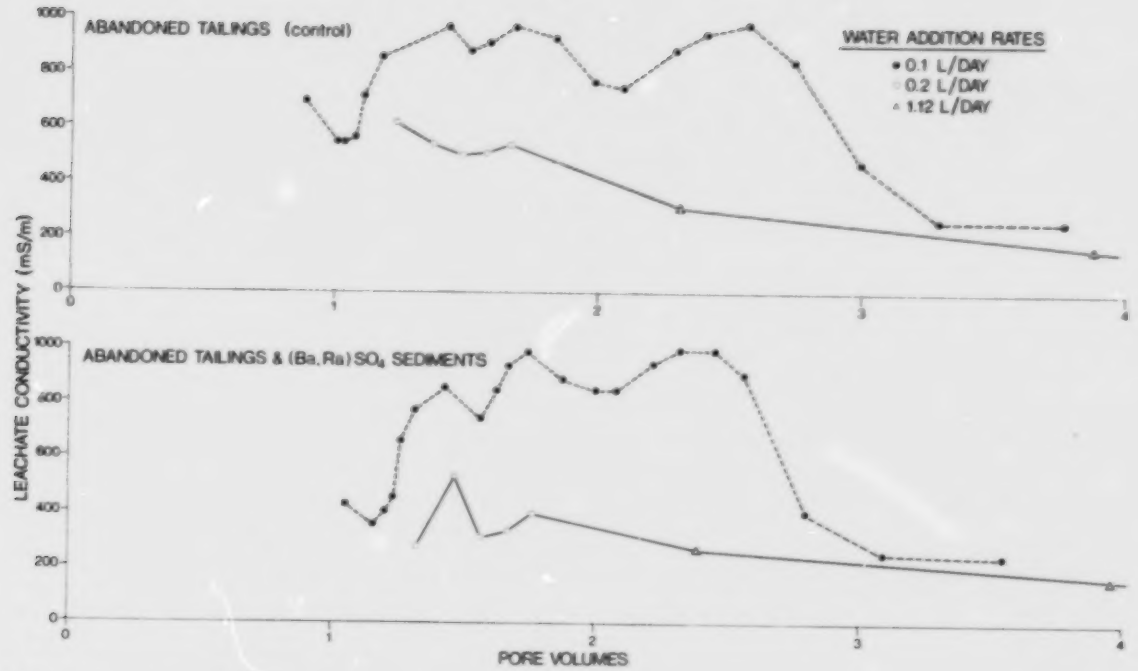

(a) During First Four Volumes

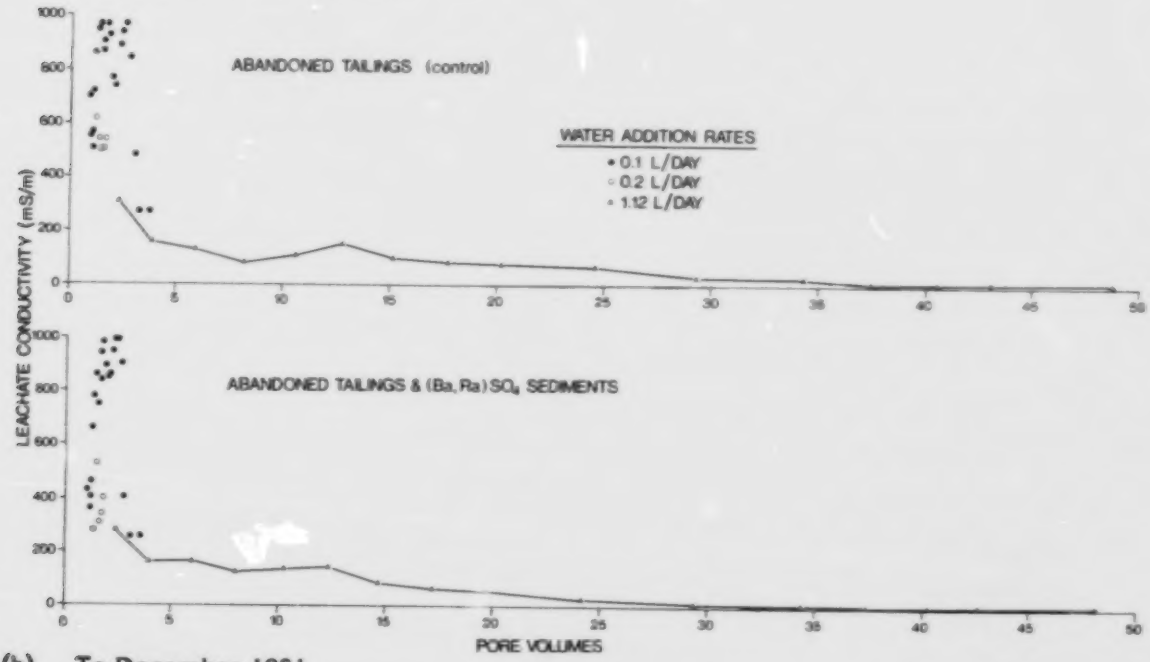

(b) To December 1981

FIGURE 11 EXPERIMENT 1: PORE-VOLUMETRIC VARIATIONS IN LEACHATE CONDUCTIVITY

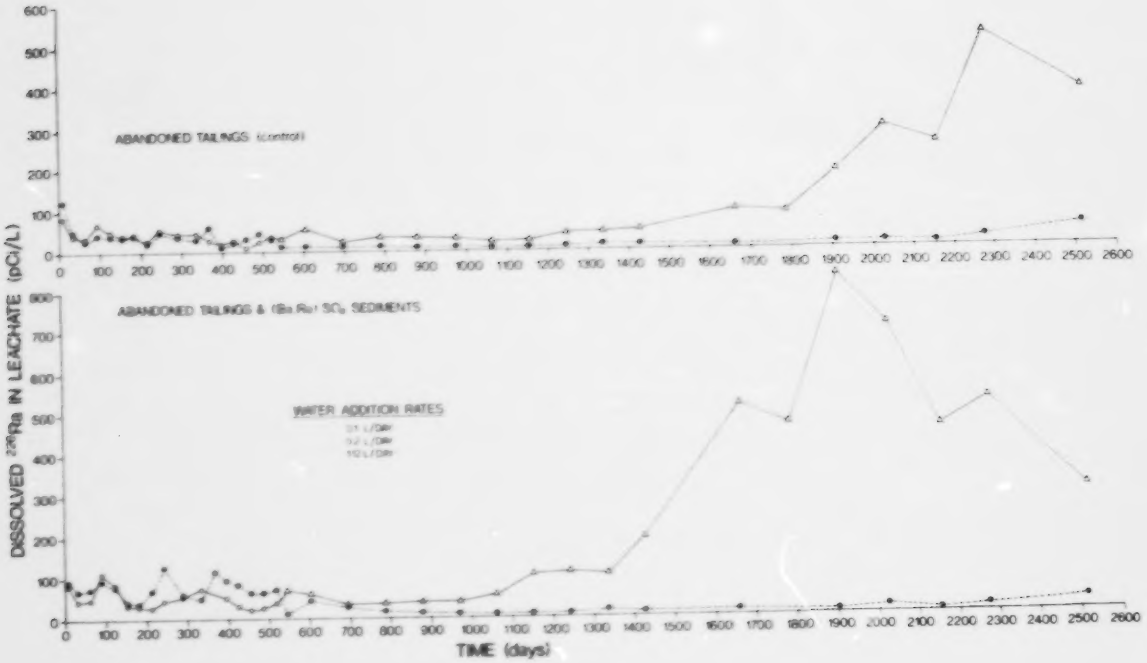

FIGURE 12 EXPERIMENT 1: TEMPORAL VARIATIONS IN DISSOLVED Ra-226

Initial thorium levels in leachates were about 300 to 500 pCi/L (11 to 19 Bq/L) for Th-228, 200 to 400 pCi/L (7.4 to 15 Bq/L) for Th-230, and 20 to 100 pCi/L (0.74 to 3.7 Bq/L) for Th-232. In general, thorium levels peaked around 100 days in the tailings-sediment leachates and 300 days in the control leachates, then decreased (Figures 17 to 22). After 2 200 days, levels in the low-rate leachates had generally returned to their initial values, whereas levels in most high-rate leachates had decreased to about 1 pCi/L (0.04 Bq/L). Cumulative thorium radioactivities leached from the high-rate lysimeters during the study are shown in Figure 14. A considerable amount of the thorium initially present in the lysimeters was leached during the period of this study, as indicated by the percentages given in Table 5.

Initial gross alpha and beta levels in all leachates ranged between 2 000 and 6 000 pCi/L (74 and 222 Bq/L). Their release patterns were, in general, similar to those displayed by thorium, with the exception of the decrease in gross alpha and beta levels in the high-rate leachates which was not so severe during the latter part of Phase 2 (Figures 23 to 26). About four times as much gross alpha and twice as much gross beta

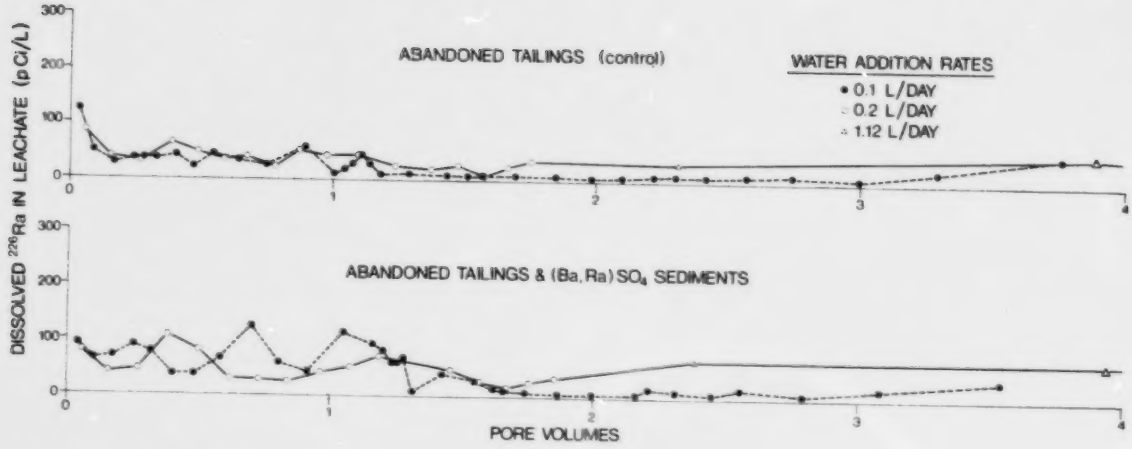

(a) During First Four Pore Volumes

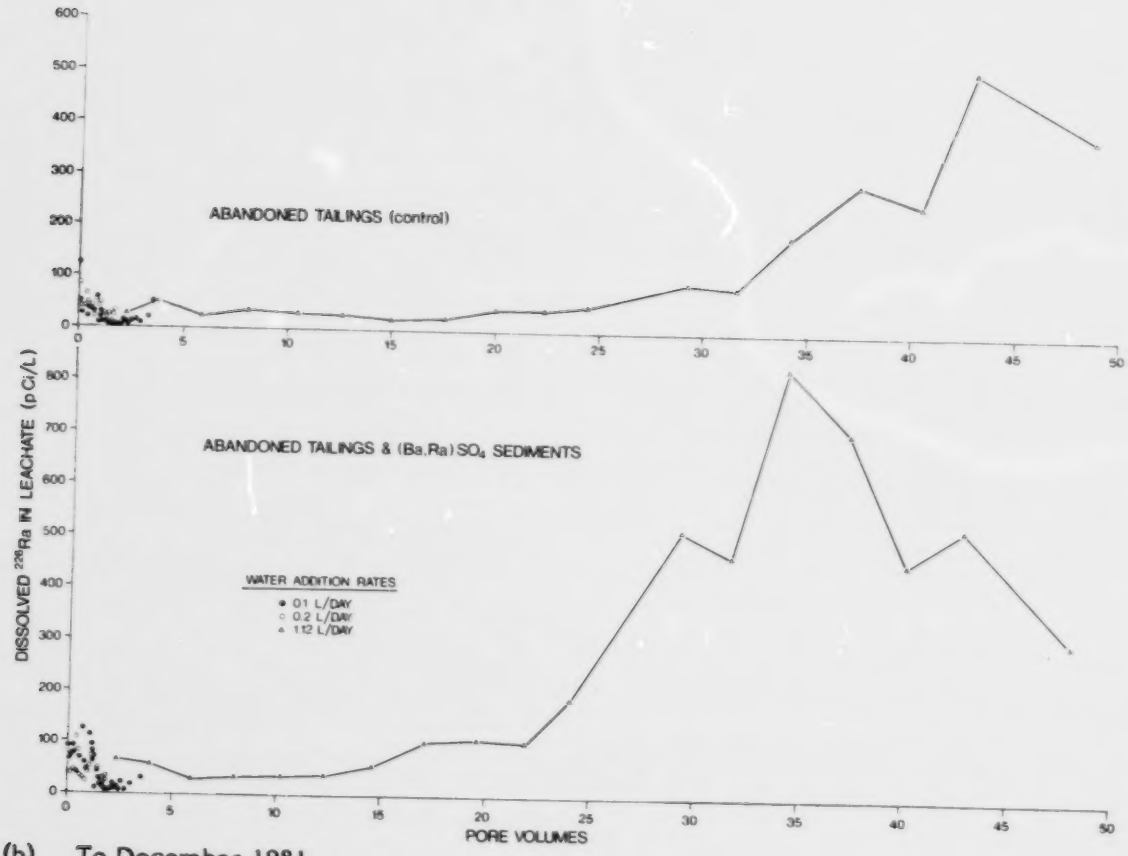

(b) To December 1981

FIGURE 13 EXPERIMENT 1: PORE-VOLUMETRIC VARIATIONS IN DISSOLVED Ra-226

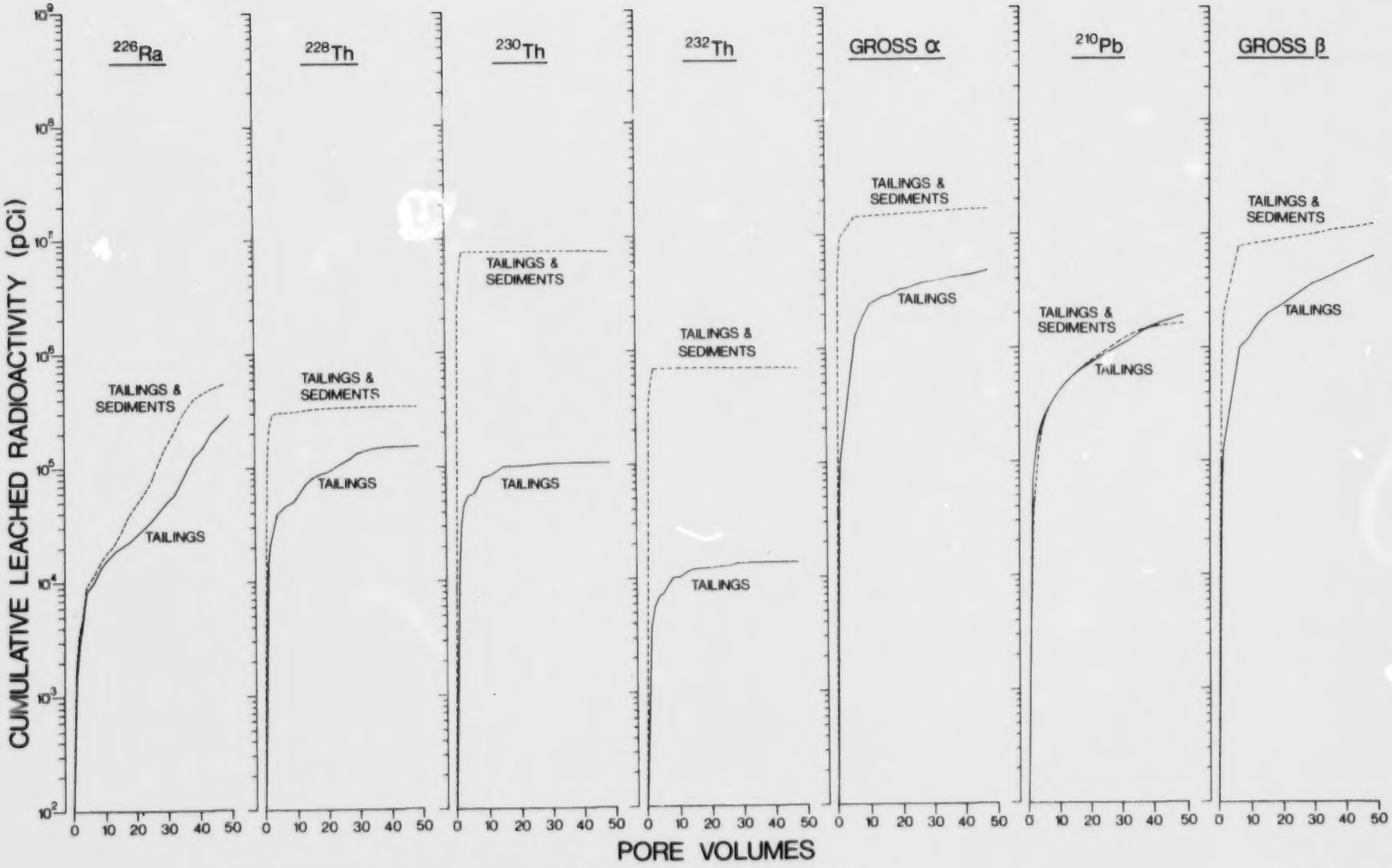

FIGURE 14 EXPERIMENT 1: CUMULATIVE LEACHED RADIOACTIVITY

TABLE 5 EXPERIMENT 1: RESIDUAL CONCENTRATIONS OF RADIOISOTOPES IN LEACHED TAILINGS

Radioisotope	Low-Rate Controls			High-Rate Controls		
	Concentration		% Leached	Concentration		% Leached
	(pCi/g)	(Bq/g)		(pCi/g)	(Bq/g)	
Ra-226	118	4.4	0.02	122	4.5	0.8
Th-230	15	0.56	6	16	0.59	9
Th-232	2.4	0.09	6	3.1	0.11	6
Th-228	4.4	0.16	8	4.3	0.16	30

were released from the tailings-sediment lysimeters than from the controls (Figure 14). Over 99 percent of the total gross alpha and beta was in the dissolved state.

The results of the analyses conducted on the control leachate samples from the last 1.5 years of the study are given in Table A.1 in Appendix A. Iron and sulphate were the major constituents in the leachates. High concentrations of Al, Ca, K, and Mg; smaller concentrations of Cl, Co, Cu, Ni, P, and Ti; and minor quantities of Ba, Cd, Mn, Pb, V, Zn, and Zr were also present.

4.3.2 Lysimeter Solids. The results of the chemical and physical tests and the scanning electron microscope and Mossbauer analyses conducted on the lysimeter solids upon termination of leaching are given in Appendices A and B. The major results of these analyses and of the washing tests with KCl and Na EDTA solutions are summarized in the following points.

1. The host grains (50 to 100 μm) from the leaching pachucas are partially covered with surface precipitates (i.e., particles) 2 to 5 μm and smaller in size. These precipitates have various physical forms including rods, polygons, and dendrites. They cover about 5 to 10 percent of the total particle surface. These precipitates are quite porous and flaky, and therefore have a large surface area. The host grains contain mainly quartz, but they also contain pyrite, alumino-silicates, and other minerals.
2. The host grains leaving the partial and final neutralization tanks are covered with surface precipitates. These precipitates contain large amounts of Ca and S, and also significant quantities of Al, Si, and K. Part of the Si results from its presence in

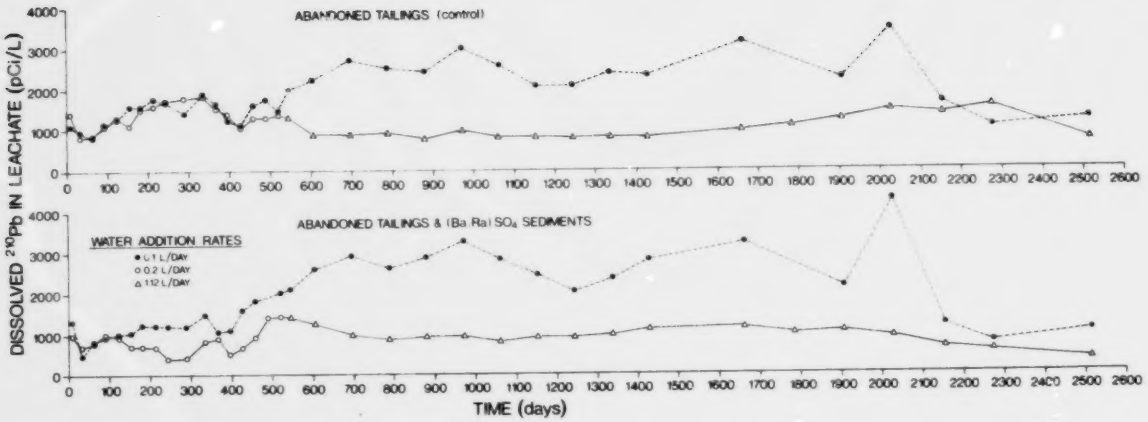

FIGURE 15 EXPERIMENT 1: TEMPORAL VARIATIONS IN DISSOLVED Pb-210

host particles; some of the Al-Si and K are found in distinct plate-shaped particles, which are assumed to be alumino-silicates.

3. The particle size distribution of the solids from control high- and low-rate lysimeters is the same. The mean grain size is about 0.25 mm; 95 percent are between 2 mm and 50 μm. The solids in the lysimeters have lost most of the surface precipitate covering the host grains, particularly from those in the upper sections of the lysimeters. The lower sections have opaque, amorphorus-appearing globules whose content is almost pure silica.
4. Some pyrite remains at all depths of the lysimeters; most of it has been oxidized throughout the top three-quarters of both the low- and high-rate lysimeters. The pyrite occurs as single cubes (of the order of 1 to 2 microns per side), attached in clusters to the host solids, and in lenses visible to the eye. The residual pyrite content in both the high- and low-rate lysimeter solids is approximately the same.
5. The upper 10 cm of one high-rate lysimeter has lost 80 percent of its Ra-226 and almost all of its pyrite. A larger fraction of Ra-226 was leached from the high-rate

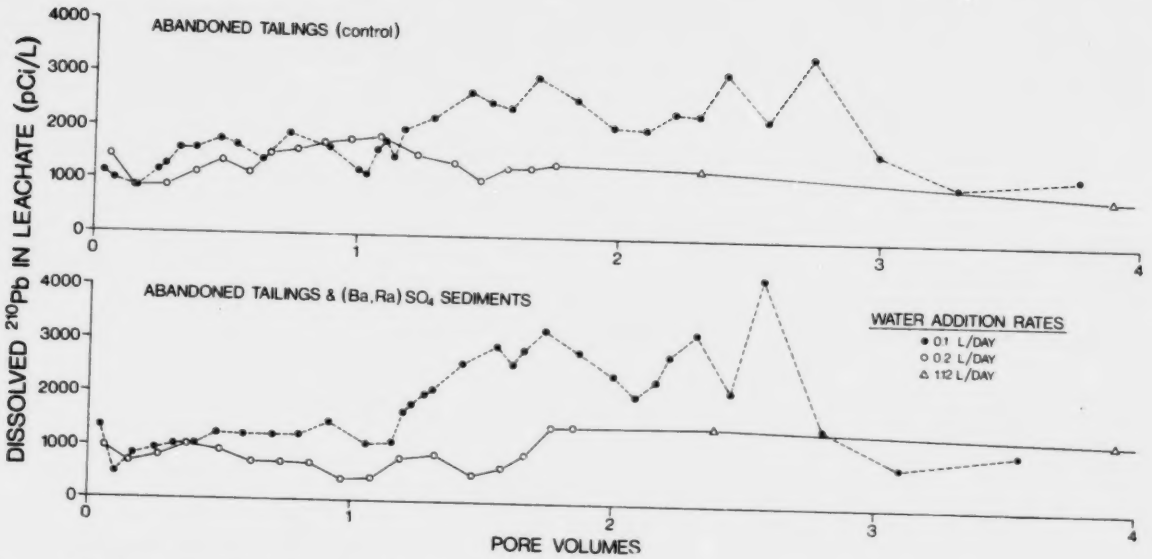

(a) During First Four Pore Volumes

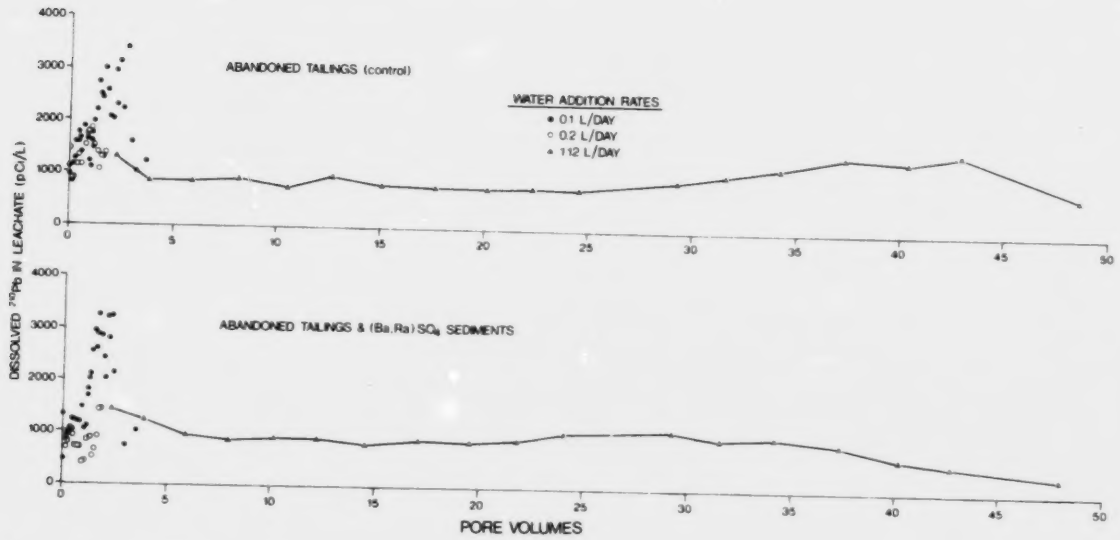

(b) To December 1981

FIGURE 16 EXPERIMENT 1: PORE-VOLUMETRIC VARIATIONS IN DISSOLVED Pb-210

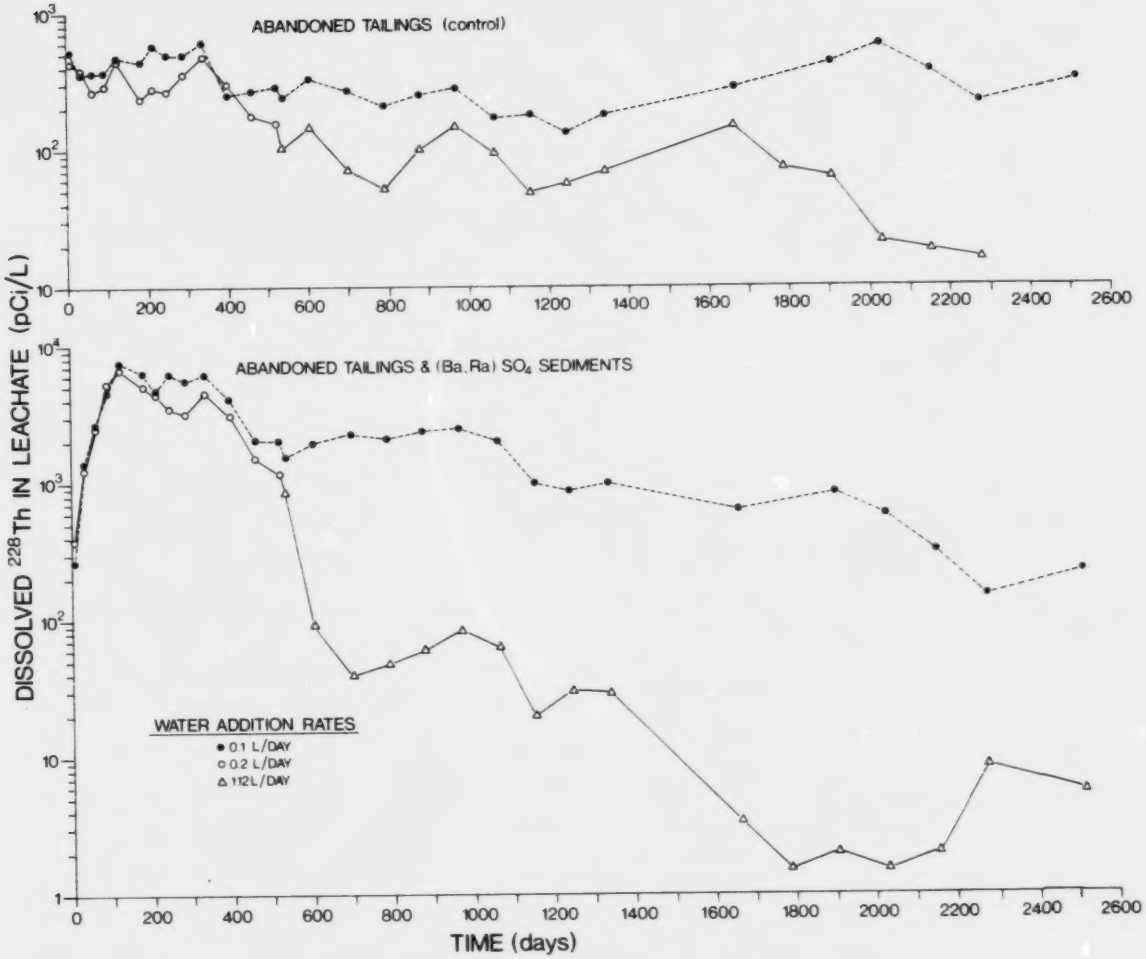

FIGURE 17 EXPERIMENT 1: TEMPORAL VARIATIONS IN DISSOLVED Th-228

lysimeters than from the low-rate lysimeters; but in total, less than 1 percent was lost over the 7 years of leaching. Low levels of Th-230 remain in the solids.

6. No carbonates and some sulphate (as gypsum) were found in the solids in the control lysimeter.
7. Bound water was found in the solids 1 year after cessation of operation.
8. The measured porosity of the lysimeter solids is 0.52; correction for compaction during coring gives a value of 0.58.

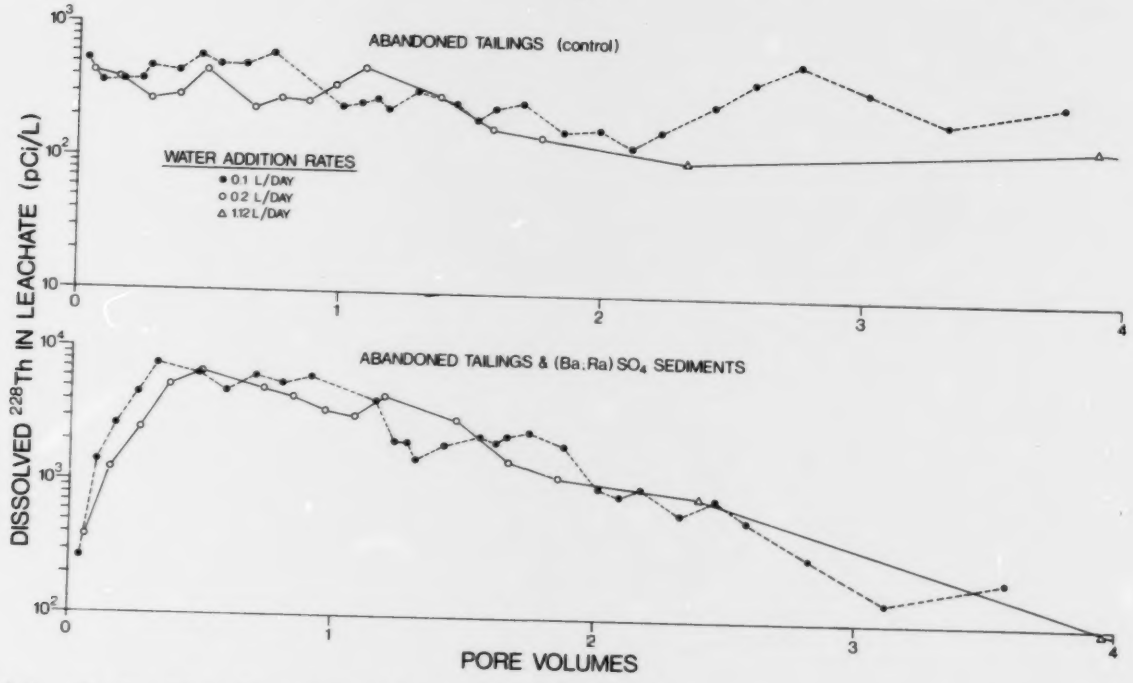

(a) During First Four Pore Volumes

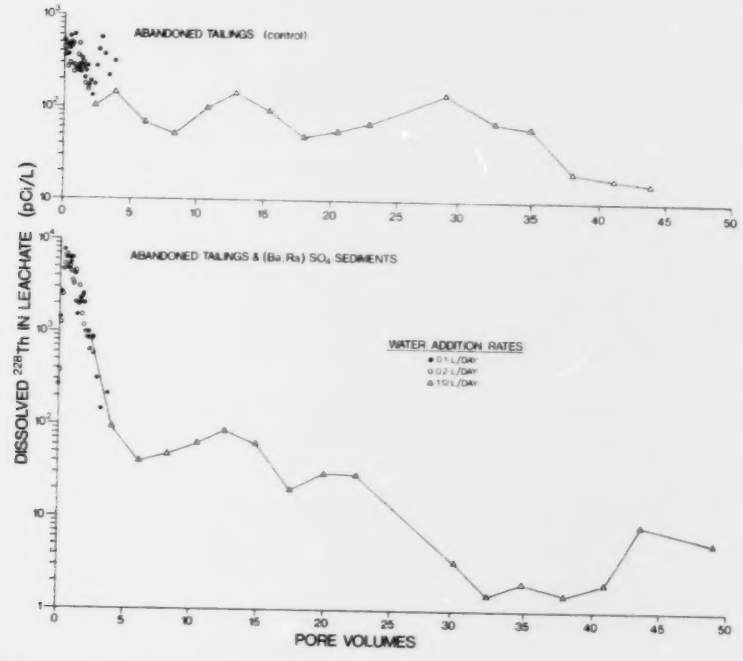

(b) To December 1981

FIGURE 18 EXPERIMENT 1: PORE-VOLUMETRIC VARIATIONS IN DISSOLVED Th-228

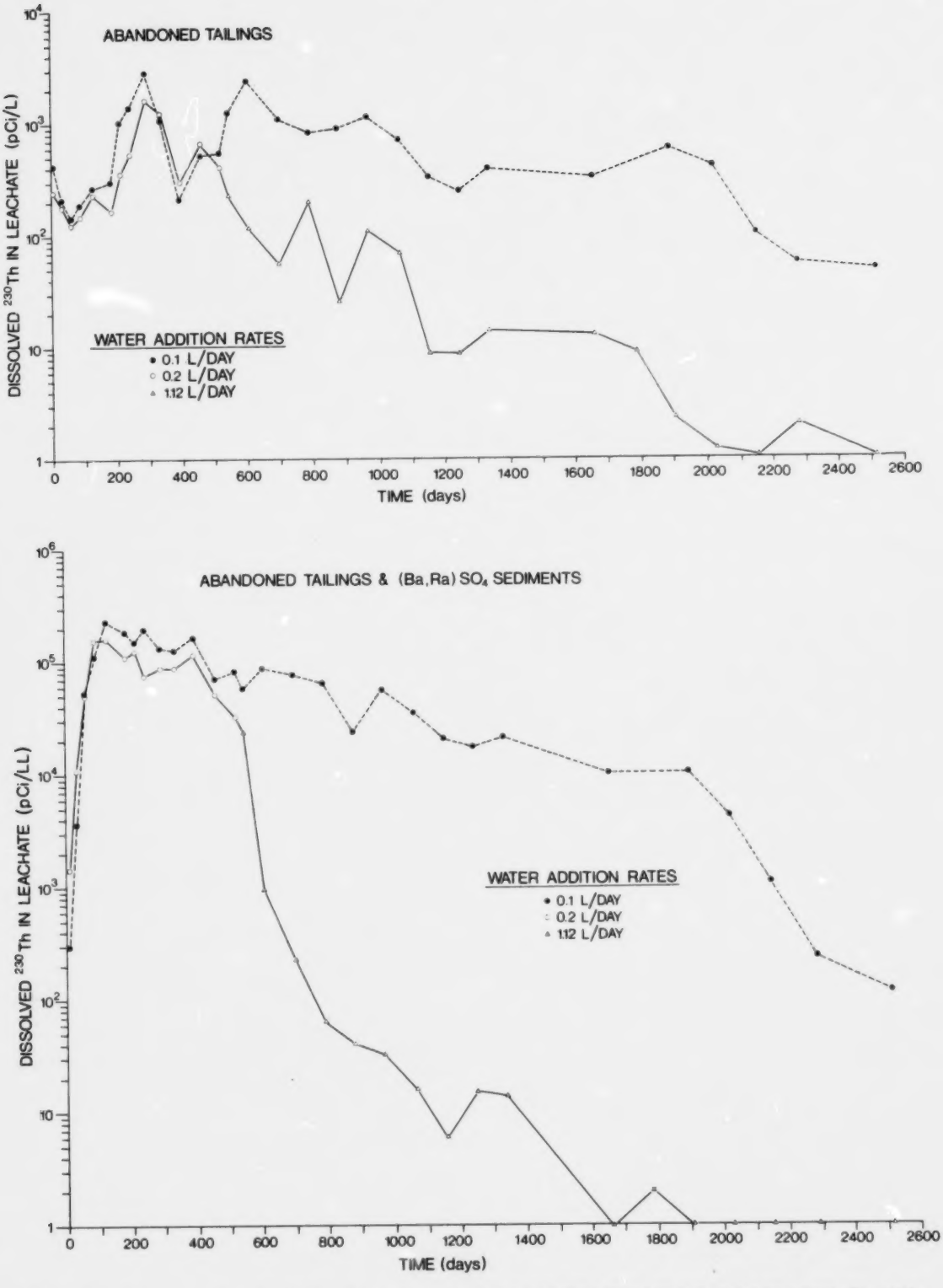

FIGURE 19 EXPERIMENT 1: TEMPORAL VARIATIONS IN DISSOLVED Th-230

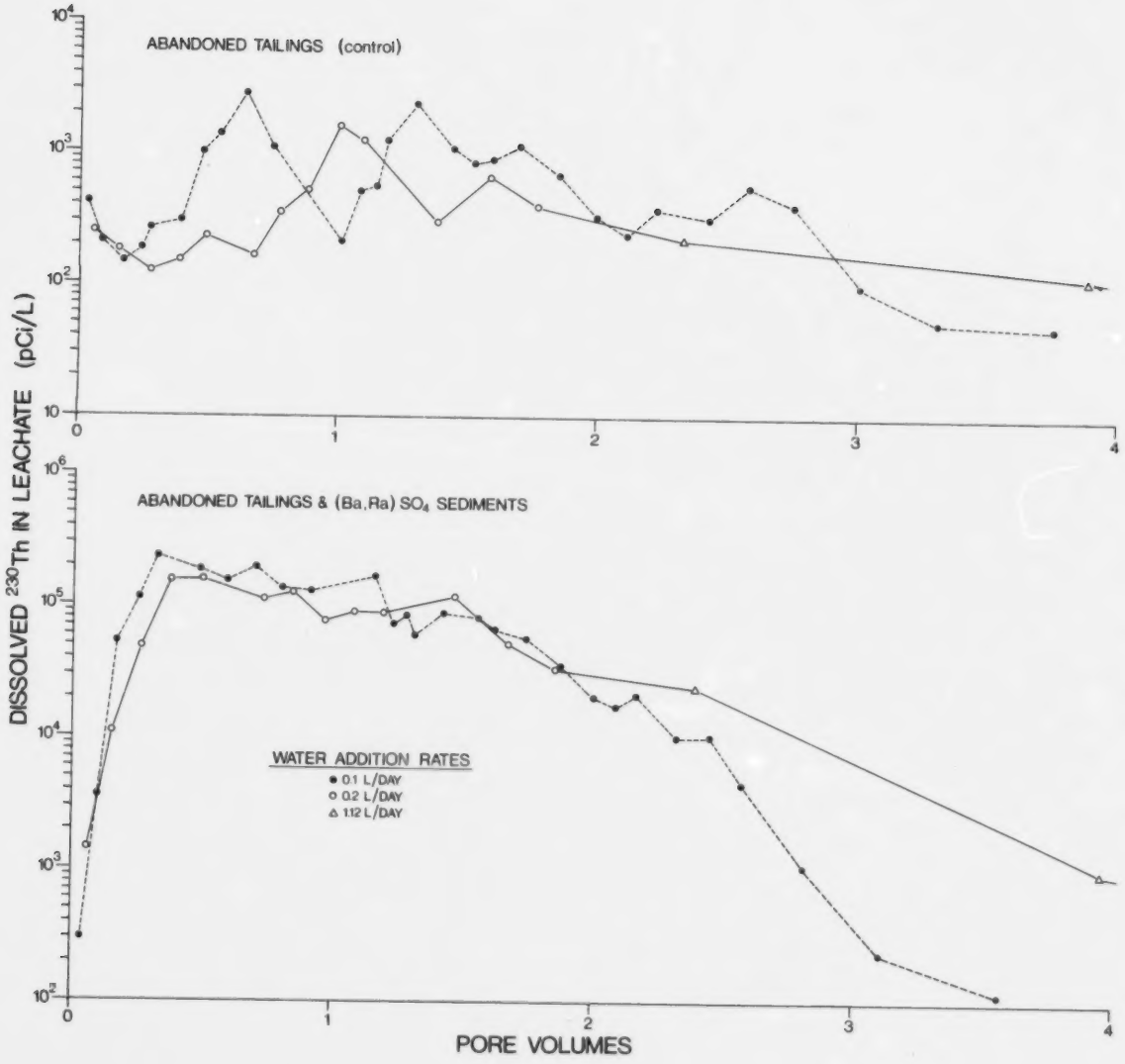

(a) During First Four Pore Volumes

FIGURE 20 EXPERIMENT 1: PORE-VOLUMETRIC VARIATIONS IN DISSOLVED Th-230

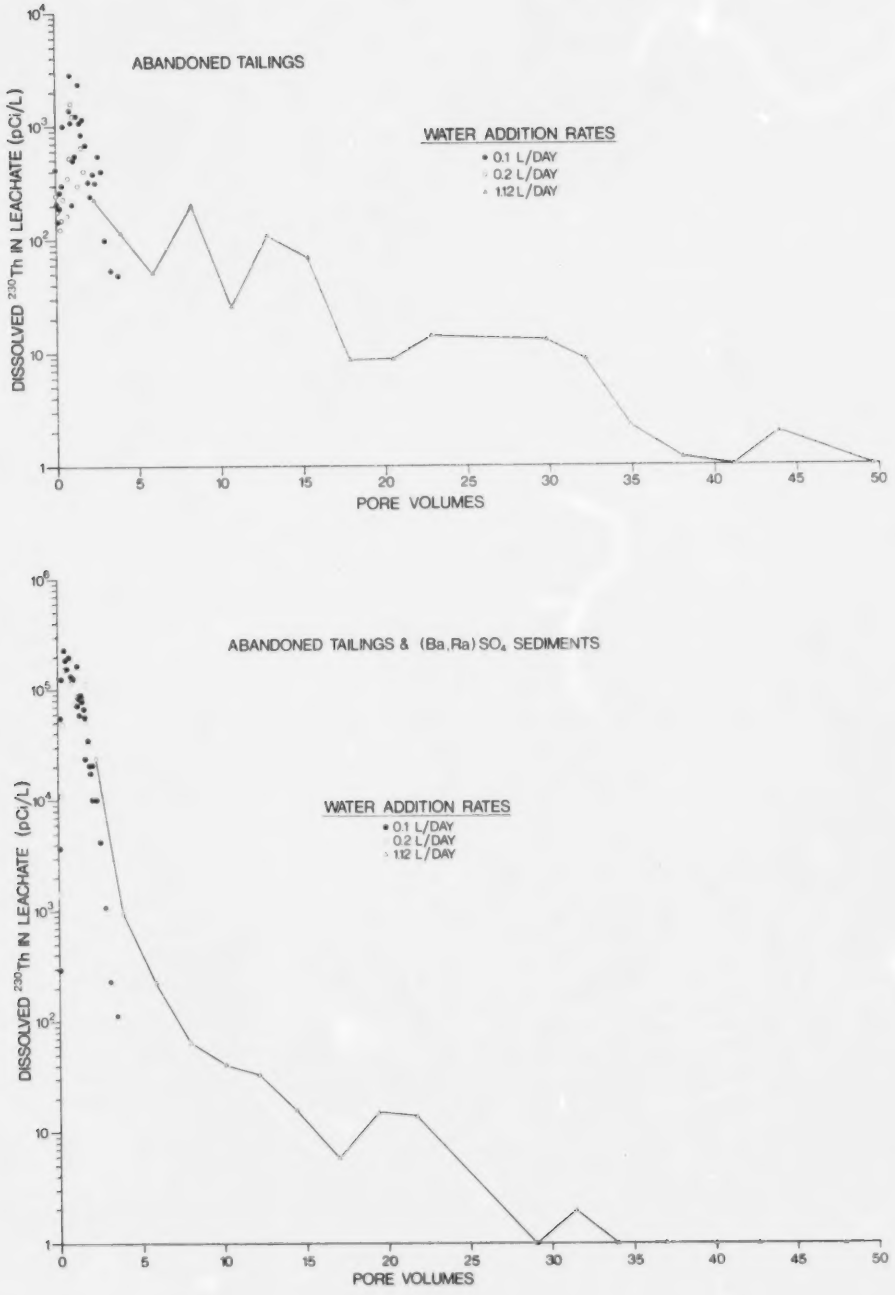

(b) To December 1981

FIGURE 20 EXPERIMENT 1: PORE-VOLUMETRIC VARIATIONS IN DISSOLVED Th-230 (Cont'd)

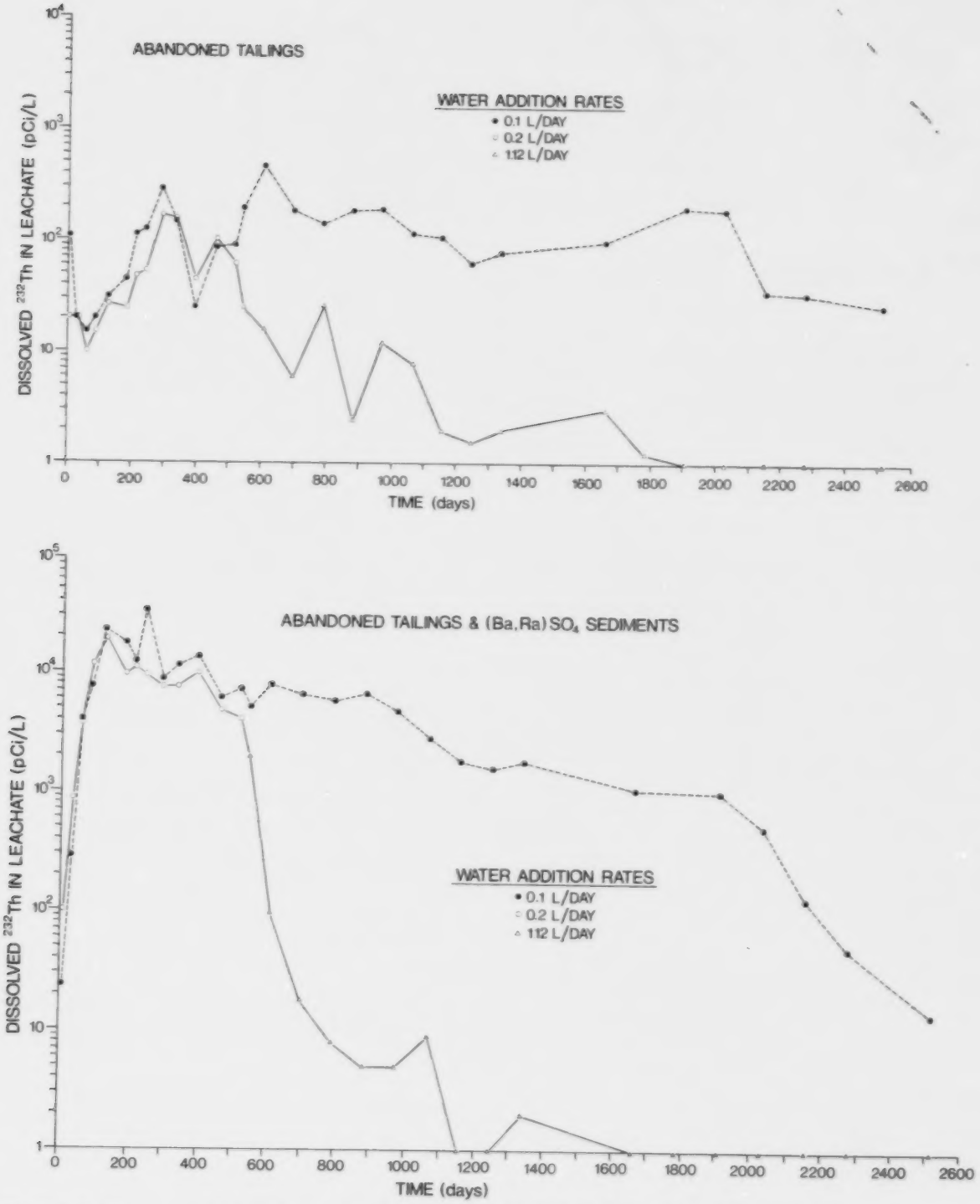

FIGURE 21 EXPERIMENT 1: TEMPORAL VARIATIONS IN DISSOLVED Th-232

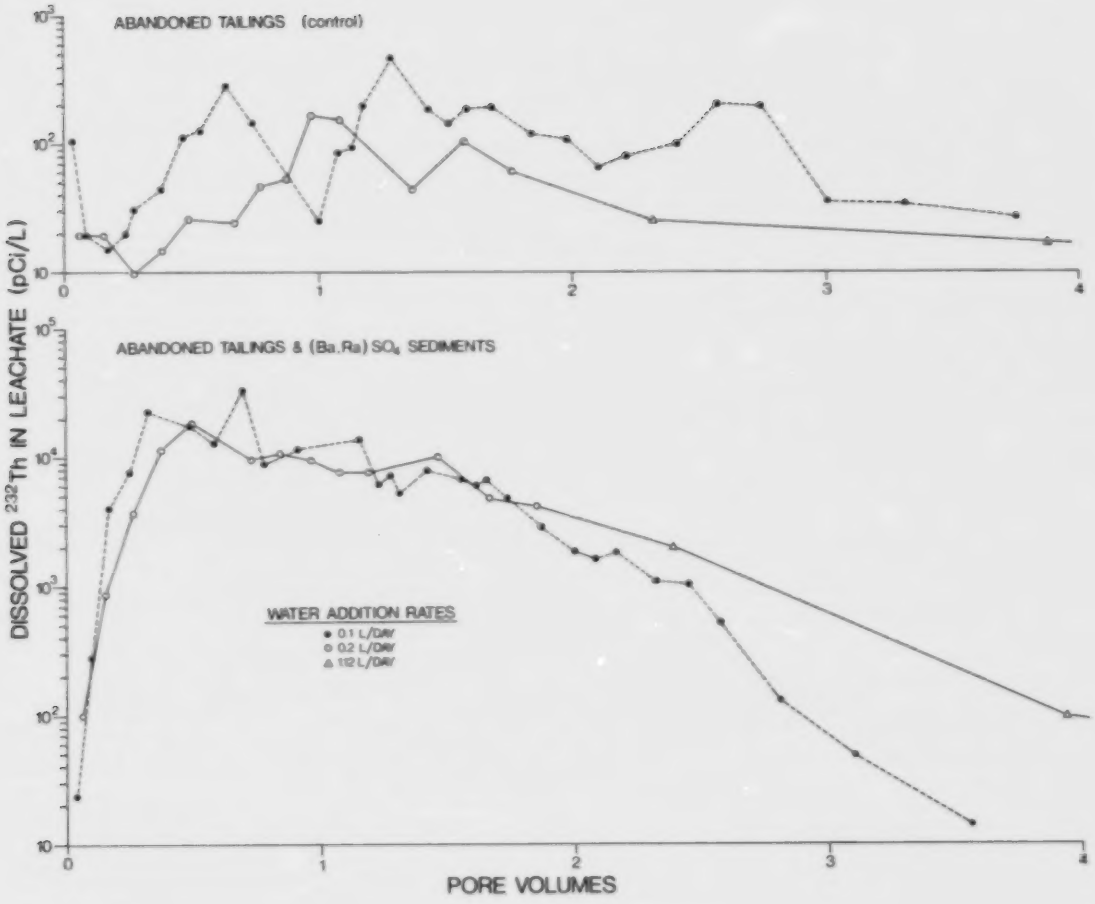

(a) During First Four Pore Volumes

FIGURE 22 EXPERIMENT 1: PORE-VOLUMETRIC VARIATIONS IN DISSOLVED Th-232

9. Plots of Ra-226 concentrations against Pb, Fe, Ba, and Ca concentrations in the KCl and Na EDTA wash waters are given in Figures 27 (a) through (d). The plot of Ra-226 against Fe (Figure 27a) is a scattergram. The plots of Ra-226 against Pb (Figure 27b) and Ra-226 against Ca (Figure 27c) show less, but still quite wide, scatter. If the data for the leaching pachuca solids or the lysimeter are considered separately, there appears to be some relationship between Ra-226 and Pb or

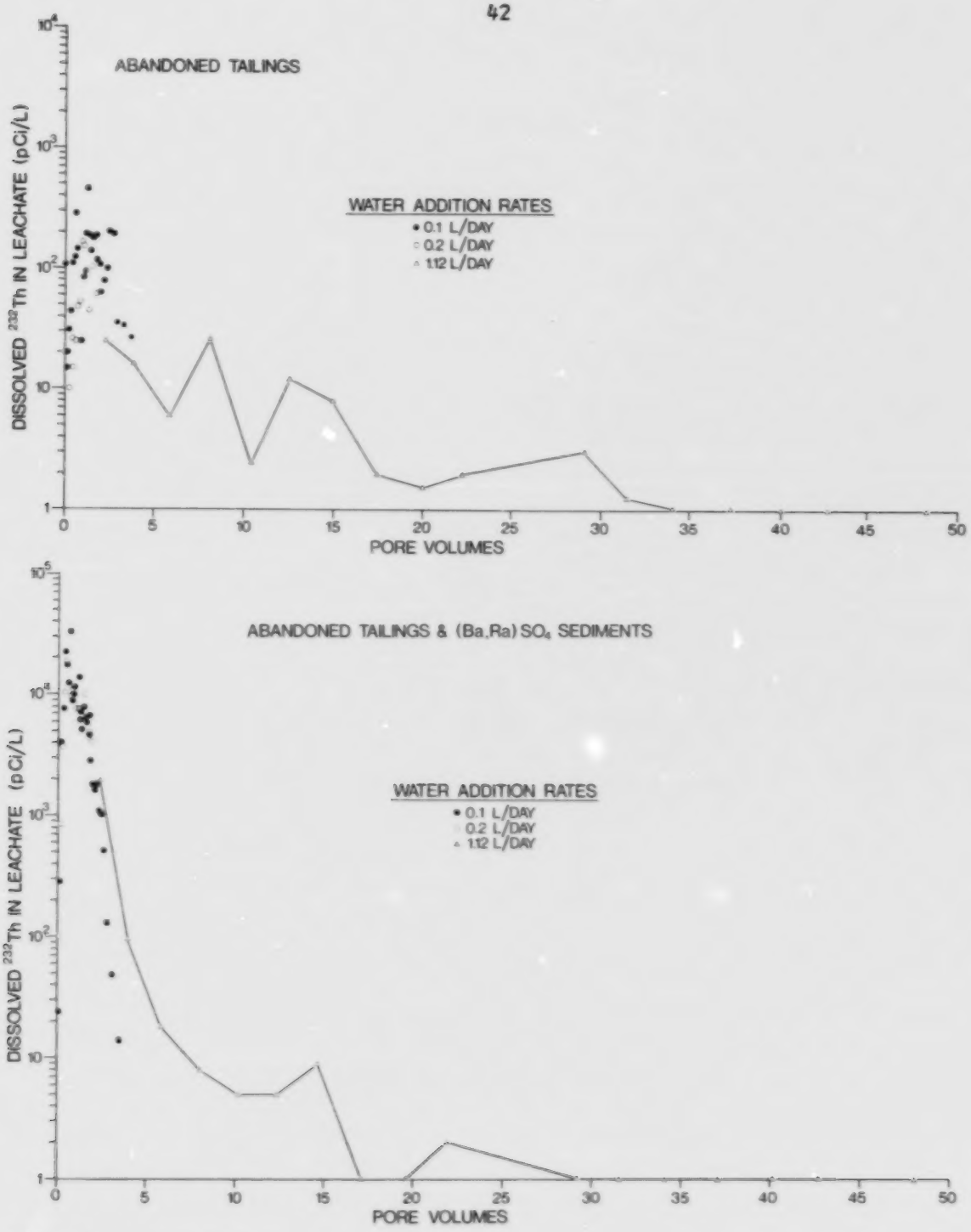

(b) To December 1981

FIGURE 22 EXPERIMENT 1: PORE-VOLUMETRIC VARIATIONS IN DISSOLVED Th-232 (Cont'd)

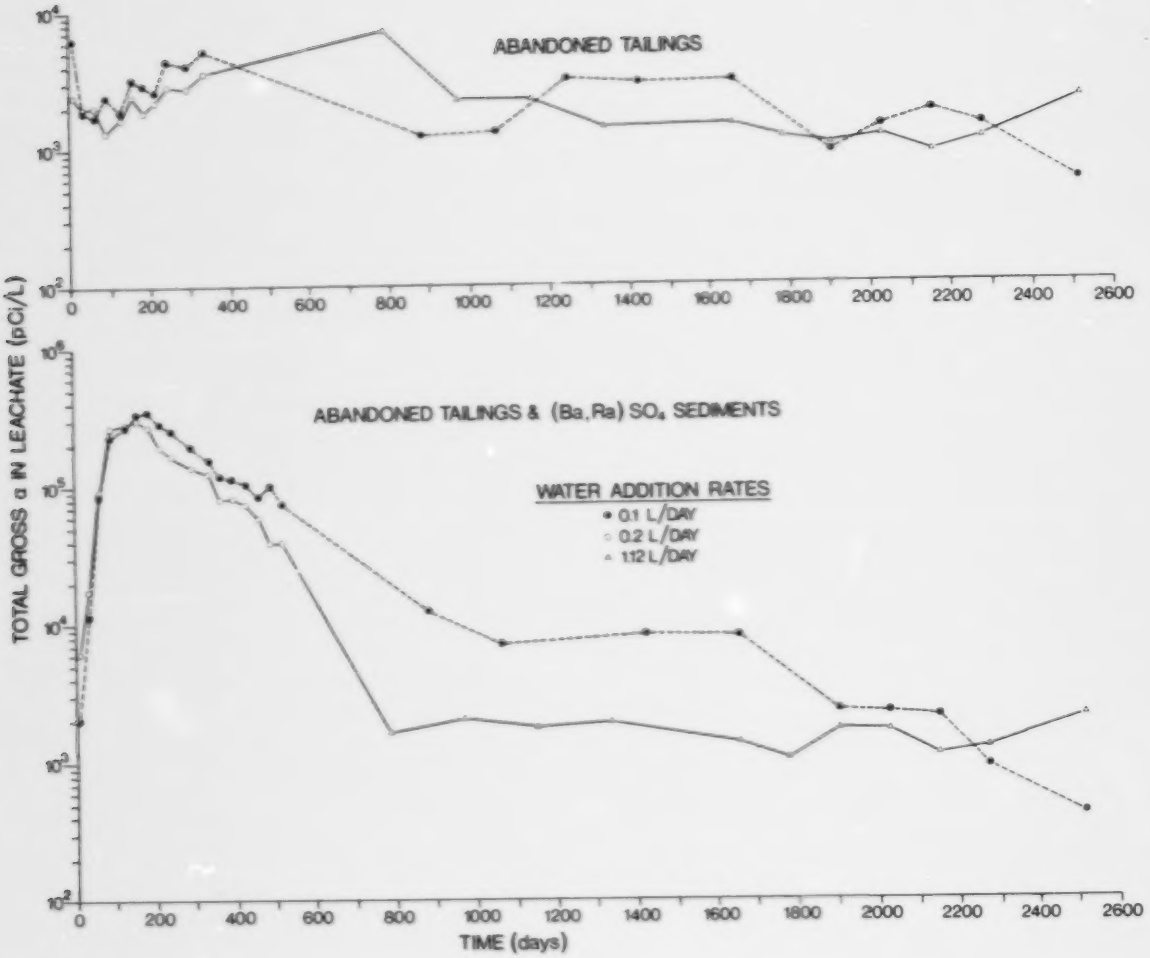

FIGURE 23 EXPERIMENT 1: TEMPORAL VARIATIONS IN TOTAL GROSS α

between Ra-226 and Ca. For Ra-226 against Ba (Figure 27d), the data from both the leaching pachuca solids and lysimeter tailings are similar.

4.4 Discussion

4.4.1 Leachate Characteristics.

Tailings-Limestone Lysimeters. The assessment of similarity between the controls and the tailings-limestone lysimeters is based upon the similarity of the pH and

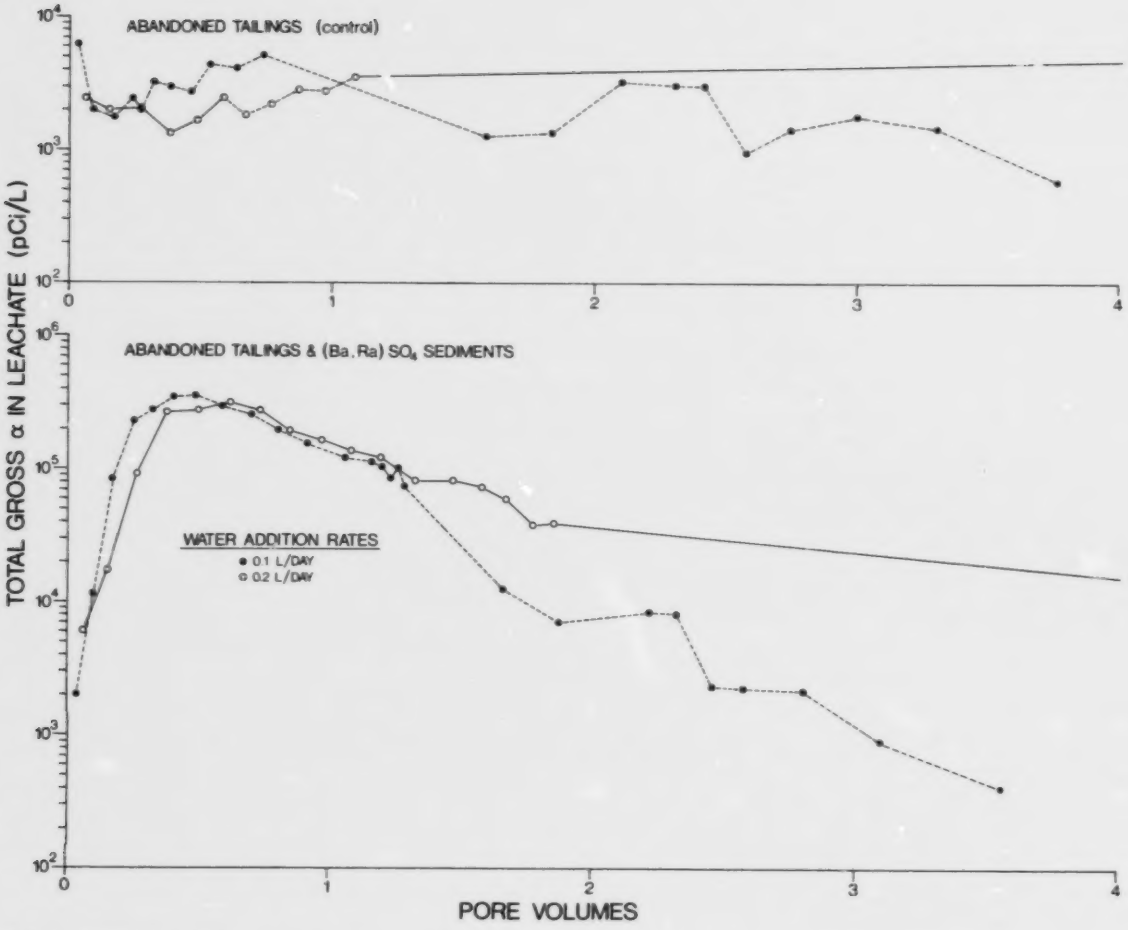

(a) During First Four Pore Volumes

FIGURE 24 EXPERIMENT 1: PORE-VOLUMETRIC VARIATIONS IN TOTAL GROSS α

that of the TDS and radioisotope concentrations. This means that despite the addition of limestone, pyrite oxidation continued unabated, and the acidity of the leachate was only minimally neutralized. This can be accounted for by at least three possible explanations: (i) surface coatings formed on the crushed limestone prevented dissolution, (ii) limestone dissolution kinetics are quite slow, relative to pyrite oxidation kinetics, and (iii) analytical chemistry cannot detect significant differences due to limestone dissolution when

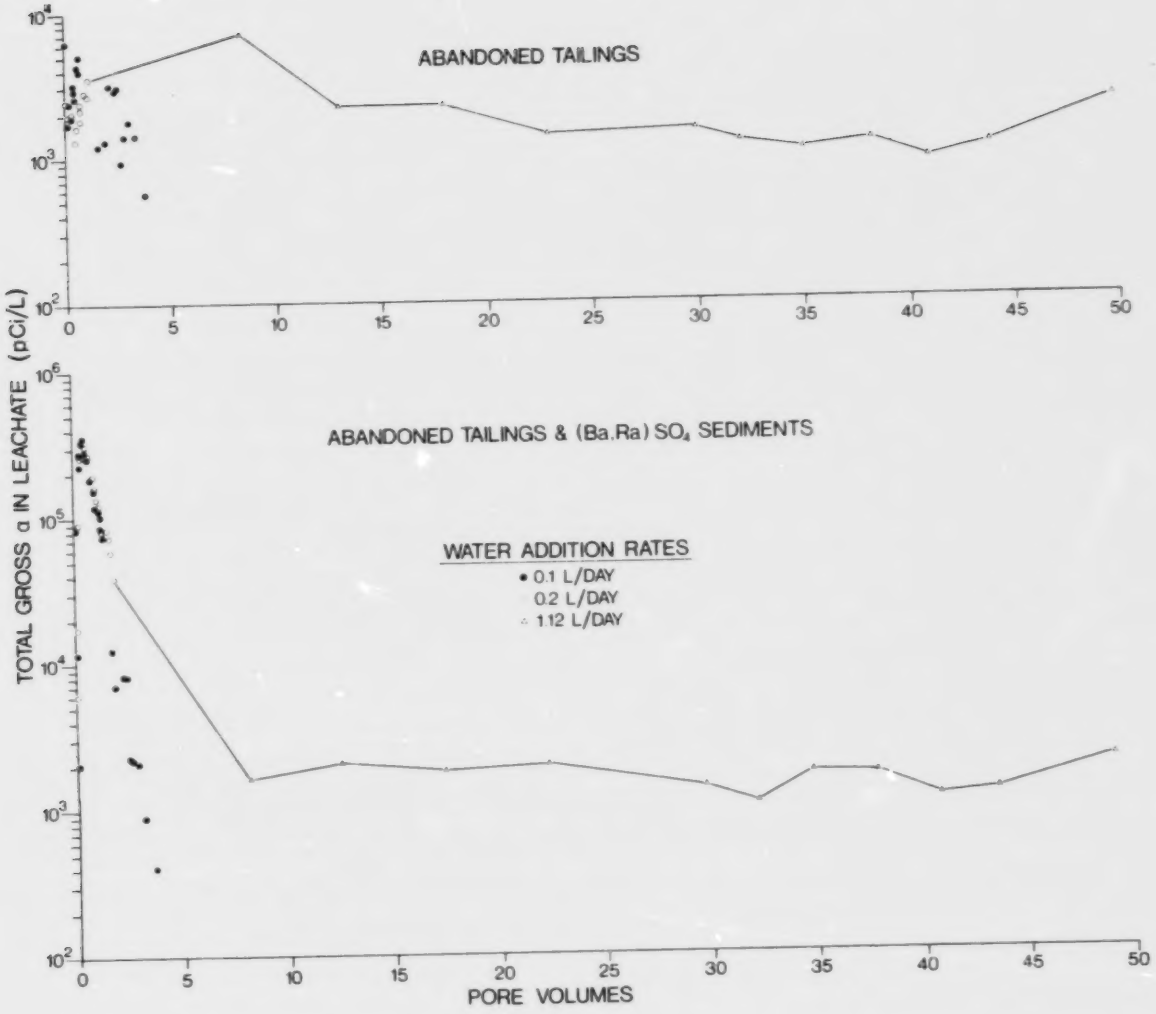

(b) To December 1981

FIGURE 24 EXPERIMENT 1: PORE-VOLUMETRIC VARIATIONS IN TOTAL GROSS α (Cont'd)

leachate pH is low and TDS is high. While the formation of surface coatings is possible, no calcium carbonate was detected in the control lysimeters at the conclusion of the experiment (see Appendix A.2.1). Thus, either surface coatings formed and then redissolved, allowing leaching of limestone, or the limestone continually dissolved. The

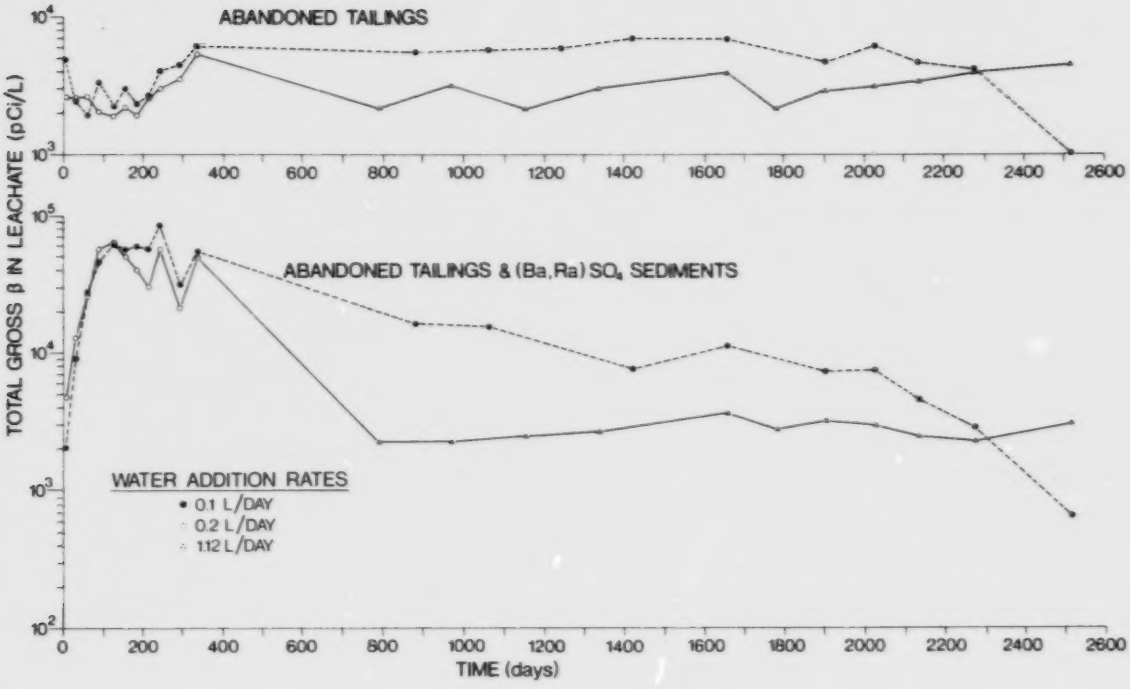

FIGURE 25 EXPERIMENT 1: TEMPORAL VARIATIONS IN TOTAL GROSS β

second explanation, slow dissolution kinetics for limestone under acidic conditions, is improbable. The third explanation is the most likely. As discussed subsequently, the TDS of control leachates during the last 2 years of the experiment are completely defined by dissolved iron sulphate. Therefore, dissolution of the limestone and its masking by the iron sulphate in the leachate is the most probable explanation for the similarities in leachate characteristics.

Leachate Production Rates. The 30- to 35-percent difference between the applied water rates and the leachate production rates in Phase 1 can be attributed to evaporation. The tops of the lysimeters were open to the atmosphere, and the lysimeter contents were not saturated with water. Water loss occurred either by evaporation of water retained in the pores being brought to the surface by capillary action, or by evaporation directly from biofilm waters to air contained in the void spaces. The 15-percent loss in applied water in the high-rate lysimeters during Phase 2 was due partly to evaporation and partly to constriction of the peristaltic pump tubing, preventing

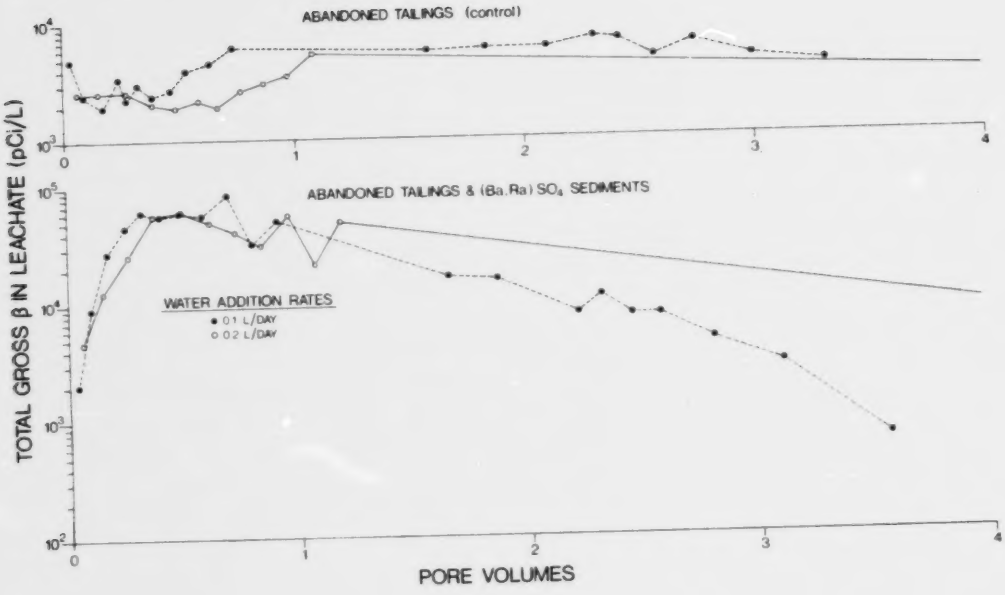

(a) During First Four Pore Volumes

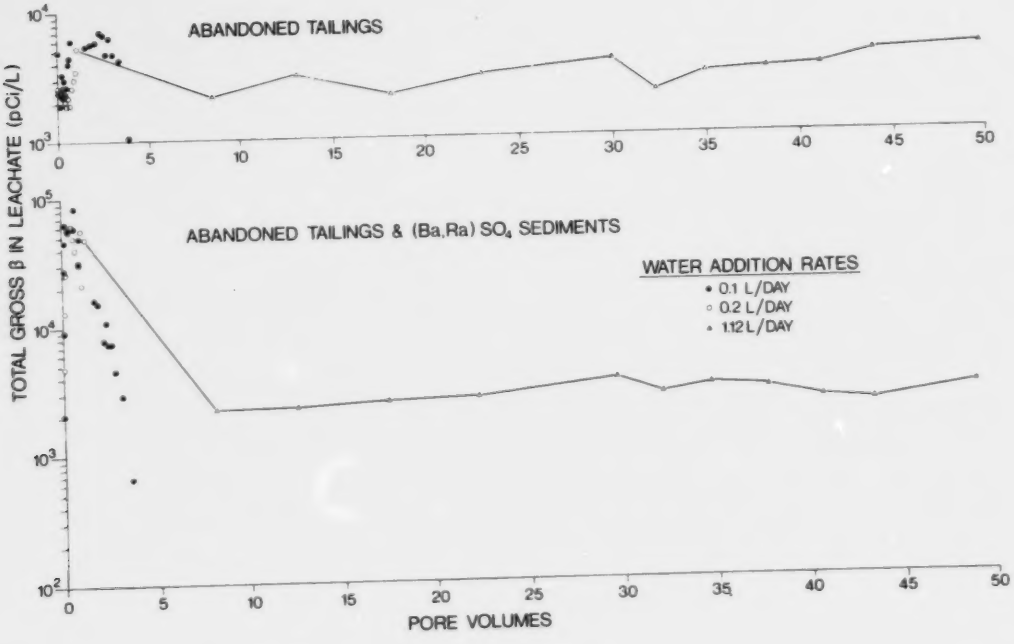

(b) To December 1981

FIGURE 26 EXPERIMENT 1: PORE-VOLUMETRIC VARIATIONS IN TOTAL GROSS β

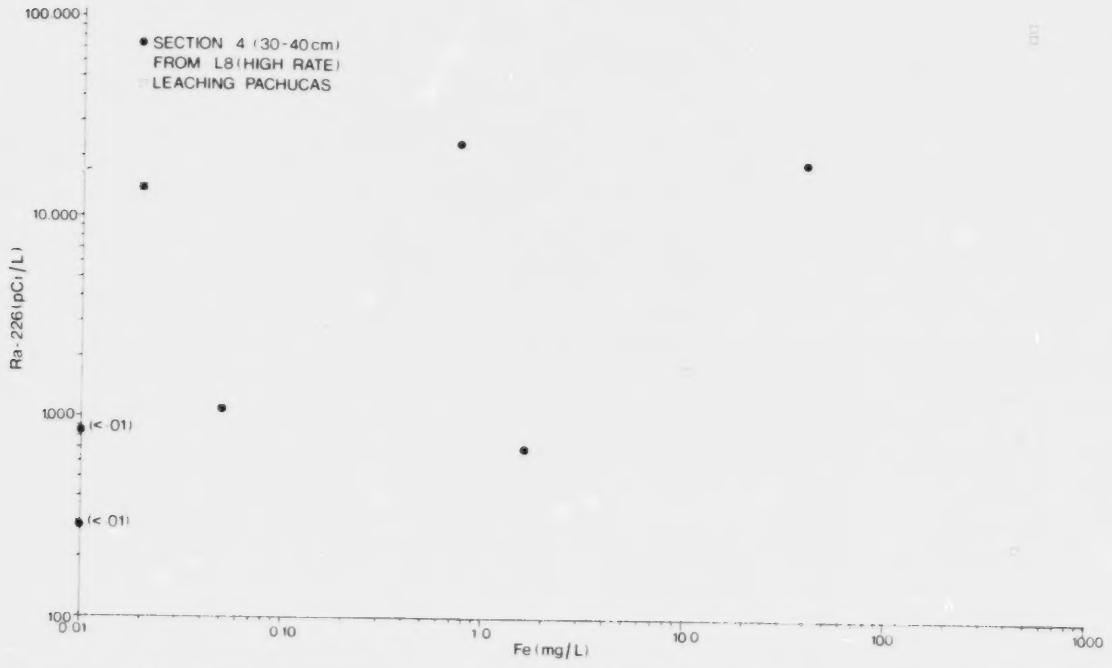

FIGURE 27(a) EXPERIMENT 1: SCATTERGRAPH FROM WASHING EXPERIMENT FOR Ra-226 vs. IRON

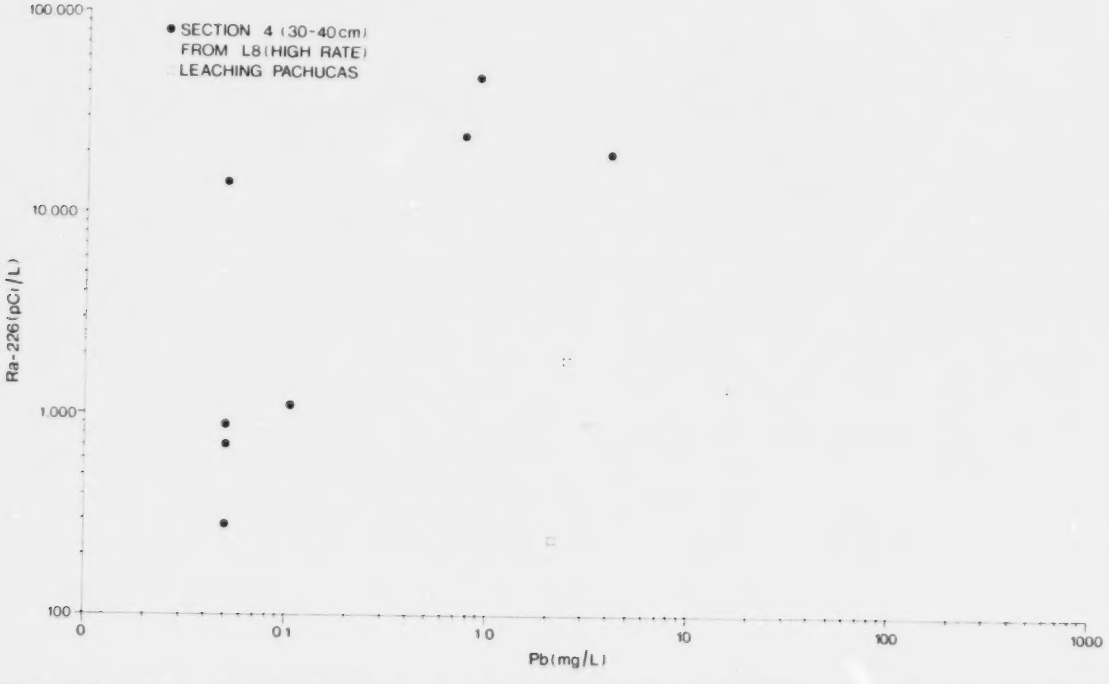

FIGURE 27(b) EXPERIMENT 1: SCATTERGRAPH FROM WASHING EXPERIMENT FOR Ra-226 vs. LEAD

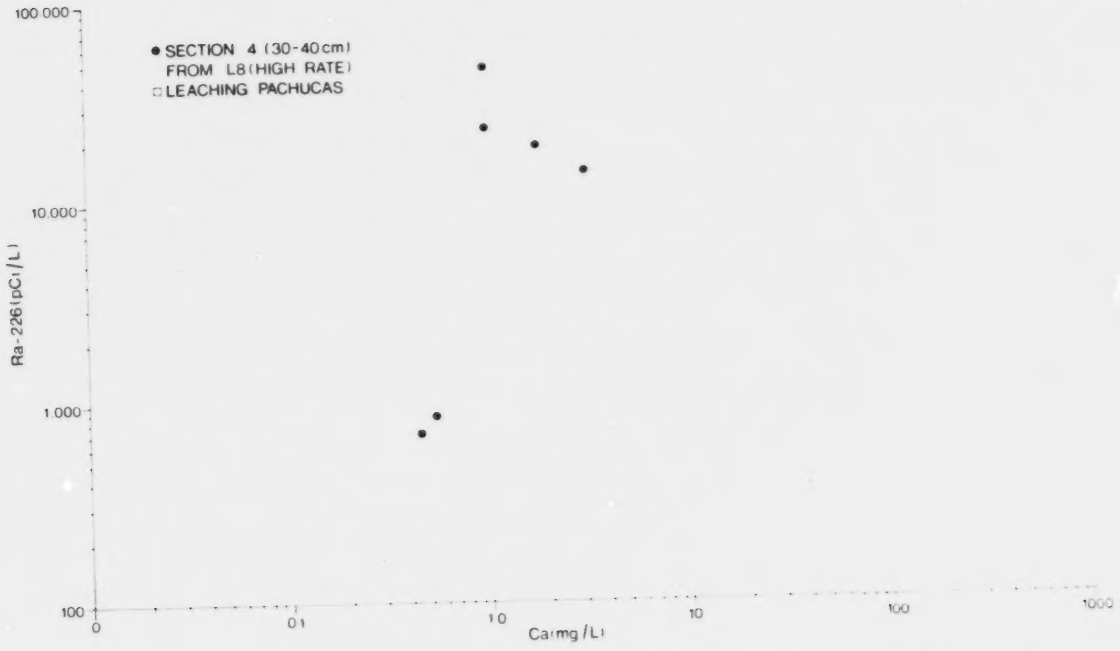

FIGURE 27(c) EXPERIMENT 1: SCATTERGRAPH FROM WASHING EXPERIMENT FOR Ra-226 vs. CALCIUM

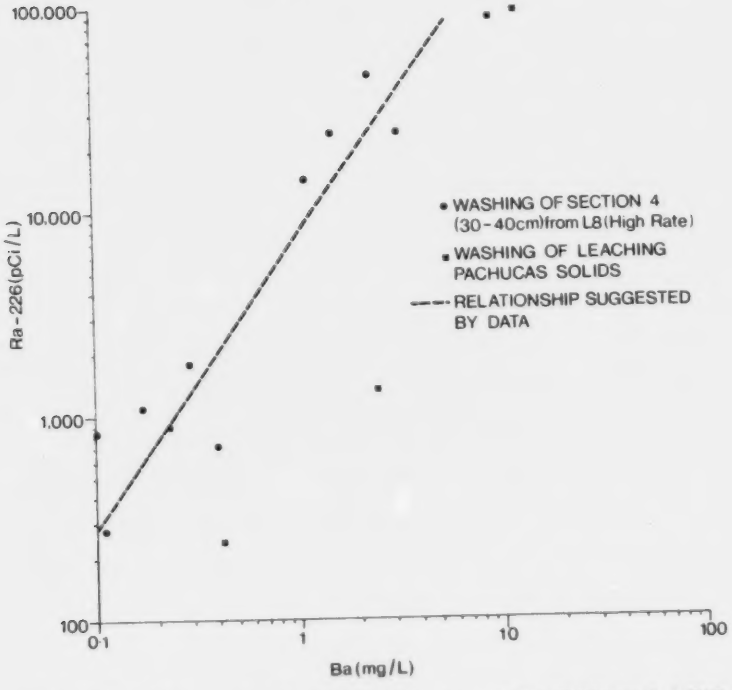

FIGURE 27(d) EXPERIMENT 1: SCATTERGRAPH FROM WASHING EXPERIMENT FOR Ra-226 vs. BARIUM

delivery of the rated pump flow. The reason for the decrease in the average leachate production rate in the low-rate lysimeters from 0.07 L/day during Phase 1 to 0.05 L/day during Phase 2 is not known.

Leachate volumes collected at the end of each sampling period from the controls and tailings-sediment lysimeters are significantly different at the low and middle rates of water application, but not at the high rate (Table 4). However, the total leachate volumes produced during the study at each flow rate were approximately the same for both treatment systems. This indicates that volumetric differences at the end of each sampling period were due to temporal lags in leachate release from the low- and middle-rate lysimeters.

pH - Conductivity - TDS. When the tailings were collected in the field, they contained acidic biofilm water. Subsequent drying of the tailings in the laboratory resulted in storage of the acid in mineral form. Drying may have killed some, but not all, of the pyrite-oxidizing bacteria. Because of an initial rapid decrease in pH, (Figure 7(a)), it is assumed that the mineral acid was redissolved and released immediately at the start of the leaching tests. After this initial decrease, the low pH and the unsaturated nature of the tailings allowed the establishment and maintenance of aerobic conditions in the lysimeters. This not only promotes active growth and recolonization of the pyrite-oxidizing bacteria, but also provides an ideal environment for microbial oxidation of the pyrite in the tailings, which caused the pH of the leachate to decrease even further. After this initial period, an approximate equilibrium condition was reached. In the low-rate lysimeters, a constant production rate of iron sulphate occurred giving a constant pH.

During Phase 2, leachate pH remained below 1.5 in the low-rate control lysimeters but increased in the high-rate control lysimeters. This increase may have been due to the increased rate of water application, which may have inhibited the rate of microbial pyrite oxidation because of the decreased flux of oxygen into the tailings. Inhibition would also occur if physical perturbation significantly influenced the bacteria, if Fe concentrations in biofilm waters are too low, or if the pH is too high. Physical perturbation is unlikely and the pH appeared to be in the optimum range for pyrite-oxidizing bacteria. Because the mass flux of TDS (i.e., iron sulphate) in the leachates and the quantity of pyrite remaining in the control lysimeters at the end of the study was the same in the low- and high-rate controls (Table A.12),

(a) the rate of pyrite oxidation remains unchanged in the high-rate lysimeter;
(b) the decreased flux of oxygen does not measurably slow the rate of oxidation; and
(c) the pyrite oxidation rate is the same in the low- and high-rate lysimeters.

Hence, the increase in pH and the reduced TDS concentrations in the high-rate leachates can be assumed to be mainly due to dilution. The order of magnitude by which conductivity differs (Figure 11b) can be explained on the basis of the order of magnitude of change in flushing rate, assuming that the pyrite oxidation rate remained constant.

Patterns in leachate conductivity were reflected in changes in pH; e.g., an increase in conductivity was accompanied with a decrease in pH. Whereas statistical analyses indicate that coincident conductivity measurements were significantly different in the control and tailings-sediment leachates (Table 4), the same general trends were observed in both types of leachates. Thus it appears that the addition of (Ba, Ra)SO_4 sediments to tailings had little effect on leachate conductivity.

Radium-226. Radium-226 levels in low-rate leachates generally decreased during the study, whereas those in high-rate leachates remained relatively constant for the first 1 000 days or so (12 to 17 pore volumes), and then increased to a peak at about 2 000 days (34 to 43 pore volumes). The results of the chemical tests conducted on the lysimeter cores (Appendix A) suggest that all Ra-226 observed in the peak was derived from the top 10 cm of the contents in the lysimeters, and that most of the Ra-226 lost from this area was resorbed (adsorbed, coprecipitated) on lower solids. Release of this radium was retarded until a geochemical mechanism (assumed to be $BaSO_4(s)$ and discussed below), controlling its release from the lysimeter solids, had been removed. Blair et al. (1980) found similar retardation of Ra-226 release in the in-situ abandoned Nordic tailings. They estimated that the Ra-226 plume from the tailings only advances at a rate of about 0.05 percent of the average groundwater velocity.

Lead-210. The addition of (Ba,Ra)SO_4 sediments to tailings had little effect on Pb-210 levels in leachates during the study. After 50 pore volumes, the high-rate control and tailings-sediment lysimeters had released about the same amounts of Pb-210, even though the tailings-sediment lysimeters initially contained more Pb-210.

Thorium. The addition of (Ba,Ra)SO_4 sediments to tailings had a significant effect on the amounts of thorium released from the lysimeters. The patterns of thorium release can be explained by considering variations in leachate pH during the study (Figures 6 and 7). During Phase 1, the rapid decrease in leachate pH during the first 0.2 pore volumes was followed by a large increase in thorium levels during the first 0.4 to 0.9 pore volumes, as thorium which had been adsorbed and precipitated on the tailings and sediments during the drying process was desorbed. Thorium levels generally remained the

same for the balance of Phase 1, during which time leachate pH decreased slightly. This suggests that the rate of proton attack upon thorium-containing residual minerals was constant after all thorium, precipitated during the drying process, had been flushed from the lysimeters. During Phase 2, the pH of the low-rate leachates decreased even more, to less than 1; and thorium continued to be solubilized, although at a slower rate, so that, after 2 200 days, levels had returned to approximately their initial values. In contrast, the pH of the high-rate leachates slowly increased to between 2.5 and 3.0 during this same period. This increase in pH resulted in less proton attack upon residual minerals, allowing thorium levels to decrease until they were close to 1 pCi/L (0.04 Bq/L) in most high-rate leachates. Thus, because there is a correlation between thorium concentration and pH, it is concluded that thorium patterns resulted from the capability of protons to attack thorium-containing, residual minerals.

Gross alpha and gross beta. The addition of $(Ba,Ra)SO_4$ sediments to tailings resulted in an almost four-fold increase in gross alpha release and a doubling of gross beta release in the high-rate leachates over 50 pore volumes. Uranium-238 is the first member of a long series of radioactive isotopes which decay to stable Pb-206 (Figure 28). The series contains eight alpha emitters and six beta emitters. The alpha-emitting radionuclides that were measured (Ra-226, Th-232, Th-230, and Th-228) only accounted for about 11 percent of the gross alpha measured in the control leachates and 54 percent in the tailings-sediment leachates. The beta-emitting Pb-210 that was measured accounted for only 31 percent of the gross beta in the control leachates and for 14 percent in the tailings-sediment leachates. These results indicate that effluent guidelines or regulations based solely on only a few radionuclides, such as those measured in this study, will only monitor a small fraction of the total radioactivity released.

Cations and anions. It appears that major biogeochemical changes occurred during the last 1.5 years of the study, because TDS concentrations declined by an order of magnitude and pH increased by an order of magnitude, whereas leachate chemistry was fairly constant during the previous 2 to 3 years of the study. An in-depth analysis and technical discussion of the chemical constituents measured in the control leachate samples from the last 1.5 years of the study are given in Appendix A. The degree of charge balance attained in the measurements and a comparison of measured and calculated TDS concentrations are presented in Appendix A.1.1. The probable speciation of most cations and anions is given in Appendix A.1.2. The estimates were made by selecting 10 of the leachate samples and using equilibrium chemistry constants to

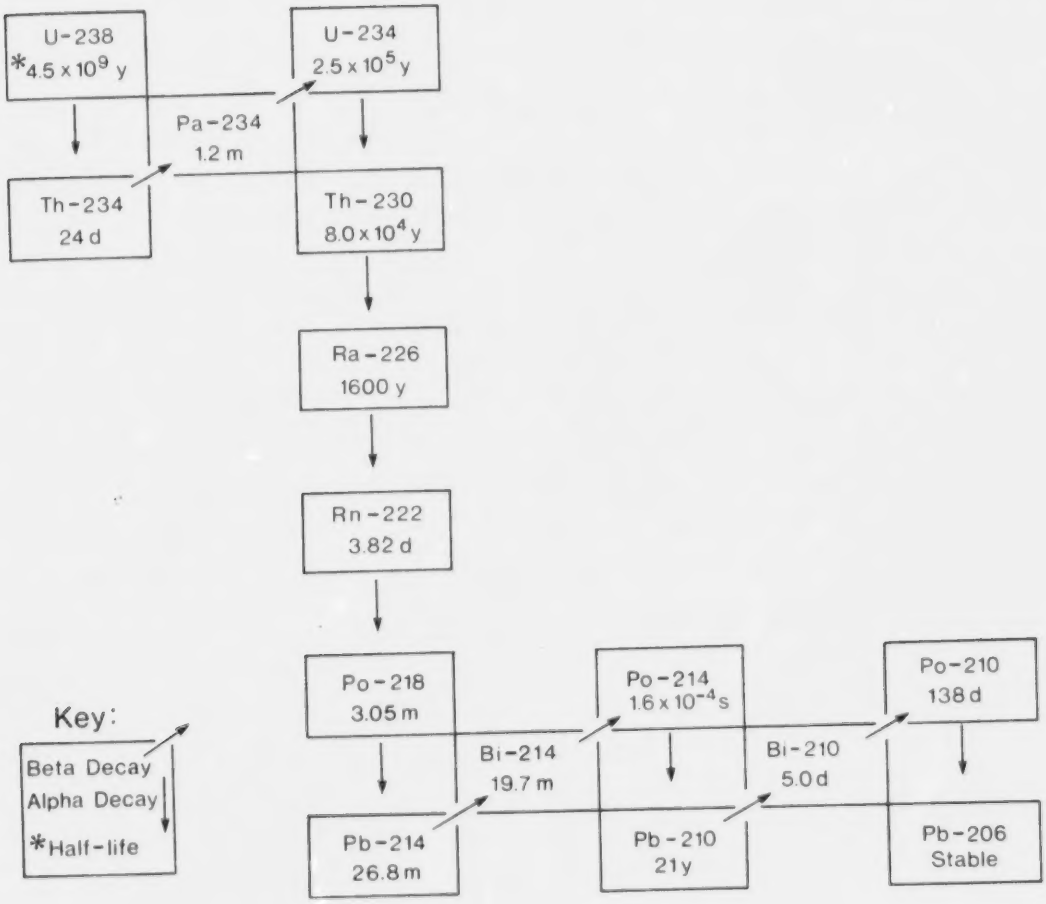

FIGURE 28 PRINCIPAL DECAY SCHEME OF THE URANIUM SERIES

calculate speciation. For example, for iron and sulphate, the calculations provide estimates of the concentrations of H^+, HSO_4^-, SO_4^{2-}, Fe^{3+}, $FeSO_4^+$, and $Fe(SO_4)_2^-$.

The possible formation of various solids such as $BaSO_{4(s)}$, $CaSO_{4(s)}$, amorphous $SiO_{2(s)}$ and secondary alumino-silicates are also examined in Appendix A.1.2 using both the speciation calculations and ratios of various metals (e.g., K/Al, F/Al, Ca/Al, Mg/Al, Si/Al and K/Mg). Assuming that the metal used as the normalizing quantity (the denominator) is conservative, deviation of the ratio in a leachate from that in the lysimeter solids infers that the metal in the numerator is being dissolved but partially retained in the solids. Bejurrum diagrams, which show changes in chemical speciation

with changing pH, are also presented in Appendix A.1.2 for "model water" samples from a low-rate and high-rate lysimeter. The terminology "model water" is used instead of leachate water to emphasize that the specification of all chemical constituents of the leachate water is incomplete, the thermodynamic data which describe the complexation and precipitation-dissolution reactions may have errors associated with them, and the number of complexes known to form, given present day knowledge, may actually be incomplete. In Appendix A.1.3, the biochemical characteristics of the leachates are examined using ammonia or carbon produced per mole of iron or sulphate oxidized.

The major findings described in Appendix A are summarized in the following paragraphs:

The major ions in the leachates are iron, sulphate, and their complexes. If the oxidation state of these ions is assumed to be Fe^{3+} and SO_4^{2-}, iron chemistry is calculated to be dominated by sulphate complexes ($Fe(SO_4)^+$, $Fe(SO_4)_2^-$) in leachates from the low-rate lysimeters and by hydroxo complexes and $Fe(OH)_{3(s)}$ in leachates from the high-rate lysimeters. Because the iron leaves the lysimeter in soluble form, its kinetic transformation to solid form must be sufficiently slow to prevent the precipitation of aqueous iron, because the calculations suggest some $Fe(OH)_{3(s)}$ should form in the tailings solids. Sulphate chemistry is dominated by iron sulphate complexes in the low-rate lysimeter leachates and by its free form (SO_4^{2-}) in the high-rate lysimeter leachates. Minor amounts of HSO_4^- are calculated to occur in all leachates.

The shift in dominant species between the low-rate and the high-rate lysimeter leachates occurs because the higher pH in the high-rate leachates provides more hydroxyl ions for complexing iron and because the sulphate concentration is lower. In most leachate waters with pH<2, HSO_4^- would be the dominant complex, if iron were not present.

High concentrations of Al, K, Mg, Ca, F, and Si were also present in the leachates as well as low concentrations of Cu, Co, Ti, and Ni. The Al, K, Mg, F, and Si concentrations are attributed to the dissolution of primary alumino-silicates by proton attack, since the concentration of these elements increased with increasing H^+ (i.e., decreasing pH). SEM-XRE analyses suggest that plate-shaped particles of 2 µm by 10 µm by 10 µm in size are likely candidates for these elements. It is also possible that some of the host solids whose size dominate the particle size distribution measurements (i.e., 50 µm to 2 mm) were also undergoing proton attack. The other metals measured in the leachates are assumed to result from proton attack upon trace quantities of minerals containing those elements or from oxidation of their sulphides.

Analyses of various metal ratios in the control leachates suggest that some of the K, Al, and F liberated during proton attack is reprecipitated in the tailings solids, probably as secondary alumino-silicates and amorphorus $SiO_{2(s)}$. The formation of amorphorus $SiO_{2(s)}$ is probable, because the concentration of Si in the leachates appears to have been constant until the switch in pH occurs in the high-rate lysimeters; the concentration of Si is that expected when the leachate is at equilibrium with amorphorus $SiO_{2(s)}$. Furthermore, particles, which are mainly Si and whose morphology is consistent with that of amorphorus $SiO_{2(s)}$, were found in the lower sections of the control lysimeters.

The sum of anions and cations by weight (i.e., the calculated TDS) is consistently less than the measured TDS by approximately 30 percent. While this could be due either to unknown ions not measured or to volatilization of ions such as sulphate, these causes are improbable. The difference may be due to the retention of two of the six waters of hydration in an iron sulphate salt formed during the TDS analysis (i.e., drying at 105°C). Similar arguments can be made for the retention of two waters of hydration in gypsum, in waters dominated by calcium sulphate (see Section 7.3.7). These findings suggest that reported TDS concentrations should be decreased by about 30 percent.

Measurements for volatile dissolved solids (VDS) were also made on these leachates. When VDS is added to the sum of anions and cations, the resulting quantity approximately equals measured TDS. VDS normally is a measure of organic carbon and carbonate solids formed during evaporation. These leachates, however, have almost no carbonate; TOC is less than 1 percent of TDS. Thus VDS can be explained as being the loss of water of hydration from the iron sulphate salt formed during the TDS measurement.

A linear relationship can be observed between the log of TDS and log of conductivity in the control leachates; if HNO_3 had been added (for sample preservation), the data points lie off this line. Therefore, conductivity can be used as a surrogate parameter to estimate TDS concentrations provided the leachate is dominated by one major cation (e.g., iron or calcium) and one major anion (e.g., sulphate).

The Fe:S molar fraction varies from 0.5 to 0.75 (average: 0.677 ± 0.069) in leachates from the low-rate control lysimeters and from 0.1 to 0.65 (average: 0.344 ± 0.198) in leachates from the high-rate lysimeters. Theoretically, the ratio should be 0.5 for pyrite (FeS_2). The higher fraction in the low-rate leachates could arise from incomplete sulphate oxidation; however, this is unlikely. It is possible that two different iron sulphides are being oxidized. For example, a source consisting of 1/3 FeS (e.g.,

mackinawite) and 2/3 FeS_2 (e.g., pyrite) would explain the higher fraction. FeS could be present because much of the iron found in the leaching pachacus would result from the leaching of FeS in acid solution; pyrite dissolution is relatively unaffected by H_2SO_4 because of its slow dissolution rate.

The low Fe:S ratios in the high-rate leachates can be explained by precipitation of iron as $Fe(OH)_{3(s)}$ in the lysimeters; this is consistent with speciation calculations (Appendix A.1.2).

Within reasonable limits, one can estimate the pH in the control leachates by using the following: (i) the TDS of the leachate, (ii) the assumption that the Fe:S molar ratio in the tailings is 1:2, and (iii) solution electroneutrality (see Appendix A.1.1). Errors in the calculated pH arise from the Fe:S molar ratio not being equal to 1:2, and from the nonlinear decrease of the pH as TDS (conductivity) increases, because pH is a log scale and, below pH 1.9, a larger percentage of the H^+ complexes with SO_4^{2-} to form HSO_4^-, and increasing amounts of Fe^{3+} and SO_4^{2-} form complexes with species of lower charge [$FeSO_4^+$, $Fe(SO_4)^{2-}$]. Overall, an increase in conductivity causes an increase in H^+ concentration and hence a decrease in pH.

The chemical speciation calculations (Appendix A.1.2) suggest that of the minerals which could control Ra-226 dissolution, only $BaSO_{4(s)}$ and jarosite are close to saturation in low-rate lysimeter leachates, and only $Fe(OH)_{3(s)}$ in high-rate lysimeter leachates. However, no significant quantities of jarosite or $BaSO_{4(s)}$ were identified either by examination with the SEM beam of individual precipitated particles (1 to 5 μm in size) located on the host solids or by ultrasonication to remove surface materials from the host solids. For iron, the lack of clear identification of either hydroxide or jarosite in some samples results from the presence of pyrite preventing the clear identification of other iron solids. But the colour of the solids, particularly those from the high-rate lysimeter, is consistent with the presence of iron hydroxide or iron sulphate solids (bands of reddish-brown and yellow-orange - see Appendix A.2).

In the KCl-EDTA experiments, barium is the only metal whose concentration gives a consistent correlation with Ra-226 activity in the wash waters. The chemical speciation calculations suggest that Ba in the leachate is at equilibrium with $BaSO_{4(s)}$ throughout the lysimeter leaching history. Over 80 percent of the Ra-226 and almost all the pyrite has been lost from the top 10 cm of one of the high-rate lysimeters. All of these observations lead to the hypothesis that Ra-226 is coprecipitated with $BaSO_{4(s)}$ on the surface of quartz solids in the leaching pachucas, and that release of this Ra-226 is retarded through maintenance of $BaSO_{4(s)}$ solubility limits until sufficient pyrite has been

removed to allow sulphate concentrations in biofilm waters to decrease and the $BaSO_4(s)$ containing Ra-226 to dissolve.

The possible coprecipitation of Ra-226 with secondary minerals, such as alumino-silicates, amorphorus silica, and jarosite, cannot be completely ruled out. Recent evidence that jarosite formation is particularly mediated by oxidizing bacteria as well as Kaiman's observation of 80 000 pCi (2960 Bq) Ra-226/g of jarosite in tailings (Kaiman, 1977) shows that such associations exist. This evidence also suggests that while jarosite formation is thermodynamically possible in the leaching pachucas, its role as an agent influencing Ra-226 behaviour in the mill is much less probable than that assumed by Snodgrass et al. (1982) in their generic model. Jarosite formation and Ra-226 incorporation into the secondary precipitate in the tailings pile is a much more probable explanation of Kaiman's observation. Also Kaiman's observation could be the exception rather than the rule or the Ra-226 could be reversibly adsorbed rather than coprecipitated with jarosite. The significance of secondary mineral formation to Ra-226 migration requires further assessment.

Furthermore, although the plots of Ra-226 against Fe, Pb, and Ca concentrations in the KCl-EDTA wash waters showed wide scatter, relationships of Ra-226 with these metals cannot be completely rejected. The KCl and Na EDTA solutions are sequestering agents which dissolve precipitates and act in several ways. The KCl solution should increase the solubility of sulphate and hence the tendency for a sulphate precipitate to dissolve due to a decrease in activity coefficients at higher ionic strengths; K can substitute for the 2^+ metal (isomorphic substitution) in the metal sulphate lattice leading to precipitate breaking. Na EDTA can act in two ways:

- Na may isomorphically substitute for the 2^+ metal leading to precipitate breakup, and
- the EDTA complex can increase the solubility of the metal sulphate by rapidly chelating each metal ion which dissolves from the precipitate.

It is expected that substantial portions of the metals in the wash waters resulted from the dissolution and complexation with EDTA of non-sulphate solids, but the association of Ra-226 with small quantities of the metals in solid sulphate form is possible. However, these relationships do not appear to be very significant.

The mineral acidity (titration with base to pH 4.5) of the leachates agrees reasonably well with measurements of sulphate and nitrate concentrations in the leachates. Nitrate is derived from sample preservation with nitric acid. The

electroneutrality of these waters is explainable by Fe^{3+} and SO_4^{2-} concentrations, provided the complexation of SO_4^{2-} with H^+ and Fe^{3+} is properly accounted for. This suggests that it is reasonable to assume that both iron and sulphur in leachate waters leaving the lysimeters are fully oxidized. Because the leachate samples were stored for 1 to 2.5 years before analysis for ion concentrations, this cannot be thoroughly proven. The occurrence of coloured compounds (see Table A.1a) and the remains of bacteria (presumed to be T. ferrooxidans) in samples from the low-rate lysimeters suggest that some iron oxidation occurred in the sample bottles and hence that some iron leaves the lysimeter in a 2^+ oxidation state (i.e., as Fe^{2+}).

The biochemical yield from the high-rate lysimeter is 170 millimol C/mol Fe. The yield from the low-rate lysimeter is only about 10 percent of that. However, the yield from the two lysimeters should be the same. The value for the low-rate lysimeter is probably a net yield, resulting from the decay by other organisms such as heterotrophs or saprophytic fungi living on lysed pyrite-oxidizing bacterial cells.

A similar difference in yields is observed for nitrogen. It is improbable that the nitrogen is lost by decay because nitrifiers are inactive at low pH. Calculations are presented in Appendix A.2 which show that loss of ammonia by volatilization (at pH 1) is the probable mechanism, despite the concentration of NH_3, the volatile form of ammonia, being approximately 8 orders of magnitude lower than that of total NH_3-N (i.e., $NH_3 + NH_4^+$).

4.4.2 Lysimeter Solids. Detailed assessments of the chemical and physical tests and the SEM-XRE and Mossbauer Spectroscopy analyses conducted on the solids from the control lysimeters upon termination of leaching are given in Appendices A and B, and summarized in the following paragraphs.

The solids in the control lysimeters at the end of the study are much coarser than those classified by Murray and Moffett (1977). It is possible that leaching consumed many of the fine particles in the lysimeter tailings, but it is improbable that this caused such a large shift from the size distribution observed by Murray and Moffett.

The average radium content of the high-rate lysimeter solids (122 pCi/g (4.5 Bq/g)) is less than the coarse fraction of Murray and Moffett (166 pCi/g (6.1 Bq/g)). The difference can be explained by the smaller surface area of these coarser tailings, assuming Ra-226 is in surface precipitates that have a uniform surface density in coarse and fine fractions.

The density of the surface precipitates covering the host solids is greater on solids from the partial and final neutralization tanks of the mill than on solids from the leaching pachucas, and substantially lower on the lysimeter solids. This observation is consistent with dissolution of gypsum after placement in a tailings pile. Gypsum-type particles as well as rod-shaped particles whose composition and morphology are consistent with ettringite (calcium sulphate aluminate hydrate), a mineral formed during concrete reactions, were observed on the solids. The existence of ettringite, the relative importance of ettrigite and gypsum in the surface precipitates, and their subsequent dissolution in the tailings pile, requires further assessment. The plate-shaped particles found on the host solids leaving the partial and final neutralization tanks are probably alumino-silicates.

The results of Experiment 1 suggest that the pyrite oxidation rate is fairly constant in all lysimeters and independent of flushing rate. First, if more oxidation had occurred in the high-rate lysimeters, it is expected that they would contain less pyrite. This pattern is observed for two lysimeters (compare L7 and L8, Table A.12) but is inconsistent for two others (L1 and L2). Surface coatings on pyrite particles of one high-rate lysimeter (L2) may explain part of these results. But it appears that, in general, the mass of pyrite in the low- and high-rate lysimeter solids is the same. Second, the mass flux rate of TDS in the high-rate lysimeter is approximately the same as it had been at the middle flow rate. Furthermore, although the conductivity and TDS graphs do not show it, the concentrations of TDS, iron, and sulphate in both the low- and high-rate leachates decreased an order of magnitude at approximately the same time (see Table A.1b). Hence the main effect of the rate of water application appears to be the dilution of a constant production of iron sulphate.

The generally low levels of pyrite found in the solids explain the decrease in TDS concentrations in the low-rate lysimeter leachates near the end of the study. After approximately 2 000 days of leaching, the pyrite content had decreased sufficiently so that insufficient pyrite was available to maintain the iron sulphate concentrations of the previous years. Accordingly pH increased and TDS concentrations decreased.

The appearance of pyrite in the tailings cores in lenses visible to the eye indicates that the layering and lens characteristics of the tailings pile were not completely eliminated when the solids were homogenized before being put into the lysimeters.

A larger fraction of Ra-226 was leached from the high-rate lysimeters than from the low-rate lysimeters (see Table 5), but overall less than 1 percent was lost over the 7 years of leaching. The larger loss from the high-rate lysimeters resulted mainly from the loss of over 80 percent of the Ra-226 from the top 10 cm, but most of the Ra-226 lost from this area appears to have been resorbed on lower solids. Most pyrite had also been lost from the top 10 cm. This suggests that when sulphate production from pyrite oxidation is complete, a sulphate mineral, containing Ra-226 and formed in the leaching pachucas, begins to solubilize and release Ra-226.

Possible minerals that could control Ra-226 release are discussed in Section 4.4.1 (Item 7).

The low levels of Th-230 in the solids (Table 5) are consistent with the residual levels expected in solids after acid leaching of the ore in the leaching pachucas, assuming the leached thorium was reprecipitated in the final neutralization tank and then redissolved in the tailings pile. For example, assuming that 95 percent uranium minerals and associated daughters (e.g., Th-230) are leached in the pachucas (Skeaff, 1978), 5 percent of 325 pCi/g (12 Bq/g) or 16.3 pCi/g (0.6 Bq/g) should remain. The observed value of Th-230 is 16 pCi/g (0.6 Bq/g). Because of this, and because there is a correlation between thorium concentration and leachate pH (Section 4.4.1), thorium in the leachate waters must originate from residual minerals not attacked in the leaching pachucas and the amount of thorium liberated must be controlled by the acidity of biofilm waters.

The residual concentration of Th-228 is somewhat enriched relative to that of Th-232 whereas they should be the same. That is, the activity of the radioisotopes should be the same if all Th-228 results only from Th-232 decay. Because Th-228 is a daughter of Ra-228 and assuming that the chemistry of Ra-228 is similar to that of Ra-226, it is probable that significant amounts of Th-228 have ingrown from Ra-228. Hence it is probable that two different minerals contain Th-228: the mineral containing Th-232 and the mineral containing Ra-228.

There is a substantially larger amount of Pb-210 than Th-230 left in the tailings. Since both Pb-210 and thorium should be mobilized equally in the leaching pachucas, it might be expected that an equal quantity of thorium and lead would be found in the gypsum formed in the final neutralization tank. Because thorium readily forms $Th(OH)_{4(s)}$ and has few sulphate complexes, it is probable that thorium exists mostly as $Th(OH)_{4(s)}$. Lead has a larger fraction in sulphate complexes at pH 8 (see Figure A.12),

and is probably coprecipitated as $(Ca,Pb)SO_4$ in the gypsum solid or as a distinct $PbSO_4(s)$ precipitate, when the tailings leave the final neutralization tank.

Some sulphate (as gypsum) is still left in the control lysimeter solids. Accordingly, it is probable that most Pb-210 in the leachates resulted from the slow dissolution of residual sulphates. The rate of dissolution would be lowest at the depth of most active pyrite oxidation because the high sulphate concentration from biofilm waters would suppress dissolution of gypsum. After dissolution, it is doubtful that reprecipitation would occur because the speciation calculations (Appendix A.1.2) indicate that neither Pb nor Ca should precipitate given their concentrations in leachate waters.

Without further measurements and theoretical evaluation, it is not possible to conclude that dissolution of residual sulphate controls Pb-210 release, however, because of the following points:

(i) the increase in Pb-210 levels with decreasing pH indicates that the Pb-210 in the tailings, unlike Ra-226, is readily soluble at low pH and is not controlled to the same extent by adsorption and co-precipitation; and

(ii) the activity levels of Pb-210 in leachates from the control and $(Ba,Ra)SO_4$ sediment lysimeters are the same.

In the mill, gypsum forms in the partial neutralization tanks after addition of carbonates. More gypsum yet is added to the solids in the final neutralization tank. There were no carbonates present on the lysimeter solids, but some sulphate remained. It is probable that the carbonate dissolved many years before these lysimeter solids were obtained for the leaching studies.

Leaching patterns are unaffected by carbonate dissolution at any time during lysimeter operation and some or all of the calcium observed in the leachates results from slow dissolution of the residual sulphates. The slow dissolution results partly from coatings (e.g., secondary minerals formed in the tailings) and partly from the high sulphate concentrations of biofilm water. Because the saturation index for gypsum in leachate waters is much less than 1, slow dissolution kinetics are suggested. But the effect of sulphate concentration cannot be ruled out because the sulphate concentration of biofilm waters may be 1 to 2 orders of magnitude higher; only at the biofilm scale can actual solubility controls be irrefutably evaluated.

The bound water found in the solids, one year after cessation of operation, would provide a suitable environment for the maintenance of a viable but sessile community of pyrite oxidizers. The higher moisture content at the bottom of the

lysimeters suggests that bound water constituted a minimum of 0.2 percent of the lysimeter volume during its operation.

The difference between the porosity of 0.58 measured in the cores at the end of the study and the value of 0.55 calculated at the beginning of the study (Section 4.2.2) is probably due to leaching.

The depth of penetration of the electron beam of the SEM is about 1 μm. Penetration of the beam through surface precipitates causes reflection off of the host solids (quartz particles) and, consequently, an XRE spectrum dominated by Si. Samples were ultrasonicated to produce particles free from the host quartz. Some success was attained. The small particles are primarily composed of pyrite, and also contain Ca, Al, Si, K, and S. Further creative work is required to allow full exploitation of the SEM-XRE technology. Such work would include ultrasonic techniques coupled with separation of the vibrated particles by centrifugation or flotation.

Mossbauer analysis for amorphorus and crystalline Fe^{3+} forms of iron sulphate (e.g., jarosite) is complicated by the fact that the doublet peak for FeS_2 (in which Fe is assigned a low spin number of +2) is at approximately the same location on the spectrum and has approximately the same shift as Fe^{3+}. Hence, to exploit the potential of Mossbauer spectroscopy fully, removal of pyrite is recommended. No significant quantities of ferric minerals must remain on the surface of the pyrite particles.

4.5 Summary and Conclusions

The addition of $(Ba,Ra)SO_4$ sediments to tailings results in considerable increases in leached radioactivity for all measured radionuclides except Pb-210. After 50 pore volumes, the ratios of cumulative radioactivity leached from the high-rate tailings-sediment lysimeters to that leached from the controls are:

1.9:1 for Ra-226,
51:1 for Th-232,
72:1 for Th-230, and
2.3:1 for Th-228.

While the increases are substantial, the results should be considered in the context of the amount of $(Ba,Ra)SO_4$ sediments added to the tailings. The sediment-to-tailings ratio used in the lysimeters was about four orders of magnitude larger than the current sediment-to-tailings mass production ratio. If sediments were homogeneously codisposed

with tailings at the current mass production ratio, the results indicate that this would, under aerobic conditions, likely have little effect on radionuclide levels in seepage from the tailings. The stability of such sludges under anaerobic (sulphate-reducing) conditions requires further evaluation.

Evidence gathered suggests that Ra-226 is maintained in a solid form until biofilm concentrations of sulphate decrease to permit dissolution of the $(Ba,Ra)SO_4$ coprecipitate. This is true even for tailings without $(Ba,Ra)SO_4$ sludges. Hence, Ra-226 release is ultimately proportional to the initial Ra-226 content, but its history depends upon the amount of pyrite initially present and its history of oxidation. A similar argument can be made for thorium contained in the $(Ba,Ra)SO_4$ sludge. The amount of thorium released is a function of the initial mass present, but the history of thorium evolution is a function of biofilm acidity and the length of time during which it is maintained.

5 EXPERIMENT 2: LEACHABILITY OF $(Ba,Ra)SO_4$ SEDIMENTS FROM THE BOTTOM OF SETTLING PONDS

The sediments used in Experiment 2 were dredged in 1976 from the bottom of the North Nordic Lake settling pond near the City of Elliot Lake, Ontario, which receives the effluent from the Nordic tailings area (Figure 4). Since the effluent contains large amounts of dissolved Ra-226, barium chloride ($BaCl_2$) is added to precipitate barium-radium sulphate ($(Ba,Ra)SO_4$) according to a reaction of the type (Moffett, 1976):

$$BaCl_2 + Ra^{2+} + SO_4^{2-} \rightarrow 2\ Cl^- + (Ba,Ra)SO_4$$

The sediments are stored at the bottom of the treatment pond, and the treated effluent is discharged to a local water course. However, redissolution of Ra-226 from these sediments may occur after the tailings area has been abandoned, and cause contamination of receiving waters.

Experiment 2 was conducted to investigate the rate at which this dissolution occurs, and to determine whether this rate could be decreased by solidification of the sediments. Solidification (also referred to as chemical fixation or encapsulation) involves mixing the sediments with chemicals to produce a solid matrix analogous to concrete.

5.1 Experimental Procedure

Four rectangular steel-supported polyethylene tubs - 61 cm wide, 91 cm long, and 81 cm deep - were used to simulate settling ponds for holding two replications of two $(Ba,Ra)SO_4$ sediment compositions (Figure 29). Each tub contained 0.07 m^3 of sediments over a base of silica sand. Two of the tubs received untreated sediments (the control ponds), and two received sediments which had been treated using the proprietary Chemfix^R process (Sales, 1979). This solidification process increased the volume of the sediments by 23 percent. The treated sediments were cured for 2 weeks, after which all loose material on top of the treated sediments was removed by vacuum, and all ponds were filled with distilled water. The tubs were located inside the Wastewater Technology Centre in Burlington, Ontario, and were kept at 18 to 20°C.

A constant head of 41 cm of water was maintained in each pond during the 1616-day monitoring period. A peristaltic pump was used to add distilled water continuously to the settling ponds at a flow rate of approximately 1 L/day, giving a hydraulic loading of 0.18 cm/day and a detention time of 228 days. Effluent was collected continuously from an outflow port located opposite to the inflow port at the same hydraulic head, and composited for 1, 2, or 4 months. The compositing periods increased

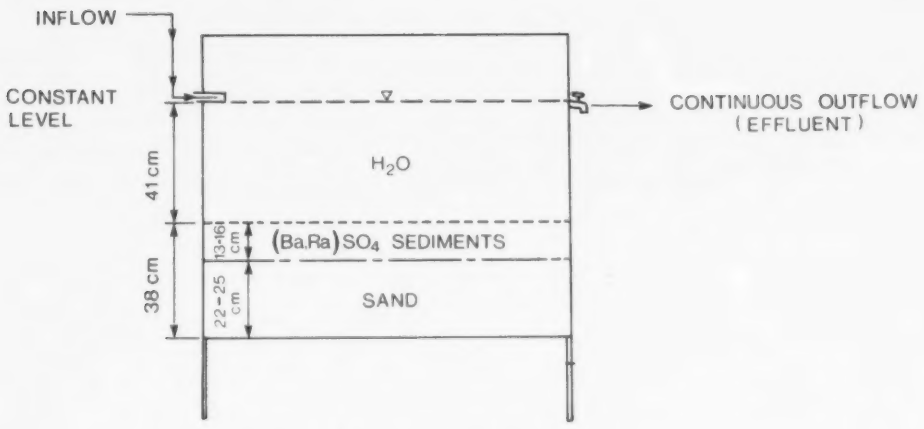

Rectangular Polyethylene Lysimeter
(61 cm Wide x 91 cm Long x 81 cm Deep)

FIGURE 29 TYPICAL SIMULATED SETTLING POND USED IN EXPERIMENT 2

as the study progressed. The composited effluent samples were analyzed for pH, conductivity, dissolved and suspended solids, selected trace metal concentrations, and radionuclide levels (dissolved Ra-226, Pb-210, Th-232, Th-230, Th-228, gross alpha and gross beta, and suspended gross alpha and gross beta).

The acute lethality of the effluents was examined using static 96-hour bioassay tests with daphnia (*Daphnia pulex*) for the initial screening tests and rainbow trout (*Salmo gairdneri*) for the rest of the tests. Initial tests with daphnia and rainbow trout were conducted in undiluted effluents.

Since it was expected that high pH might be causing the toxicity observed in these initial tests, subsequent tests with rainbow trout were conducted in undiluted effluents which were adjusted prior to testing to pH 7 by adding, as appropriate, either concentrated sulphuric acid or sodium hydroxide.

For the initial screening tests, eight juvenile *Daphnia pulex* (less than 72 hours old) were each exposed to 20 mL of undiluted sample. Observations were made at elapsed times of 0.25, 0.5, 1, 2, 4, 8, 24, 48, 72, and 96 hours, and the number of living and dead daphnia recorded. A coincident control test was conducted using daphnia exposed to filtered water from Lake Ontario. Dissolved oxygen, pH and temperature were measured at elapsed times of 0 and 96 hours.

The remainder of the bioassays were conducted with rainbow trout, according to the EPS Standard Procedure for Testing the Acute Lethality of Liquid Effluents to Fish (EPS, 1977). Juvenile rainbow trout were exposed to samples of undiluted effluent

(usually 80 L) for 96 hours, at a loading density of 1.0 L/gm of fish·day. Observations were made at the same elapsed times used for the daphnia bioassays, and the number of living, dead, and moribund fish recorded. Dissolved oxygen, pH, and temperature were measured daily. All samples were aerated at 5 $cm^3/L \cdot min$ throughout the tests. Coincident control tests were conducted using rainbow trout exposed to dechlorinated water.

5.2 Results

The results of statistical analyses conducted on the measured effluent characteristics are given in Table 6, in the form of coefficients of variation. These were calculated both by comparing effluent characteristics for each pair of replicated ponds (to obtain an estimate of the variation in parameter magnitudes between two ponds having the same sediments) and also by comparing effluent characteristics for ponds containing treated and untreated sediments (to obtain an estimate in the variation in parameter magnitudes between two ponds having different sediments).

Coefficients of variation for the activity of the three dissolved thorium isotopes and suspended gross alpha and beta could not be calculated because many of the analyses were less than the detection limit of 1 pCi/L (0.04 Bq/L). Coefficients of variation for dissolved metal concentrations could not be determined because effluent samples from replicate ponds were composited prior to metal analyses.

In general, reproducibility of measured effluent characteristics in duplicated ponds was better for non-radioactive parameters (volume, pH, conductivity, total solids) than for radioactive constituents (dissolved gross alpha and beta, dissolved Ra-226). Differences in effluent characteristics between treated and untreated ponds were significant for all detectable parameters except dissolved gross alpha. Larger values were measured in effluents from the treated ponds for all the significantly different parameters (see the "Between Treatments" column in Table 6) except volume and dissolved Ra-226.

The pH of the treated pond effluent gradually decreased from 10 to 9 during the study, whereas the pH of the control pond effluent remained relatively stable at about 8 (Figure 30). The control effluent pH is within the range of 6.5 to 9.0 measured in decants from active tailings areas (Vivyurka, 1974).

Effluent conductivity for treated ponds peaked at 30 mS/m at 200 days, and then gradually declined to 14 mS/m at 800 days (Figure 31). It continued to decrease during the rest of the study but at a much slower rate, and had reached 10 mS/m after

TABLE 6 EXPERIMENT 2: VARIATIONS WITHIN AND BETWEEN TREATMENTS

Effluent Parameter	Coefficient of Variation (Number of Pairs of Observations)		
	Within Replicated Treatments		
	Untreated Sediments	Solidified Sediments	Between Treatments
Volume	5.5(25)	6.7(25)	* 10.1(25)
pH	2.1(21)	1.0(22)	* 18.2(25)
Conductivity	13.0(23)	13.2(23)	*144.0(23)
Total Solids	18.5(14)	14.4(14)	*156.0(14)
Suspended Solids	57.0(7)	117.0(12)	*220.0(11)
Dissolved Gross α	23.2(5)	35.4(5)	35.8(5)
Dissolved Gross β	58.9(5)	46.5(6)	*118.0(5)
Dissolved Ra-226	20.0(24)	30.7(13)	*122.0(16)

1. Variations within replicated treatments could not be calculated for some parameters because most of the replicated observations were below detection limits.
2. The coefficients of variation within and between treatments were calculated using the equations given in Tables 3 and 4.
3. An asterisk (*) preceeding a coefficient of variation in the "Between Treatments" column indicates that the between-treatment variance is significantly greater than the within-treatment variance (F-test, 95-percent level of confidence).
4. The number of pairs of observations used in each determination is indicated in brackets.

1616 days. Effluent conductivity for the control ponds decreased steadily throughout the study from 6 to 3 mS/m.

Suspended and dissolved solids concentrations in the effluents are shown in Figure 32. Suspended solids concentrations were low in all pond effluents, and were usually less than 3 mg/L in the control pond effluent and less than 10 mg/L in the treated pond effluents. Dissolved solids concentrations were two to three orders of magnitude larger than the suspended solids concentrations, and decreased steadily during the study. Approximately four times more suspended and dissolved solids were released from the treated ponds than from the controls during the study (Figure 33).

During the first 100 days, Ra-226 levels in control effluents decreased from 9 to 2 pCi/L (0.33 to 0.07 Bq/L), whereas levels in treated sediment effluents remained

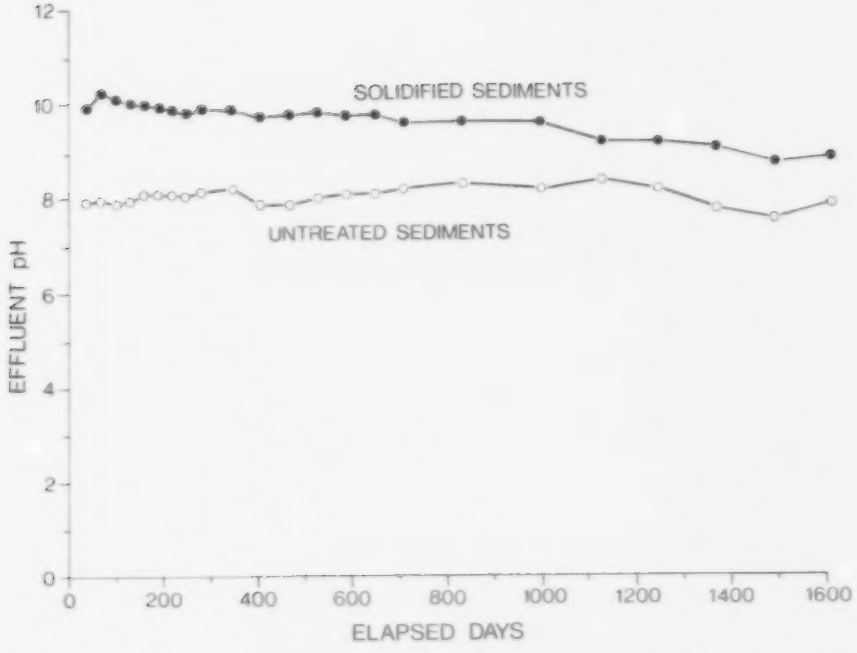

FIGURE 30 EXPERIMENT 2: TEMPORAL VARIATIONS IN EFFLUENT pH

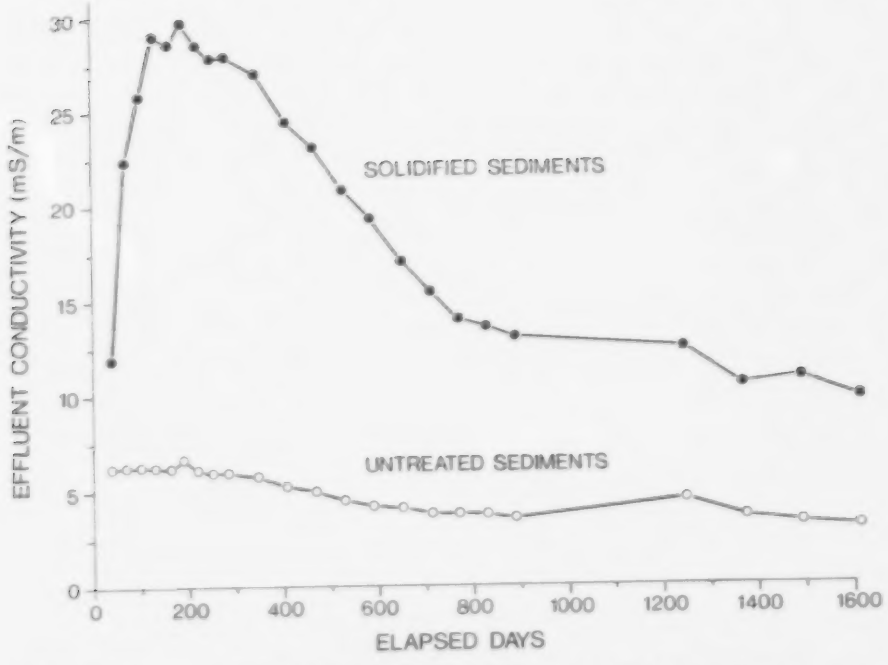

FIGURE 31 EXPERIMENT 2: TEMPORAL VARIATIONS IN EFFLUENT CONDUCTIVITY

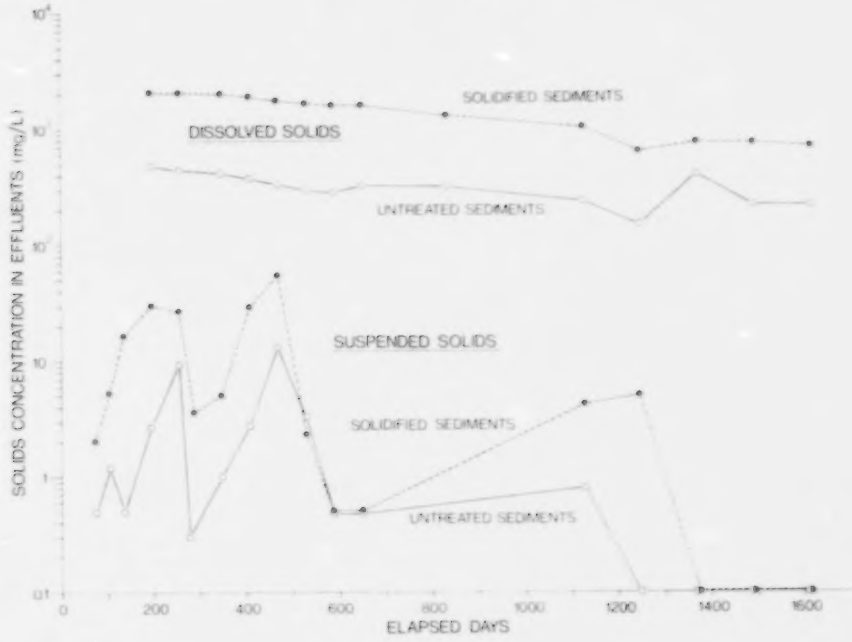

FIGURE 32 EXPERIMENT 2: TEMPORAL VARIATIONS IN DISSOLVED AND SUSPENDED SOLIDS

less than the detection limit of 1 pCi/L (0.04 Bq/L) (Figure 34). Levels in both effluents then increased over the next 150 days to 5.4 pCi/L (0.2 Bq/L) for the controls and 2.4 pCi/L (0.09 Bq/L) for the treated ponds. During the balance of the study, Ra-226 levels fluctuated between 4.8 and 8.0 pCi/L (0.18 and 0.30 Bq/L) for the controls and between 1.0 and 3.1 pCi/L (0.04 and 0.11 Bq/L) for the treated ponds. By the end of the study, three times more Ra-226 had been released from the control ponds than from the treated ponds (Figure 35).

Levels of dissolved Pb-210 in all pond effluents remained less than the detectable limit of 15 pCi/L (0.56 Bq/L) during the entire study, with the exception of the period July and August 1977 (elapsed time: 346 to 407 days). At this time, levels of 22 and 29 pCi/L (0.81 and 1.07 Bq/L) were measured in the control pond effluents.

Dissolved Th-228, Th-230, and Th-232 levels in all pond effluents were generally less than the detection limit of 1 pCi/L (0.04 Bq/L) during the entire monitoring period.

Suspended gross alpha and beta in all pond effluents were less than 5 pCi/L (0.19 Bq/L) throughout the study, with the majority of the measurements less than the detection limit of 1 pCi/L (0.04 Bq/L).

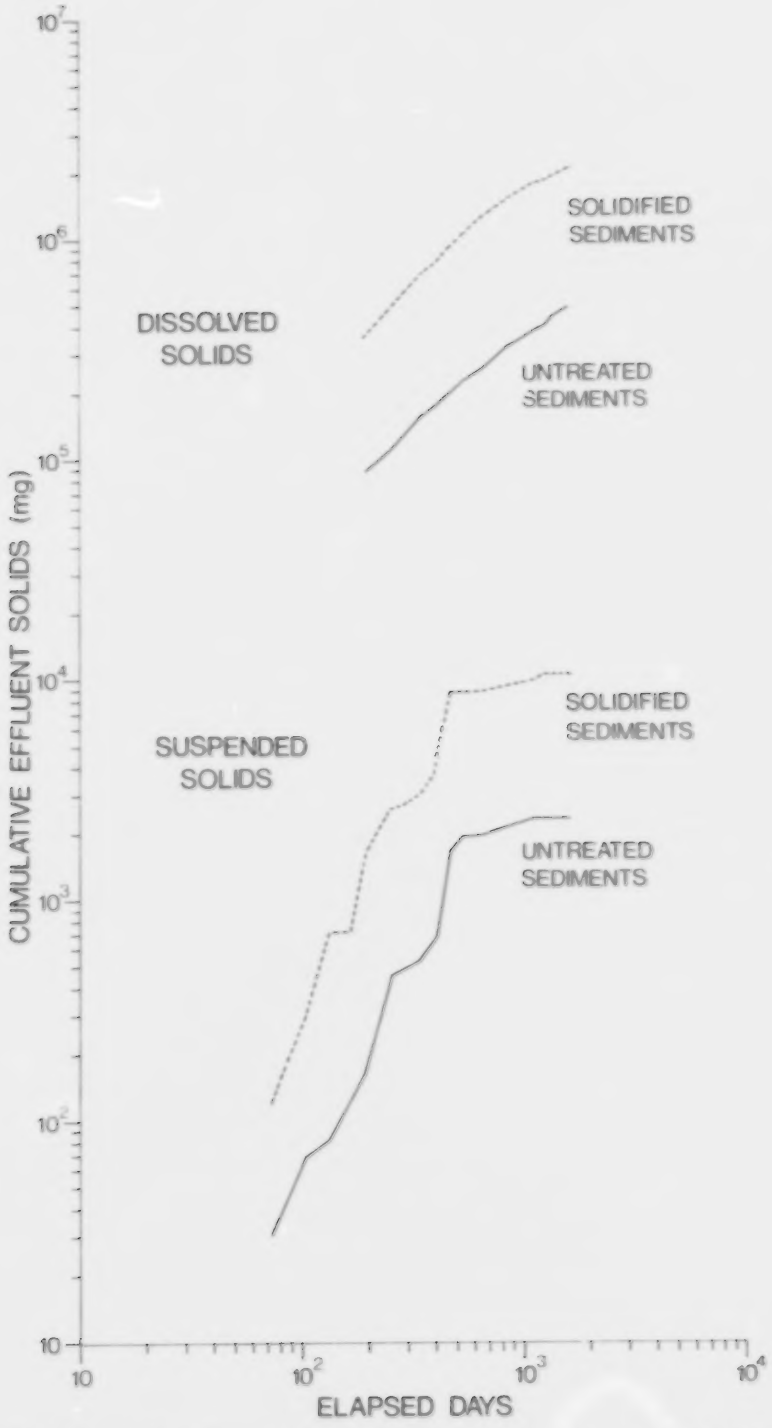

FIGURE 33 EXPERIMENT 2: CUMULATIVE MASS OF DISSOLVED AND SUSPENDED SOLIDS vs. TIME

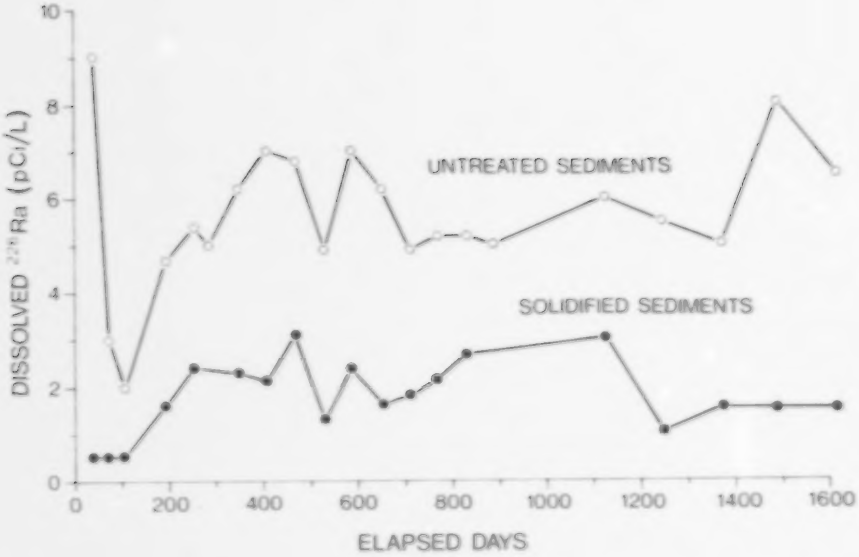

FIGURE 34 EXPERIMENT 2: TEMPORAL VARIATIONS IN DISSOLVED Ra-226

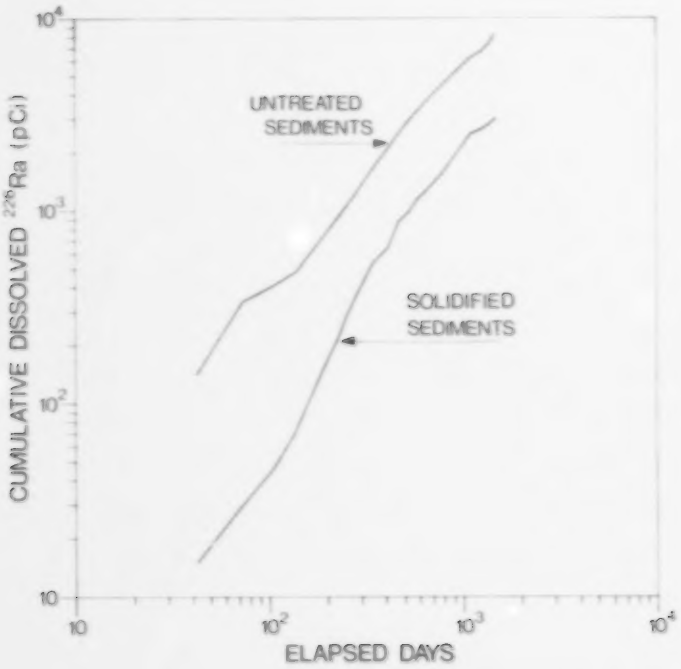

FIGURE 35 EXPERIMENT 2: CUMULATIVE LEACHED Ra-226 vs. TIME

Dissolved gross alpha levels were approximately the same in all effluents. Levels remained relatively constant at about 120 pCi/L (4.4 Bq/L) during the first 840 days, and then decreased. After 1616 days, effluent levels in all ponds ranged between 5 and 13 pCi/L (0.19 and 0.48 Bq/L).

Dissolved gross beta levels during the first 840 days were less than 1 pCi/L (0.04 Bq/L) in control pond effluents and approximately 30 pCi/L (1.11 Bq/L) in treated pond effluents. Levels then increased to reach about 25 pCi/L (0.93 Bq/L) in control pond effluents and 110 pCi/L (4.07 Bq/L) in treated pond effluents at 1100 days. For the balance of the study, levels ranged between 15 and 40 pCi/L (0.56 and 1.48 Bq/L) in control pond effluents and between 50 and 105 pCi/L (1.85 and 3.89 Bq/L) in treated sediment pond effluents.

In the initial static bioassay tests in which there was no pH adjustment, no mortality occurred in effluent from the control ponds but 100 percent mortality occurred to both daphnia and rainbow trout in effluent from the treated sediment ponds. It was expected that the high effluent pH of 10 was responsible for the toxicity, but 100 percent mortality also occurred after adjustment of the treated pond effluent pH to 7.

Subsequent bioassays were conducted in undiluted effluents which were adjusted to pH 7. Effluent pH prior to adjustment ranged between 7.5 and 8.8 for the control ponds and between 9.0 and 10.0 for the treated sediment ponds. Generally, effluents from the treated sediment ponds were toxic, whereas those from the control ponds were not. However, the results are not consistent. For example, 20 percent mortality occurred in control pond effluents in September 1978 and 100 percent mortality in December 1978, whereas no mortality occurred in treated sediment pond effluents in September and December 1978, and in January 1979.

Several chemical constituents in the effluents were measured to identify those that could be toxic in the bioassay tests. The annual average concentrations of these constituents are given in Table 7. Concentrations generally remained relatively constant or decreased throughout the study, although there were some exceptions, such as sodium in the control pond effluents; calcium in the treated sediment pond effluents; and iron and zinc in both types of effluent. Higher concentrations of aluminum, copper, iron, potassium, silicon and sodium were usually found in the treated pond effluents than in the control effluents, whereas the reverse occurred for calcium, magnesium and sulphate. Cadmium, chromium, copper, lead, manganese, nickel and zinc concentrations were near or below detection limits in effluents from all ponds, with the exception of zinc concentrations in 1980 effluents.

TABLE 7 EXPERIMENT 2: CONCENTRATIONS OF VARIOUS CONSTITUENTS IN LEACHATES

Constituents	Treatment	Average Concentration[1] (mg/L) 1976	1977	1978	1979	1980
Aluminum	Controls	0.15	0.19	0.19	0.10	0.12
	Solid. Sediments	1.20	0.73	0.49	0.34	0.29
Cadmium	Controls	< 0.001	< 0.001	< 0.002	< 0.002	< 0.003
	Solid. Sediments	0.001	< 0.001	0.002	< 0.002	< 0.003
Calcium	Controls	62.0	41.0	39.0	27.0	31.0
	Solid. Sediments	0.71	1.7	2.4	2.5	4.0
Chromium	Controls	< 0.01	0.01	< 0.01	< 0.01	< 0.01
	Solid. Sediments	0.02	0.02	< 0.01	< 0.01	< 0.01
Copper	Controls	0.02	0.02	0.02	0.01	0.03
	Solid. Sediments	0.05	0.05	0.03	0.03	0.05
Iron	Controls	0.08	0.09	0.16	0.09	0.80
	Solid. Sediments	0.09	0.18	0.17	0.33	0.20
Lead	Controls	< 0.01	< 0.01	< 0.01	< 0.02	0.01
	Solid. Sediments	< 0.01	< 0.01	0.02	0.02	0.01
Magnesium	Controls	29.4	24.3	17.6	15.0	16.0
	Solid. Sediments	0.9	0.7	0.3	0.4	0.1
Manganese	Controls	0.03	0.03	< 0.01	--	0.002
	Solid. Sediments	0.04	0.05	< 0.01	--	0.002
Nickel	Controls	< 0.01	< 0.01	0.01	< 0.02	< 0.01
	Solid. Sediments	0.02	0.02	0.01	0.01	0.01
Potassium	Controls	13.5	12.4	--	--	5.7
	Solid. Sediments	154.0	134.0	--	--	60.0
Silicon	Controls	1.1	0.5	0.3	--	< 3.0
	Solid. Sediments	41.0	46.0	1.8	--	< 3.0
Sodium	Controls	21.0	26.0	54.0	--	17.0
	Solid. Sediments	477.0	542.0	373.0	--	238.0
Sulphate	Controls	165.0	151.0	--	--	51.0
	Solid. Sediments	84.0	81.0	--	--	31.0
Zinc	Controls	0.01	< 0.01	0.02	0.02	0.10
	Solid. Sediments	< 0.01	< 0.01	0.02	0.02	0.13

[1] Averages are weighted by effluent volumes

5.3 Discussion

The main chemical constituents in the control effluents were sulphate, calcium, magnesium, and potassium, whereas those in the treated effluents were sodium, potassium, sulphate and silicate. These constituents probably resulted from the diffusion of pore water constituents into the pond water. The gradual decrease of conductivity in the controls suggests that the constituents in the solid portion of the $(Ba,Ra)SO_4$ sediment were at equilibrium with those in the pore water, whereas the peak in the conductivity of the treated sediment effluent suggests that the constituents in the solids and pore waters were not at equilibrium.

Only low levels of Ra-226 were observed in the control pond effluents, indicating that only small quantities of the $(Ba,Ra)SO_4$ sediments dissolved. Ra-226 concentrations in the treated pond effluents were approximately one-half of those in the control effluents. It appears that the Chemfix® treatment forms a (Na,K)-(silicate, sulphate) solid that can partially suppress dissolution of Ra-226 and (Ca,Mg, Ba) sulphate, which are the main constituents of the sediments. However, the increase in calcium concentrations and the continued release of Ra-226 in treated pond effluents suggests that this solid was dissolving or that the sediments were incompletely encapsulated by the Chemfix® process, or both.

In general, dissolved Th-228, Th-230, and Th-232 levels in effluents from all ponds were below the detection limit of 1 pCi/L (0.04 Bq/L) during the entire monitoring period. This is consistent with the theory presented in Section 9.0; namely that the high pH of the sediment pore water would maintain any thorium present in solid form as $Th(OH)_{4(s)}$.

In general, effluents from the treated ponds were toxic to daphnia and rainbow trout, whereas those from the control ponds were not. The radioactivity of the effluents does not appear to be a contributing factor because of the low levels involved and the small differences in the radioactivity levels of the control and treated pond effluents. The elevated levels of aluminum could explain the observed toxicity. Adjustment of pH in some of the tests would have caused a change in the ratio of dissolved to precipitated species for some elements, but the net effect on toxicity is not known.

5.4 Summary and Conclusions

The leaching of Ca, Mg, SO_4, and Ra-226 from $(Ba,Ra)SO_4$ sediments is consistent with dissolution reactions in sediment pore water and the diffusion of these

constituents into the overlying water. Leaching from treated sediments is consistent with the dissolution of a (Na,K)-(silicate, sulphate) solid that can partially suppress dissolution of Ra-226 and (Ca,Mg,Ba) sulphate, which are the main constituents of the sediments. Solidification decreased the amount of dissolved Ra-226 released from the ponds during the study by about 65 percent. The increase in calcium concentrations in the treated pond effluents suggests that the encapsulating material may be slowly dissolving. These results and those of Experiment 3 suggest that solidification of tailings and $(Ba,Ra)SO_4$ sediments by the Chemfix^R process may only delay the release of radionuclides and other constituents from these residues, but not prevent it from eventually occurring.

6 EXPERIMENT 3: LEACHABILITY OF NEW TAILINGS SUBJECTED TO VARIOUS TREATMENTS

Experiment 3 was conducted to examine the leachability of radioactive constituents and selected chemical species from freshly milled uranium tailings, and to determine whether leachability could be decreased by solidification or revegetation of the tailings. Revegetation programs have been implemented on several tailings deposits in the Elliot Lake area (Schmidt and Moffett, 1979). Solidification has been suggested as a means of limiting acidic and radioactive seepage from tailings basins, and possibly eliminating water and wind erosion.

The freshly milled tailings were obtained in 1976 from the discharge site of Rio Algom Quirke Mine in the Elliot Lake area of Ontario (Figure 3). One of the largest uranium ore reserves in the world is located in this area. The ore consists mainly of quartz and orthoclase, with minor amounts of pyrite (2 to 7 percent), feldspar, chlorite, uranium-bearing minerals and radioisotopes (the most important of which are radium and thorium). Besides the radioisotopes, the ores also contain a small amount of heavy metals, mainly in the form of oxides (Raiecevic, 1979). The uranium oxide content of the ore ranges between 0.8 and 1.25 kg/tonne, and thorium is present in quantities of 0.25 to 0.5 kg/tonne (Murray and Moffett, 1977). The most common heavy metals which may be present are copper, zinc, manganese, lead, iron, nickel, and arsenic.

Quirke Mine produces and concentrates about 4000 tonnes of ore/day, using an acid leach/ion-exchange extraction process (Moffett, 1976). This results in the generation of about 10000 to 16000 tonnes of tailings discharged to the tailings basin every day.

The solid portion of the tailings is made up of quartz, pyrite, calcium sulphate (from the neutralization reaction caused by lime addition in the neutralization tanks), metal hydroxides, precipitated thorium, and rare earths (Vivyurka, 1976). The solid portion of a sample of fresh Quirke tailings obtained by Silver and Ritcey (1980) contained 2.5 to 3.5 percent pyrite, 0.72 percent sulphate (as sulphur), 2.82 percent total iron, 0.007 percent uranium, 0.025 percent thorium and 170 pCi/g (6.3 Bq/g) Ra-226. The tailings have the potential to become acidic after abandonment through the generation of sulphuric acid by chemical or microbial oxidation of pyrite.

The liquid portion of the tailings is an alkaline, saturated calcium sulphate solution (pH 8 to 10), containing ammonia (120 mg/L as N), nitrate (650 mg/L as N), and sulphate (2 000 mg/L). The concentration of dissolved solids is approximately 3 500 mg/L, and that of dissolved Ra-226 4 500 pCi/L (167 Bq/L) (Scott, 1979).

Less than 1 percent of the radioactivity is in the liquid portion of the tailings; the remainder is in the solid phase. The solid phase of the tailings is composed of two distinct size types: coarse sands and fine solids or slimes. The slimes account for about one-third of the total mass of the tailings, but contain about 75 percent of the radioactivity. Approximately 90 percent of the Ra-226 is in the -200 mesh fraction of the tailings (Skeaff, 1977).

6.1 Experimental Program

Eight rectangular steel-supported polyethylene lysimeters - 61 cm wide, 91 cm long and 81 cm deep - were used to hold the tailings (Figure 36). The eight lysimeters consisted of two replicates of each of the following tailings treatments:

1. fresh tailings (control),
2. fresh tailings which were solidified using the Chemfix^{R} process (Sales, 1979),
3. fresh tailings mixed with sewage sludge and vegetated, and
4. solidified fresh tailings mixed with sewage sludge and vegetated.

Each lysimeter contained approximately 490 kg of fresh tailings (excluding sewage sludge and the solidification chemicals). The four lysimeters with fresh tailings contained 36 cm of tailings over 30 cm of silica sand. The other four lysimeters contained 58 cm of solidified tailings over 8 cm of sand, because the solidification process caused a 61-percent increase in volume. The initial radionuclide contents of each lysimeter are given in Table 8.

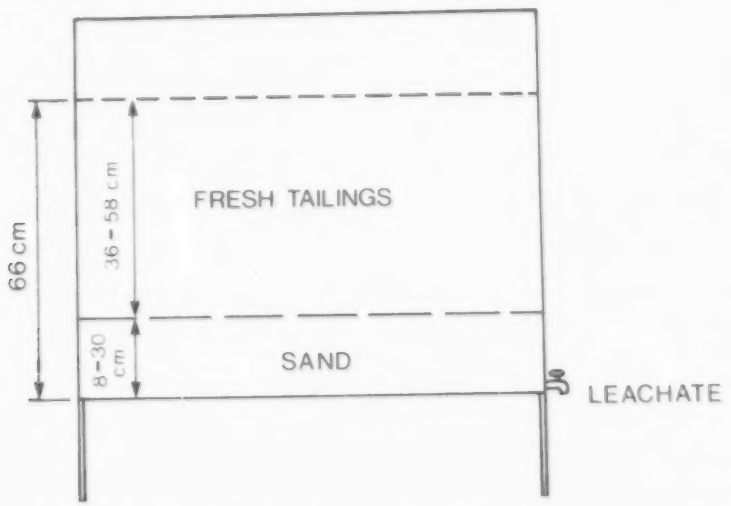

FIGURE 36 TYPICAL LYSIMETER USED IN EXPERIMENT 3

TABLE 8 EXPERIMENT 3: INITIAL RADIONUCLIDE LEVELS

	Tailings		Each Lysimeter	
	pCi/g	Bq/g	μCi	Bq
Ra-226	538	19.9	262	9.7×10^6
Pb-210	503	18.6	245	9.1×10^6
Th-232	34	1.26	17	6.3×10^5
Th-230	402	14.9	196	7.3×10^6
Th-228	34	1.26	17	6.3×10^5

* $\mu Ci = 10^6$ pCi

Air-dried (90 percent dry matter) anaerobically digested sewage sludge, treated with $FeCl_3$ for phosphorus removal, was applied on August 24, 1976 to the four lysimeters to be vegetated. This addition, applied to the top 15 cm at the rate of 323 tonne/ha, increased the organic matter of the top layer to 3 percent. Sludge constituent concentrations and loading rates to the tailings are given in Table 9.

A grass seed mixture of 40 percent fescue and 60 percent red top by weight was broadcast seeded on August 31, 1976. A chemical fertilizer (5-20-20) was applied to the vegetated lysimeters in April, 1980 and April, 1981, at an application rate of 0.066 kg/m^3. This vegetation procedure is similar to that of Murray and Moffett (1977).

The lysimeters were located outside the Wastewater Technology Centre in Burlington, Ontario, and received natural precipitation and sunlight. During the growing seasons, 14 L of water were added once a week to each lysimeter to generate sufficient amounts of leachate for analysis and bioassay tests.

Crops from the vegetated lysimeters were harvested two to three times per year. The grass cuttings were washed to remove tailings particles adhering to the surface of the grasses, dried in a warm air oven at 70°C for 48 hours, ground to 40-mesh size in a Wiley mill, and analyzed for yield and for the presence of Ra-226, Pb-210, Th-232, Th-230 and Th-228.

Leachate was collected through a perforated drainage pipe located at the base of each lysimeter. Composited leachate samples were analyzed at each harvest and at the end of each dormant season. The leachates were analyzed for pH, conductivity, selected chemical species, and dissolved Ra-226, Pb-210, Th-232, Th-230, and Th-228.

TABLE 9 EXPERIMENT 3: SLUDGE CONSTITUENT CONCENTRATIONS AND LOADING RATES

Constituents	Concentration (%)	Loading Rate (kg/ha)
TKN-N	2.31	3 470
Total P	4.98	7 470
Total C	21.30	32 000
Total S	0.94	1 410
Ca	3.90	5 850
Mg	0.4033	605
Na	0.0572	86
K	0.0792	119
Fe	7.245	10 900
Mn	0.0475	71
Al	0.9390	1 410
Cu	0.1210	182
Zn	0.2130	320
Ni	0.0020	3
Cr	0.0489	73
Pb	0.1700	255
Cd	0.0026	4
Mo	0.0033	5
Total Solids	90.0	135 000
Volatile Solids (600°C)	40.0	60 000

The acuite lethality of undiluted leachates from the four treatments was examined using static 96-hour bioassays with daphnia and rainbow trout. Leachates from replicated treatments were composited, and their pH adjusted when necessary to approximately 7.5 prior to the tests. The procedures followed in the bioassays were similar to those used in Experiment 2 (Section 5.1).

6.2 Results

To assist in data interpretation, the results are presented as seasonal averages for each vegetation growing and dormant season. April and November were considered to be the start and end of each growing season. The seasonal averages were determined by weighting the results of samples collected over a season by their corresponding leachate volumes.

The reproducibility of the replicated treatments and the significance of differences in parameter magnitudes between pairs of treatments were examined by

calculating coefficients of variation using coincident observations (i.e., not seasonal averages). These coefficients are presented in Tables 10 and 11 for leachate parameters and in Table 12 for vegetation parameters. Significantly different "between treatment" coefficients (F-test, 95-percent level of confidence) are indicated by an asterisk. Coefficients could not be calculated for many of the radionuclides because most or all of the measurements were below detection limits. Coefficients could not be determined for dissolved metal concentrations as leachates from replicated lysimeters were composited prior to metal analyses.

TABLE 10 EXPERIMENT 3: WITHIN TREATMENT VARIATIONS IN LEACHATE PARAMETERS

Parameter	Coefficient of Variation			
	Fresh Tailings (Control)	Solidified Tailings	Tailings + Sludge + Vegetation	Solid. Tailings + Sludge + Vegetation
Volume	140.0(30)	137.0(30)	42.4(30)	99.7(30)
pH	8.8(17)	5.4(14)	9.7(19)	12.2(17)
Conductivity	13.0(17)	23.9(14)	25.4(19)	25.5(17)
Dissolved Ra-226	96.3(12)	21.5(9)	52.0(16)	32.8(13)
Dissolved Pb-210	68.5(6)	--	29.9(2)	--
Dissolved Th-232	47.1(6)	--	45.4(10)	--
Dissolved Th-230	59.9(6)	--	54.4(9)	--
Dissolved Th-228	61.2(6)	128.0(4)	28.1(9)	62.5(4)

Notes:

1. Coefficients of variation were calculated by using the equation in Table 3.
2. Within-treatment variations could not be calculated for some parameters because most or all of the measurements were below detection limits.
3. The number of pairs of observations used in calculating each coefficient of variation is given in brackets.

The seasonal volumes of leachate produced from the four tailings treatments are shown in Figure 37. The volumes of leachate produced during each sampling period varied considerably within replicated treatments (Table 10). Differences in leachate volumes were only significant for the vegetated, solidified tailings compared to other treatments (Table 11). Leachate volumes were approximately the same from each of the

TABLE 11 EXPERIMENT 3: BETWEEN TREATMENT VARIATIONS IN LEACHATE PARAMETERS

Parameter	Coefficient of Variation				
	Controls vs. Solidified Tailings	Controls vs. Veg. Tailings	Controls vs. Solidified Veg. Tailings	Solidified Tailings vs. Solidified Veg. Tailings	Veg. Tailings vs. Solidified Veg. Tailings
Volume	173.0(30)	140.0(30)	*185.0(30)	*253.0(30)	*180.0(30)
pH	* 96.1(25)	11.8(28)	* 90.6(26)	8.8(24)	* 89.8(26)
Conductivity	*142.0(24)	* 47.4(27)	*165.0(25)	31.7(23)	*146.0(25)
Dissolved Ra-226	*224.0(22)	52.8(26)	*166.0(24)	* 90.3(21)	*181.0(24)
Dissolved Pb-210	--	110.0(8)	--	--	--
Dissolved Th-232	--	*101.0(12)	--	--	--
Dissolved Th-230	--	101.0(12)	--	--	--
Dissolved Th-228	*859.0(7)	39.4(12)	*834.0(10)	69.2(4)	*809.0(7)

1. Coefficients of variation were calculated by using the equation in Table 4.
2. The number of pairs of observations used in calculating each coefficient of variation is given in brackets.
3. A coefficient of variation preceded by an asterisk indicates that the between-treatment variance was significantly greater than the within-treatment variance (F-test, 95 percent level of confidence).

four sets of lysimeters during each dormant period, but varied considerably during the growing seasons. By the end of the study, the solidified and vegetated, solidified tailings had produced 12 to 15 percent less leachate than the controls, whereas the vegetated tailings had produced 12 percent more leachate than the controls (Figure 38).

Temporal changes in leachate pH were significantly different among the four treatments except between vegetated and non-vegetated treatments for both the fresh and solidified tailings (Table 11). In general, leachate pH remained relatively constant:

- until the end of the 1977 growing season at about 7.2 for the fresh tailings,
- until the end of the 1977/78 dormant season at about 11.7 for the solidified tailings,
- and then decreased for both types of tailings (Figure 39).

By the 1982 growing season, leachate pH had decreased to 2.2 for the fresh tailings and about 7.1 for the solidified tailings.

TABLE 12 EXPERIMENT 3: WITHIN AND BETWEEN TREATMENT VARIATIONS FOR VEGETATION PARAMETERS

Parameter	Coefficient of Variation		
	Within Treatments		
	Tailings + Sludge + Vegetation	Solidified Tailings + Sludge + Vegetation	Between Treatments
Yield	29.7(13)	37.4(18)	*170.0(13)
Ra-226	48.4(13)	62.7(18)	*143.0(13)
Pb-210	42.2(12)	43.0(15)	68.0(13)
Th-230	118.0(3)	70.1(9)	108.0(11)
Th-228	88.1(3)	68.8(9)	50.1(11)

1. Coefficients of variation were calculated by using the equations in Tables 3 and 4.
2. The number of pairs of observations used in calculating each coefficient of variation is given in brackets.
3. Coefficients of variation could not be calculated for Th-232 because most measurements were below detection limits.
4. Between-treatment coefficients of variation preceded by an asterisk were significantly different than the within-treatment coefficients (F-test, 95-percent level of confidence).

Opposing trends in leachate conductivity were observed for the fresh and solidified tailings during the first 3 to 4 years of the study (Figure 40). Conductivity levels in leachates from the fresh tailings remained relatively constant at about 25 mS/m until the 1978 growing season. They increased to peak at 90 mS/m during the 1979/80 dormant season for the vegetated lysimeters and 210 mS/m during the 1981 growing season for the controls, then decreased to 60 mS/m by the end of the study. Conductivities in leachates from the solidified tailings decreased almost continually from 130 to 20 mS/m throughout the study.

Up to the 1977/78 dormant season, dissolved Ra-226 levels were higher in leachates from fresh tailings than from solidified tailings, but this trend was reversed in subsequent seasons (Figure 41). Ra-226 levels in leachates from the non-vegetated treatments were usually equal to or greater than those in leachates from the vegetated treatments. Cumulative Ra-226 activities leached to the end of the study were approximately 40 percent less from lysimeters containing solidified and /or vegetated tailings than from the controls (Figure 42).

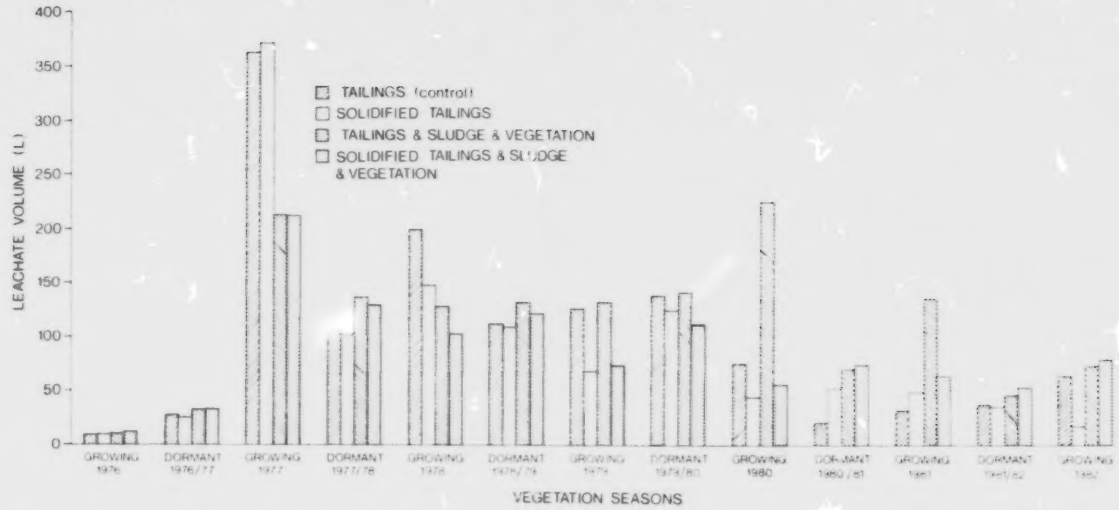

FIGURE 37 EXPERIMENT 3: SEASONAL LEACHATE VOLUMES

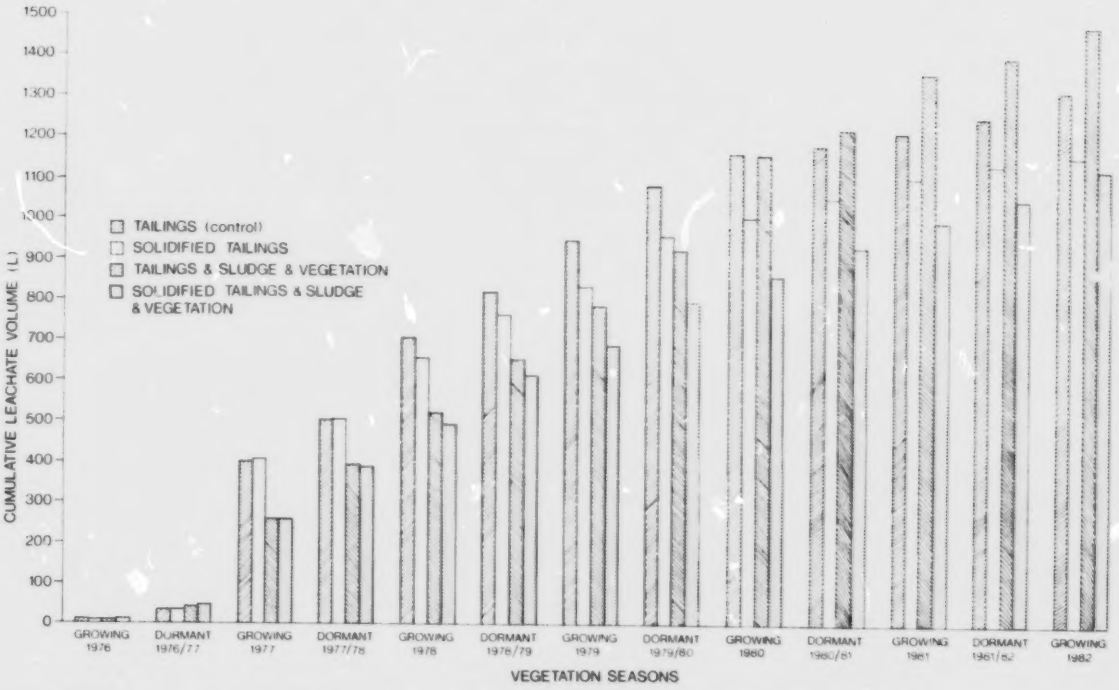

FIGURE 38 EXPERIMENT 3: CUMULATIVE LEACHATE VOLUMES

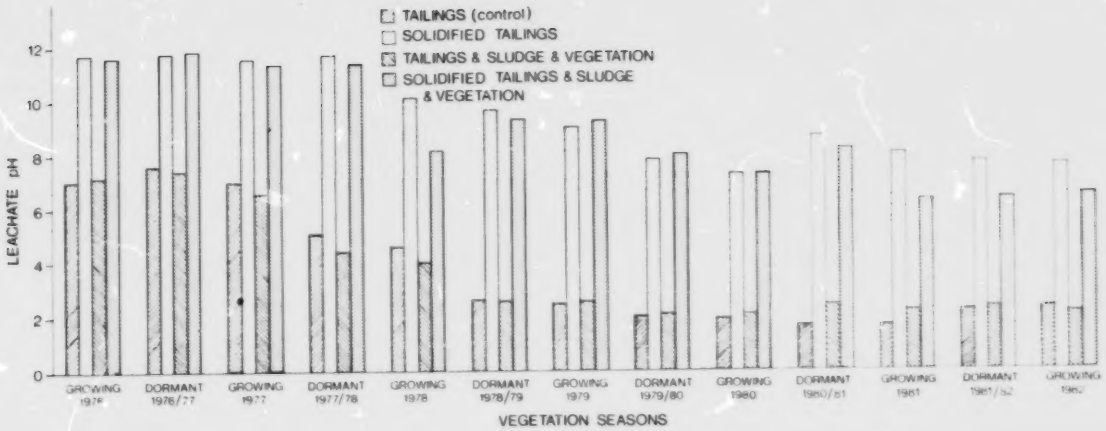

FIGURE 39 EXPERIMENT 3: AVERAGE SEASONAL LEACHATE pH

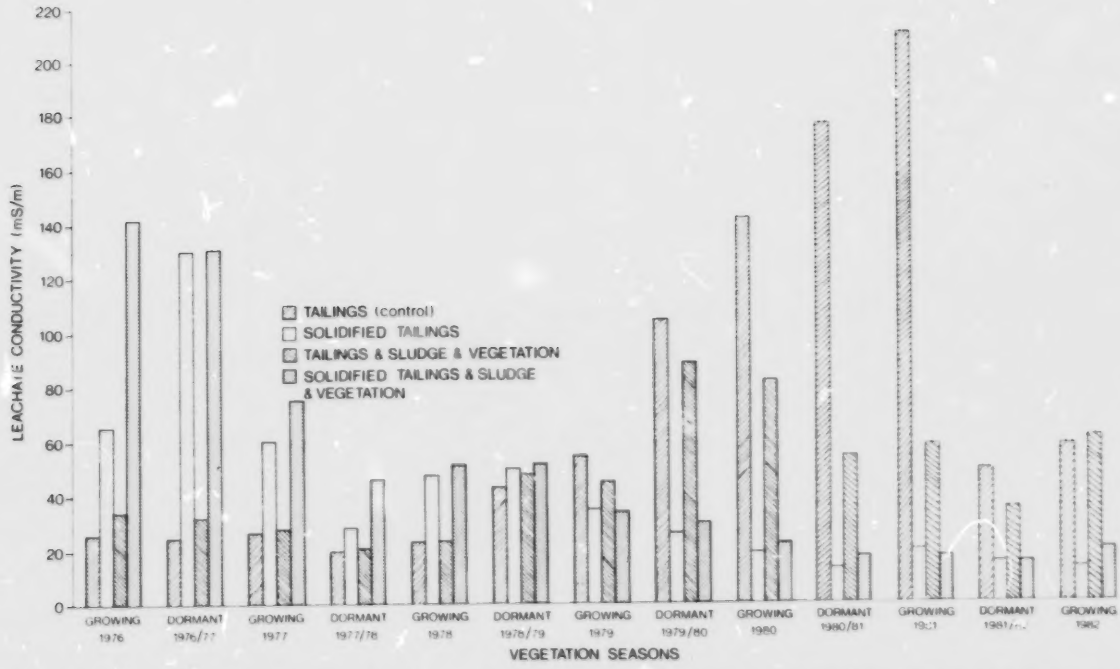

FIGURE 40 EXPERIMENT 3: AVERAGE SEASONAL LEACHATE CONDUCTIVITY

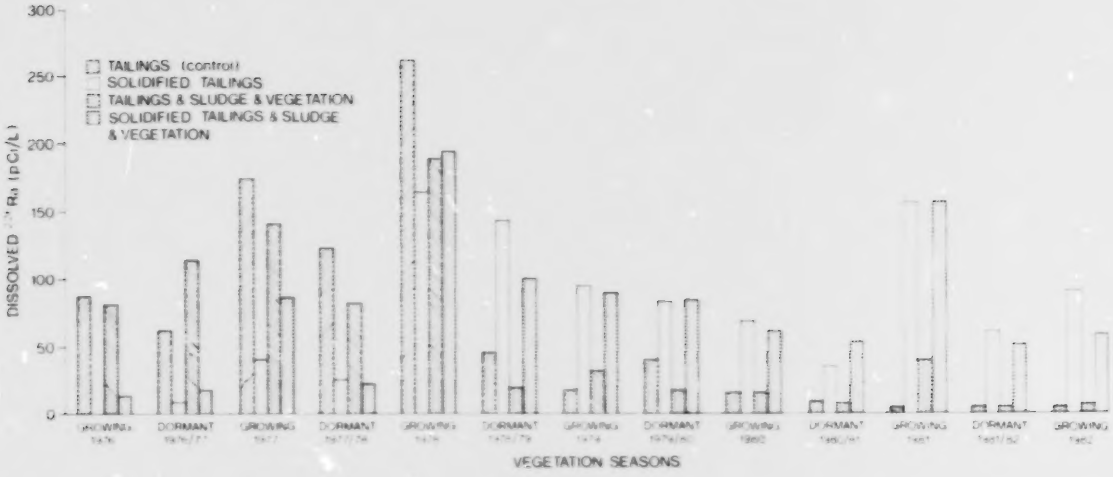

FIGURE 41 EXPERIMENT 3: AVERAGE SEASONAL DISSOLVED Ra-226 IN LEACHATES

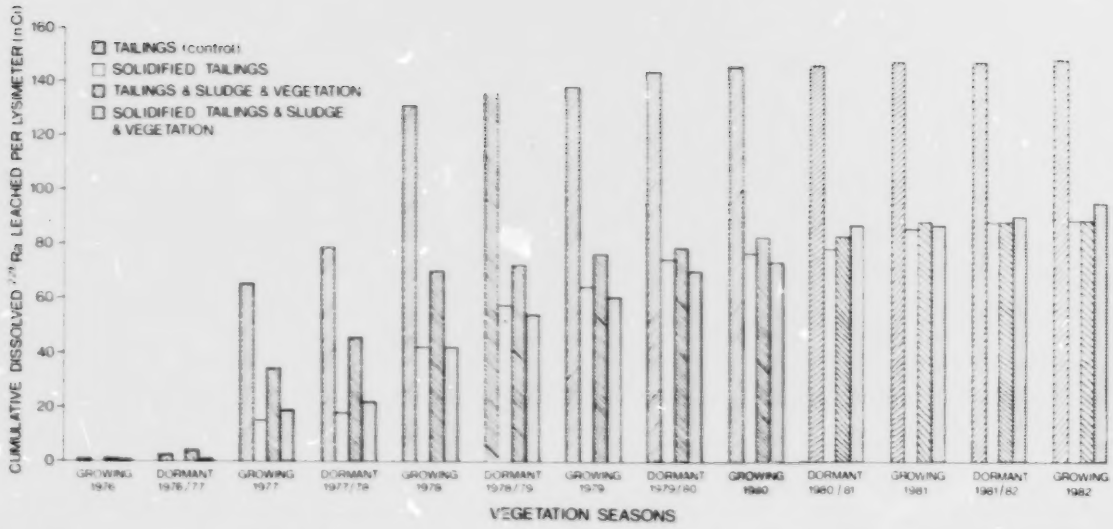

FIGURE 42 EXPERIMENT 3: CUMULATIVE DISSOLVED Ra-226 IN LEACHATES

Dissolved Pb-210 levels in leachates from all solidified tailings remained less than the detectable limit of 15 pCi/L (0.56 Bq/L) throughout the study. Pb-210 levels in leachates from fresh tailings increased from less than 15 pCi/L (0.56 Bq/L), to maximum values of 680 pCi/L (25.2 Bq/L) for the controls during the 1978 growing season and 470 pCi/L (17.4 Bq/L) for the vegetated tailings during the 1977/78 dormant season (Table 13). These peaks occurred concurrently with peaks in Ra-226 levels and initial decreases in leachate pH. By the end of the study, dissolved Pb-210 levels had decreased to approximately 20 pCi/L (0.74 Bq/L) in the control leachates and to less than 15 pCi/L (0.56 Bq/L) in the vegetated tailings leachates.

TABLE 13 EXPERIMENT 3: Pb-210 LEVELS IN LEACHATES

	Average Dissolved Levels			
	Fresh Tailings		Vegetated Tailings	
Season	pCi/L	Bq/L	pCi/L	Bq/L
Growing 1976	< 15	< 0.56	< 15	< 0.56
Dormant 1976/77	< 15	< 0.56	< 15	< 0.56
Growing 1977	< 15	0.56	< 15	0.56
Dormant 1977/78	210	7.77	470	17.4
Growing 1978	680	25.2	230	8.51
Dormant 1978/79	NA		NA	
Growing 1979	40	1.48	300	11.1
Dormant 1979/80	110	4.07	140	5.18
Growing 1980	115	4.26	23	0.85
Dormant 1980/81	240	8.88	< 15	< 0.56
Growing 1981	40	1.48	< 15	< 0.56
Dormant 1981/82	83	3.07	< 15	< 0.56
Growing 1982	24	0.89	< 15	< 0.56

NA = data not available
Pb-210 levels in leachates from all solidified tailings were less than 15 pCi/L (0.56 BqL) throughout the study

Dissolved thorium concentrations in leachates were only measured during the second half of the study. The average levels during each season are given in Table 14.

TABLE 14 EXPERIMENT 3: THORIUM LEVELS IN LEACHATES

	Seasonal Average Dissolved Levels (pCi/L)*						
	Growing 1979	Dormant 1979/80	Growing 1980	Dormant 1980/81	Growing 1981	Dormant 1981/82	Growing 1982
Th-232							
Fresh Tailings	9200	13000	1420	1660	1100	74	65
Solid. Tailings	1	< 1	< 1	< 1	< 1	< 1	< 1
Veg. Tailings	5200	8100	3060	1150	1600	455	515
Solid. Veg. Tailings	4	1	< 1	< 1	< 1	< 1	< 1
Th-230							
Fresh Tailings	94000	150000	12400	15000	8620	680	551
Solid. Tailings	5	< 1	2	5	3	< 1	1
Veg. Tailings	53000	104000	28500	12000	16200	4350	5140
Solid. Veg. Tailings	46	< 1	1	8	1	< 1	1
Th-228							
Fresh Tailings	4200	7700	2770	2130	4300	330	526
Solid. Tailings	3	< 1	1	2	5	< 1	< 1
Veg. Tailings	2300	4100	2070	2080	2670	430	903
Solid. Veg. Tailings	5	2	2	1	< 1	< 1	2

* 1 pCi/L = 0.037 Bq/L

Levels in leachates from the solidified tailings were very low throughout the monitoring period; most measurements were less than 5 pCi/L (0.19 Bq/L). Levels in the fresh tailings leachates, however, decreased between 1 and 3 orders of magnitude. Up until the 1980/81 dormant season, thorium levels were generally higher in leachates from the controls than from the vegetated tailings. This trend was reversed during the last 2 years of the study, so that, by the 1982 growing season, levels were two to ten times higher in the vegetated tailings leachates than in the control leachates.

TABLE 15 EXPERIMENT 3: CONCENTRATIONS OF VARIOUS CONSTITUENTS IN LEACHATES (mg/L)

Constituents	Treatments	Vegetation Seasons												
		Growing 1976	Dormant 1976/77	Growing 1977	Dormant 1977/78	Growing 1978	Dormant 1978/79	Growing 1979	Dormant 1979/80	Growing 1980	Dormant 1980/81	Growing 1981	Dormant 1981/82	Growing 1982
Aluminum	Tailings	0.16	0.08	0.15	0.23	3.0	86.0	428	350	203	--	--	49.0	45.0
	Solid. Tailings	4.6	3.04	0.90	0.30	0.6	--	0.44	< 0.1	< 0.2	--	< 0.1	< 0.1	< 0.1
	Veg. Tailings	0.13	0.08	7.32	22.0	193	264	147	612	237	--	78.0	38.0	46.0
	Veg. Solid. Tailings	5.1	2.19	0.31	0.25	0.5	0.01	0.2	< 0.1	< 0.2	--	< 0.1	< 0.1	< 0.1
Cadmium	Tailings	< 0.002	0.003	0.002	--	0.043	0.040	0.034	< 0.04	< 0.02	--	--	0.005	0.009
	Solid. Tailings	< 0.002	< 0.002	< 0.002	--	0.003	--	< 0.002	< 0.04	< 0.04	--	< 0.002	< 0.002	0.002
	Veg. Tailings	0.015	0.010	0.008	--	0.080	0.106	0.064	0.071	0.19	--	0.025	0.016	0.010
	Veg. Solid. Tailings	< 0.002	< 0.002	< 0.002	--	0.002	< 0.001	< 0.002	< 0.04	< 0.02	--	< 0.002	0.002	0.002
Calcium	Tailings	630	547	522	500	570	600	513	546	407	--	--	420	420
	Solid. Tailings	4.0	8.18	8.14	3.8	320	--	256	315	197	--	315	315	294
	Veg. Tailings	690	640	564	520	580	600	607	525	407	--	525	399	567
	Veg. Solid. Tailings	17.0	4.68	54.6	12.4	400	420	352	462	364	--	504	378	546
Chromium	Tailings	0.05	0.03	0.02	--	0.05	0.22	0.67	2.5	2.24	--	--	0.2	< 0.1
	Solid. Tailings	0.06	0.04	0.02	--	0.01	--	0.02	< 0.1	0.02	--	< 0.1	< 0.1	< 0.1
	Veg. Tailings	0.05	0.03	0.03	--	0.50	0.50	2.93	--	14.0	--	2.8	1.2	0.8
	Veg. Solid. Tailings	0.14	0.05	0.03	--	< 0.01	0.02	0.02	< 0.1	0.03	--	< 0.1	< 0.1	< 0.1
Copper	Tailings	0.03	0.02	0.02	0.12	2.32	6.0	7.67	31.0	434	--	--	1.45	1.24
	Solid. Tailings	0.05	0.09	0.04	0.05	0.06	--	0.04	< 0.04	0.02	--	< 0.03	< 0.03	< 0.03
	Veg. Tailings	0.14	0.10	0.41	0.28	4.43	5.4	4.09	32.0	13.0	--	5.0	2.24	2.14
	Veg. Solid. Tailings	32.6	6.97	0.59	0.69	0.30	0.24	0.21	0.07	0.05	--	< 0.03	< 0.03	< 0.03
Iron	Tailings	0.28	0.32	0.42	--	33.0	240	1390	7410	9880	--	--	794	1060
	Solid. Tailings	0.60	0.51	0.25	--	0.2	--	0.93	0.10	1.01	--	< 0.1	< 0.1	< 0.1
	Veg. Tailings	0.23	0.22	0.22	--	314	750	1290	7410	3090	--	882	529	1765
	Veg. Solid. Tailings	0.48	0.34	0.43	--	0.40	0.20	0.68	< 0.1	1.53	--	< 0.1	< 0.1	< 0.1

TABLE 15 EXPERIMENT 3: CONCENTRATIONS OF VARIOUS CONSTITUENTS IN LEACHATES (mg/L) (Cont'd)

Constituents	Treatments	Vegetation Seasons												
		Growing 1976	Dormant 1976/77	Growing 1977	Dormant 1977/78	Growing 1978	Dormant 1978/79	Growing 1979	Dormant 1979/80	Growing 1980	Dormant 1980/81	Growing 1981	Dormant 1981/82	Growing 1982
Lead	Tailings	< 0.02	< 0.02	< 0.02	--	1.96	1.12	0.56	< 0.10	< 0.07	--	--	0.004	0.030
	Solid. Tailings	< 0.02	< 0.02	< 0.02	--	0.01	--	0.03	< 0.10	< 0.01	--	<0.002	<0.002	<0.002
	Veg. Tailings	< 0.02	< 0.02	< 0.02	--	1.70	1.16	0.66	< 0.10	< 0.07	--	0.004	0.006	0.005
	Veg. Solid. Tailings	< 0.02	0.05	< 0.02	--	0.02	< 0.01	< 0.02	< 0.10	< 0.01	--	<0.002	<0.002	0.002
Magnesium	Tailings	45.0	69.1	62.9	17.0	45.0	48.0	25.0	6.0	--	--	--	4.6	4.4
	Solid. Tailings	0.50	0.17	0.19	0.09	0.80	--	0.09	< 0.10	--	--	0.1	0.1	0.2
	Veg. Tailings	240	178	133	45.0	48.0	84.0	35.7	105	--	--	6.1	4.8	4.8
	Veg. Solid. Tailings	0.20	0.13	0.44	0.15	2.80	0.60	2.51	0.20	--	--	1.7	1.4	2.2
Manganese	Tailings	0.30	0.43	2.40	--	8.9	--	5.8	--	2.11	--	--	0.78	0.49
	Solid. Tailings	0.01	0.02	0.01	--	0.20	--	0.01	--	0.01	--	<0.03	<0.03	<0.03
	Veg. Tailings	1.80	1.85	4.48	--	5.40	--	4.80	--	6.77	--	2.23	1.19	1.18
	Veg. Solid. Tailings	< 0.01	< 0.01	0.03	--	0.20	--	0.01	--	0.01	--	<0.03	<0.03	<0.03
Nickel	Tailings	0.05	0.02	0.10	--	2.90	5.40	5.22	8.40	4.67	--	--	0.7	0.9
	Solid. Tailings	0.03	0.04	0.02	--	0.10	--	0.01	< 0.10	< 0.01	--	<0.1	<0.1	<0.1
	Veg. Tailings	0.04	0.04	0.38	--	3.60	4.30	2.27	8.90	2.89	--	1.0	0.5	1.5
	Veg. Solid. Tailings	0.62	0.51	0.25	--	0.20	0.10	0.05	< 0.10	< 0.01	--	<0.1	<0.1	<0.1
Zinc	Tailings	0.09	0.08	0.11	--	3.46	6.00	5.36	15.0	2.24	--	--	0.43	0.52
	Solid. Tailings	0.03	0.15	0.04	--	0.08	--	0.02	< 0.04	0.02	--	0.06	0.22	<0.03
	Veg. Tailings	0.10	0.14	0.48	--	9.46	14.6	9.09	67.0	14.0	--	3.36	1.33	1.18
	Veg. Solid. Tailings	0.02	0.14	0.04	--	0.42	0.02	0.03	< 0.04	0.03	--	<0.03	<0.03	<0.03

Metal concentrations in leachates from the fresh tailings generally remained relatively constant up to the 1978 growing season, increased to a peak at the 1980 growing season, and then decreased (Table 15). Metal concentrations were generally 1 to 3 orders of magnitude less in solidified tailings leachates than in fresh tailings leachates, with the exception of calcium. Calcium concentrations in leachates from fresh tailings decreased during the study, whereas those in leachates from solidified tailings generally remained less than 20 mg/L during the first 2 years, then increased to about 300 to 500 mg/L.

Variable results were obtained from the bioassay tests conducted on the leachates. In the initial tests on leachates collected during the 1976/77 dormant season:

- 100 percent mortality occurred to daphnia in leachates from solidified tailings,
- no mortality occurred in leachates from the controls, and
- 37.5 percent mortality occurred in leachates from the vegetated fresh tailings.

During the 1977 growing season, however, leachates from fresh tailings were 100 percent lethal to rainbow trout, whereas those from solidified tailings were 14 percent lethal. Similar variations in leachate toxicity were observed in subsequent tests.

Larger grass yields were obtained every growing season from grasses grown on the solidified tailings than on the fresh tailings (Table 16). Yields from the solidified tailings decreased by about 50 percent each year for the first three years, then stabilized at about 4 tonnes/ha for the balance of the study. Vegetation on the fresh tailings continually decreased in yield throughout the study, and had turned black and died by the end of the 1981 growing season.

TABLE 16 EXPERIMENT 3: GRASS YIELDS

Growing Season	Grass Yield (tonne/ha)	
	Fresh Tailings	Solidified Tailings
1977	13.0	15.2
1978	5.8	6.8
1979	2.1	3.6
1980	0.8	4.4
1981	0.08	5.1
1982	0.0	3.3

Seasonal average concentrations of Ra-226, Pb-210, Th-228, Th-230, and Th-232 in the grass cuttings were relatively constant throughout the study, and were not significantly different for grasses grown on fresh and solidified tailings (Table 17). Within each growing season, however, concentrations often varied widely particularly for Ra-226 and Pb-210, as indicated by the relatively large standard deviations in Table 17.

TABLE 17 EXPERIMENT 3: AVERAGE RADIONUCLIDE LEVELS IN GRASS CUTTINGS (pCi/g)*

Radio-nuclide	Tailings	Growing Season 1977	1978	1979	1980	1981	1982
Ra-226	Fresh	32.5(19.5)[1]	32.8(15.2)	22.5(9.3)	29.1(34.7)	22.5(13.4)	--[2]
	Solid.	11.3(4.0)	8.6(5.0)	9.1(5.9)	12.0(13.4)	11.7(4.9)	5.2(4.0)
Pb-210	Fresh	3.4(1.5)	3.2(1.5)	2.5(1.3)	2.9(3.6)	9.5(2.1)	--
	Solid.	1.9(1.0)	1.6(0.9)	1.2(0.5)	8.7(14.7)	29.7(31.5)	1.2(0.5)
Th-228	Fresh	1.5(0.7)	0.9(0.9)	2.0(0.8)	0.9(0.5)	--	--
	Solid.	1.0(0.7)	0.7(0.8)	0.7(0.0)	1.1(0.6)	0.8(0.5)	0.4(0.2)
Th-230	Fresh	0.2(0.1)	0.4(0.4)	3.6(1.8)	0.7(0.5)	--	--
	Solid.	0.3(0.2)	0.3(0.4)	1.0(1.1)	0.9(1.1)	0.3(0.2)	0.4(0.3)
Th-232	Fresh	<0.1(-)	<0.1(-)	0.5(0.1)	<0.1(-)	--	--
	Solid.	<0.1(-)	<0.1(-)	0.2(0.2)	<0.3(0.2)	<0.1(-)	<0.1(-)

* 1 pCi/g = 0.037 Bq/g

1. The standard deviation of each average is shown in brackets.
2. Vegetation on the non-fixed tailings had turned black and died by the end of the 1981 growing season.

6.3 Discussion

By the end of the study, the vegetated tailings had produced 12 percent more leachate than the controls, and the solidified tailings and the vegetated solidified tailings had produced 12 to 15 percent less leachate than the controls. Since equal amounts of water were added to the lysimeters, it appears that solidifying the tailings resulted in a decrease in leachate volume, whereas vegetating the tailings resulted in an increase. The opposite was expected from vegetated tailings because of evapotranspiration losses. One

hypothesis is that solidifying the tailings reduced the infiltration rate and allowed water falling on the tailings to become ponded and to evaporate readily; whereas in the non-solidified tailings, vegetation provided pathways for percolating water through the upper crust of the tailings and thus promoted infiltration. It is also possible that the differences were due to measurement or water application errors or both.

During the first 2 years, the pH of the control leachates remained at about 7, which is within the range usually found in active tailings impoundments. The pH then decreased to reach 2.2 by the end of the study. This decrease in leachate pH, and the accompanying increases in conductivity and metal concentrations, resulted from the initiation of pyrite oxidation in the tailings after the 1978 growing season. Calcium concentrations in leachates from the controls fluctuated between 500 and 630 mg/L during the first 4 years, then decreased. Iron concentrations increased after the third year to peak at 10 000 mg/L in Year 5. This suggests that gypsum (calcium sulphate) was dissolving during the entire leaching period and that about 3 years were required before the colonization of iron-oxidizing *Thiobacillus ferrooxidans* was sufficient or before residual carbonate was consumed to allow pyrite oxidation reactions to dominate leachate chemistry. Vegetation had little influence on pyrite oxidation rates, since the concentrations of most metals in leachates from the vegetated tailings were essentially the same as in leachates from the controls.

The pH of leachates from the solidified tailings was higher than the pH of the control leachates due to the alkaline nature of the chemical additives, and because solidification prevented oxidation of the tailings by chemically bonding or encapsulating the pyrite within a solidified matrix. The concentrations of most metals in leachates from the solidified tailings were lower than those observed in the fresh tailings leachates, indicating that dissolution and pyrite oxidation reactions were inhibited.

In 1978, leachate pH started to decrease and calcium and Ra-226 concentrations increased dramatically, suggesting that the encapsulation process was breaking down and thus allowing gypsum and Ra-226 dissolution to occur. That the increases in Ra-226 concentrations occurred simultaneously with increases in calcium concentrations, leads to the hypothesis that the source of Ra-226 was Ra-226 coprecipitated with gypsum in the final neutralization tank. Since leachate pH had only decreased to 8 by the end of the study, it appears that insufficient gypsum had dissolved to allow initiation of pyrite oxidation reactions.

The pattern of aluminum concentrations in the control leachates suggests that protons formed from pyrite oxidation reactions attack alumino-silicate minerals in the

tailings. The findings of Experiment 2 concur with this suggestion. The leaching patterns of the other metals are consistent with oxidation of sulphide minerals containing chromium, copper, nickel, and zinc. The pattern of decreasing magnesium concentrations with time suggests that magnesium is initially present as a magnesium sulphate ($MgSO_4$) which dissolves. Because magnesium can also be derived from an alumino-silicate, some magnesium in the leachates could have originated from the same minerals from which aluminum originated near the end of the leaching history.

Thorium concentrations in the fresh tailings leachates initially were high but decreased 2 to 3 orders of magnitude by 1982. Thorium concentrations in leachates from solidified tailings remained very low throughout the entire study. Because thorium was lost much faster from all tailings than calcium, thorium species (Th-230, Th-232, and Th-228), precipitated mainly as thorium hydroxides ($Th(OH)_{4(s)}$) in the final neutralization tank of the uranium mill, may not have been enmeshed in the gypsum precipitates. When placed in the tailings pile, they are rapidly solubilized when the solution becomes acidic. Thus thorium dissolution may occur even if gypsum dissolution is minimal. The low thorium levels in leachates from the fresh tailings at the end of the study suggest that most of the leachable thorium may have been removed.

Vegetated tailings with a fescue/red-top grass mixture to which a layer of sewage sludge was added as a nutrient and organic matter source, was unsuccessful over the long term. Leachate from the vegetated tailings became acidic as quickly as the control tailings, and the grasses died. This is probably due to acidic solution in the root zone, although the toxic effects of elevated metal concentrations cannot be completely discounted.

Vegetated tailings which had been treated with a proprietary solidification process were more successful. The grasses had not died by the end of the 7-year study; however, vegetation yields decreased during the first three years. This decrease was probably due in part to the loss of nutrients from the tailings, because no nutrients were added, after the initial application of sewage sludge, until the 1980 growing season. Whether the vegetation would be successfully maintained over a longer term is not known. Dissolution of the encapsulating material could permit the development of pyrite oxidation reactions and the subsequent destruction of the vegetation.

The results of the bioassay tests are questionable and difficult to interpret. The results are questionable because leachate pH was adjusted to 7.5 prior to testing. This may have caused many of the potentially toxic substances to precipitate. Since only the supernatant was used in the bioassay tests, the effect of the precipitated substances

on fish mortality was not measured. Furthermore, since leachate pH prior to adjustment ranged from 2.2 to 7.2 for the fresh tailings and from 7.1 to 11.7 for the solidified tailings, most of these leachates would have been lethal, because solutions with pH values of less than 5 and more than 9 are lethal to fish even without the presence of toxic metals (EIFAC, 1969). Thus, no general conclusions can be drawn regarding the toxicity of leachates from any of the lysimeters. As noted in Experiment 2, however, the radioactivity of the leachates does not appear to be a contributing factor, because of the low levels and the short exposure times.

6.4 Summary and Conclusions

Vegetation of freshly milled uranium tailings had little effect on pyrite oxidation rates and leachate characteristics, whereas solidification had a large effect. Pyrite oxidation occurred in the fresh tailings after about 3 years, resulting in decreased pH and increased metal concentrations. This did not occur in the solidified tailings, because either (1) the pyrite was chemically bonded or encapsulated within a solidified matrix or (2) the minerals formed by the solidification process buffered the pH at a high value. The pH of the fresh tailings decreased from an initial value of 7.2 to about 2.2 by the end of the study, whereas the pH of the solidified tailings decreased from 11.7 to 7.1. However, the decreases in pH and increases in calcium and Ra-226 concentrations in leachates from the solidified tailings suggest that the encapsulation process started to break down after a few years and allowed gypsum and Ra-226 dissolution to occur. Whether acidification would develop in the solidified tailings to the same extent as in fresh tailings requires further study.

7 EXPERIMENT 4: LEACHABILITY OF NEW TAILINGS SUBJECTED TO VARIOUS FLOW RATES

Experiment 4 was initiated to examine:

- the effects of various rates of percolation on the leaching characteristics of freshly milled tailings, particularly with respect to sulphate and Ra-226 levels, and
- the effect of alternate wetting and drying periods on leaching using two modes of water application: continuous water addition and single batch additions of an equivalent amount of water once a week.

The fresh tailings were obtained in 1978 from Madawaska Mine in Bancroft, Ontario and from Rio Algom Quirke Mine in Elliot Lake, Ontario (Figure 3). (A description of the tailings from the Rio Algom Quirke Mine was given in Section 6).

Madawaska Mines Limited is located in Faraday Township, approximately 6 km southwest of Bancroft, Ontario. Before its closure in 1982, the mine/mill complex produced and concentrated about 1 500 tonnes of ore daily, using an acid leach/ion exchange extraction process. The ore grade of 0.08 to 0.1 percent U_3O_8 is approximately the same as that at Elliot Lake, but pyrite is present in very minor quantities and does not constitute the same problem with acid production that it does at Elliot Lake.

7.1 Experimental Program

Twenty-four cylindrical acrylic lysimeters, 50 mm in diameter and ranging in length from 61 to 122 cm, were filled with 48 cm (940 cm^3) of tailings on top of a 4-cm glass wool plug (Figure 43). Longer cylinders were required for some lysimeters to provide sufficient containment volume during water addition. Twelve lysimeters each received 1.6 kg of fresh tailings from Madawaska Mine, and the other twelve each received 1.65 kg of fresh tailings from Quirke Mine. The lysimeters were located inside the Wastewater Technology Centre in Burlington, Ontario, and maintained at 18 to 20°C.

Beginning May 23, 1978, distilled water was added to the top of each set of twelve lysimeters by using two modes of water addition (one batch addition per week and continuous addition by means of a peristaltic pump) and six rates of water application (154, 301, 504, 1 008, 1 610 and 3 220 mL/week). Because similar chemical results were obtained from the lysimeters receiving water at the three lowest application rates, the 504 mL/week application rate was changed to 6 440 mL/week on October 31, 1978, and the 154 mL/week application rate was changed to 24 500 mL/week on November 9, 1978.

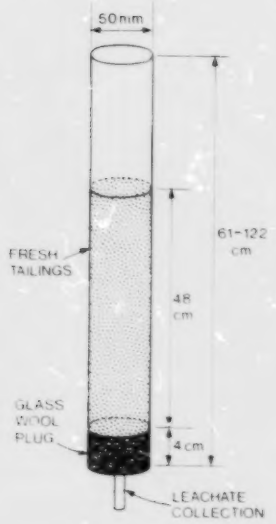

FIGURE 43 TYPICAL LYSIMETER USED IN EXPERIMENT 4

However, the rate of 24 500 mL/week could not be maintained and was discontinued on December 8, 1978. Water addition to the rest of the lysimeters ceased on January 5, 1981.

Leachate was collected from the bottom of each lysimeter, and composited samples were analyzed periodically for pH, conductivity, total solids, total sulphates (SO_4), and dissolved Ra-226.

7.2 Results

To assist in comparisons with data from other leaching studies, the results of the leachate analyses are plotted against cumulative pore volumes of leachate produced. If a porosity of 40 percent is assumed (Cherry, 1981), then one pore volume in each lysimeter was approximately equal to 0.4 L. Since the concentrations of most parameters became constant with time after 200 pore volumes of leachate production, most results are only plotted up to 250 pore volumes.

Average leachate production rates were less than the design water addition rates for all lysimeters, and were less from continuous mode lysimeters than from corresponding batch-mode lysimeters (Table 18). The amounts of water added by batch mode were equal to the design rates, and average losses of 7 to 9 percent occurred through evaporation. Average losses of 19 percent for the continuous-mode lysimeters

TABLE 18 EXPERIMENT 4: AVERAGE LEACHATE PRODUCTION RATES

Design Water Addition Rate (mL/week)	Average Leachate Production Rate* (mL/week)			
	Rio Algom		Madawaska	
	Batch	Continuous	Batch	Continuous
301	273	237	263	234
1008	939	841	914	830
1610	1491	1414	1488	1414
3220	3030	2629	3030	2667
6440 (114 wk)	6015	4720	5810	4702

* For 136 weeks unless otherwise indicated.

were due both to evaporation and to constrictions in the peristaltic pump tubing, preventing delivery of the rated pump flow.

7.2.1 Quirke Mine Tailings. The initial pH of leachates from all lysimeters containing fresh Quirke Mine tailings was approximately 8.0. This is within the range of 6.5 to 9.0 found in active tailings impoundments in the Elliot Lake area. Leachate pH decreased to 3 after 10 to 150 pore volumes (depending on the mode and rate of water addition), and remained between 2 and 3 for the balance of the study (Figure 44). Decreases generally occurred after fewer pore volumes in leachates from the batch-mode lysimeters than from continuous-mode lysimeters.

Leachate conductivities (Figure 45), total solids concentrations, and sulphate concentrations (Figure 46) followed the same pattern throughout the study. They decreased rapidly during the first 10 pore volumes, increased as leachate pH decreased, then remained relatively constant after 150 pore volumes of leachate production. In general, the magnitude of the increases was inversely related to the rates of water application. Higher concentrations were observed in leachates from the lower-rate lysimeters than from the higher-rate lysimeters at equivalent pore volumes. Increases were also larger for lysimeters receiving water by the batch mode.

The total masses of solids and sulphate released from each set of either batch-mode or continuous-mode lysimeters were approximately the same during the study, but were generally two to three times higher in batch-mode leachates (Table 19). Cumulative total solids mass and sulphate mass released from the lysimeters diverged when plotted

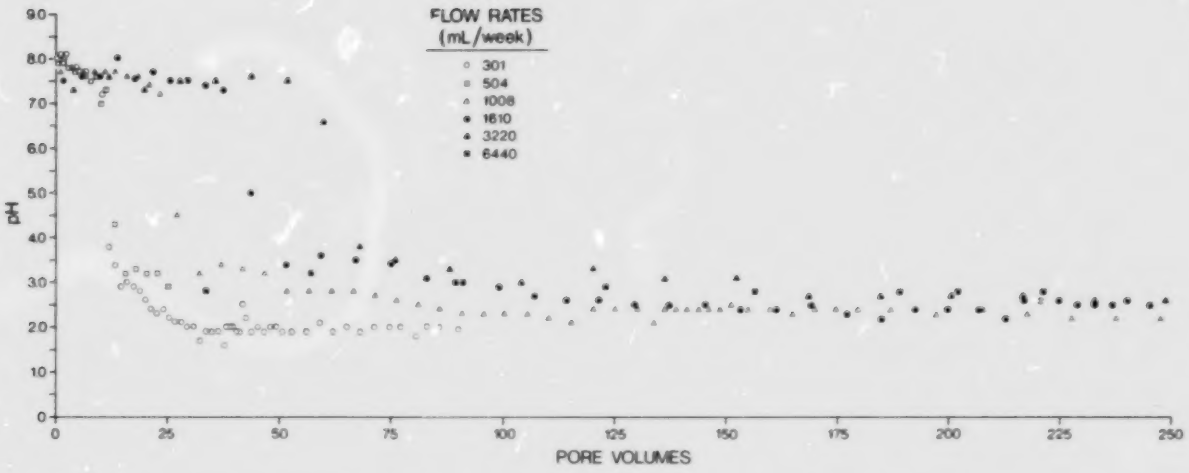

(a) Batch Water Addition

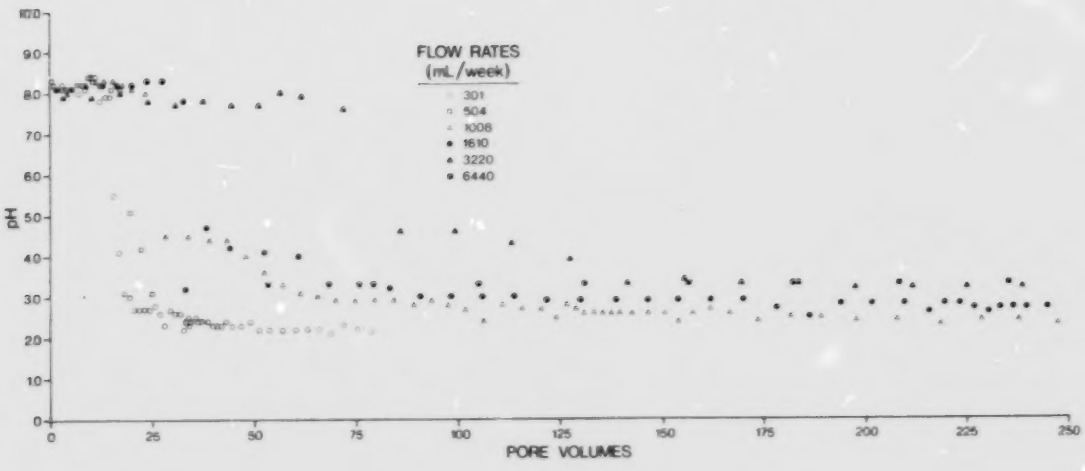

(b) Continuous Water Addition

FIGURE 44 EXPERIMENT 4: RIO ALGOM TAILINGS - PORE-VOLUMETRIC VARIATIONS IN LEACHATE pH

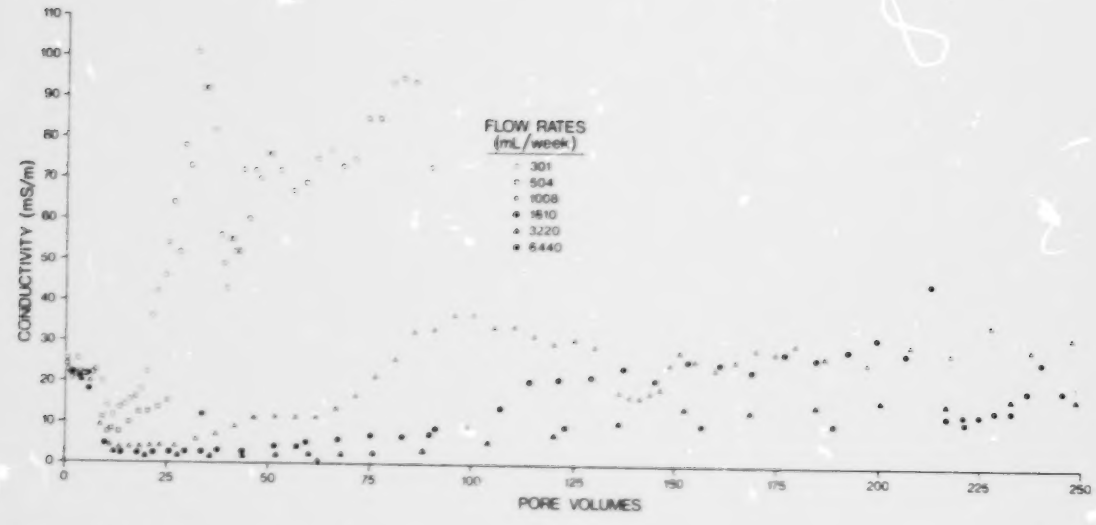

(a) Batch Water Addition

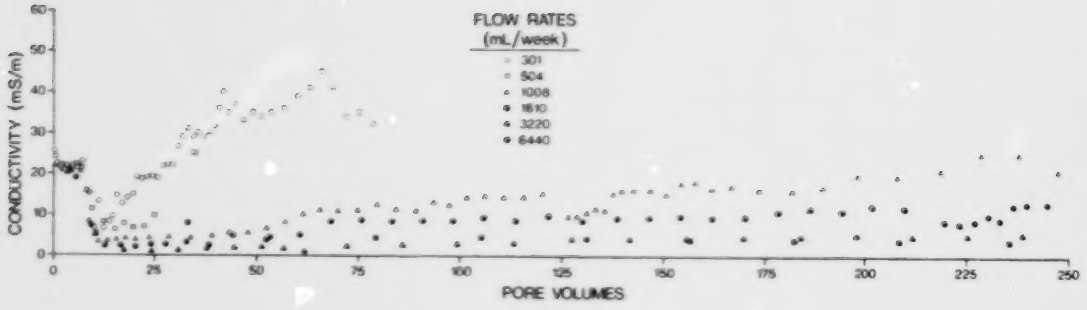

(b) Continuous Water Addition

FIGURE 45 EXPERIMENT 4: RIO ALGOM TAILINGS - PORE-VOLUMETRIC VARIATIONS IN LEACHATE CONDUCTIVITY

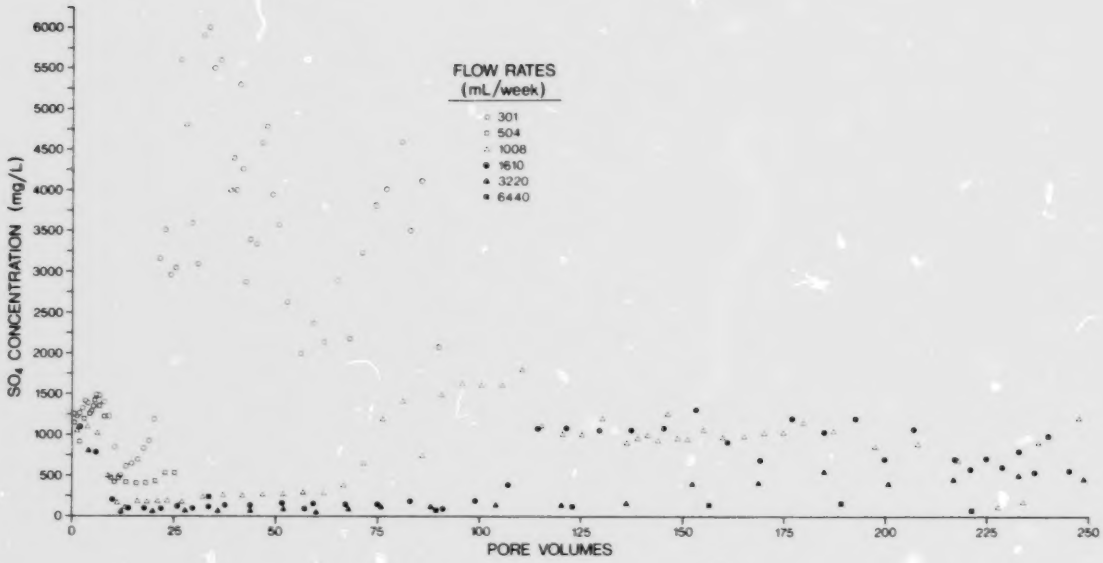

(a) Batch Water Addition

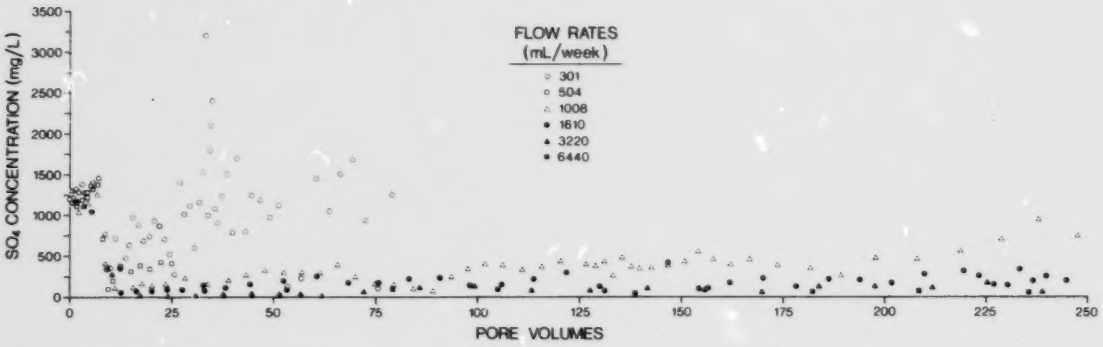

(b) Continuous Water Addition

FIGURE 46 EXPERIMENT 4: RIO ALGOM TAILINGS - PORE-VOLUMETRIC VARIATIONS IN SO_4 CONCENTRATIONS

TABLE 19 EXPERIMENT 4: CUMULATIVE Ra-226, SO_4 AND TOTAL SOLIDS MASS LEACHED DURING 136-WEEK STUDY PERIOD

Design Water Addition Rate (mL/week)	Average Cumulative Leachate Volume (L)		Dissolved Ra-226 Leached (nCi)*				Sulphate Mass Leached (g)				Total Solids Mass Leached (g)			
			Rio Algom		Madawaska		Rio Algom		Madawaska		Rio Algom		Madawaska	
	Batch	Cont.	Batch	Cont.	Batch	Cont.	Batch	Cont.	Batch	Cont.	Batch	Cont.	Batch	Cont.
301	36.4	32.1	2.9	2.7	11.0	8.8	115	34.0	26.0	25.1	317	96.0	55.5	54.3
1008	126	114	44.1	14.3	14.5	15.0	119	48.6	27.5	29.2	315	123	62.9	62.6
1610	203	192	75.3	43.4	15.4	25.9	153	50.0	26.7	26.0	369	131	70.2	68.1
3220	412	360	101	99.7	30.5	37.7	170	42.8	27.2	26.2	424	115	78.4	74.4
504 & 6440	685	548	106	140	52.8	37.5	129	44.3	32.6	29.3	384	103	82.2	72.2

* 1nCi = 37 Bq

against cumulative pore volumes of leachate (Figures 47 and 48), but converged when plotted against time (Figures 49 and 50).

Radium-226 levels generally fluctuated between 50 and 300 pCi/L (1.85 and 11.1 Bq/L) at the start of the study, increased to peaks of 900 pCi/L (33.3 Bq/L) in the batch-mode leachates and 700 pCi/L (25.9 Bq/L) in the continuous-mode leachates, then decreased to less than 100 pCi/L (3.7 Bq/L) (Figure 51). The start of the increase in levels generally corresponded to the achievement of acidic pH in the tailings, although this was more prevalent in the batch-mode leachates. Peaks and subsequent declines to Ra-226 levels less than 100 pCi/L (3.7 Bq/L) occurred earlier in the batch-mode leachates. The Ra-226 levels near the end of the study compare favourably to the levels of 35 to 100 pCi/L (1.3 to 3.7 Bq/L) measured in the in-situ abandoned Nordic tailings in 1979 (Blair et al., 1980).

The cumulative totals of dissolved Ra-226 released from the tailings during the study are given in Table 19, and are shown versus cumulative pore volumes of leachate production in Figure 52. Cumulative Ra-226 release patterns during the study were similar for batch-mode lysimeters at the three highest flow rates, particularly after 100 pore volumes, but were different for all other lysimeters. Total Ra-226 release at equivalent pore volumes from the continuous-mode lysimeters generally increased with increasing rate of water addition.

7.2.2 Madawaska Mine Tailings. Leachate pH was approximately the same at equivalent pore volumes for all lysimeters containing fresh Madawaska tailings (Figure 53). Values remained relatively constant at pH 8 during the first 200 pore volumes of leachate production, but then decreased slowly to pH 5 - 6 at 1 000 pore volumes.

Conductivities (Figure 54), total solids concentrations and total sulphate concentrations (Figure 55) in Madawaska leachates displayed the same trends during the study, with an initial rapid decrease during the first two pore volumes, a relatively constant period during the next 20 to 60 pore volumes, and then a gradual decrease. After 170 pore volumes, leachate conductivities had decreased to less than 1 mS/m, total solids concentrations had decreased to less than 100 mg/L, and sulphate to less than 10 mg/L. Most of the solids and sulphate were released during the first 100 pore volumes of leachate production (Figures 56 and 57). By the end of the study, each lysimeter had leached between 54 and 82 g of solids and between 25 and 33 g of sulphate, depending on the water addition rate used (Table 19).

Radium-226 levels decreased rapidly from 2200 to 900 pCi/L (81.4 to 33.3 Bq/L) during the first two pore volumes, decreased steadily to less than 100 pCi/L

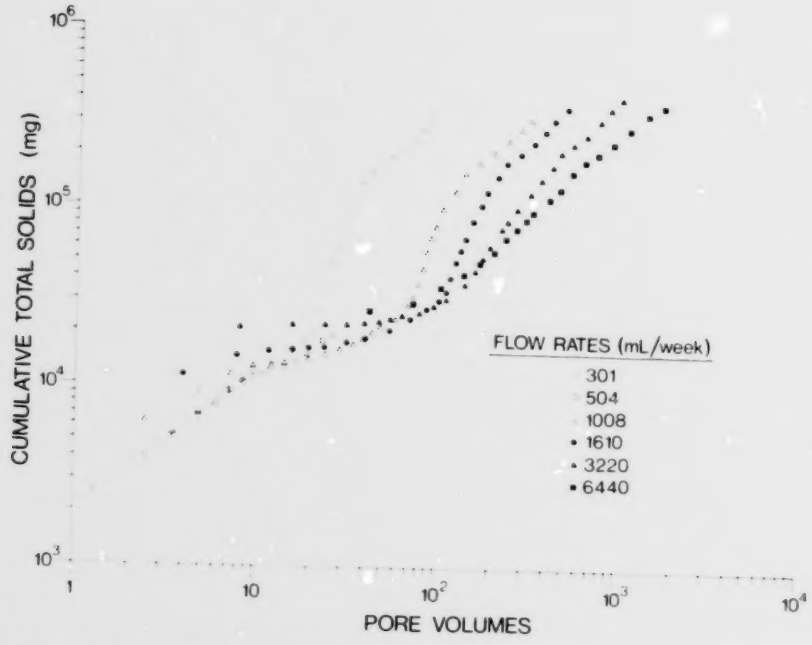

(a) Batch Water Addition

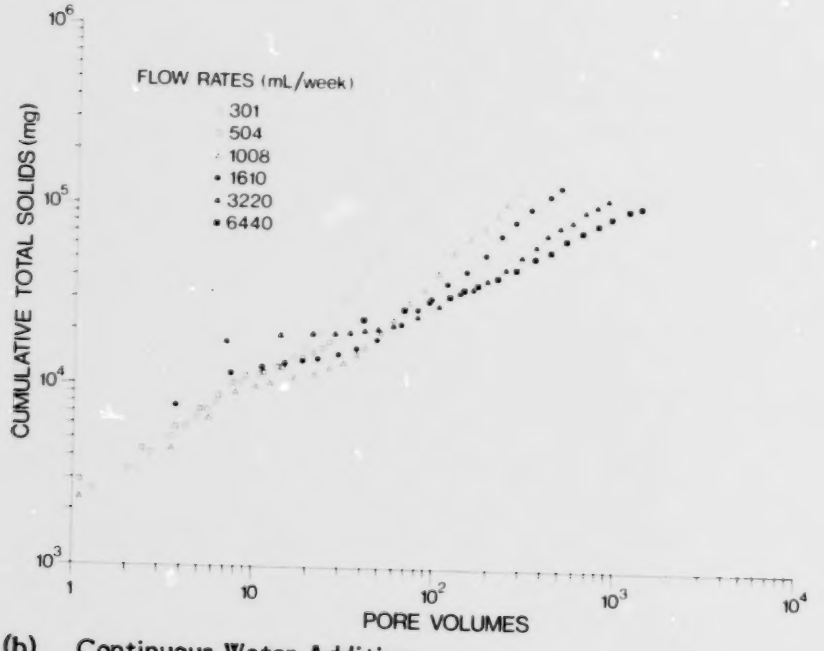

(b) Continuous Water Addition

FIGURE 47 EXPERIMENT 4: RIO ALGOM TAILINGS - CUMULATIVE MASS OF TOTAL SOLIDS LEACHED vs. PORE VOLUMES OF LEACHATE

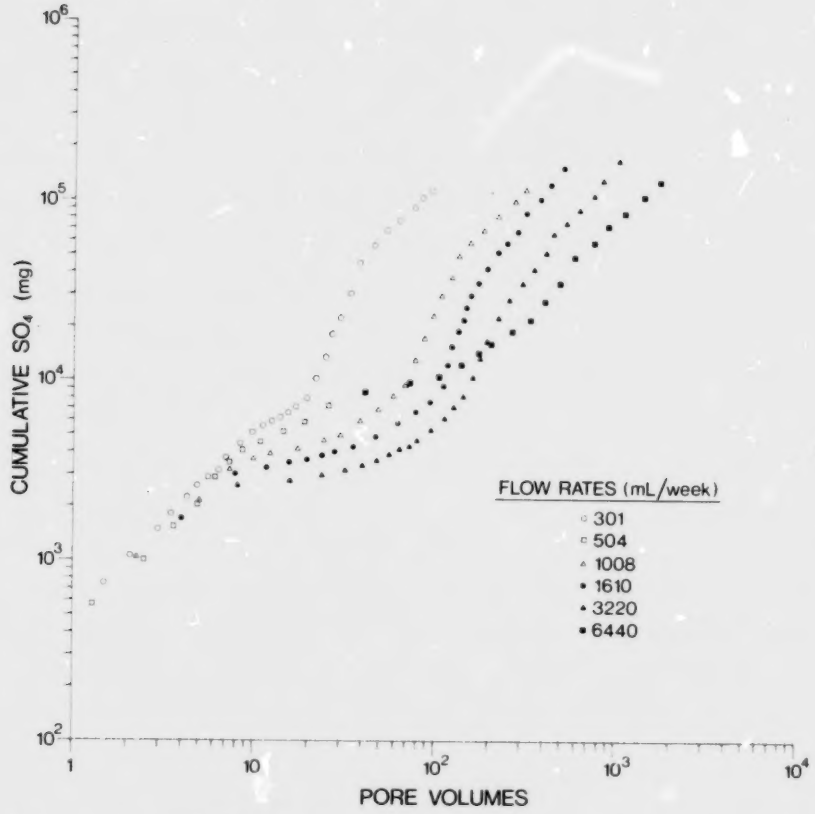

(a) Batch Water Addition

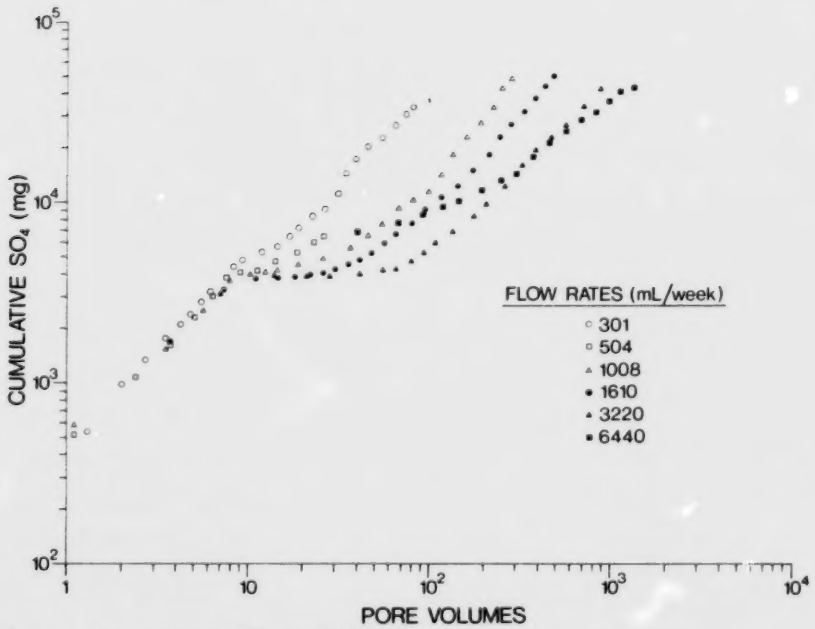

(b) Continuous Water Addition

FIGURE 48 **EXPERIMENT 4: RIO ALGOM TAILINGS - CUMULATIVE MASS OF SO_4 LEACHED vs. PORE VOLUMES OF LEACHATE**

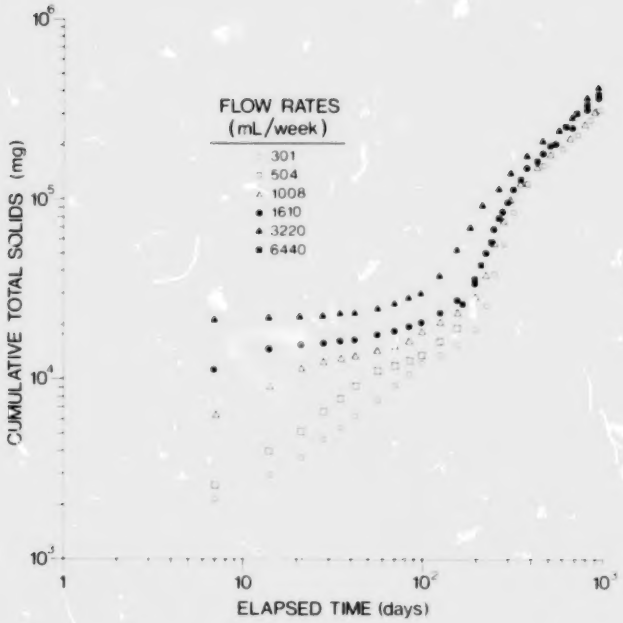

(a) Batch Water Addition

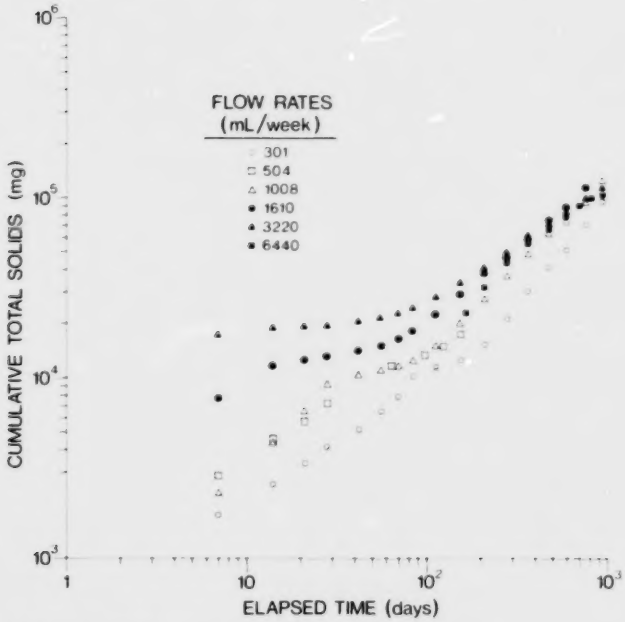

(b) Continuous Water Addition

FIGURE 49 EXPERIMENT 4: RIO ALGOM TAILINGS - CUMULATIVE MASS OF TOTAL SOLIDS LEACHED vs. ELAPSED TIME

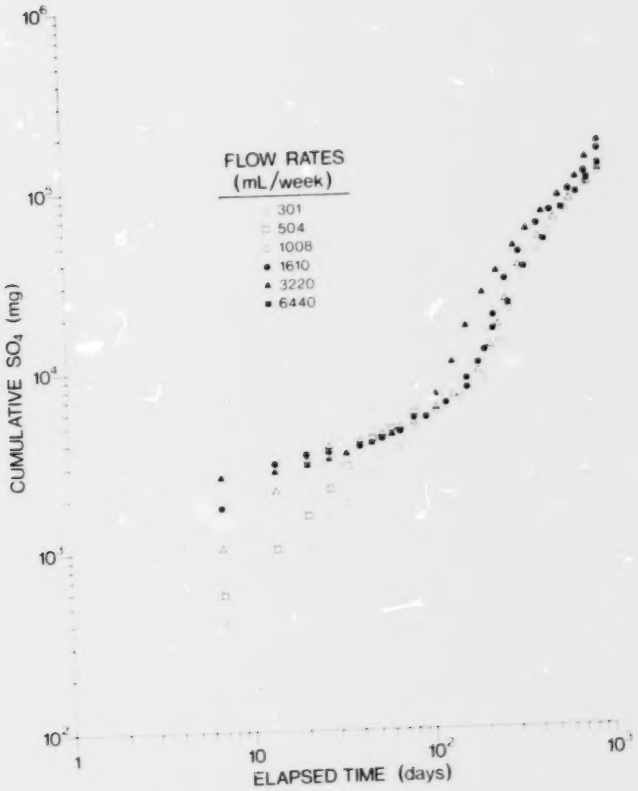

(a) Batch Water Addition

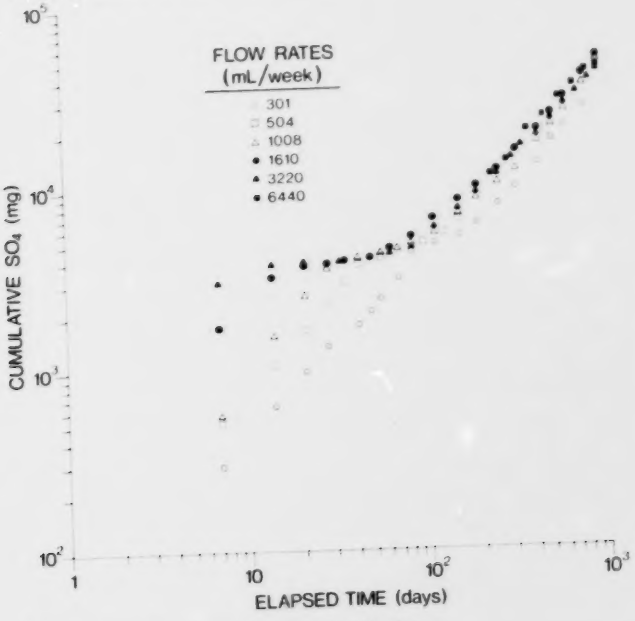

(b) Continuous Water Addition

FIGURE 50 EXPERIMENT 4: RIO ALGOM TAILINGS - CUMULATIVE MASS OF SO_4 LEACHED vs. ELAPSED TIME

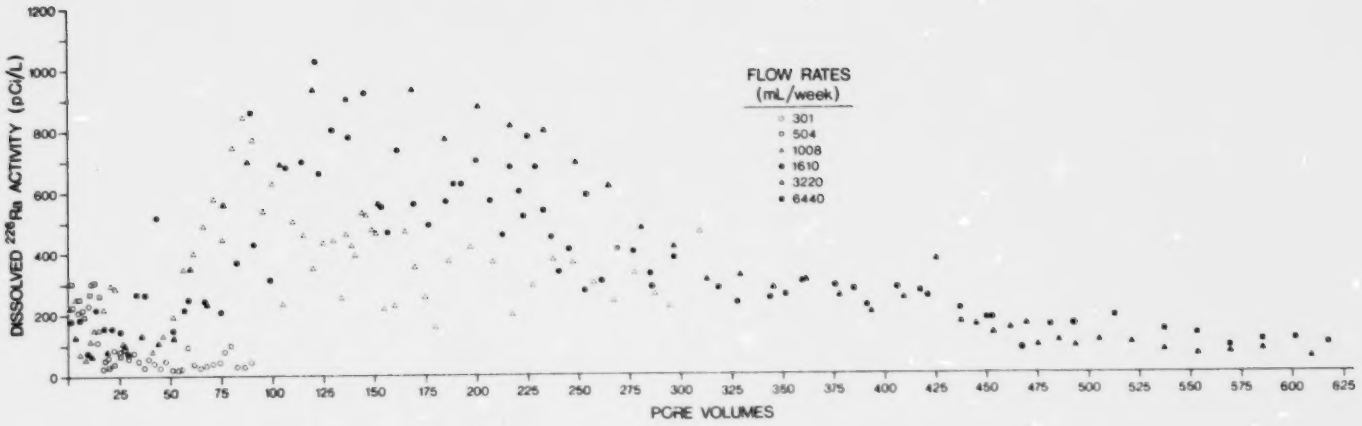

(a) Batch Water Addition

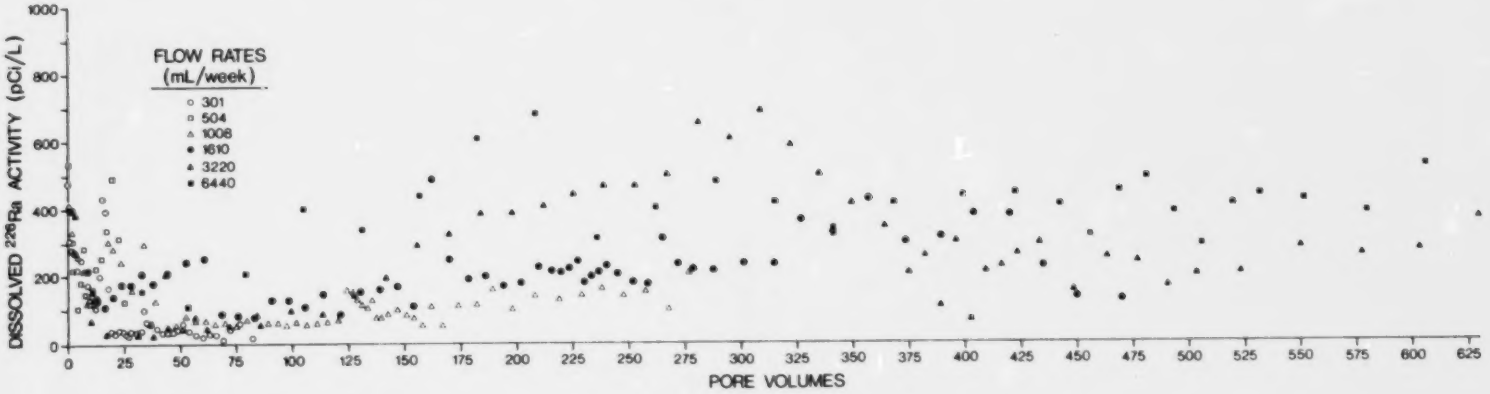

(b) Continuous Water Addition

FIGURE 51 EXPERIMENT 4: RIO ALGOM TAILINGS - PORE-VOLUMETRIC VARIATIONS IN DISSOLVED Ra-226

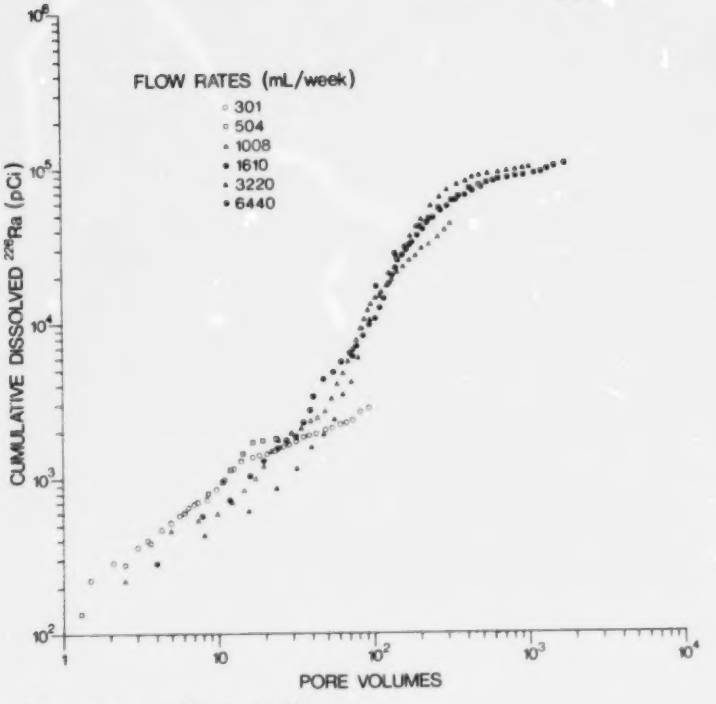

(a) Batch Water Addition

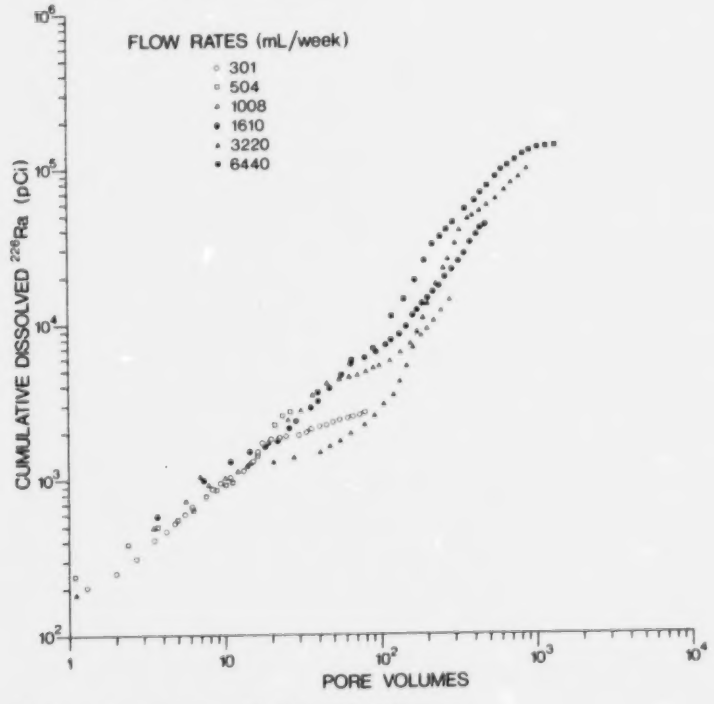

(b) Continuous Water Addition

FIGURE 52 EXPERIMENT 4: RIO ALGOM TAILINGS - CUMULATIVE DISSOLVED Ra-226 LEACHED vs. PORE VOLUMES OF LEACHATES

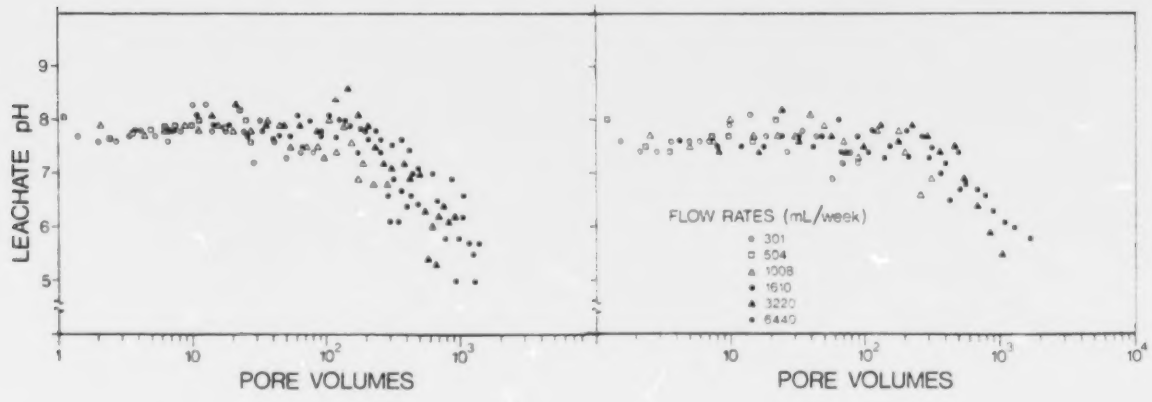

(a) Continuous Water Addition (b) Batch Water Addition

FIGURE 53 EXPERIMENT 4: MADAWASKA TAILINGS - PORE-VOLUMETRIC VARIATIONS IN LEACHATE pH

(3.7 Bq/L) after approximately 100 pore volumes, and then remained less than 100 pCi/L (3.7 Bq/L) for the balance of the study (Figure 58). The cumulative totals of dissolved Ra-226 released from the Madawaska tailings were identical for the batch-mode lysimeters and similar for the continuous-mode lysimeters at equivalent pore volumes (Figure 59). By the end of the study, each lysimeter had leached between 9 and 53 nCi (333 and 1960 Bq) of dissolved Ra-226, depending on the rate of water addition used (Table 19).

7.3 Discussion

One of the purposes of the experiment was to examine the effect of alternately wetting and drying the tailings on leachate characteristics, as opposed to keeping the tailings wet throughout the study. Since water addition to the batch-mode lysimeters was done once a week, however, and because a head of water was often maintained on the higher-rate batch-mode lysimeters for 2 or 3 days after water addition, these tailings never had an opportunity to dry out completely. It was not possible to determine whether the tailings in the other lysimeters had drained completely (i.e., whether they were in an unsaturated state) by the end of each weekly period. Based on the delayed decrease in leachate pH in the higher-rate Quirke Mine lysimeters (Figure 44), it appears that tailings in all lysimeters receiving water in excess of 1.0 to 1.5 L a week

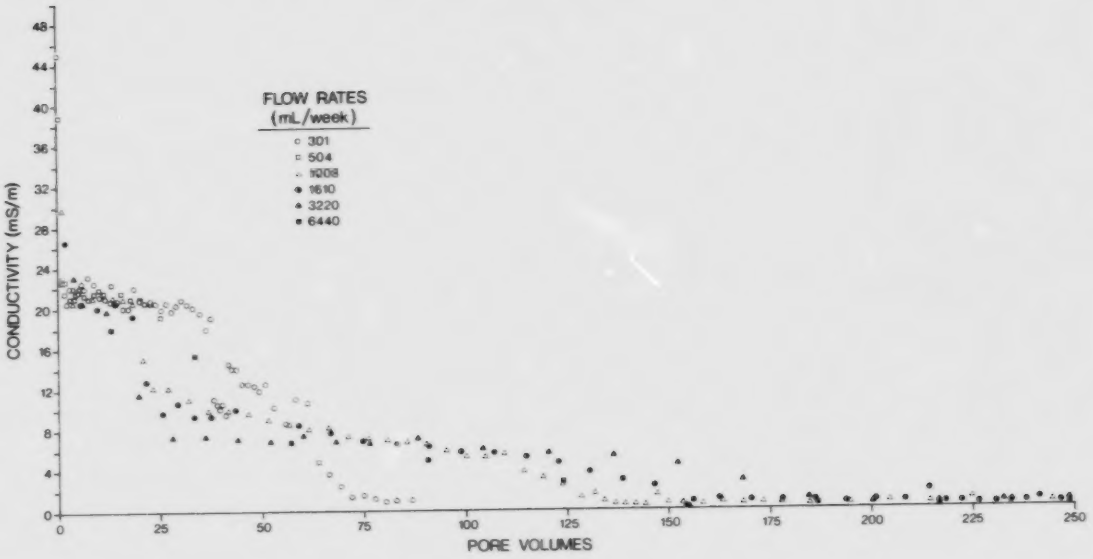

(a) Batch Water Addition

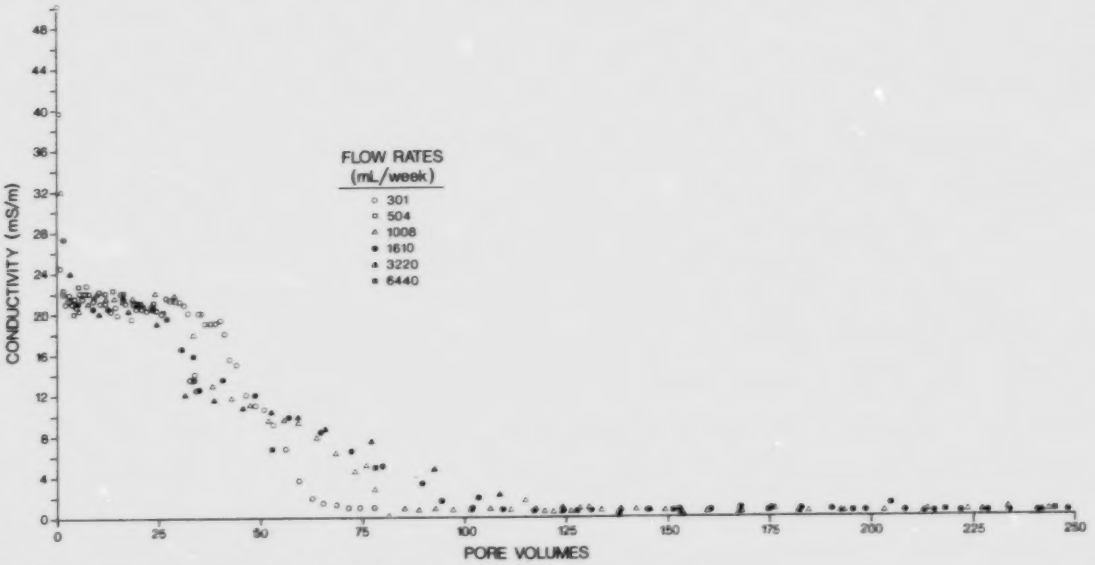

(b) Continuous Water Addition

FIGURE 54 EXPERIMENT 4: MADAWASKA TAILINGS - PORE-VOLUMETRIC VARIATIONS IN LEACHATE CONDUCTIVITY

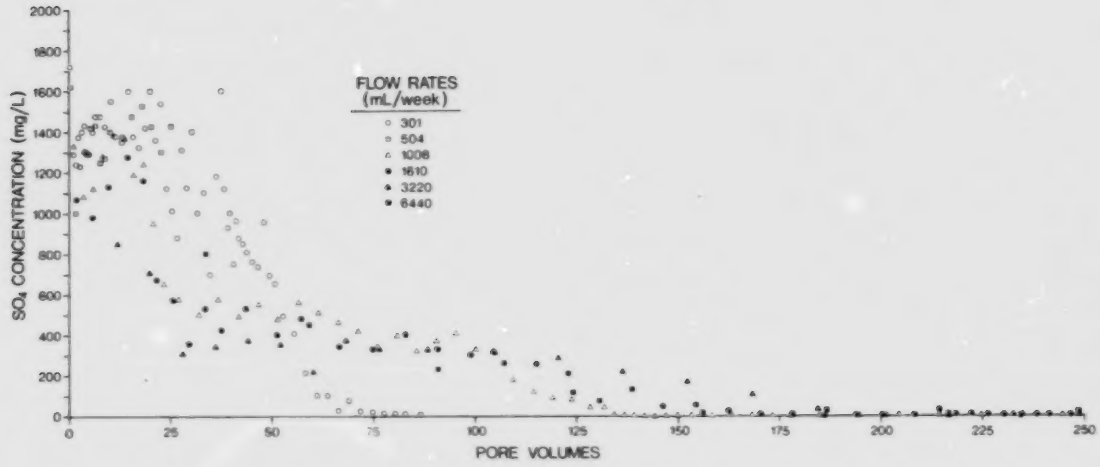

(a) Batch Water Addition

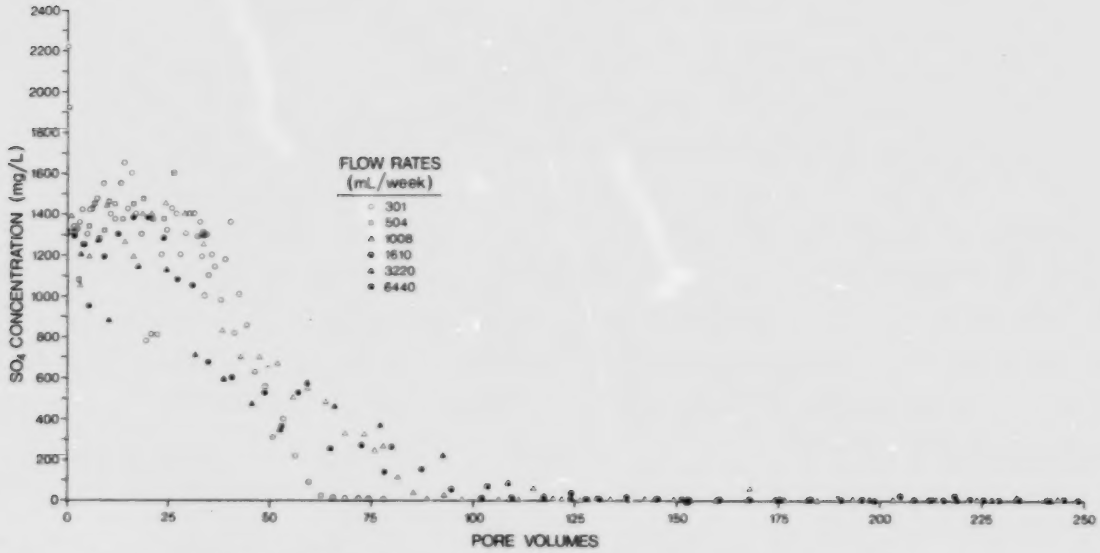

(b) Continuous Water Addition

FIGURE 55 EXPERIMENT 4: MADAWASKA TAILINGS - PORE-VOLUMETRIC VARIATIONS IN SO_4 CONCENTRATIONS

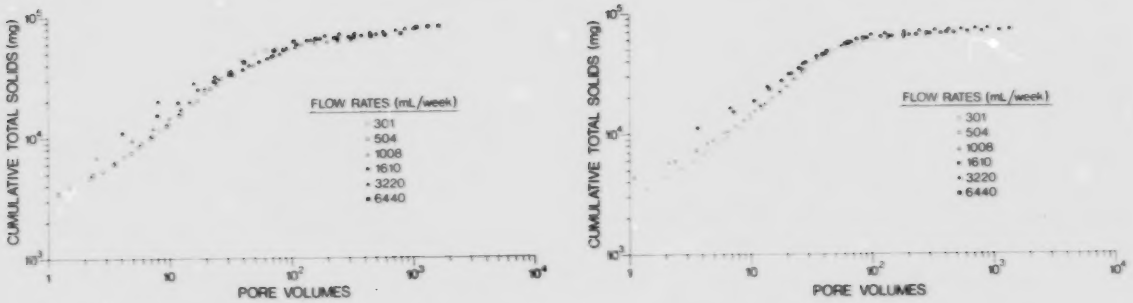

(a) Batch Water Addition (b) Continuous Water Addition

FIGURE 56 EXPERIMENT 4: MADAWASKA TAILINGS - CUMULATIVE MASS OF TOTAL SOLIDS LEACHED vs. PORE VOLUMES OF LEACHATE

(both by batch and by continuous modes of addition) were at least partially saturated at all times.

7.3.1 Quirke Mine Tailings. Leachate pH generally decreased more rapidly in the lysimeters receiving water at the lower rates and by batch mode. This suggests that microbial oxidation was established earlier in these lysimeters, probably because air diffusion was easier into the tailings that were mostly maintained in an unsaturated state. However, in Experiment 1, microbial oxidation was not significantly retarded when the flow rates to the lysimeters were increased so that the tailings were maintained in an intermittent saturated state. This suggests that higher flushing rates slow down the rate of colonization of tailings by *T. ferrooxidans*, but not the rate of oxidation once the bacteria are colonized, provided that a sufficient source of oxygen is available.

The initial decrease in conductivity, total dissolved solids concentrations, and sulphate concentrations in all leachates was probably caused by the flushing of readily soluble ions from the tailings. The decrease in sulphate concentrations is consistent with complete removal of the readily dissolvable portion of gypsum (thought to be that formed in the final neutralization tanks). At the same time, pyrite-oxidizing bacteria started to colonize the tailings. This resulted in increased sulphide oxidation, decreased pH, and

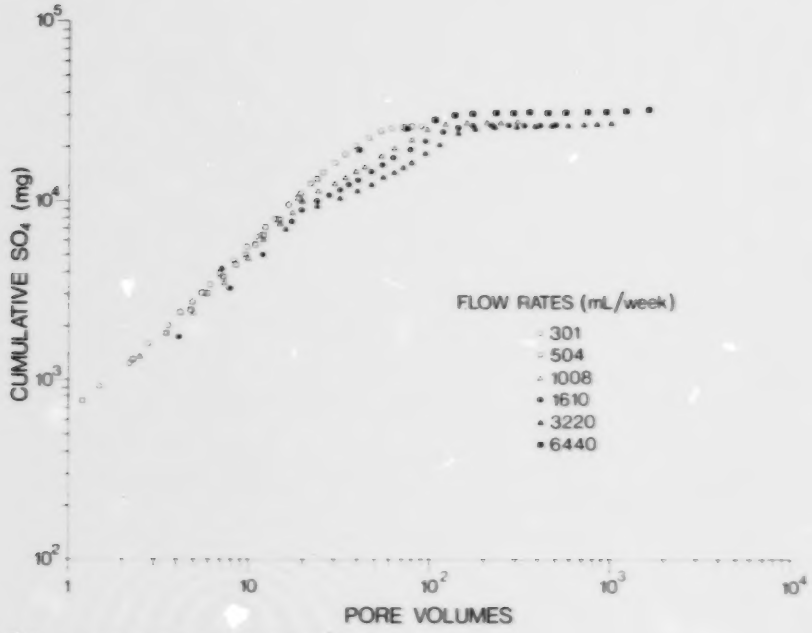

(a) Batch Water Addition

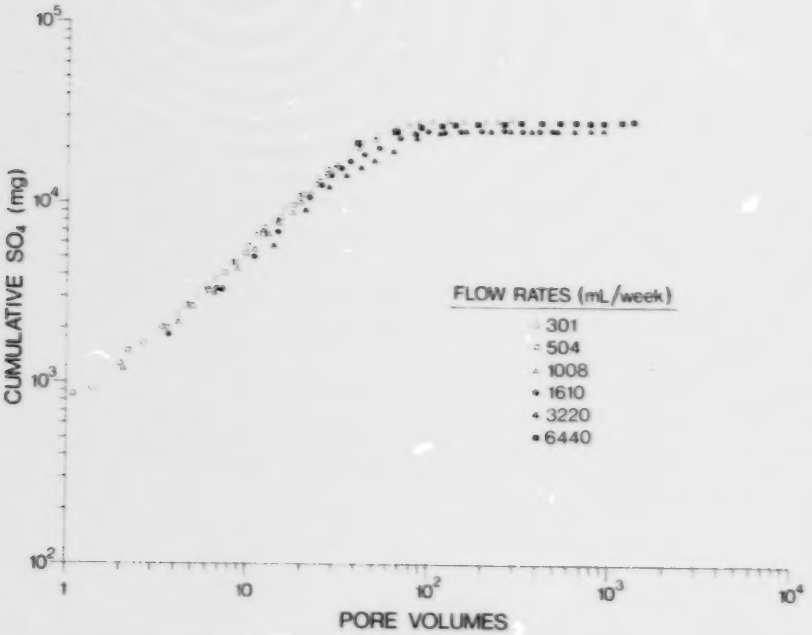

(b) Continuous Water Addition

FIGURE 57 EXPERIMENT 4: MADAWASKA TAILINGS - CUMULATIVE MASS OF SO_4 LEACHED vs. PORE VOLUMES OF LEACHATES

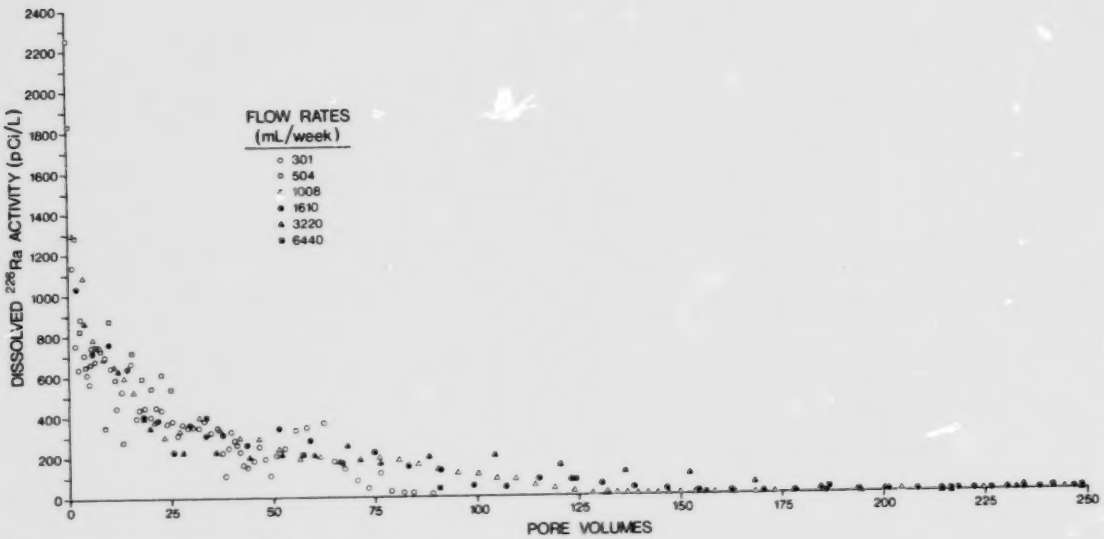

(a) Batch Water Addition

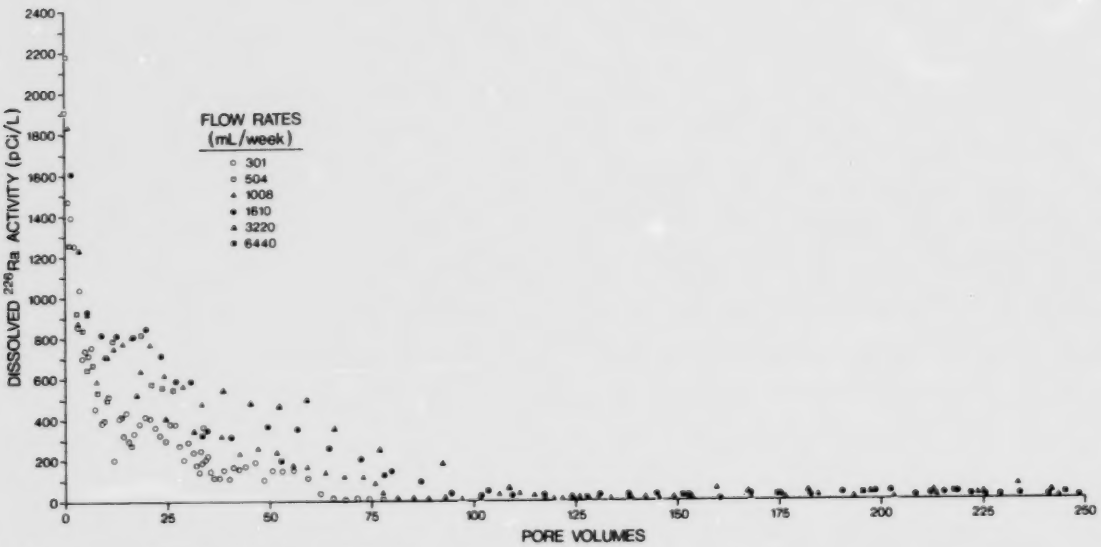

(b) Continuous Water Addition

FIGURE 58 EXPERIMENT 4: MADAWASKA TAILINGS - PORE-VOLUMETRIC VARIATIONS IN DISSLOVED Ra-226

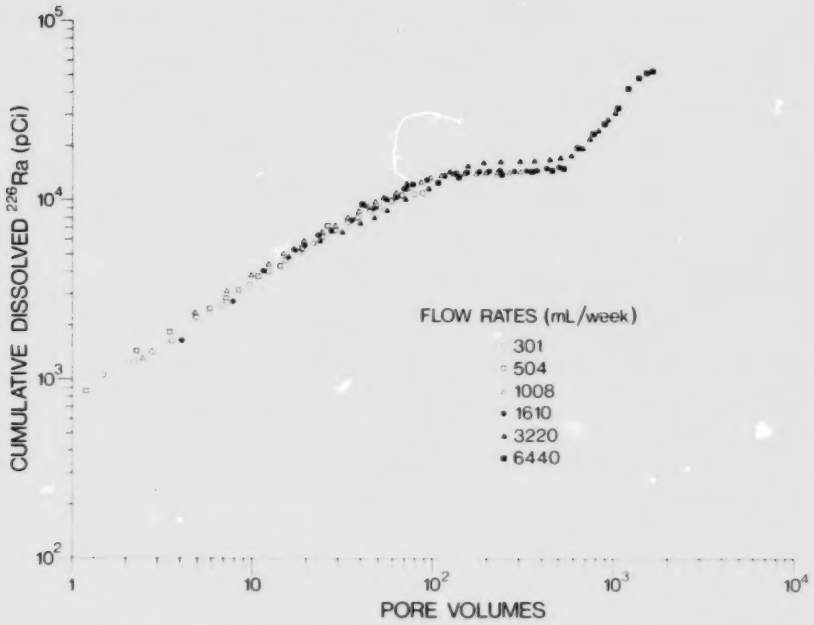

(a) Batch Water Addition

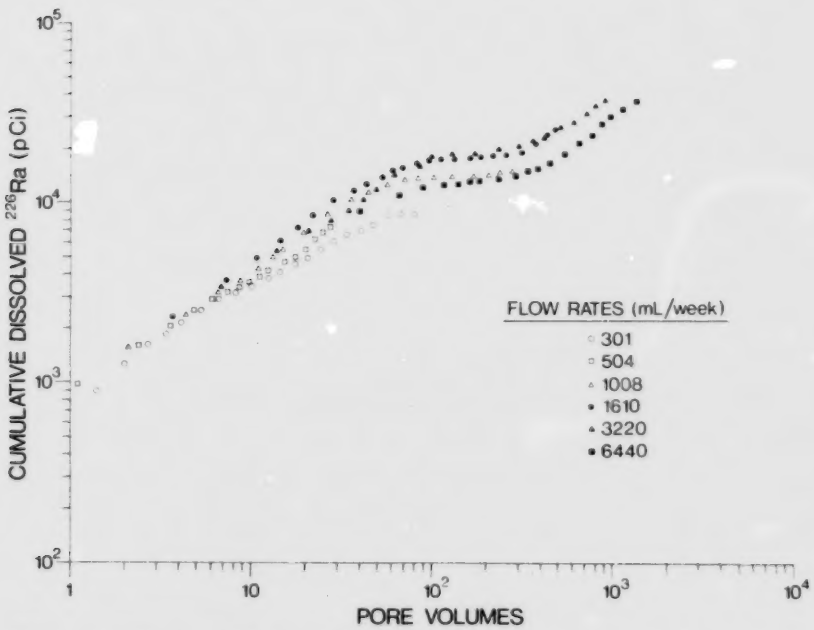

(b) Continuous Water Addition

FIGURE 59 EXPERIMENT 4: MADAWASKA TAILINGS - CUMULATIVE DISSOLVED Ra-226 LEACHED vs. PORE VOLUMES OF LEACHATES

increased sulphate and other dissolved ion concentrations. However, pH considerations alone do not appear to be sufficient to explain the much larger increases in conductivity and sulphate concentrations in the 301-mL/week lysimeters. Concentrations were at least twice as high in these leachates than in leachates from any of the other lysimeters.

The divergence of cumulative total solids mass and sulphate mass when plotted against pore volumes (Figures 47 and 48) and the convergence of these cumulative masses when plotted against time (Figures 49 and 50), indicate that solids release depends on time rather than flushing rate. This suggests that the concentration of total solids in a leachate depends on the contact time between the water percolating through a lysimeter and the tailings: the slower the water moves through the tailings, the more solids it dissolves and removes. Adding water intermittently to the lysimeters rather than continuously removed three to four times more solids and sulphate from the Rio Algom tailings. This may have resulted from pyrite-oxidizing communities being able to colonize earlier in the batch-mode lysimeters. This may also have occurred because a head of water was created over the batch-mode lysimeters which flushed very small particles through the tailings.

The observed Ra-226 patterns are consistent with the dissolution of mill-formed gypsum forms of Ra-226. The Ra-226 may be carried with the leach waters from the leaching pachucas and coprecipitated with gypsum in the partial and final neutralization tanks.

An extensive set of calculations is presented in Appendix A.1.2 describing the probable concentrations of different complexes in the leachates from the control lysimeters of Experiment 1. A similar, but more limited, set of calculations using REDEQL (Morel and Morgan, 1972) is given in the following paragraphs to determine whether TDS concentrations (assumed to be equal to total solids concentrations) and electroneutrality can be used to predict the pH of leachates from Experiment 4.

For leachates at the beginning of the study, all total dissolved solids in the leachates were assumed to be gypsum. Hence, the molar Ca^{2+} or SO_4^{2-} concentration was calculated as being equal to the measured total solids concentration divided by (40.1 + 96.1). It was also assumed that only gypsum dissolution controlled pH. These assumptions result in a predicted pH of 6.95 compared to observed values of 8.1 (Table 20). Under these conditions, about 24 percent of the TDS (Ca, SO_4) were predicted to precipitate. Furthermore, the SO_4^{2-}/TDS ratios for the initial leachates averaged 0.33 for the continuous systems and 0.34 for the batch systems. The actual value should be 0.7. The measured total solids concentrations were higher than the equilibrium solubility

TABLE 20 EXPERIMENT 4: ESTIMATION OF pH CONTROLLING MECHANISM (301 mL/week CONTINUOUS FLOW LYSIMETER)

Mechanism	pH		Comments*
	Observed	Predicted	
$CaSO_4$ dissolution	8.11±0.057	6.95	24% TDS (2830 mg/L) lost by $CaSO_4$ precipitation
$CaSO_4$ dissolution, plus carbonate alkalinity of 100 mg/L as $CaCO_3$	8.11±0.057	8.81	23.5% of Ca and 22.2% of SO_4 lost by precipitation

* Predictions were calculated by using measured TDS concentration and an assumed gypsum saturation state. Measured TDS concentrations probably over-estimated the actual TDS concentrations (see text), causing the model to predict Ca and SO_4 precipitation.

concentration of gypsum (about 2400 mg/L) and probably overestimated actual total solids concentrations. If at least two waters of hydration are assumed to form during evaporation (at 105°C) for total solids determinations, the measured total solids concentrations are high by 2 x 18/(2 x 18 + 40.1 + 96.1) or 21 percent. These waters of hydration are lost from gypsum at 175°C. Factoring these waters of hydration into the calculation means that the TDS value used for calculating pH should be 21 percent lower and that only a marginal amount of TDS would precipitate, a condition consistent with leachate being at equilibrium with gypsum.

Because the predicted pH is lower than the observed pH, some other buffering system (e.g., carbonate system) could have influenced the initial pH. This possibility was examined by performing a second calculation for which 10^{-3} M of total inorganic carbon was assumed to be present (equivalent to a carbonate alkalinity of 100 mg/L as $CaCO_3$). The predicted pH of 8.8 (Table 20) is closer to the observed pH of 8.1, indicating that carbonate is influencing pH. A more precise series of calculations would be required to ascertain the composition of the solution that gives the observed pH of 8.1.

For leachates at the middle and end of the study, when the pH was less than 5, the TDS was assumed to be an iron sulphate (with an Fe:S ratio of 1:2). For leachates near the middle of the study, predicted and observed pH values agree, if it is assumed that no $Fe(OH)_{3(s)}$ forms (Table 21). However, near the end of lysimeter operation, agreement occurs only if it is assumed that $Fe(OH)_{3(s)}$ precipitation does occur.

TABLE 21 EXPERIMENT 4: COMPARISON OF CALCULATED AND OBSERVED pH AND TDS FOR RIO ALGOM TAILINGS (CONTINUOUS FLOW)

Time Period	Lysimeter Flow (mL/week)	Observed pH	Calculated pH				Percent TDS Loss by $Fe(OH)_{3(s)}$ Precipitation	
			pE>13, no $Fe(OH)_{3(s)}$	pE>13, with $Fe(OH)_{3(s)}$	pE = 10, no $Fe(OH)_{3(s)}$	pE = 10, with $Fe(OH)_{3(s)}$	pE>13	pE = 10
Days 224 to 373	301	2.70±0.19	2.64	2.30	3.23	2.73	17.2	8.1
	1008	2.78±0.14	2.76	2.40	3.33	2.83	32.2	13.9
	1610	2.85±0.11	2.89	2.43	3.39	2.89	45.2	19.5
	3220	3.13±0.085	3.03	2.60	3.47	2.97	62.0	28.4
	6440	3.24±0.14	3.12	2.74	3.55	3.05	74.0	37.9
Days 620 to 950	301	2.22±0.075	2.67	2.32	3.28	2.78	16.2	7.4
	1008	2.40±0.064	2.80	2.44	3.29	2.88	31.7	13.3
	1610	2.56±0.14	2.88	2.50	3.44	2.94	45.4	18.3
	3220	2.76±0.086	3.10	2.72	3.58	3.08	71.2	33.1
	6440	2.97±0.18	3.33	2.99	3.71	3.22	86.1	52.0

Similar calculations were also carried out to examine whether the iron actually leaves the lysimeter in the 2+ or 3+ oxidation state. The results, given in Table 21, show that the predicted pH is considerably higher than the observed pH, if the pE is assumed to be 10 and more iron is present as Fe^{2+} than as Fe^{3+}. This suggests that the iron must be essentially in the 3+ state.

The question arises whether it is reasonable to consider iron hydroxide precipitation to explain the pH of the lysimeters during the later stages. The percentage of TDS lost by $Fe(OH)_{3(s)}$ precipitation is given in Table 21 for those cases in which precipitation is thought to occur. The proportion to precipitate is extremely high in the high-rate lysimeters but not unreasonable in the low-rate lysimeters. The proportion of iron which is tied up with different complexes is given in Table 22, both with and without assuming the occurrence of iron hydroxide precipitation. The large fraction of iron tied up with soluble hydroxo-polymeric forms of iron (Fe^{3+} with OH), when precipitation is prevented in the calculations, becomes an iron hydroxide solid when precipitation is allowed to occur. Because thermodynamic equilibrium is assumed in the speciation calculations, kinetics rather than thermodynamics may actually control the speciation of iron. This would apply particularly in the high-rate lysimeter, since it is unlikely that large amounts of iron hydroxide precipitates are continuously carried from the lysimeter. Furthermore, the values for TDS are probably high because of the formation of waters of hydration during evaporation for the TDS measurements, as noted before.

Therefore, the observed TDS and pH patterns of the Quirke Mine tailings for pH values in the 2.5 to 3.3 range can be explained on the basis of an iron sulphate system. Nevertheless, the kinetics of $Fe(OH)_{3(s)}$ precipitation, the concentration of intermediate hydroxo-polymeric complexes of iron (e.g., $Fe_2(OH)_2^{4+}$, etc.) and the possibility of colloidal $Fe(OH)_{3(s)}$ in the leachate, are also influential in determining the actual pH. A more involved analysis of Fe^{3+} hydrolysis kinetics and Fe^{3+} polymeric species, and more precise data giving the concentration of iron and other major cations and anions, is required to give more accurate predictions of pH than are given here.

7.3.2 Madawaska Mine Tailings. Leachate pH in all Madawaska lysimeters followed the same trend: the pH remained constant at about 8 during the first 200 pore volumes of leachate production, and then decreased slowly to 5-6 at 1 000 pore volumes (Figure 53). This is in marked contrast to the Quirke Mine leachate pH, which decreased rapidly from 8 to 3 within the first 150 pore volumes. The differences can be attributed to the different pyrite contents of the two tailings. Pyrite is present in only very small quantities in the Madawaska tailings, whereas it constitutes between 2 and 7 percent of

TABLE 22 EXPERIMENT 4: TYPICAL PREDICTED COMPOSITION OF LEACHATE FROM RIO ALGOM TAILINGS

Species	Composition	
	301 mL/week	3220 mL/week
(a) Without $Fe(OH)_{3(s)}$ Formation (Days 224 to 378)		
Fe^{3+} - as free metal (%)	2.7	1.5
- combined with SO_4 (%)	69.1	15.2
- combined with OH (%)	28.2	83.4
SO_4^{2-} - as free ligand (%)	55.7	88.3
- combined with Fe^{3+} (%)	39.5	7.6
- combined with H^+ (%)	4.8	4.0
Total Fe (moles/L)	1.1×10^{-2}	8.1×10^{-4}
Total SO_4 (moles/L)	2.2×10^{-2}	1.6×10^{-3}
TDS (mg/L)	2790	328
Calculated pH	2.64	3.03
(b) With $Fe(OH)_{3(s)}$ Formation (Days 224 to 378)		
Fe^{3+} - as free metal (%)	2.8	0.8
- combined with SO_4 (%)	67.4	6.9
- combined with OH (%)	12.7	18.3
- as $Fe(OH)_{3(s)}$ (%)	17.2	74.0
SO_4^{2-} - as free ligand (%)	52.0	88.3
- combined with Fe^{3+} (%)	38.1	3.4
- combined with H^+ (%)	9.9	8.3

the Quirke Mine tailings. The Quirke Mine tailings thus have a greater potential to become acidic through the generation of sulphuric acid by the oxidation of pyrite. Therefore pyrite oxidation never played a significant role in the Madawaska tailings.

The conductivity, total solids, and total sulphate concentration patterns observed in the Madawaska leachates are interpreted to mean that conductivity was completely dominated by the dissolution of gypsum. The patterns suggest that readily dissolvable gypsum, formed in the final neutralization tank, was dissolved during the first

part of the study and that a gypsum which was harder to dissolve (e.g., gypsum formed in the partial and final neutralization tanks) controlled conductivity during the second phase of the study. Because the pH never fell below 5 to 6, and because little pyrite existed in these tailings, no sulphate from pyrite oxidation existed in the leachates.

The cumulative mass of total solids and total sulphate released from each lysimeter was the same at equivalent pore volumes (Figures 56 and 57), indicating that their release from the Madawaska tailings, unlike the Quirke Mine tailings, was a function only of the amount of water contacting the tailings and did not depend on the mode of water application.

The observed Ra-226 patterns result from the dissolution of gypsum containing Ra-226, except during the initial two pore volumes, when high Ra-226 levels suggest an initial release of Ra-226 that was loosely adsorbed. The subsequent more constant rate resulted from the dissolution of Ra-226 contained in gypsum. The slow rate of change of cumulative Ra-226 leached during 100 to 1000 pore volumes corresponds to the period when little gypsum (i.e., total solids) was dissolving. The total solids and sulphate concentrations did not increase significantly beyond 1000 pore volumes, whereas Ra-226 concentrations increased rapidly. This suggests that the sulphate particles (assumed to be a $(Ba,Ra)SO_4$ precipitate which was formed in the leaching pachucas and which holds the Ra-226 on the surface of host solids) began to dissolve, releasing Ra-226. These rates were substantially faster (by approximately an order of magnitude) than those associated with Ra-226-gypsum dissolution.

7.3.3 Effect of Sulphate Concentrations on Ra-226 Leaching. To determine whether sulphate concentrations had any significant effect upon the leaching patterns of Ra-226, plots were constructed of the ratio of radium leached/TDS leached against TDS concentration, and of the ratio of radium leached/SO_4 leached against sulphate concentration. These are given in Figures 60(a) and 60(b) for the Madawaska leachates, and in Figures 60(c) and 60(d) for the Quirke Mine leachates. Plotting the ratio of mass Ra-226 leached to mass TDS or sulphate leached normalizes the Ra-226 leaching pattern to that of gypsum. If Ra-226 mobilization depends only on the rate of gypsum leaching, the ratio is fairly constant and independent of sulphate concentration. Plots involving both sulphate and TDS concentrations are given to demonstrate that variations in SO_4:TDS ratios do not affect the plots adversely. The TDS of the Madawaska tailings is assumed to be calcium sulphate, whereas that of the Quirke Mine tailings is assumed to be iron sulphate. The period used to calculate the cumulative leaching characteristics of

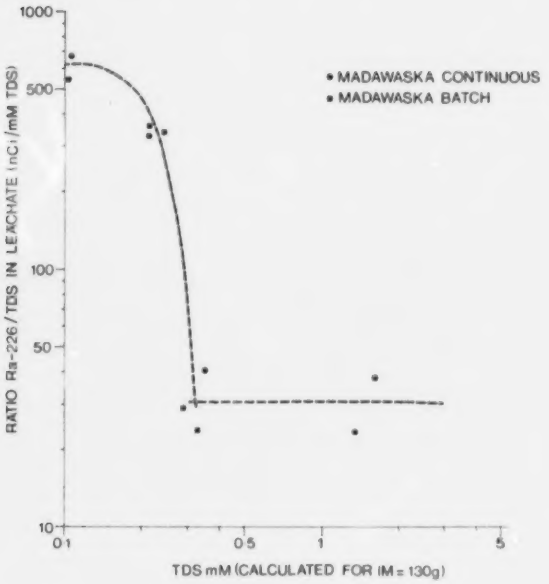

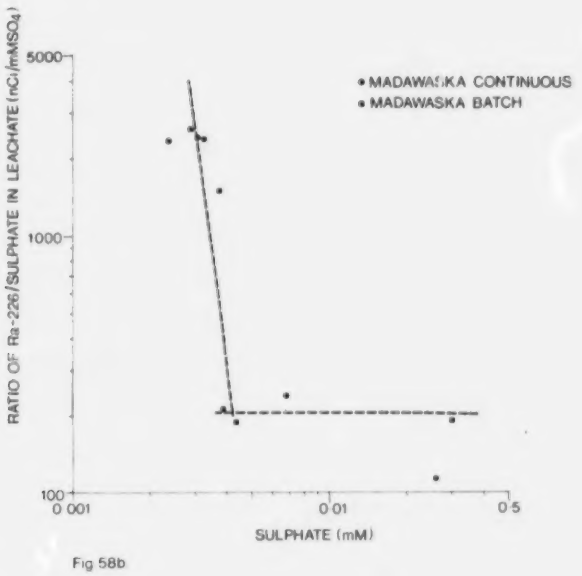

Fig 58b

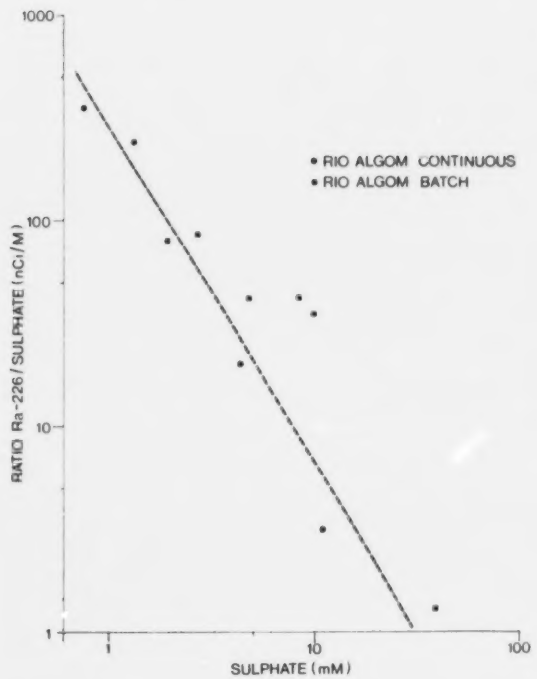

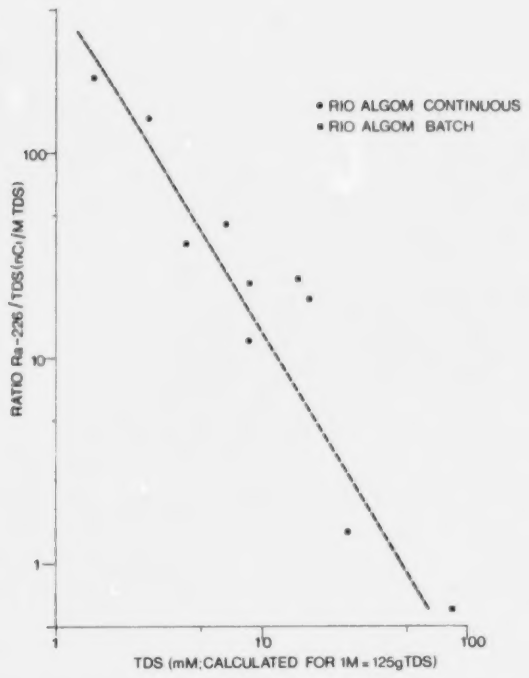

FIGURE 60 EXPERIMENT 4: RATIO OF RADIUM TO TDS (OR SULPHATE) LEACHED vs. TDS (OR SULPHATE) CONCENTRATION

Madawaska tailings was the last 300 days of operation, whereas the period for the Quirke Mine data was the last 500 to 600 days, i.e., the period when the leachates were acidic, at a pH of about 2.5 to 3.5.

The plots of the Madawaska leachates show that the ratio of radium leached to TDS (or SO_4) leached is independent of the TDS (SO_4) concentration for sulphate concentrations greater than 0.5 mMol. However, for lower sulphate concentrations, the ratio becomes quite dependent upon sulphate concentrations. Whether the ratio continues to be dependent upon SO_4 at concentrations lower than 0.3 mMol (e.g., Figure 60(b)) or whether it becomes independent at lower SO_4 concentrations equivalent to 40 mg/L TDS (e.g., Figure 60(a)) is unclear because of the variability in the SO_4 and TDS concentration data. These plots suggest that some of the lysimeters (the high-rate ones near the end of their operation) had reached the stage where the sulphate mineral controlling the Ra-226 concentrations on the solids had started to dissolve, thus allowing the release of Ra-226. These plots also suggest that the point of dissolution can be explained by solubility considerations of the sulphate mineral (presumed to be $BaSO_{4(s)}$) and the sulphate concentration of the leachate water.

The plots of Ra-226 leached against TDS and SO_4 leached for the Quirke Mine tailings (Figures 60(c) and 60(d)) show a different behaviour. They suggest that leaching behaviour is a function of the sulphate concentration in all lysimeters after acidic conditions are reached. Some care must be taken in comparing these plots to those for the Madawaska tailings because the TDS here was an iron sulphate rather than a calcium sulphate. Hence the absolute values of the Ra-226:TDS leaching ratios are not directly comparable. However, the conclusion remains that the leaching behaviour is in part a function of the sulphate concentration of the leachate water. This conclusion is further substantiated by data from the old tailings in Experiment 1, where Ra-226 was released from the top 10 cm of the high-rate lysimeters when sulphate concentrations became quite low. However, since inconsequential amounts of Ra-226 were released from the old tailings until the pyrite was nearly exhausted, the relationship given by Figures 60(c) and 60(d) may represent only a small amount of the total leachable Ra-226 from the Quirke Mine tailings until pyrite oxidation reactions are complete.

7.4 Summary and Conclusions

During the initial leaching of the Quirke Mine and Madawaska tailings, dissolution of gypsum and small amounts of carbonates explain the conductivity, total dissolved solids (TDS) concentration, and pH of leachate waters. TDS characteristics

during this initial phase are controlled by the mass of gypsum available for leaching, provided that the solubility of gypsum is maintained. That is, the mass of TDS lost during the initial leaching phase is a function only of the rate of water application.

Upon completion of dissolution of most gypsum from tailings containing little or no pyrite (Madawaska), Ra-226 concentrations rapidly increase and the leachate pH stabilizes at 5 to 6. This leachate has approximately the same pH as the distilled water applied to the tailings. The whole leaching history was controlled by dissolution reactions, and biochemical reactions appeared to have no significance because of the absence of pyrite. Thus, Madawaska tailings are good candidates for further studies to examine geochemical controls upon Ra-226 evolution without the complication of sulphate formation from pyrite oxidation reactions.

In tailings containing pyrite (Quirke Mine), pyrite oxidation becomes possible after:

(i) dissolution of a sufficient mass of gypsum has exposed pyrite crystals to biofilm waters containing oxygen,
(ii) the tailings are colonized by pyrite oxidizers, and
(iii) residual carbonates are dissolved or coated to allow the pH to decrease.

A continuous mode of water application is thought to slow the rate of colonization compared to a batch mode of application. Pyrite oxidation then results in a decrease in leachate pH to between 2 and 3. The rate of decrease is influenced by hydraulic loading rates; the rate is slower at higher loading rates, because H^+ ions produced by pyrite oxidation are diluted. Since the rate of production of TDS is independent of the hydraulic loading rate during acidic leaching phases, this implies that the pyrite oxidation rate is also independent of the hydraulic loading rate, once pyrite-oxidizing bacteria have colonized the tailings. After the start of pyrite oxidation, leachate pH can be reasonably predicted from TDS concentrations. These predictions are based on the assumption that the chemical condition is electroneutral, TDS is an iron sulphate, and pyrite is the main source of Fe and S.

From a tailings management viewpoint, the results indicate that maintaining a Madawaska tailings site in either a saturated or unsaturated state would not have any effect on leachate properties. Maintaining a Quirke Mine tailings site in a near-saturated rather than unsaturated state would initially result in lower Ra-226 and SO_4 concentrations. These concentrations would, however, likely be similar, once pyrite-oxidizing bacteria had colonized the tailings.

8 EXPERIMENT 5: MICROBIOLOGY OF EXPERIMENTS 2 AND 3

Microbes play an important role in plant-soil systems and biogeochemical cycling processes because they can:

- mineralize organic molecules,
- regenerate nutrients in forms available to higher plants,
- destroy toxic chemicals, and
- release products that are important in geochemical cycles.

In view of the fact that their activities are highly sensitive to environmental disturbances, such as changes in pH values and high concentrations of heavy metals, Experiment 5 was undertaken to examine the effects of solidification on key microbiological processes. These effects were determined by establishing the identity and quantity of aerobic and anaerobic microorganisms present in untreated and solidified $(Ba,Ra)SO_4$ sediments (Experiment 2) and tailings (Experiment 3). In addition, rates of microbial respiration in the presence and absence of added organic matter (glucose) were measured to assess overall microbial activity.

8.1 Experimental Program

Samples of all treatments in Experiments 2 and 3 were obtained by coring. The two samples from Experiment 2 consisted of untreated and solidified $(Ba,Ra)SO_4$ sediments. The four samples from Experiment 3 consisted of untreated and solidified tailings from the non-vegetated and vegetated lysimeters. The samples were shipped to the Chemistry and Biology Research Institute of Agriculture Canada. The experiments described below were conducted and documented by Dr. K.C. Ivarson.

Approximately 1 kg of each sample was placed in a 2-L plastic container under constant environmental conditions (moisture level 50 to 55 percent, 15°C) for 45 days, and then chemically and microbiologically analyzed.

Fungi, bacteria and actinomycetes were counted by the plate count technique (Pramer and Schmidt, 1964). Plates were poured in quadruplicate and incubated at 20°C. Other organisms were counted using the most probable number (MPN) method (Alexander, 1965). All counts were averages of quadruplicates. The media used, the types of organisms counted and isolated and their significance are recorded in Table 23. For rates of microbial respiration, standard respirometric techniques were used (Umbreit et al., 1972). Samples (4 g, oven-dry basis) were placed in 15-mL Warburg respirometer flasks,

TABLE 23 EXPERIMENT 5: MEDIA INOCULATED WITH H_2O SUSPENSION OF SAMPLES TO ISOLATE AND CHARACTERIZE ORGANISMS PRESENT IN THE SAMPLES, AND TO DETERMINE THE SIGNIFICANCE OF THE ORGANISMS

Media	Organisms	Significance
Soil Extract Agar	Total bacterial and actinomycetes	In well-aerated, neutral environments, dominate and account for much of the microbial activity of the community.
Rose Bengal Agar	Total fungi	Also very active at neutral reactions but, unlike bacteria and actinomycetes, are insensitive to high H^+ concentrations, and thus dominate at low pH values.
Soil Extract Agar (H_2O Suspensions of samples heated to 80°C for 10 min.)	Aerobic spore forming bacteria, mainly bacilli	In aerobic environments comprise approx. 10% of total bacteria; are resistant to heat, drying and other destructive agencies.
Deep cultures, NH_4-glucose solutions (H_2O suspensions of samples heated to 80°C for 10 min.)	Anaerobic spore forming bacteria, mainly clostridia	In anaerobic environments comprise a very large percentage of the bacteria; are also resistant to destructive agencies.
KNO_2-$CaCO_3$ solution	Bacteria (nitrobacter group)	Produce nitrate which is the major nitrogen source assimilated by growing plants.
Peptose-glucose solution	Bacteria and fungi (ammonifiers)	Convert organic nitrogen to inorganic nitrogen.
$NaNO_3$ - glucose solution	Bacteria (denitrifiers)	Transform inorganic nitrogen to gaseous nitrogen.
N-free medium (shallow solution)	Aerobic N-fixers (*Azotobacter* species)	Fix atmospheric - N.
N-free medium (deep solution)	Anaerobic N-fixers (*Clostridium* species)	Fix atmospheric - N.
SO_4 - lactate solution	*Desulfovibrio*	Reduce sulphate to gaseous sulphides.
NH_4 - $FeSO_4$ solution	*Thiobacillus ferrooxidans*	Oxidize ferrous iron (pyrite) to ferric iron (jarosites) with production of H_2SO_4.
Inorganic salt solutions + cellulose strips (aerobic)	Bacteria, actinomycetes, and fungi (aerobic cellulose decomposers)	Carbonaceous materials (plant residues) transformed to CO_2.
Inorganic salt solution + cellulose strips (anaerobic)	Bacteria (anaerobic cellulose decomposers)	Same as above.

and brought to 70 percent water-holding capacity with distilled water or a solution of glucose and distilled water. Oxygen utilization rates were recorded for a period of 7 days. The results are the averages of triplicate runs.

8.2 Results and Discussion

The organic carbon and the organic nitrogen (oven-dry basis) along with the pH values are reported in Table 24. In the tailings, the carbon and nitrogen contents, which reflect the presence of decomposable organic matter, were increased substantially by solidification, whereas the reverse occurred in the sediments. The highest pH values were, as expected, found in the solidified materials.

TABLE 24 EXPERIMENT 5: SOME CHEMICAL PROPERTIES OF THE SAMPLES

	$(Ba,Ra)SO_4$ Sediments		Fresh Tailings			
			Non-vegetated		Vegetated	
	Not Solid.	Solid.	Not Solid.	Solid.	Not Solid.	Solid.
Carbon (%)	2.91	1.62	0.13	1.08	1.16	3.28
Nitrogen (%)	0.28	0.12	0.05	0.09	0.16	0.28
pH	7.8	12.1	2.1	10.1	2.7	7.8
C/N ratio	10.4	13.5	2.6	12.0	7.3	11.7

The microbial populations of the samples are presented in Table 25. In general, except for fungi, ammonifiers and iron-oxidizing bacteria (*Thiobacillus ferrooxidans*), solidifying the tailings markedly increased the counts of most microbes. These increases were far more pronounced in vegetated samples than in non-vegetated samples; this is probably due to a combination of several factors, the main ones being the presence of more decomposable organic matter and a more favorable pH in the solidified tailings than in the corresponding untreated samples (Table 24). In comparison to the tailings, solidifying the sediments has had an effect opposite to the above observations and again the above-mentioned factors are likely responsible. The autotrophic acidophilic, iron-oxidizing microbe, *T. ferrooxidans*, would, as expected, be more numerous in an environment characterized by low pH and low organic content. Some of the ammonifiers are fungi. Since fungi are relatively insensitive to hydrogen ion

TABLE 25 EXPERIMENT 5: TOTAL COUNTS OF MICROBIAL POPULATIONS

Organism	$(Ba,Ra)SO_4$ Sediments		Fresh Tailings			
			Non-vegetated		Vegetated	
	Not Solid.	Solid.	Not Solid.	Solid.	Not Solid.	Solid.
Bact.+Act.	1.1×10^5	4.0×10^2	<10	5.0×10^3	<10	8.0×10^6
Fungi	2.7×10^2	<10	<10	<10	5.0×10^2	8.0×10^2
Aerobic Spore Formers	2.5×10^4	<10	<10	3.5×10^2	<10	1.4×10^5
Anaerobic Spore Formers	1.1×10^3	<10	<10	0.7×10^2	<10	1.3×10^2
Nitrobacter	1.0×10^2	<10	<10	<10	<10	1.0×10^4
Ammonifiers	1.0×10^2	<10	2.3×10^1	<10	<10	1.0×10^3
Denitrifiers	1.7×10^5	1.0×10^3	<10	3.3×10^3	1.8×10^5	1.6×10^6
Aerobic N-fixers	3.0×10^2	<10	<10	<10	<10	1.5×10^2
Anaerobic N-fixers	7.0×10^2	<10	<10	<10	<10	2.3×10^2
Sulphate Reducers	<10	2.3×10^2	<10	<10	<10	1.0×10^2
Fe-oxidizers	7.0×10^3	2.0×10^2	4.0×10^5	3.0×10^2	3.0×10^5	3.0×10^4
Aerobic Cellulose Decomposers	3.5×10^4	<10	2.3×10^1	1.1×10^2	2.0×10^2	4.9×10^4
Anaerobic Cellulose Decomposers	<10	<10	<10	<10	2.4×10^2	6.8×10^2

concentrations, increasing the acidity would remove competitive groups of microbes and in the end appear to enhance the establishment of the fungal and ammonifying organisms.

Very few important groups of microbes, such as nitrifiers (form nitrate) and nitrogen fixers (fix atmospheric nitrogen), existed in the unfavorable environment of low pH and low organic content but their number definitely increased when conditions improved. Further studies showed that the aerobic nitrogen fixers belong to the genus

Azotobacter. Vegetating the tailings apparently improved activities of the cellulose decomposers, whereas solidifying the sediments reduced their activities.

The linear rate over the 7 day period (Figure 61) suggests that microbes were not substrate or oxygen limited, 1 day after addition of the glucose.

Microbial respiration, a reflection of the ability of microbes to decompose the organic matter either present or added, has been shown to be well correlated with pH and microbial numbers (Pramer and Schmidt, 1964). In all cases in this study, the addition of glucose stimulated the respiration rate (Figure 61) and increased the final microbial count (Table 26). The respiration rate was considerably higher in the vegetated tailings than in the non-vegetated tailings. In both the non-amended and glucose-amended tailings, solidification increased the potential of the soil microorganisms to utilize indigenous or added growth substrates. However, in the sediments, solidification again reversed the microbiological trend found in the tailings. In other words, although solidification stimulates microbiological activity in the tailings, it retards the process in the sediments because of unfavorable pH and low organic content.

Solidifying the sediments decreased its microbial activity. This in general is in agreement with the bioassays of Experiment 2, where usually it was found that the effluents from the solidified sediments were toxic to both daphnia and rainbow trout, whereas those from the untreated sediments were not. Thus, it appears that solidifying the sediments exerts a toxic effect on much of the biological life that is associated with the material.

8.3 Summary and Conclusions

The results indicate that a higher level of microbial activity is found in both solidified, vegetated tailings and solidified, non-vegetated tailings compared to the corresponding untreated samples. On the other hand, solidifying the sediments decreases microbial activity. This increase or decrease in microbial activity is due to the fact that solidification produces a more favorable pH and a higher organic content in the tailings, yet it produces an unfavorable pH and a lower organic matter content in the sediments.

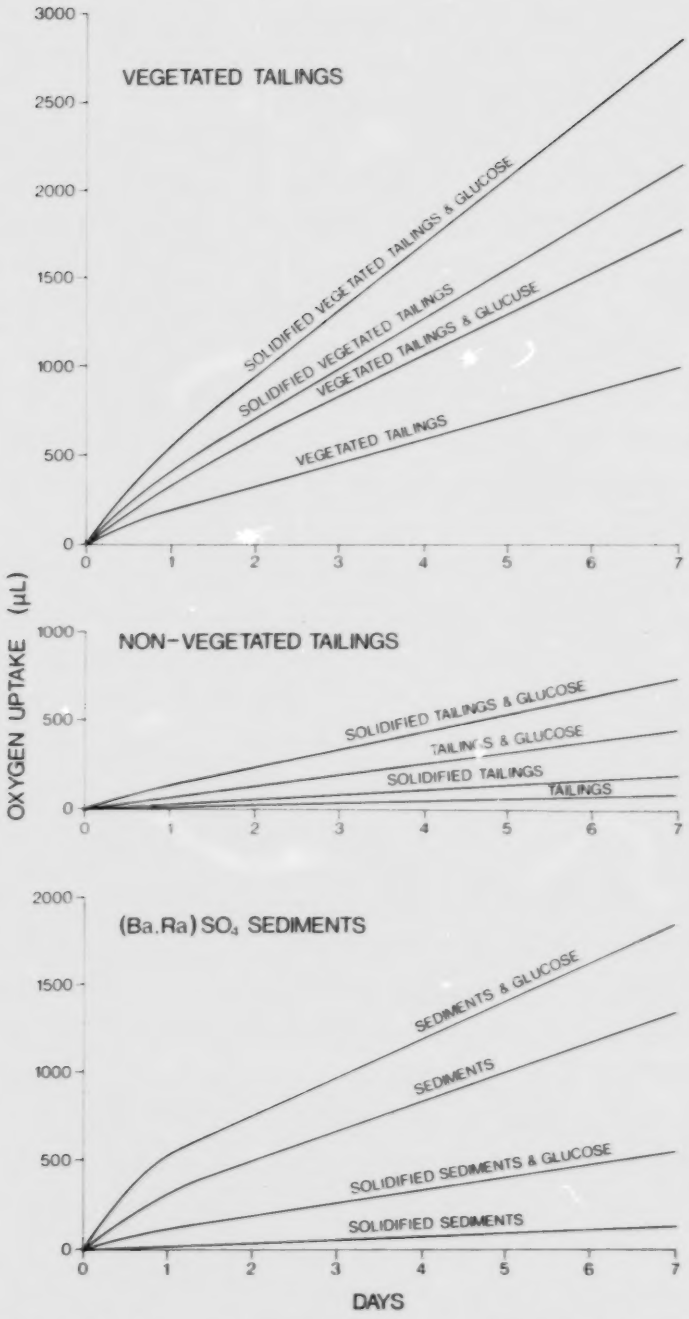

FIGURE 61 EXPERIMENT 5: MICROBIAL RESPIRATION IN VEGETATED AND NON-VEGETATED TAILINGS AND (Ba,Ra)SO_4 SEDIMENTS

TABLE 26 EXPERIMENT 5: FINAL MICROBIAL COUNTS FOR RESPIRATION TESTS

	Microbial Counts After 7 days of Incubation			
	Bacteria + Actinomycetes		Fungi	
	Non-amended	Glucose Amended	Non-amended	Glucose Amended
1. $(Ba,Ra)SO_4$ Sediments				
Not solidified	0.2×10^6	1.0×10^6	0.4×10^3	0.4×10^3
Solidified	1.0×10^2	1.0×10^3	0.0	0.0
2. Non-vegetated Tailings				
Not solidified	0.0	0.0	3.0×10^2	3.0×10^4
Solidified	1.0×10^2	1.0×10^4	0.0	0.0
3. Vegetated Tailings				
Not solidified	0.0	0.0	4.1×10^4	9.0×10^4
Solidified	1.5×10^7	4.5×10^9	3.4×10^4	4.5×10^4

9 CONCEPTUAL MODEL OF TAILINGS LEACHING PROCESSES

Three experiments in this study aid in evaluating the processes of tailings leaching. First, Experiment 1 monitored the composition of leachate from old tailings for 6 years. These tailings had been placed in a tailings pile several years before the start of the experiment. The probable water chemistry of this leachate (major and minor cations and anions) was assessed. The lysimeter solids were characterized using chemical analysis and Scanning Electron Microscope - X-ray Emission techniques. The results suggest that secondary minerals were formed by acid attack on the parent minerals. These data are useful for characterizing the expected behaviour of tailings during acid reactions and near the end of the acid period when pyrite oxidation is complete. Experiment 1 also examined leaching from tailings containing 30 percent $(Ba,Ra)SO_4$ sludge formed from the chemical precipitation of tailings overflow water containing Ra-226. The results provide not only evidence for the behaviour of $(Ba,Ra)SO_4$ sludges disposed of in the unsaturated zone of a tailings pile but also an indication of the behaviour of $BaSO_{4(s)}$ solids formed upon the surface of host solids.

Experiment 3 provides evidence for leachate behaviour from tailings that were solidified using the Chemfix^R technique. It also provides evidence for the length of time that grasses can survive on such tailings and their radionuclide accumulation rates. Because the solids produced in Experiment 3 were not characterized at the end of the study as were those of Experiment 1, the evidence they provide for management options has been emphasized rather than the biogeochemical processes in the tailings. The results of Experiment 5 (characterization of the bacteriology of Experiments 2 and 3) are treated similarly.

Experiment 4 examined the leaching characteristics of fresh tailings from Rio Algom's Quirke Mine and from the Madawaska Mine. The data provide evidence for the leaching behaviour of tailings during the first years after placement. The main difference between the leaching characteristics of the two sets of tailings is that leachates from the Quirke tailings acidified to pH 2, whereas those from the Madawaska tailings decreased only to approximately pH 5.

A conceptual model of the evolution of the tailings through time is given in Figure 62. The history is divided into four different phases:

(i) tailings characteristics upon placement and the mill processes which control these characteristics,

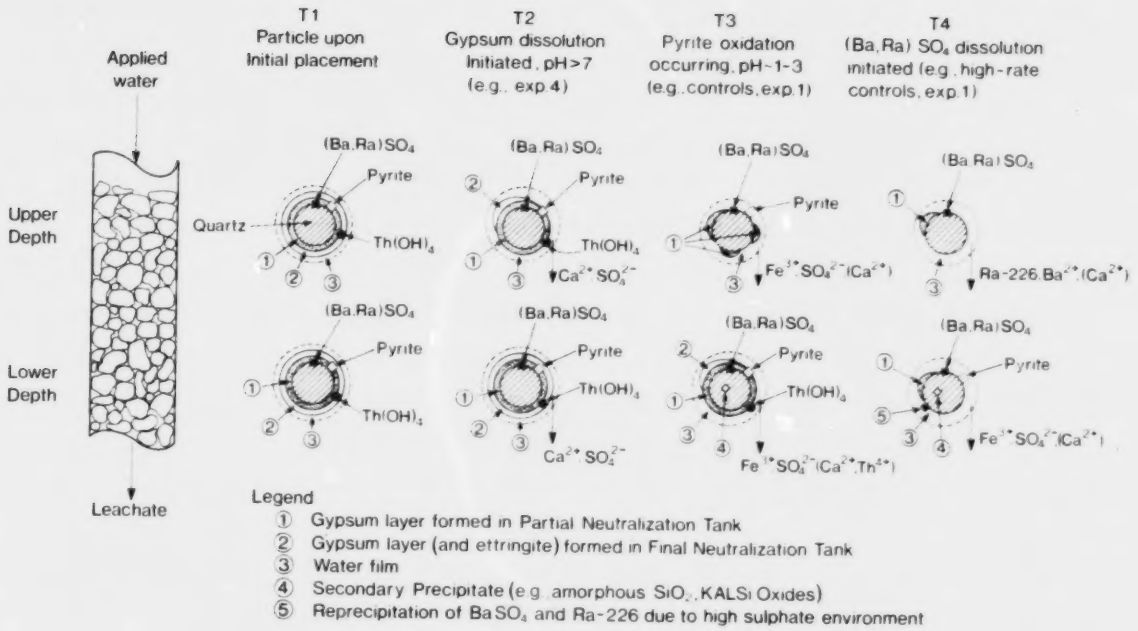

FIGURE 62 CONCEPTUAL MODEL OF THE EVOLUTION OF TAILINGS IN A LYSIMETER

(ii) tailings processes during gypsum dissolution but before acidification starts,

(iii) tailings processes during pyrite oxidation, and

(iv) tailings processes after completion of pyrite oxidation in surface layers.

The diagram under Time T1 in Figure 62 shows that when milled solids leave the mill, they are coated with three different forms of precipitates (or layers). These precipitates are formed in the leaching pachucas, the partial neutralization tank, and the final neutralization tank. In the leaching pachucas, uranium, thorium, Ra-226, and Pb-210 are leached along with various metal sulphides. Oxidation of the reduced metals occurs and metal sulphates precipitate. Due to the similarity in behaviour between Ba^{2+} and Ra-226, one may describe Ra-226 as having an affinity for Ba^{2+}. Data presented in Section 4.3 suggest that Ra-226 is associated with $BaSO_{4(s)}$ in the leached solids. Hence it is thought that coprecipitation of Ra-226 with $BaSO_{4(s)}$ occurs in the leaching

pachucas, thus removing Ra-226 from solution. Furthermore, the coprecipitation process prevents significant quantities of Ra-226 from being measurable in solution; rather its chemistry is essentially controlled by reactions occurring on the surface of host (quartz) and other solids in the leaching pachucas. Ra-226 is leached from its host uraninite and other uranium minerals by proton attack on the structure, but it does not migrate far from the surface of the mineral matrix from which it is leached.

Ra^{2+} forms $RaSO_4^o$ complexes (see Appendix A.1.2) and is rapidly incorporated into a $BaSO_{4(s)}$ structure. For solution concentrations of 100 pCi/L (3.7 Bq/L) of Ra-226 and 1 mg/L of Ba^{2+}, there is approximately 1 ion of Ra^{2+} for every 1 000 000 Ba^{2+} ions present. Accordingly in such solutions, the number density of Ra-226 incorporated into the $BaSO_{4(s)}$ lattice is so small that significant effects upon crystal growth of $BaSO_{4(s)}$ are quite small. Because the ionic sizes of Ra^{2+} and Ba^{2+} are quite similar, significant effects upon crystal growth would occur only when the molar ratio of Ra-226/Ba^{2+} is much larger. At very high concentrations of Ra-226, formation of a $RaSO_{4(s)}$ may be possible; such concentrations are generally not observed in mills or in the environment.

For this conceptual model, thorium species leached in the leaching pachucas are carried through the mill until the final neutralization tank. Pb-210 forms sulphate complexes in the leaching pachucas with other lead species. The number of $PbSO_4$ complexes may increase in the partial neutralization tanks because the number of SO_4^{2-} ions increases and the number of HSO_4^- ions decreases as the pH is raised. The behaviour of Pb-210 in the partial neutralization tanks may depend upon competition for SO_4^{2-} by Ca^{2+} and Pb^{2+} or the formation of a $(CaPb)SO_4$ coprecipitate. Some thorium species are expected to precipitate or to adsorb in the partial neutralization tank, because the thorium concentration on the solids increases process by process through the mill (Table A.12). Most of the thorium species are thought to precipitate in the final neutralization tanks as hydroxides (see speciation of thorium at pH 4 to 6 in Figure A.6), which then become enmeshed in the gypsum-ettringite (Ca-S) precipitates formed in these tanks.

All precipitates can be viewed as forming in successive layers. The total layer is only a few microns thick. While the precipitates are conceptualized here as being in layers, they are, in fact, a fairly porous structure with interwoven rods, dendrites, and polygons. Pore spaces are readily discernable from SEM photographs of tailings. If the precipitates do not dissolve in the tailings pile, they significantly increase the surface area of the tailings particulate compared to the surface area of the host solids.

Furthermore, because of incomplete covering of the host solids, the layers have irregular thicknesses (from negligible to substantial thickness). The precipitates coat individual small particles (e.g., alumino-silicate plates) and help bond these small particles to the large coarser quartz solids formed by the milling of the mined silica-ore solids. Disposal of the final neutralization tank slurry to the tailings pond/pile allows for separation of fines (agglomerations of small-diameter, less dense particles) from larger, denser quartz tailings.

Upon placement in the tailings pile, the data of Experiment 4 show that the leaching water remains basic for a relatively long time. Dissolution of gypsum should give a pH of about 7 (see Section 7.3.1). Because the observed pH is higher, a buffering system, such as carbonate, must be influencing the pH. The amount of calcium oxides and carbonates added in the mill is in excess of that required to neutralize the acidity of the mill water (Snodgrass et al., 1982). Measurements on the final neutralization tank solids show that they contain 0.02 to 0.04 percent carbonates (see Appendix A.2). Dissolution of $CaCO_{3(s)}$ into a water saturated with CO_2 from the air gives a pH of 8.3. Hence, both $CaCO_{3(s)}$ and $CaSO_{4(s)}$ dissolution is occurring. The dominant solids dissolved during the time period are thought to be $CaSO_{4(s)}$ with minor amounts of $CaCO_{3(s)}$.

During this dissolution process (Time T2 on Figure 62), the $Th(OH)_4$ solids originally enmeshed within the gypsum in the final neutralization tank remain on the particles until the pH decreases sufficiently to allow for their dissolution. Because formation of Th-floride and Th-sulphate complexes is important, $Th(OH)_{4(s)}$ dissolution is more favoured if the complexes are present.

During this period of gypsum dissolution, Ra-226 enmeshed by the $CaSO_4$ precipitates is the main source for Ra-226 in the leachates. This concept is supported by the correlations between the mass of Ra-226 leached per mass of TDS leached, a correlation determined in Experiment 4.

When pyrite grains are exposed to dissolved oxygen and organisms in the film water covering the solids (Time T3 in Figure 62), pyrite oxidation starts, provided that sufficient gypsum has dissolved to expose the grains. But not all grains are covered by gypsum. Also, oxidation proceeds chemically in the absence of bacteria. Atmospheric oxygen penetrating to various depths of the lysimeter between applications or surges of infiltrating water is the main source for oxygen in the tailings waters. Biofilms containing *T. ferrooxidans* develop. The actual origins of such bacteria are not specified here, but the results of Experiment 5 and those of Ritcey and Silver (1980) demonstrate

that pyrite oxidizers develop both in tailings fresh from the mill (Experiment 3 and 4) and in old tailings which are dried and then leached (Experiment 1).

As pyrite oxidation continues, the pH starts to decrease. The pH is maintained in the 5 to 7 range as the pyrite-oxidizer community develops and as carbonates are continually attacked. The carbonates, if exposed to acid pore waters, are probably rapidly attacked. The rate-limiting factors for carbonate removal may be the rate of acid production and the rate of exposure of carbonate surfaces to acidic biofilms, not the rate of dissolution of $CaCO_{3(s)}$. This assumes that some of the carbonate added in the mill is also covered by precipitates formed in the mill.

As the pH decreases, concentrations of sulphate increase and minimize the rate of dissolution of gypsum. In waters in which the pH is 2 to 3 and the TDS is 2 000 to 3 000 mg/L, equilibrium chemistry calculations suggest that the pH can be explained by:

(i) the sum of the concentrations of Fe^{3+} and SO_4 being equal to the concentration of TDS,

(ii) the acidity constant for the HSO_4^- complex, and

(iii) the chemical condition of electroneutrality in the leachate.

Hence gypsum dissolution makes a small contribution to TDS during pyrite oxidation. This mechanism provides for the maintenance of gypsum on solids in the porous zone of tailings until the completion of pyrite oxidation reactions, as observed on the lysimeter solids (old tailings) of Experiment 1.

In older tailings (13 to 21 years old), pyrite oxidation is not complete; sufficient pyrite remains for pyrite oxidation reactions to continue (see data in Appendix A.2). For rainfall rates (water application rates) which are smaller than normal precipitation, biofilm reactions allow Fe^{3+} and SO_4^{2-} to increase above 2 000 mg/L and to cause high H^+ concentrations (pH in the range of 0.8 to 1.0). At higher water application rates, the pH ranges are higher, because the continual dilution of biofilm waters by percolating water decreases the Fe^{3+}, SO_4^{2-} and H^+ concentrations. In these waters, electroneutality is dominated by $Fe(SO_4)^+$ and $Fe(SO_4)_2^-$ complexes.

Weathering reactions also become important. Analyses of leachates from the old tailings demonstrate that Al, K, Si, and Mg concentrations are present in significant amounts (see Appendix A.1.2). These elements originate from a proton attack on alumino-silicates. Plate-shaped, 10-micron particles (see Appendix B.1) are probable sources for these elements. Examination of metal ratios and concentrations of metals in the leachates show that Al, K, and Si are retained in the solids, if Mg is conservative. The

concentration of Si suggests that the formation of amorphorus $SiO_{2(s)}$ and its solubility in water controls the Si concentration. Although the formation of $Fe(H_2SiO_4)_x$ complexes is possible, their concentration does not appear to be significant. Al and K may be coprecipitated in amorphorus $SiO_{2(s)}$, or they may form secondary K-alumino-silicates. Using SEM-XRE on surface precipitates shows a large variation in ratios of Al-K-Si in these precipitates; this suggests that various secondary precipitates are formed.

The Fe and S ions from pyrite oxidation reactions may all be leached from the tailings. Reprecipitation of Fe^{3+} and SO_4^{2-} in minerals, such as jarosite, is thermodynamically possible, particularly in the low-rate lysimeters where the saturation index is large (see Appendix A.1.2). Such formation is most likely observed in solutions containing *T. ferrooxidans*. Above pH 2, $Fe(OH)_{3(s)}$ is predicted to form rapidly (see Appendix A.1.2). However, Mossbauer analysis (see Appendix B.1) indicates that the quantity of Fe^{3+} minerals, such as jarosite, is less than 5 percent in all samples analyzed (mill and lysimeter tailings). Hence most of the Fe and SO_4 may escape with the leachates, and the colour in the lysimeter solids attributed to $Fe(OH)_{3(s)}$ (see Appendix A.2) may represent a very small quantity of total iron.

When the pH is below about 3 in both Experiments 1 and 4, the TDS is dominated by Fe_T (total iron) and SO_4^{2-}. The oxidation state of Fe_T is not precisely defined because leachate samples analyzed herein had been stored for 1 to 2.5 years. To assume that nearly all the Fe occurs as Fe^{3+} is justified by the electroneutrality balance for the old tailings (see Appendix A.1) and for predictions of pH for the new tailings of Experiment 4 (see Appendix A.1.2).

Measurements of TDS are estimated to be too high by about 20 percent in calcium sulphate solutions and 30 percent in iron sulphate solutions. This is attributed to two waters of hydration not being removed from $CaSO_4.2H_2O$ during evaporation of water from the calcium sulphate solution and to two of the six waters octohedrally coordinated to Fe^{3+} not being lost during evaporation (i.e., drying at 105°C for TDS measurements). The waters of hydration of gypsum are lost in the 150 to 175°C range. For the calcium sulphate solution, this error brings the TDS measurements into agreement with TDS predicted by the solubility product for gypsum (approximately 1.8 E-04). Note that this solubility product predicts approximately 1700 mg/L TDS, if activity corrections are ignored; and approximately 2400 mg/L, if activity corrections are included. For iron sulphate solution, the sums of anions plus cations agree with TDS measurements when volatile dissolved solids (VDS) are included (see Appendix A.1). VDS are assumed to be waters of hydration associated with Fe^{3+}. Accordingly, TDS values measured during the

experiments must be decreased by approximately 30 percent when the pH is less than 3.5 to 4 to give an accurate estimate of the TDS.

The source of Ra-226 in the old tailings in Experiment 1 during the time that the leachate is acidic requires some explanation. Dissolution of small amounts of $BaSO_{4(s)}$ and of residual gypsum minerals containing Ra-226 is possible, but the high sulphate concentrations observed in the leachates prevent substantial dissolution.

Another source of the Ra-226 in the leachates is the residual uranium minerals containing Th-230 and Ra-226. A 0.084 (mCi (3110 Bq) quantity of Th-230 and 0.0021 mCi (77.7 Bq) of Ra-226 were leached from the low-rate lysimeters; and 0.15 mCi (5550 Bq) of Th-230 and 0.085 mCi (3150 BQ) of Ra-226 were leached from the high-rate lysimeters. Much of the Ra-226 in the high-rate lysimeter is derived from the pulse near the end of leaching. The leachate chemistry shows that the thorium concentrations (Th-230, Th-232 and Th-228) increase as the pH decreases. This suggests that residual minerals containing thorium are attacked by protons and that the residual minerals are the main source of thorium in the leachate from the old lysimeters. It can be assumed that similar quantities of Th-230 and Ra-226 are found in these residual minerals which remain after the leaching pachucas. Hence, if Th-230 is liberated by weathering (H^+ from pyrite oxidation), Ra-226 would likewise be liberated.

$BaSO_{4(s)}$ is close to equilibrium with $BaSO_4$ concentrations in the biofilms. These biofilms have higher concentrations of Fe and SO_4 than the percolating leachate. Since the mass of Ra-226 leached in Experiment 1 is significantly less than that of Th-230 during the 6 years of leaching, the Ra-226 and Th-230 must be released by proton attack on residual minerals containing these radioisotopes, but much of the Ra-226 liberated is retained by coprecipitation reactions with $BaSO_{4(s)}$ or secondary alumino-silicates and amorphorus $SiO_{2(s)}$.

When pyrite oxidation is nearly complete and hence when the production rate of sulphate decreases, the Ra-226-containing coprecipitate on the host particles begins to dissolve because of the low sulphate concentration in the pore water (Time T4 in Figure 62). The dissolution occurs at the top of the tailings (see data in Appendix A.2). It is estimated that 80 percent of Ra-226 is dissolved in 1.5 years (the length of time of the Ra-226 peak from the high-rate lysimeters) from 10 cm of tailings. The subsequent behaviour of the high-rate lysimeters suggests that this does not occur continuously. The Ra-226 seems to have reprecipitated at lower depths of the tailings, because this mass has not left the tailings. Reprecipitation is probable, but why the peak declines is not

known. Local variations in deeper zones of the tailings are thought to provide large enough concentrations of sulphate to prevent continuous dissolution of $BaSO_{4(s)}$.

The results of Experiment 3 show that grasses can grow in tailings that have been solidified using the ChemFix^{R} process. However, if dissolution of the solidifying agents is sufficient to allow exposure of pyrite grains to the atmosphere, reactions leading to acidity occur. The acidity may reach a magnitude sufficient to poison vegetative growth, if the grasses are not able to maintain neutral conditions about their root zone. The key to avoiding such reactions is the ability of the solidifying agents to maintain a coating over the pyrite particles.

10 SUMMARY

The mining and milling of uranium-bearing ores has the following effects:

- it removes a mineral assemblage that is stable in a reducing environment,
- it mobilizes some of the reduced minerals by leaching and oxidation,
- it reprecipitates most of the mobilized substances as secondary precipitates upon the surfaces of the host minerals and solids (e.g., as gypsum in the case of an acid-leach mill), and
- it disposes of them within a tailings management area.

In the new environment, aerobic conditions may prevail, particularly in unsaturated zones, and water flow pathways may allow percolating waters to pass through the tailings (the solid wastes resulting from mining/milling) and carry mobilized elements to ground and surface waters. In particular, an aerobic environment is conducive to the oxidation of reduced sulphide minerals. This is the basic principal used in milling uranium. Uranium in the oxidized state (UO_2^{2+}) is considerably more soluble than in the reduced state. Leaching with sulphuric acid thus oxidizes and puts the uranium-containing mineral (e.g., U(IV)) into solution (e.g., U(VI)). In tailings such as those at Elliot Lake in which pyrite (FeS_2) occurs in significant quantities (1 to 3 percent), the major elements in leachate from aerobic tailings are Fe^{3+}, SO_4^{2-} and H^+, resulting in a very acidic water. Other heavy metals (e.g., Cu, Ni), which occur as sulphides, are also released because of oxidation of their sulphides.

In addition to acidity and heavy-metal mobilization, the release of radioisotopes through atmospheric and aquatic pathways are of concern to regulatory authorities involved with environmental quality (e.g., Environment Canada) and nuclear safety (e.g., Atomic Energy Control Board). Past work has suggested that Ra-226 is the radioisotope of most concern to regulatory authorities due to its radio-toxicity. Thorium species are also of concern because of their long half-life and because Th-230 is the parent of Ra-226. More recent work has suggested that Pb-210 and Po-210 are of equal or even greater importance to regulatory authorities than Ra-226. Both Pb-210 and Po-210 may result in a potentially larger "dose commitment" (a measure of committed damage to the human body) to humans through aquatic pathways than does Ra-226.

In response to these concerns, Environment Canada's Wastewater Technology Centre (WTC), in Burlington, Ontario, initiated a series of studies in 1974 to examine the leachability of major constituents (TDS, heavy metals, H^+) and radioisotopes from two

uranium mining/milling wastes: tailings and settling pond sludges. The study also attempted to assess the effect of two tailings treatment methods (solidification and vegetation) upon the characteristics of leachates from these wastes. The original study design was formulated in consultation with the Radioactivity Subgroup of the Federal Mining Task Force, whose purpose is to assist the development of effluent guidelines and regulations for the uranium mining industry, and the Abatement and Compliance Branch of Environment Canada. Subsequent modifications were made by internal expertise developed during the course of the study and at the suggestion of CANMET personnel. Final characterization of the solids remaining from one experiment (13- to 21 year old tailings) was conducted by IEC Beak Consultants.

Four bench-scale experiments were conducted to examine the leachability of:

(1) old tailings and those containing a large portion of $(Ba,Ra)SO_4$ sludges,
(2) untreated and solidified $(Ba,Ra)SO_4$ sludges located at the bottom of settling ponds,
(3) new tailings that had been vegetated and/or solidified, and
(4) new tailings subject to varying flow rates.

A fifth study was conducted to examine the microbiology of Experiments 2 and 3. In addition a conceptual model was developed which integrates the results from all experiments. Several of the major findings of this study are summarized in the following text.

1. During the initial leaching of tailings, dissolution of gypsum and minor amounts of carbonates explains the conductivity, total dissolved solids (TDS) concentration and pH of leachates. After the pyrite grains are exposed to biofilm waters containing oxygen, pyrite oxidation becomes possible.

2. Upon the exposure of pyrite crystals to oxygen, the colonization of tailings by pyrite oxidizers, and the dissolution of carbonate minerals, the pH of leachates rapidly decreases to 2-3. Higher pH values result from the flux of water diluting the mass of H^+ produced by pyrite oxidation. After dissolution of gypsum and at equivalent pore volumes of leachate production, the amounts of sulphate and TDS produced are less in continuous-mode lysimeters than in batch-mode lysimeters. Thus a continuous mode of water application appear to slow the rate of colonization compared to a batch mode of application.

3. Upon completion of dissolution of most gypsum from tailings containing little or no pyrite, the leachate stabilizes at pH 5 to 6. This is approximately the same pH as that of the distilled water applied to the tailings.

4. During the initial leaching phase, TDS leaching characteristics are controlled by the mass of gypsum available for leaching provided that the solubility of gypsum is maintained. That is, the mass of TDS lost during the initial leaching phase is a function only of the rate of water application.

5. During acidic leaching phases, TDS characteristics are independent of pyrite leachability. That is, during pyrite oxidation, the rate of producing TDS is independent of flushing rate (Experiments 1 and 4), implying that once bacteria have colonized the tailings, the pyrite oxidation rate is independent of the hydraulic loading (flushing) rate. This occurs provided that sufficient oxygen is available to allow pyrite oxidation to continue.

6. During acidic leaching phases, the pH can be reasonably predicted from TDS concentrations, if one assumes that the chemical condition is one of electroneutrality and that pyrite is the main source of Fe and S. Leachate analysis data from the old tailings (Experiment 1) suggest that the source is 1/3 FeS and 2/3 FeS_2. The lack of an Fe:S ratio of 0.5 cannot be explained by iron precipitation in the lysimeter. This suggests that a slight alteration from an Fe:S ratio of 0.5 is in order for mathematically modelling some tailings.

7. Below pH 2, the pH of iron sulphate waters does not decrease per unit increase in TDS as fast as it does above pH 2 because of the formation of chemical complexes. For leachate with a pH in the range of 0.8 to 1.5, $Fe(SO_4)_2^-$, $FeSO_4^+$, and HSO_4^- are the dominant chemical complexes.

8. Chemical measurements of TDS overestimate the actual TDS (the sum of anions and cations) of iron sulphate waters by about 30 percent, and of calcium sulphate waters by about 20 percent. The measurement error for the iron sulphate waters correlates well with the value for volatile dissolved solids. This error is attributed to the incomplete loss of water of hydration surrounding ions; some of these water molecules are retained in the solid formed during evaporation at 105°C. For iron sulphate waters, this error probably results from incomplete loss (1/3) of the six molecules of water of hydration which are coordinated as innersphere complexes with Fe^{3+}. For calcium sulphate (gypsum) waters, the error probably represents the two waters of hydration of gypsum formed during evaporation; these two water molecules are lost at 175°C.

9. Protons formed from pyrite oxidation attack alumino-silicate minerals in the tailings, releasing Al, F, Mg, K, and Si. However, solubility controls limit the amount

of Si that can be released in the leachate, inducing the reprecipitation of Si as amorphorus $SiO_{2(s)}$.

Substantial quantities of Al, F, and K are also retained in the tailings after proton attack. Whether they are constituted in secondary alumino-silicates formed from the incongruent dissolution of the parent minerals or are enmeshed in the amorphous $SiO_{2(s)}$ is unclear.

10. Minor amounts of other heavy metals are also found in the lysimeter leachates. Metals such as Ni and Cu are probably derived from oxidation of their sulphides; whereas others, such as Ti, probably originate from a proton attack upon oxides (e.g., rutile) and uranium minerals (e.g., brannerite).

11. Because thorium appears to be lost much faster from the tailings than gypsum, it is suggested that thorium species (Th-230, Th-232, Th-228) are precipitated mainly in the final neutralization tank as $Th(OH)_{4(s)}$, which is only partially encapsulated in the gypsum precipitates. When placed in the tailings pile, they are rapidly solubilized when the pH becomes acidic.

12. Over the long term, thorium species observed in the leachate from old tailings are derived from a proton attack upon residual minerals containing thorium which was not mobilized in the leaching pachucas of the mill.

13. About 20 years after placement, the solids concentration of Ra-226 in the tailings is approximately the same as that when the tailings were originally placed.

14. The average Ra-226 concentration of 120 pCi/g (4.4 Bq/g) in the old tailings of Experiment 1 is lower than the 165 pCi/g (6.1 Bq/g) conventionally associated with coarse tailings. This difference is due to the smaller surface area of these tailings. These tailings are coarser (95 percent of their mass is found in the size class 2 mm to 50 μm) than those conventionally described as coarse tailings (64 percent between 2 mm and 50 μm). Coarser tailings have a smaller surface area per gram than finer tailings. If it is assumed that Ra-226 is in surface precipitates that have a uniform surface density in coarse and fine fractions (i.e., Ra-226 has a constant value of "x" Bq/cm^2 of surface area), then a lower concentration of Ra-226 per gram of tailings can be expected in coarser tailings.

15. Over 80 percent of the Ra-226 was lost from the top 10 cm of one of the lysimeters containing old tailings (Experiment 1). Release of this Ra-226 coincided with a decrease in sulphate concentration in the leachate. In addition, there was essentially no

pyrite left in this layer. This suggests that when sulphate production from pyrite oxidation is complete, a sulphate mineral containing Ra-226 and formed in the leaching pachucas begins to solubilize, releasing the Ra-226. Hence, these tailings appear to be on the verge of releasing all their Ra-226.

16. The loss of Ra-226 upon completion of sulphate dissolution is substantiated by data from tailings containing little or no pyrite (Madawaska). After almost complete dissolution of gypsum in these tailings, the loss of Ra-226 increased by an order of magnitude. The increase in Ra-226 is attributed to the decrease of sulphate concentration in the pure water which permits a substantial increase in dissolution of a sulphate precipitate containing Ra-226. Such tailings thus provide an excellent source for studying geochemical controls upon Ra-226 evolution without the complication caused by pyrite oxidation.

17. Washing experiments were conducted on tailings from the leaching pachucas and the middle section of a high-rate, old tailings lysimeter to ascertain which minerals might be maintaining Ra-226 on the surface of tailings solids. Correlations were sought between Ra-226 and concentrations of various metals (Pb, Fe, Ba, and Ca) in the wash water. Barium is the only metal whose concentration gives a consistent correlation with the Ra-226 activity in the water. The chemical speciation measurements show that only $BaSO_{4(s)}$ and jarosite $(KFe_3(SO_4)_2(OH)_6)$ in the low-rate lysimeter leachates, and only $BaSO_{4(s)}$ and $Fe(OH)_{3(s)}$ in the high-rate lysimeter leachates, are close to solubility limits. Therefore, $BaSO_{4(s)}$ must be the precipitate controlling Ra-226 behaviour through the mill and into the tailings pile. Barium can be derived from dissolution of trace quantities of barium minerals in the ore and their subsequent rapid reprecipitation as precipitates (probably less than 1 μm in size) on the surface of the host tailings solids in the leaching pachucas.

18. Scanning Electron Microscope-X-Ray Emission (SEM-XRE) analyses were made on solids from the old tailings of Experiment 1 and on fresh samples from the leaching pachucas (LP), partial neutralization (PN) tanks and final neutralization (FN) tanks of the Rio Algom mill. The analyses show that many particles are formed on the host tailings solids in the LP and substantially more in the PN and FN tanks. Many of the particles are composed of Al, Si, K, Ca, Fe, and S, suggesting alumino-silicates, gypsum and pyrite. Some precipitates in the tailings have a morphology consistent with jarosite. Several particles have a composition and morphology consistent with ettringite, a mineral formed in concrete reactions. No significant quantities of $BaSO_{4(s)}$ were identified either

by examination with the SEM beam of individual precipitated particles (1 to 5 μm in size) located on the host solids or by ultrasonication to remove surface materials from the silicate mineral background. The weathered tailings solids were found to have a substantially lower surface coverage of secondary precipitates than the coarse particles taken fresh from the mill. This observation is consistent with dissolution of gypsum from tailings after placement in a tailings pile.

19. The leaching of Ca, Mg, SO_4, and Ra-226 from (Ba,Ra)SO_4 sludges in settling pond sediments is consistent with dissolution reactions in sediment pore water and the diffusion of these constituents into the overlying water. Leaching from sludge sediments treated with a proprietary solidification process is consistent with the dissolution of a (Na,K)-(silicate, sulphate) precipitate which can be dissolved. The subsequent appearance of Ca in leachates from both sediments and tailings treated with this solidification process suggests that the encapsulating material dissolved sufficiently to allow the $CaSO_4$ and $MgSO_4$ contained in these wastes to start to dissolve. Thus the solidification process provides, at least initially, neutralization capacity to the tailings, but may only delay the development of acidification of the sludges and tailings, if pyrite is present.

20. Vegetating tailings with a fescue/red-top grass mixture, to which a layer of sewage sludge was added as a nutrient and source of organic matter, was unsuccessful over the long term. The leachate from the tailings became acidic as quickly as that from the controls, and the grasses died.

21. Vegetating tailings which had been treated with a proprietary solidification process was more successful. The grasses had not died by the end of the 7-year study; however, vegetation yields continually decreased during the experiment. It is not known whether the vegetation could be successfully maintained over a longer term. Dissolution of the encapsulating material, as observed in other experiments, could permit the development of pyrite oxidation reactions and the subsequent destruction of the vegetation.

REFERENCES

Alexander, M., "Most Probable Number Method for Microbial Populations", Methods of Soil Analysis, Part 2. Editor: C.A. Black, American Society of Agronomy, Inc., Madison, Wisconsin, 1965.

Atomic Energy Control Board, The Management of Uranium Mill Tailings - An Appraisal of Current Practices. Advisory Panel on Tailings, Report AECB-1156, September, 1978.

Beak, Dose Commitment Calculations for a Generic Uranium Mill Tailings Site in Northern Ontario, Report for Atomic Energy Control Board of Canada, 1982.

Benes, P., M. Odrzalek, and M. Cejchanova, "The Physicochemical Forms of Traces of Radium in Aqueous Solutions Containing Chlorides, Sulphates and Carbonates", Radiochem. Radionanal Letters 50(4), 227-242, 1982.

Blair, R.D., J.A. Cherry, T.P. Lim and A.J. Vivyurka, "Groundwater Monitoring and Contaminant Occurrence at an Abandoned Tailings Area, Elliot Lake, Ontario", Presented at the First International Conference on Uranium Mine Waste Disposal, Soc. Mining Engineers of AIME, Vancouver, May 19 to 21, 1980.

Blakeman, W.B., "Management of Uranium Mine/Mill Wastes", Presented at the EPS Nuclear Industry Seminar, March 27 to 28, 1979.

Bland, C.J. and D.E. Gonzalez. "A Report on a Study to Determine the Chemical and Physical Stability of Barium/Radium Sulphate Sludges under Varying Conditions of Temperature, pH and Dissolved Sulphate Concentrations", Energy, Mines and Resources, Canada, Contract No. OSU76-00147, March, 1977.

Box, G.E.P., W.G. Hunter, and J.S. Hunter, Statistics for Experimenters, John Wiley & Sons, Inc., 1978.

Brown, J.B., "Jarosite-Goethite Stabilities at 25°C", Mineral Deposita, (Berl)6, 245-252, 1971.

Bryant, D.N., D.B. Cohen, and R.W. Durham, "Leachability of Radioactive Constituents from Uranium Mine Tailings - Status Report (June 1974 to January 1977)", Environment Canada Water Pollution Control Directorate, Technology Development Report, EPS 4-WP-79-4, April 1979.

Cherry, J.A., Personal Communication, April, 1981.

Cherry, J.A., R.J. Blackport, N. Dubrovsky, R.W. Gillham, T.P. Lim, D. Murray, E.J. Reardon, and D.J.A. Smyth, "Subsurface Hydrology and Geochemical Evolution of Inactive Pyritic Tailings in the Elliot Lake Uranium District, Canada", Proceedings, Third Symposium on Uranium Tailings Management, Colorado State University, Fort Collins, Colorado, November 24 to 25, 1980.

Clark, D.A., "State-of-the-Art: Uranium Mining, Milling and Refining Industry", U.S. Environmental Protection Agency, Corvallis, Oregon, Report No. EPA-660/2-74-038, June, 1974.

Coady, J.R. and L.C. Henry, "Regulatory Principles, Criteria and Guidelines for Site Selection, Design, Construction and Operation of Uranium Tailings Retention Systems", Seminar on Management, Stabilization and Environmental Impact of Uranium Mill Tailings, Albuquerque, New Mexico, July 24 to 28, 1978.

Davies, O.L., and P.L. Goldsmith, "Statistical Methods in Research and Production", Oliver and Boyd, Edinburgh, 1972.

De Hek, H., R.J. Stol, and P.L. De Bruyn, "Hydrolysis Precipitation Studies of Aluminum (III) Solutions 3. The role of Sulphate Ion". J. Colloid Interface Science, 64(1), p. 72-89, 1978.

Durham, R.W. and S.R. Joshi, "Determination of ^{210}Pb, ^{226}Ra and ^{137}Cs in Sediments", Chemical Geology, 18, p. 155-160, 1976.

Durham, R.W. and S.R. Joshi, "Determination of ^{228}Th, ^{230}Th and ^{232}Th in Environmental Samples from Uranium Mining and Milling Operations", Journal of Radioanalytical Chem., 52(1), 1979.

EIFAC (European Inland Fisheries Advisory Commission), "Water Quality Criteria for European Freshwater Fish - Extreme pH Values and Inland Fisheries", Water Research, 3, p. 593-611, 1969.

EPA (Environmental Protection Agency, USA), Nitrogen Removal Technology Transfer Series Document, 1980.

EPS, "Standard Procedure for Testing the Acute Lethality of Liquid Effluents to Fish", 1977.

Gorber, D.M. and B.G. Ibbotson, "Environmental Assessment of Uranium Mining in Elliot Lake, Ontario", Symposium on Uranium Mill Tailings Management, Fort Collins, Colorado, November 19 to 20, 1979.

IUPAC, Stability Constants of Metal-Ion Complexes Part A Inorganic Ligands. (ed. by Eric Hogfeldt). IUPAC Chem. Data Series No. 21, Pergamon Press (New York), 1982.

Kaiman, S., "Mineralogical Examination of Old Tailings from the Nordic Lake Mine, Elliot Lake, Ontario", Report ERP/MSL 77-190 (IR), CANMET, Dept. of Energy, Mines and Resources, Ottawa, 1977.

Landolt-Bornstein. Zahlenwerte und Funktionen aus Physik Chemie II Band Eigenschaften Der Materie in Ihren Aggregatzustanden 7. Teili Elektrochemische Systeme, p. 259-260, 1950.

Lind, C.J., "Specific Conductance as a Means of Estimating Ionic Strength". U.S. Geol. Survey Prod. Paper 700-D, p. 272-280, 1970.

MacLaren, James F., Limited, "Environmental Assessment of the Proposed Elliot Lake Uranium Mines Expansion: Volume 4 - Environmental Assessment", April, 1978.

Moffett, D. and M. Tellier, "Radiological Investigations of an Abandoned Uranium Tailings Area", Journal of Environmental Quality, 7(3), p. 310-314, 1978.

Moffett, D. and M. Tellier, "Uptake of Radioisotopes by Vegetation Growing on Uranium Tailings", Canadian Journal of Soil Science, 57(4), p. 417-424, 1977.

Moffett, D., "Environmental Aspects of Thorium", CANMET Report MRP/MRL 77-43(OP), March, 1977.

Moffett, D., "The Disposal of Solid Wastes and Liquid Effluents from the Milling of Uranium Ores", CANMET, Dept. of Energy, Mines and Resources, Canada, Report 76-19, July, 1976.

Morel, F., and J.J. Morgan, Environ. Sci. Technol., 6,58, 1972.

Murray, D. and D. Moffett, "Vegetating the Elliot Lake Uranium Mine Tailings", Journal of Soil and Water Conservation, 32(4), p. 171-174, 1977.

Nikitin, B., and P. Tolmatscheff. "Einbetrag zur Gultigkeit des Massenwirkungsgesetzes II. Quantitative Bestimmung der Loslichkeit des Radium Sulfates in Natrium Sulfatlosungen und in Wasser". Z. Physikat Chem. 167A, p. 260-272, 1933.

Pramer, D. and E.L. Schmidt, Experimental Soil Microbiology, Burgess Publishing Co., Minneapolis, Minn., 1964.

Radioactivity Subgroup, "Draft Report of Radioactivity Subgroup to the Mining Task Force for the Development of Effluent Guidelines and Regulations for the Canadian Mining Industry", Environmental Protection Service, July, 1974.

Raicevic, D., "Decontamination of Elliot Lake Uranium Tailings", The Canadian Mining and Metallurgical Bulletin, August, 1979.

Reilly, P.M. and G.E. Blau, "The Use of Statistical Methods to Build Mathematical Models of Chemical Reacting Systems", The Canadian Journal of Chemical Engineering, 52, p. 289-299, June, 1974.

Ringbom, A., Complexation in Analytical Chemistry, Wiley-Interscience, New York, 1963.

Ritcey, G.M. and M. Silver. "Lysimeter Investigations on Uranium Tailings at CANMET". CIM Bulletin 75(846)), p. 134-143, 1980.

Robertson, J.A., Geology of Township 149 and Township 150, Geological Report 57, Ontario Department of Mines, 1968.

Rossum, J.R., "Checking the Accuracy of Water Analyses through the Use of Conductivity", J. Am. Water Works Assoc., 67, p. 204-205, 1973.

Roy, A.C. and W. Keller, "Water Pollution in the Serpent River", Status Report, Ontario Ministry of the Environment, Toronto, Ontario, 1976.

Sales, R.K., "Disposal of Liquid Wastes by Chemical Fixation Solidification - The Chemfix^{R} Process", Toxic and Hazardous Waste Disposal, Vol.1, R.B. Projasek (ed.), Ann Arbor Science Publishers Inc., Ann Arbor, Mich., 1979.

Schmidt, J.W. and D. Moffett, "Overview of Canadian Environmental Research in the Uranium Mining Industry", Presented at BCWWA and FACE "Uranium Mining and the Environment Seminar", Vancouver, British Columbia, April 11, 1979.

Scott, J.S., "Uranium Mining and Milling Waste Treatment", EPS Nuclear Industry Seminar, March 27-28, 1979.

Sill, C.W., "Decomposition of Refractory Silicates in Ultramicro Analysis", Anal. Chem. 16(12), 1961.

Sill, C.W. and R.L. Williams, "Preparation of Astinides for α Spectrometry without Electrodeposition", Anal. Chem. 53(3), 1981.

Sillen, L.G. and A.E. Martell. Stability Constants, Special Publication 17, The Chemical Society (London), 1964.

Sillen, L.G. and A.E. Martell. Stability Constants - Supplement No. 1, Special Publication 25, The Chemical Society (London), 1971.

Silver, M. and G.M. Ritcey, "A Simulated Study on the Effects of Bacteria, Organics and Salt Solutions on Uranium Mine Mill Tailings from Elliot Lake, Ontario", CANMET, Dept. of Energy, Mines and Resources, Canada, Report MRP/MSL 80-82(OP&J), June, 1980.

Skeaff, J.M., "Distribution of Radium-226 in Uranium Tailings", Report MRP/MSL 77-340(J). CANMET, Dept. of Energy, Mines and Resources, Ottawa, Canada, June, 1976.

Snodgrass, W.J., D.L. Lush, and J. Capobianco. "Implications of Alternative Geochemical Controls on the Temporal Behaviour of Elliot Lake Tailings", in Management of Wastes from Uranium Mining and Milling, International Atomic Energy Agency, Vienna (Publ.) p. 285-310, 1983.

Umbreit, W.W., R.H. Burris, and J.F. Stauffer, Manometric and Biochemical Techniques, Fifth Ed., Burgess Publishing Co., Minneapolis, Minn., 1972.

Vivyurka, A.J., "Rehabilitation of Tailings Areas of Uranium Mines", 7th Annual Meeting of the Canadian Mineral Processors, Ottawa, Ontario, January 21 to 23, 1975.

Zahary, G., D. Murray, and B. Hoare, "Reclamation - A Challenge to Open Pit Mining Operations in Canada", Presented at the World Mining Congress, Lima, Peru, November, 1974.

Zimmerman, J.B. and V.C. Armstrong, "The Determination of Radium-226 in Uranium Ores and Mill Products by Alpha Energy Spectrometry", CANMET Report 76-11, 1976.

ACKNOWLEDGMENTS

Many people have participated in this project since its conception in 1974. Those people originally active in its initiation and management are acknowledged in the Status Report by Bryant et al. (1979) describing the results of the experiment up to January 1977. The senior author of this report was responsible for the management of the study after June 1979. Technical maintenance and operation of the experiments during that part of the study were provided by several technicians. The technical contributions of Mr. Don Bartels, Ms. Margaret Gregory, Mr. Don Hamilton, Mr. Kevin Hosler, Mr. Tim Little, Mr. Steve Sawell, Mr. Terry Sway, and Mr. Adrian Van Kester to this study are gratefully acknowledged. The chemical, radiochemical, and bioassay tests performed by the Analytical Services Section of the Wastewater Technology Centre are gratefully acknowledged, particularly the contributions of Mess'rs Peter Fowlie, David Ide, Serge Metikosh, and Jerry Rajkumar.

Experiment 5 on the microbiology of solidified tailings was conducted at the Chemistry and Biology Research Institute of Agriculture Canada by Dr. Karl C. Ivarson. Dr. Ivarson's report on the conductance and results of Experiment 5 was incorporated into Chapter 8 of this report, and his contribution is gratefully acknowledged.

The first draft of this report was reviewed by Dr. John Cherry and Mr. Ron Nicholson of the Earth Sciences Department of the University of Waterloo, and Dr. Marvin Silver of CANMET. Based on their helpful suggestions, a contract was issued to IEC-Beak Consultants Ltd. to characterize the leached tailings from Experiment 1 and interpret the results of the study. The funding provided by CANMET and the contribution of Dr. Jim Skeaff as Scientific Authority for this contract are greatly appreciated.

The authors also acknowledge the contributions of the following people to the IEC-Beak contract. Professor Ron Mills of the Department of Civil Engineering at the University of Toronto enthusiastically helped in our examination of tailings morphology with the SEM-XRE. Mr. Ron Nicholson and Mr. Neil Dubrowsky sampled and physically characterized the residual tailings. Mr. Nicholson also coordinated the chemical measurements for sulphate, sulphide, and carbonate in the tailings. Dr. Michael Bancroft, University of Western Ontario, conducted Mossbauer analyses on several samples. Mr. Al Vivyurka, Rio Algom, kindly provided some leached ore samples from the leaching pachucas, partial neutralization tanks, and final neutralization tanks for the washing experiments. Dr. Donald Lush reviewed aspects of the report. Mr. John Robertson

organized the analyses of samples for solids characterization, water chemistry, etc., and technically reviewed the interpretations of some of the results.

APPENDIX A
CHARACTERIZATION OF LEACHATES AND TAILINGS SOLIDS

A.1 Chemical Characteristics of Leachate from Experiment 1

Representative leachate samples from the final 1.5 years of the study were analyzed for all major ions and various trace metals. The actual samples analyzed are listed in Table A.1(a). The last 1.5 years correspond to the period when a major shift in geochemistry occurred. During this period, the pH of the low-rate lysimeter increased from 0.7 to 1.5 and its TDS concentration decreased from about 200 g/L to near 20 g/L, whereas the pH of the high-rate lysimeter increased from 2.4 to 3.1 and its TDS concentration decreased from 1.5 g/L to 0.15 g/L. Measured concentrations in the leachates are given in Table A.1(b). Cations were measured by inductively coupled argon plasma (ICAP), anions by ion chromatography.

In general, each leachate sample is an iron sulphate solution, reflecting the fact that its composition is largely determined by the aerobic oxidation of pyrite minerals (by the bacteria *T. ferrooxidans*). Next to iron, aluminum and potassium are the most abundant cations; they probably originated from proton attack upon alumino-silicates such as K-feldspar. Calcium and magnesium are the next most abundant cations; Ca probably originated from residual sulphates formed during milling, whereas Mg resulted from proton attack upon alumino-silicates. The negligible concentration of sodium suggests that sodium alumino-silicates were not present in the lysimeter solids. The high concentrations of copper and nickel suggest that oxidation of chalcopyrite ($CuFeS_2$) and of a nickel sulphide may have occurred; however, the quantity of metal sulphide is small relative to pyrite. The concentration of titanium may have originated from proton attack on titanium minerals such as rutile (TiO_2), titanite ($CaTiSiO_5$), and uranium minerals such as brannerite [$(U, Ca, Ce)(TiFe)_2O_6$]. The concentration of other cations (Ag, Ba, Be, Cd, Co, Cr, Mn, P, Pb, Sr, Th, V, Zn) has a negligible effect on the pH of the solution, although the potential control of cations, such as Ba and Pb, on Ra-226 transport cannot be disregarded.

Sulphate is the dominant anion. Nitrate is present in significant amounts in certain samples because of the addition of nitric acid for sample preservation; nitrate production during leaching is assumed to be negligible. Because the samples were diluted 1:100 to allow measurement of sulphate, the detection limits of ion chromatography preclude conclusive statements about the patterns of phosphorus and nitrate in these

TABLE A.1(a) DESCRIPTION OF LEACHATE SAMPLES ANALYZED

Water*	IEC Beak Sample No.	Date Sampled from Lysimeter	Lysimeter[a]	Sample Volume (mL)	WTC Analyses TDS (mg/L)	WTC Analyses pH	Description of Sample Condition (Jan/83) pH	Description of Sample Condition (Jan/83) Visual
1	28	Dec/79-Apr/80	L1	50	215.0	0.7	1.1x	slightly cloudy, dark amber
	29	Apr/80-Aug/80	L1	1000	166.0	1.2	1.2	slightly cloudy, brown
	30	Aug/80-Jan/81	L1	1000	63.0	1.4	1.3	slightly cloudy, dark amber, some bacterial remains
2	31	Apr/81-Aug/81	L1	1000	26.8	1.5•	1.5	slightly cloudy, amber
3	32	Dec/79-Apr/80	L7	1000	187.0	0.8	1.3	dark brown
	33	Dec/79-Apr/80	L7	150	187.0	0.8	1.1x	dark brown
	34	Dec/79-Apr/80	L7	750	187.0	0.8	1.4	dark brown
4	35	Apr/80-Aug/80	L7	1000	126.0	1.0	1.4	brown
	36	Aug/80-Jan/81	L7	1000	61.6	1.2	1.5	clear, amber
	37	Jan/81-Apr/81	L7	1000	27.3	1.5	1.7	clear, amber, some bacterial remains
5	38	Apr/81-Aug/81	L7	1000	29.9	1.5•	-	clear, amber, some bacterial remains
6	39	Dec/79-Apr/80	L2	50	1.5	2.3	1.5x	clear, colourless
	40	Apr/80-Aug/80	L2	500	0.778	2.5	2.6	clear, colourless
	41	Apr/80-Aug/80	L2	1000	0.778	2.5	1.6x	clear, colourless, some bacterial remains
7	42	Aug/80-Jan/81	L2	1000	0.443	2.6	2.2	clear, colourless except for reddish-orange specs
	43	Jan/81-Apr/81	L2	450	0.222	3.0	1.7x	clear, colourless
	44	Jan/81-Apr/81	L2	500	0.222	3.0	1.9x	clear, colourless
8	45	Apr/81-Aug/81	L2	1000	0.100	3.2•	2.0x	clear, colourless
9	46	Dec/79-Apr/80	L8	75	1.2	2.3	1.6x	clear, colourless
	47	Apr/80-Aug/80	L8	1000	0.502	2.5	2.1	clear, colourless
	48	Apr/80-Aug/80	L8	1000	0.502	2.5	2.2	clear, colourless
	49	Aug/80-Jan/81	L8	1000	0.483	2.5	1.8x	clear, colourless
10	50	Apr/81-Aug/81	L8	1000	0.150	3.1•	-	clear, colourless

• data not recorded, value is average of Periods 35 and 37
+ waters used for speciation calculations, Section A.12
x samples to which HNO_3 was added as preservative
a L1, L7 = low-rate control lysimeters; L2, L8 = high-rate control lysimeters, from Experiment 1

TABLE A.1(b) CONCENTRATIONS OF ANIONS AND CATIONS MEASURED IN EXPERIMENT I LEACHATES BY ICAP-IC

IEC Beak Sample No.	Al (mM/L)	Ba (μM/L)	Ca (mM/L)	Cd (μM/L)	Co (mM/L)	Cu (mM/L)	Fe (mM/L)	K (mM/L)	Mg (mM/L)	Mn (μM/L)	Ni (μM/L)
28	31.4	0.42	3.39	1.4	0.714	0.538	958.0	8.57	1.10	30.6	174.0
29	19.9	0.39	1.47	3.5	0.602	0.545	673.0	5.09	0.691	21.3	140.0
30	3.53	0.20	0.579	1.9	0.214	0.394	245.0	0.639	0.121	7.65	64.7
31	0.83	0.12	0.399	0.8	0.086	0.301	89.7	0.128	0.0173	1.8	25.7
32	20.4	0.39	0.546	2.0	0.635	0.395	770.0	5.19	0.744	23.1	184.0
33	20.6	0.39	0.671	2.0	0.584	0.405	791.0	5.42	0.761	23.8	152.0
34	20.1	0.39	0.546	2.9	0.609	0.397	754.0	5.24	0.749	22.9	167.0
35	9.15	0.30	0.297	2.9	0.428	0.423	485.0	2.43	0.362	13.3	106.0
36	3.18	0.20	0.134	2.2	0.210	0.340	238.0	0.691	0.109	5.8	61.0
37	0.86	0.12	0.0624	0.9	0.0872	0.233	105.0	0.163	0.023	2.0	26.9
38	0.76	0.11	0.0312	0.09	0.0854	0.244	89.5	0.0512	0.018	1.5	28.1
39	0.11	0.20	0.0472	0.09	0.0058	0.0187	4.22	0.0767	0.0086	4.9	1.97
40	0.10	0.24	0.017	0.09	0.0039	0.0178	2.22	0.102	0.0053	5.1	1.2
41	0.10	0.24	0.0157	0.09	0.0041	0.0181	2.40	0.0767	0.0053	4.7	1.5
42	0.057	0.26	0.0165	0.09	0.002	0.0116	0.371	0.0767	0.0045	5.3	1.0
43	0.035	0.55	0.0267	0.09	0.0009	0.00708	0.218	0.0767	0.0045	5.3	0.9
44	0.034	0.55	0.0220	0.09	0.001	0.00705	0.229	0.0767	0.0033	5.1	0.9
45	0.032	0.65	0.0157	0.09	0.0009	0.00801	0.0471	0.128	0.0053	5.3	0.9
46	0.10	0.20	0.0250	0.09	0.00051	0.0168	3.21	0.102	0.0066	5.5	1.9
47	0.11	0.24	0.0157	0.09	0.0031	0.0113	1.40	0.128	0.0053	4.9	1.0
48	0.11	0.24	0.0172	0.09	0.0032	0.0112	1.40	0.128	0.018	5.3	1.4
49	0.11	0.20	0.015	0.09	0.0029	0.0091	0.790	0.102	0.0045	5.3	0.9
50	0.04	0.37	0.0013	0.09	0.0009	0.00513	0.0451	0.0512	0.002	0.2	0.9

IEC Beak Sample No.	Pb (μM/L)	Th (μM/L)	Ti (mM/L)	V (mM/L)	Zn (mM/L)	Zr (mM/L)	P (mM/L)	Cl^- (mM/L)	NO_3^- (mM/L)	SO_4^- (mM/L)
28	8.93	10.6	0.420	0.0448	0.0203	0.109	0.42	0.014	49.4	1290.0
29	10.1	7.02	0.278	0.353	0.0176	0.0509	0.68	0.014	0.08	971.0
30	11.6	0.733	0.0532	0.00987	0.0095	0.0067	0.03	1.81	0.08	370.0
31	11.1	0.259	0.0132	0.00328	0.0049	0.0011	0.03	0.86	0.08	133.0
32	10.9	7.11	0.276	0.0379	0.0178	0.0353	0.29	4.01	0.08	1060.0
33	11.1	6.94	0.286	0.0351	0.0178	0.0569	0.55	4.15	54.8	1090.0
34	10.4	7.03	0.282	0.0347	0.0187	0.0555	0.47	3.98	0.08	1060.0
35	12.8	3.41	0.132	0.021	0.013	0.0232	0.37	3.24	0.08	703.0
36	11.6	0.60	0.0482	0.0104	0.009	0.0061	0.11	2.03	0.08	337.0
37	9.65	0.04	0.0141	0.00471	0.0043	0.0013	0.03	1.52	0.08	167.0
38	8.69	0.17	0.00095	0.00318	0.0319	0.0006	0.022	0.296	0.08	185.0
39	13.8	0.04	0.00228	0.0001	0.0009	0.0006	0.03	0.395	41.4	6.45
40	15.0	0.09	0.00089	0.0002	0.0008	0.0006	0.03	0.14	0.08	4.40
41	15.0	0.09	0.00089	0.0001	0.0008	0.0006	0.03	0.17	15.4	3.90
42	17.6	0.04	0.00048	0.0001	0.0008	0.0006	0.03	0.395	0.08	2.81
43	21.0	0.04	0.00065	0.0001	0.0008	0.0006	0.03	0.451	16.8	0.85
44	20.3	0.04	0.00081	0.0001	0.0008	0.0006	0.03	0.333	13.2	0.67
45	4.83	0.04	0.0013	0.0001	0.0008	0.0006	0.03	0.113	16.6	0.59
46	14.7	0.09	0.0011	0.0001	0.0008	0.0006	0.03	0.395	31.2	5.55
47	14.3	0.09	0.00083	0.0001	0.0008	0.0006	0.03	0.282	0.08	4.40
48	15.0	0.09	0.00079	0.0001	0.0008	0.0006	0.03	0.212	0.08	4.32
49	13.8	0.09	0.00058	0.0001	0.0008	0.0006	0.03	0.14	20.8	2.81
50	11.3	0.04	0.0001	0.0001	0.0003	0.0006	0.22	0.15	16.3	1.07

Note: Units are mM/L unless indicated otherwise.

waters. The occurrence of orthosilicic acid and fluoride result from proton attack upon alumino-silicates; chlorides result from similar attack. The TOC and ammonia result from biomass formation during pyrite oxidation; CO_2 and N_2 from air or the applied water are probable sources of bacterially formed carbon and nitrogen. Probably no significant amount of carbon is available in the lysimeter solids, although organics are applied during milling. The work of Ritcey and Silver (1980) suggests that organics are not significant in pyrite oxidation reactions. Furthermore, 20 years after discharge to the tailings pile, any such compounds are expected to be present only in trace amounts.

The majority of the leachate parameters measured by the WTC from the 20-year old tailings are TDS, pH, and radionuclides (Th-230, Ra-226, Pb-210, Th-232, Th-228). To understand the chemistry of radionuclides in the leachates, it is useful to examine the solid-solution equilibria of major cations and anions, their complexes, the buffering system which controls pH, and the biochemistry of leachates. Before conducting this examination, the limits of analytical chemistry to measure total concentrations of anions and cations have to be understood. Hence, the precision of analytical chemistry is discussed by comparing measurements of TDS made by various laboratories and the electroneutrality of the anionic-cationic balances (Appendix A.1.1). Calculations of the speciation of the major ions and metal-ligand complexes are then described (Appendix A.1.2). Stoichiometric concepts are then used to describe the pyritic oxidative metabolism of the lysimeters (Appendix A.1.3).

A.1.1 TDS Measurements and Electroneutrality Balances. A comparison for the high-rate lysimeter between TDS measured by IEC-Beak and TDS calculated from the ICAP (cations) and ion chromotography (anions) analyses by Barringer is given in Figure A.1. These TDS values include the dissolved solids derived from HNO_3 addition for sample preservation. The calculated values for TDS are consistently less than the measured values. The degree of difference is not a function of concentration, but is random throughout the wide range of concentrations. The plot of TDS measured by the WTC before HNO_3 addition and that calculated from the anion-cation analyses by Barringer (Figure A.2) suggests increased deviation from the 1:1 relationship compared to that of Figure A.1. The increased deviation results either from the method used to calculate TDS (a large number representing the weight of the dish plus evaporated solids minus a large number representing the weight of the dish) or from changes in TDS concentrations between the time that the samples were first taken and analyzed for TDS (by the WTC in 1980-81) and the time that were reanalyzed (by IEC-Beak in Jan.

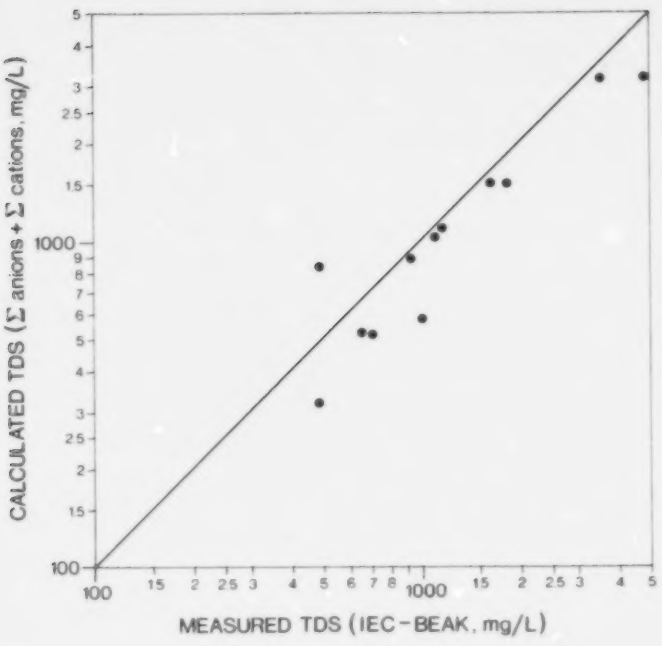

FIGURE A.1 CALCULATED vs. MEASURED TDS CONCENTRATIONS IN LEACHATE FROM THE HIGH-RATE LYSIMETERS

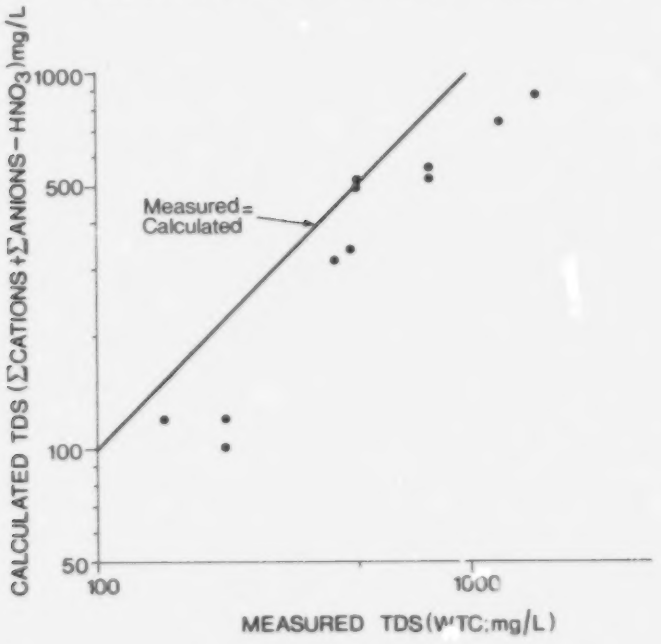

FIGURE A.2 CALCULATED vs. MEASURED TDS CONCENTRATIONS IN LEACHATES FROM THE HIGH-RATE LYSIMETERS WHEN NITRIC ACID CONCENTRATIONS ARE SUBTRACTED FROM CALCULATED TDS CONCENTRATIONS

1983). Due to the addition of HNO_3 for sample preservation in the high-rate lysimeter samples, a direct comparison of the two sets of TDS measurements by the two different laboratories is most appropriate on the leachates from the low-rate lysimeters because they did not have significant quantities of HNO_3 added as preservative.

As shown in Figure A.3, the calculated TDS values for the low-rate lysimeters again are lower than those measured by the WTC. The effect of HNO_3 on these samples is less than 5 percent for the two samples to which HNO_3 was added. Hence, the difference is not caused by HNO_3.

The difference could be caused by precipitation of products from reactions during the time between analyses for TDS and the ICAP-IC measurements for cations and anions (1 to 2 years). A comparison between TDS measured by IEC-Beak and those measured by the WTC (Figure A.4) suggests that the WTC measurements are slightly and consistently higher than those of IEC-Beak. This allows for some degree of precipitation, but the difference is quite small compared to the difference between measured and calculated TDS. The differences between the two sets of TDS measurements in Figure A.4 can easily be attributed to differences in analytical results from two different laboratories.

Differences between ICAP-IC measurements and TDS measurements have also been observed by IEC-Beak on other waters, particularly groundwaters. Parts of the measured TDS can be water molecules which are bound to a metal and do not evaporate during the drying process used for TDS analysis. For example, hydrated iron is octahedrally coordinated with six water molecules as innersphere complexes. For a solution containing 56 000 mg/L Fe (i.e., 1 mol Fe), there are 108 000 mg/L of water associated with the iron (i.e., 6 mols H_2O for 1 mol Fe). One needs about 30 000 mg/L TDS in the form of water to equal the TDS concentration measured in such a water. This would be supplied if one third of the water molecules coordinated with iron did not evaporate during drying. Another possibility is the formation of ferric hydroxo-polymers which do not break up during drying. The existence of such compounds at pH 0.8-1.5 is a matter of debate. The calculations given in the next section suggest that $Fe_2(OH)_2^{2+}$ is not a probable species at these low pH ranges.

Another possible error is that sulphate is inaccurately measured. For oxidation of pyrite, a Fe:S ratio of 0.5 is expected. For the low-rate lysimeter leachates, the ratio varies from 0.5 to 0.75, whereas it varies from 0.1 to 0.65 for most of the high-rate lysimeter leachates. This would suggest that the sulphate concentration is too low in the low-rate lysimeter and that some Fe^{3+} is precipitating out of solution in the high-rate

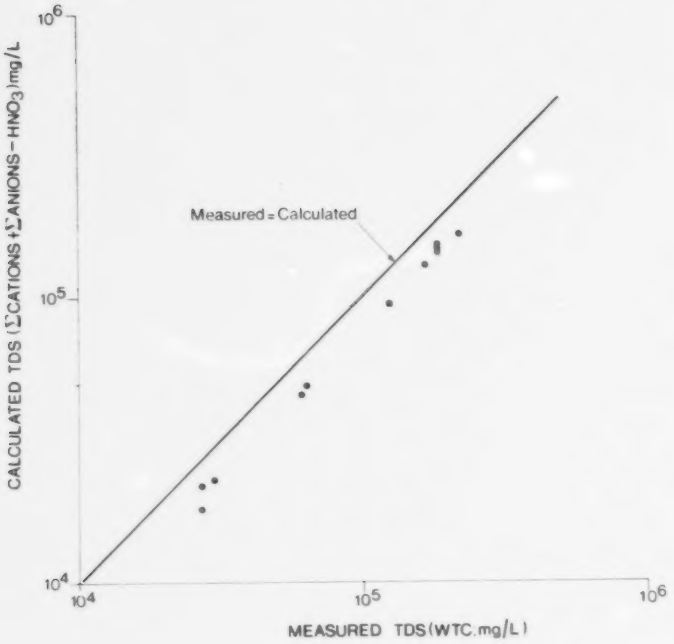

FIGURE A.3 CALCULATED vs. MEASURED TDS CONCENTRATIONS IN LEACHATES FROM THE LOW-RATE LYSIMETERS

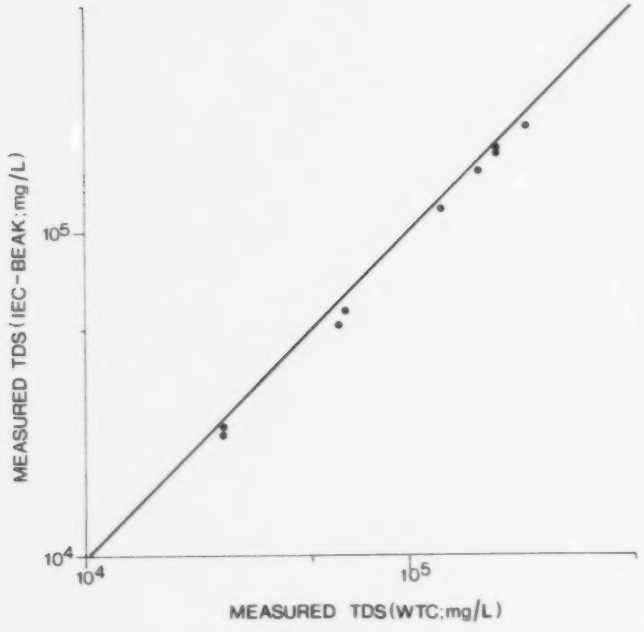

FIGURE A.4 WTC MEASUREMENTS OF TDS CONCENTRATIONS vs. IEC-BEAK MEASUREMENTS IN LEACHATES FROM THE LOW-RATE LYSIMETERS

lysimeter (i.e., for those samples where the Fe:S ratio is less than 0.5). Incomplete oxidation of FeS_2 may occur, yielding an SO_3^{2-} ion which is not picked up in the normal domain of ion chromatography. However, this possibility is contrary to the thermodynamics of the redox reaction; oxidation of sulphide should be complete at a much lower redox potential than that of Fe^{2+}.

Another method for checking the sulphate measurements is by comparing them with acidity measurements and electroneutrality calculations. The sum of sulphate plus nitrate agrees with measured acidity (measured to a pH 4.5 operationally defined end point) for the high-rate lysimeter leachates (Figure A.5), although most of the measurements of acidity are somewhat higher than the levels of SO_4^{2-} and NO_3^- would suggest. Nitrate is included in the diagram because considerable quantities of nitrate were added to the samples for preservation. When the effects of HNO_3 are removed from measured values, the deviation from a 1:1 relationship between measured acidity and SO_4^{2-} (see Figure A.6) for the high-rate lysimeter does not increase substantially, although the scatter about the 1:1 line has increased. For the low-rate lysimeter (see Figure A.7), measured acidity is consistently higher than measured sulphate by 10 to 20 percent. This suggests that sulphate concentrations are low, provided that an operationally defined end point of pH 4.5 does not substantially overshoot neutralization of acidity incorporated in the proton complexed with sulphate.

How one perceives the electroneutrality balances depends upon one's interpretation of the redox chemistry of iron and the speciation of SO_4^{2-}. If all Fe is assumed to occur as Fe^{3+}, the sum of cations is larger than the sum of anions for the low-rate lysimeters (see Table A.2); a less consistent but similar pattern is observed for the high-rate lysimeters. Samples showing negative values for cations in the high-rate lysimeters are associated with samples to which HNO_3 was added or samples in which Fe^{3+} precipitation is probable (i.e., the Fe/S ratio is less than 0.5) or both. If we assume that all Fe occurs as Fe^{2+}, the sum of cations is less than the sum of anions for the low-rate lysimeters. A mixed pattern is observed in a comparison between total anions and total cations (based upon Fe^{2+}) for the high-rate lysimeters (see Table A.2). Because sulphate exists mainly as HSO_4^- at low pH's, the sum of the anions decreases considerably when HSO_4^- is factored into the calculations. However, calculations given below show that Fe^{2+} often competes more successfully for SO_4^{2-} than H+ does. Thus, the sum of anions based on HSO_4^- can be erroneously low. It is difficult to do electroneutrality balances for these waters without proper consideration of complexes.

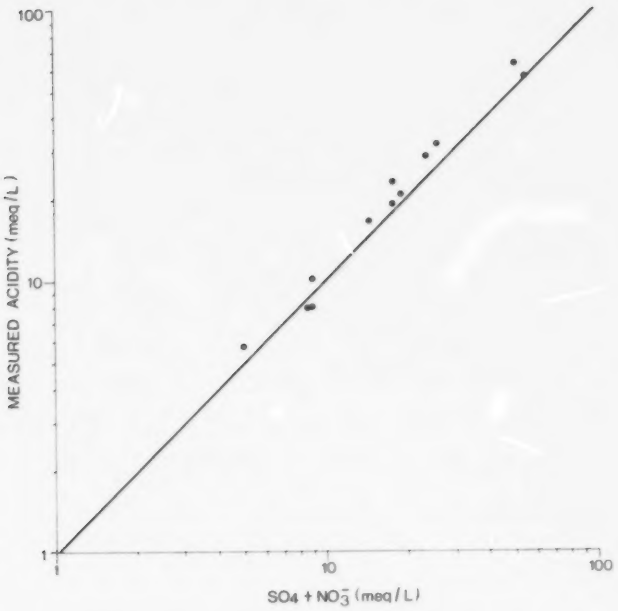

FIGURE A.5 MEASURED ACIDITY vs. THE SUM OF THE SULPHATE AND NITRATE CONCENTRATIONS IN LEACHATES FROM THE HIGH-RATE LYSIMETERS

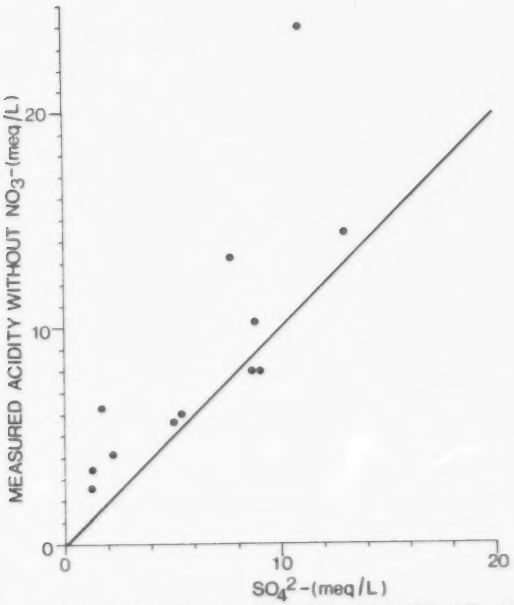

FIGURE A.6 MEASURED ACIDITY WITHOUT HNO_3 vs. SULPHATE CONCENTRATIONS IN LEACHATES FROM THE HIGH-RATE LYSIMETERS

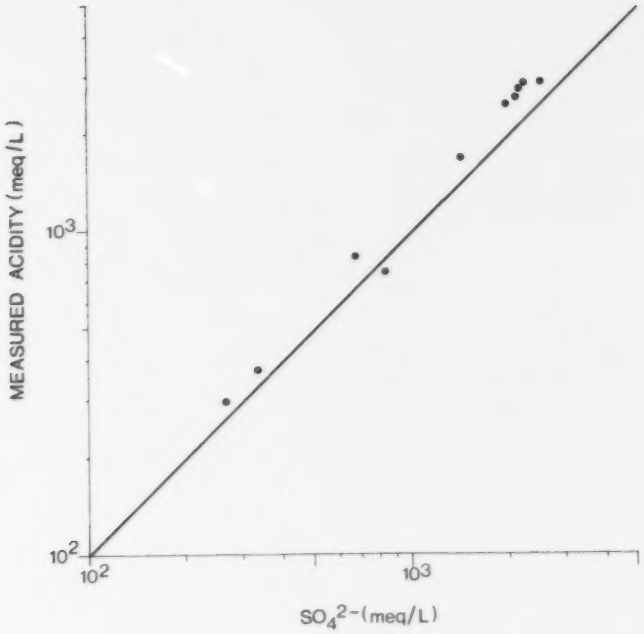

FIGURE A.7 MEASURED ACIDITY vs. SULPHATE CONCENTRATION IN LEACHATES FROM THE HIGH-RATE LYSIMETERS

Another way to check the lack of balance for measured versus calculated TDS is the use of volatile dissolved solids (VDS). VDS is often used as a measure of organic carbon. But TOC is less than 1 percent of TDS in all these waters; hence VDS must represent another material. VDS is the difference between TDS left after evaporation at 105°C and TDS left after drying at 456°C. The only probable explanation for VDS in these leachates is that they represent volatilization of water of hydration. When VDS is added to the sum of anions plus cations, the total sum approximately equals the measured TDS for all waters.

Accordingly, the lack of balance between measured TDS and calculated TDS is due to the incomplete loss of water of hydration of Fe^{3+}. Hence, the TDS values measured throughout this project are overestimated by about 30 percent. This suggests that, for leachates with a pH of less than 3, estimates of Fe and SO_4 concentrations can be made from TDS measurements, provided the TDS values are decreased for the water of hydration not lost during the TDS measurement. Precise determinations for the water of hydration of different leachates should be made by measurement. As a rule of thumb, an estimate of the order of 30 percent seems appropriate for Fe-SO_4 waters. For $CaSO_4$ waters, the TDS values should be reduced by 2(18)/(40.1 + 96.1 + 2 x 18) or about 20 percent. The two water molecules of hydration for gypsum are lost at 175°C; this

TABLE A.2 Fe:S RATIO AND ELECTRONEUTRALITY BALANCE FOR LEACHATE FROM OLD TAILINGS

Sample No.	Lysimeter+	$Fe_T/(SO_4)_T$ Ratio	$\sum$Anions** (meq/L)	$\sum$Anions*** (meq/L)	$\sum$Cations (based on Fe^{2+}) (meq/L)	$\sum$Cations (based on Fe^{3+}) (meq/L)
28	L1	0.748	2560	1460	2110	3060
29	L1	0.693	1940	1230	1530	2200
30	L1	0.662	742	446	567	812
31	L1	0.674	267	172	215	305
32	L1	0.726	2120	1270	1660	2430
33	L7	0.726	2190	1250	1670	2460
34	L7	0.711	2120	1320	1610	2370
35	L7	0.690	1400	866	1040	1530
36	L7	0.706	676	436	520	758
37	L7	0.629	331	229	234	339
38	L7	0.484	370	260	258	348
39*	L2	0.654	13.3	8.70	-	4.3
40	L2	0.505	8.97	7.91	9.0	11.2
41*	L2	0.615	8.00	5.40	14.9	17.3
42	L2	0.132	6.01	5.24	7.4	7.8
43*	L2	0.257	2.18	1.66	4.0	4.2
44*	L2	0.342	1.71	1.38	0.6	0.8
45*	L2	0.080	1.34	1.08	-6.2	-6.1
46*	L8	0.578	11.5	7.80	-7.2	-4.7
47	L8	0.318	9.11	7.00	11.3	12.7
48	L8	0.324	8.88	7.45	9.7	11.1
49*	L8	0.281	5.77	4.20	2.0	-1.9
50*	L8	0.042	2.51	2.45	13.3	-3.5

* Substantial quantity of HNO_3 was added to sample. The measured (NO_3^-) and associated H^+ was subtracted from values for $\sum$anions and $\sum$cations.

** Based on the assumption that all sulphate is SO_4^{2-}

*** Based upon calculating actual speciation of SO_4^{2-} with H+

\+ L1, L7 = low-rate lysimeters; L2, L8 = high-rate lysimeters

calculation assumes that $CaSO_4 \cdot 2H_2O$ forms during the drying of gypsum solution. Similar theoretical calculations are not available for the Fe-SO_4 solution, because no information was found on the temperature for hydrated water loss from Fe^{3+}.

To calculate the probable TDS pattern over time, one could either calculate the aqueous species in leachates by assuming that they are dominated by the oxidation of FeS_2 or by using conductivity-TDS relationships. Conductivity is a useful surrogate;

unfortunately it is difficult to calculate conductivity at these high levels of TDS, because the normal theory for electrical contribution of different ions to conductivity is wrong at high ionic strength. For example, the data of Landolt-Bornstein (1950) for equivalent conductance for H^+, HSO_4^-, and SO_4^{-2}, and a calculation of the speciation of HSO_4^- - SO_4^{2-} using the method of Rossen (1973) and Lind (1970), suggest a conductance of 1100 mS/m; yet the observed value is much larger. Accordingly, a plot of conductivity against TDS (Figure A.8) must be used. For all leachate samples to which HNO_3 was not added, a linear relationship was observed, except for one sample. The effect of HNO_3 is to displace the relationship towards a higher conductance for the same TDS. Accordingly, a TDS-conductivity relationship may be used, provided that the major charge determining species (e.g., iron sulphate or calcium sulphate) does not change.

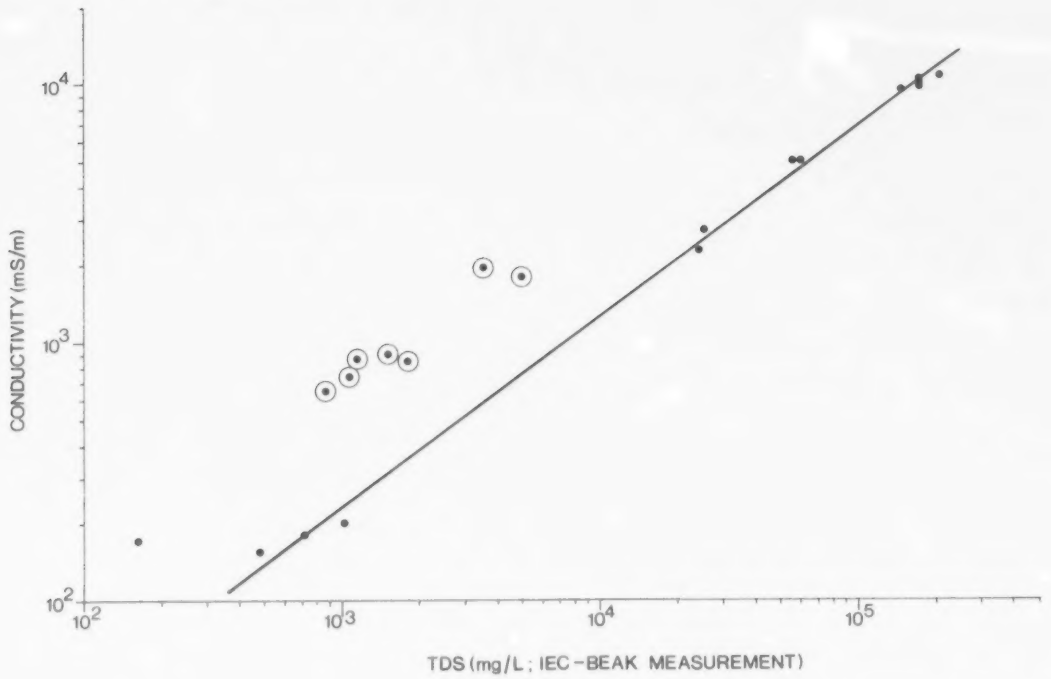

FIGURE A.8 CONDUCTIVITY vs. TDS CONCENTRATIONS IN LEACHATES FROM ALL LYSIMETERS (CIRCLED POINTS HAD NITRIC ACID ADDITION)

A.1.2 Cation-Anion Speciation. The formation of various complexes can significantly influence the transport characteristics of cations and anions from the lysimeter. The measurement of the concentration of different complexes is difficult in solutions of several anions and cations. Hence, speciation calculations may be used based upon knowledge of total concentration of anions and cations, and thermodynamic constants that describe the solubility of metal-ligand solids and the formation of soluble metal-ligand complexes. Such calculations provide guidance to estimating the probable chemistry of the water, but the calculations cannot be viewed as absolutely precise, because an actual equilibrium may not exist or the values assigned to the thermodynamic constants may be incorrect.

The algorithm by Morel and Morgan (1972) was used to make speciation calculations for sample waters. The thermodynamic data is from the compilation of Sillen and Martell (1964, 1971) and Ringbom (1963), which was then updated by a review of constants for complexes and solids of metal sulphates, fluorides, and chlorides from IUPAC (1982). Constants for thorium fluoride species are those of Beak (1982); the constants for radium sulphate and radium chloride species have been recently measured by Benes et al. (1981). The identification of a $RaSO_4^o$ species by Benes et al. infers that the original solubility product for $RaSO_4$ measured by Nikiten and Tolmatseheff (1932) is somewhat in error, because they do not appear to have considered the $RaSO_4^o$ complex. Inclusion of the $RaSO_4^o$ complex gives a solubility constant for $RaSO_{4(s)}$ of $10^{-10.41}$. The adjustment to the value calculated by Nikiten and Tolmatseheft ($10^{-10.37}$) is small.

Ten leachate samples were selected for speciation calculation (see Table A.3). The samples are designated by the terminology "model water" or "water". This terminology has been selected to emphasize that:

(i) the concentrations of all chemical constituents in the leachate samples may be incomplete,

(ii) the thermodynamic data that describe the complexation and precipitation-dissolution reactions may have errors associated with them, and

(iii) the number of complexes known to form (given current knowledge) may actually be incomplete.

Waters 1 and 2 are the initial and Waters 3 and 5 the final leachate samples analyzed by ICAP-IC from the low-rate lysimeters (L1 and L7 respectively); Water 4 is an intermediate sample, in time between Waters 3 and 5. Similarly, Waters 6 and 8 are the initial and Waters 9 and 10 the final leachate samples analyzed from the high-rate

TABLE A.3 CATION-ANION CONCENTRATIONS USED FOR SPECIATION CALCULATIONS FOR 10 WATERS

Metal/ Ligand	pC Total for Water Number									
	From Low-Rate Lysimeters					From High-Rate Lysimeters				
	1	2	3	4	5	6	7	8	9	10
Al	1.5	3.08	1.69	2.04	3.13	3.96	4.24	4.5	4.0	4.5
Ba	6.38	6.92	6.41	6.52	7.0	6.7	6.6	6.2	6.7	6.4
Ca	2.46	3.4	3.26	3.53	4.51	4.33	4.78	4.8	4.6	5.5
Cd	6.85	6.1	5.7	5.54	7.05	7.05	7.0	7.0	7.0	7.0
Co	3.15	4.066	3.2	3.37	4.07	5.24	5.7	6.0	5.3	6.0
Cu	3.27	3.52	3.4	3.37	3.61	4.73	4.9	5.1	4.8	5.3
Fe	0.0186	1.047	0.144	0.314	1.048	2.375	3.431	4.327	2.493	4.346
K	2.07	3.89	2.28	2.614	4.29	4.12	4.12	3.89	4.0	4.3
Mg	2.96	4.76	3.13	3.44	4.74	5.07	5.3	5.3	5.2	5.7
Mn	4.51	5.75	4.64	4.88	5.82	5.31	5.3	5.3	5.3	6.7
Na	3.52	4.4	3.76	4.06	5.0	5.0	5.0	5.0	4.3	5.0
Ni	3.76	4.59	3.74	3.97	4.55	5.7	6.0	6.0	5.7	6.0
Pb	5.04	4.95	4.96	4.89	5.06	4.9	4.8	5.32	4.83	4.95
Th	2.63	3.4	2.8	3.5	4.0	4.9	5.0	5.3	5.3	5.3
Ti	3.38	4.88	3.56	3.88	5.0	5.6	6.3	5.9	6.0	7.0
Zn	4.69	5.3	4.75	4.89	4.5	6.0	6.1	6.1	6.1	6.1
Ra	13.5	12.8	13.2	13.0	12.8	12.2	11.9	11.7	12.0	11.7
F	3.38	4.52	3.54	3.434	4.66	4.5	4.5	4.5	4.5	3.66
Cl	4.85	3.07	2.4	2.49	3.53	3.4	3.4	3.94	3.4	3.82
SO_4	0.107	0.885	0.0253	1.53	0.745	2.19	2.55	3.23	2.255	2.971
H^+	0.7	1.5	0.8	1.0	1.5	2.3	2.55	3.2	2.4	3.1

lysimeters (L2 and L8 respectively); Water 7 is an intermediate sample, in time between Waters 6 and 8 for lysimeter L2. The time covered by the initial and final samples is the period over which the TDS decreased by an order of magnitude (see Table A.1).

Waters 1 (low-rate) and 6 (high-rate) were selected for calculations of aqueous chemical speciation over a pH range (the actual metal and liquid concentrations were taken to be constant but the pH was allowed to vary). These model waters describe the actual concentrations for TDS, iron, etc. which were observed in the lysimeter leachate for most of the leaching period. Ionic strength was calculated by the algorithm of Morel and Morgan (1972); corrections for activity coefficients were calculated according to the Davies equation (Stumm and Morgan, 1981). The ionic strength (I) of Water 1 is approximately 1.3 M. Because the Davies equation begins to give some errors at I = 0.5 M, the calculations for Water 1 entail some uncertainty.

Water 1 was allowed to vary over the pH range of 0 to 3 (see Figures A.9 and A.10).

Aluminum	Al^{3+} dominates to pH 1.5; above pH 1.8, sulphate complexes dominate (Figures A.9a, A.10a).
Barium	Ba^{2+} is dominant to pH 1.5, but $BaSO_{4(s)}$ becomes important at higher pH's (Figure A.9b, A.10b).
Iron	Iron sulphate complexes dominate from pH 0 to pH 1.8; above pH 2, iron hydroxide dominates (Figures A.9c, A.10c).
Calcium	Ca^{2+} is important to pH 1.9, above which $CaSO_4^o$ is most important (Figure A.9d, A.10d).
Thorium	Thorium has several species of interest (sulphate, fluoride, hydroxide - see Figure A.9e) but sulphate dominates throughout the pH range (Figure A.10e).
Radium	$RaSO_4^o$ dominates throughout most of the pH range (Figures A.9f, A.10f).
Sulphate	The graph reflects the HSO_4 - SO_4^{2-} speciation predicted by a pK = 1.9 (Figure A.9g) but iron sulphate is the dominant species over much of the pH range (Figure A.10g).
Titanium	$TiO(SO_4)_x$ complexes are of some importance, but the 2^+ complex is most important below pH 1.5 whereas TiO^{2+} precipitates above pH 1.7 as the hydroxide (Figure A.10h).

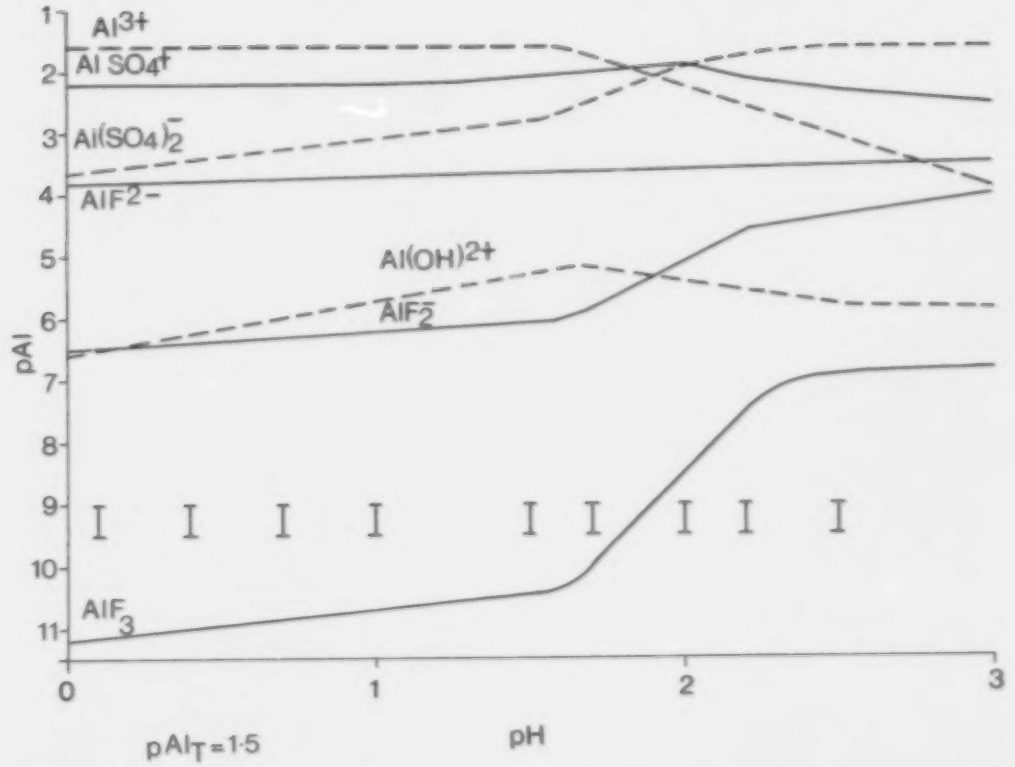

(a) Aluminum

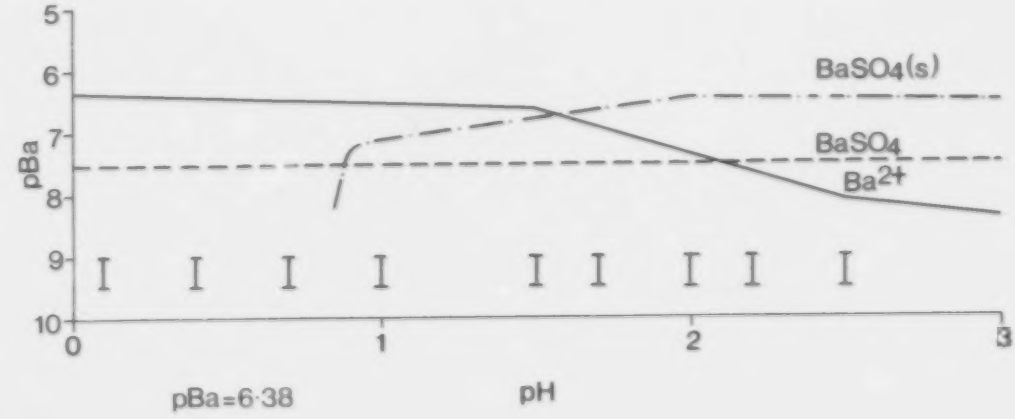

I = POINT OF EVALUATION

(b) Barium

FIGURE A.9 BJERRUM DIAGRAM FOR WATER I (ACTUAL pH = 0.7)

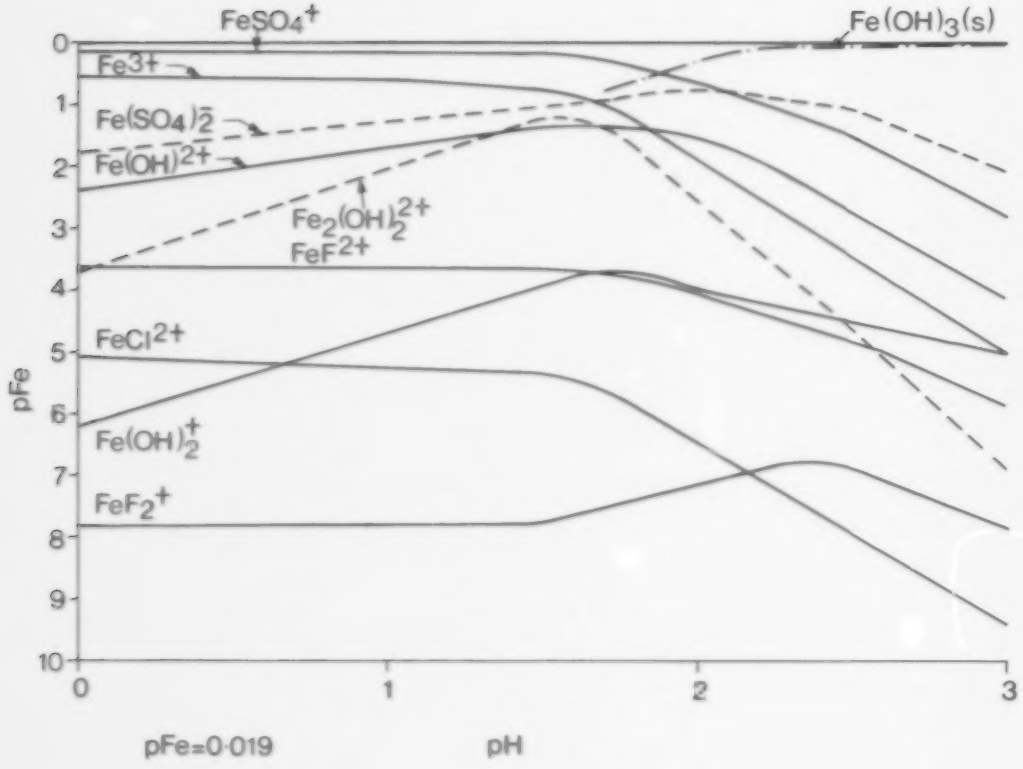

(c) Iron

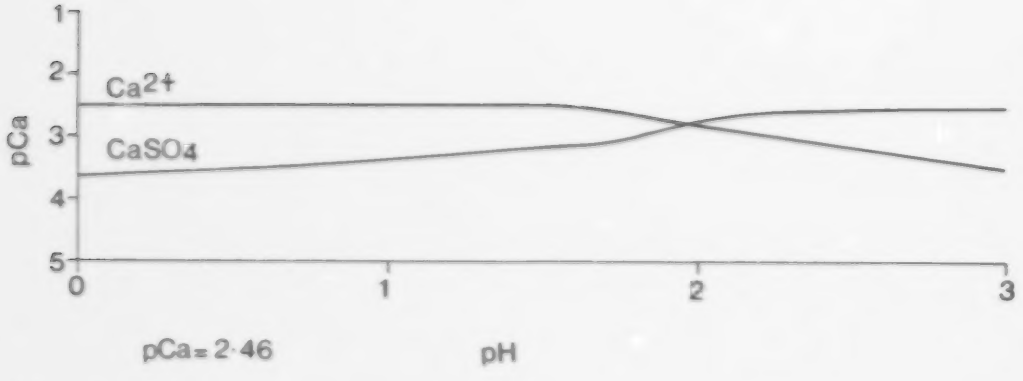

(d) Calcium

FIGURE A.9 BJERRUM DIAGRAM FOR WATER 1 (ACTUAL pH = 0.7) (Cont'd)

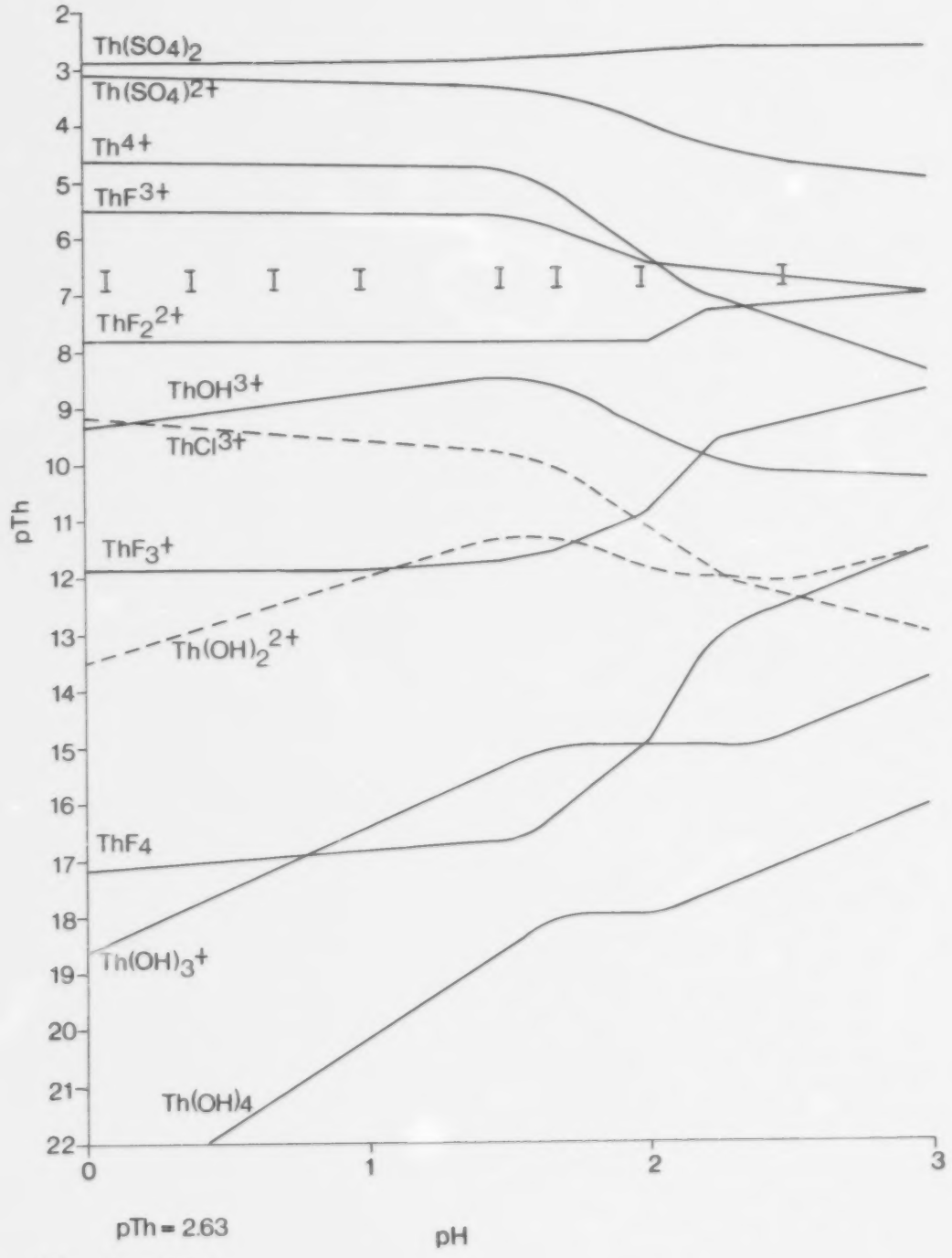

pTh = 2.63

(e) Thorium

FIGURE A.9 BJERRUM DIAGRAM FOR WATER 1 (ACTUAL pH = 0.7) (Cont'd)

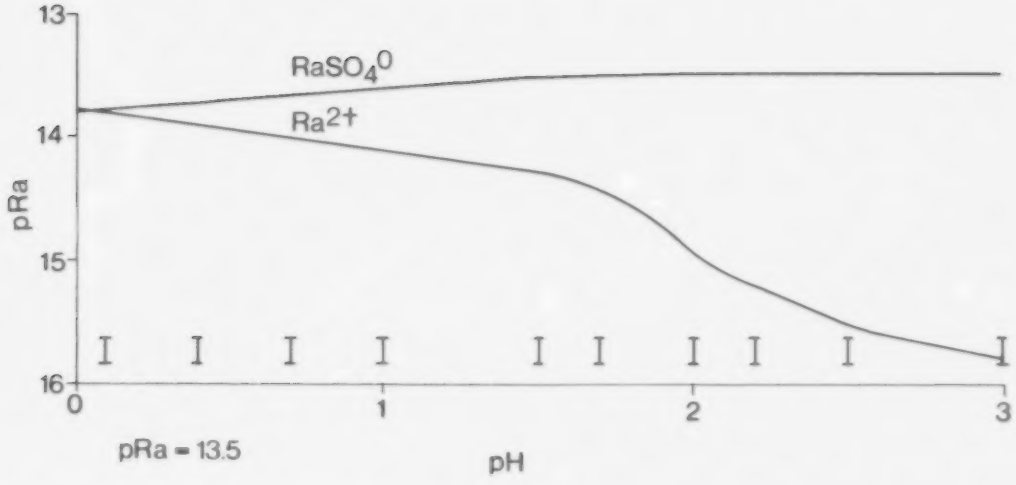

(f) Radium

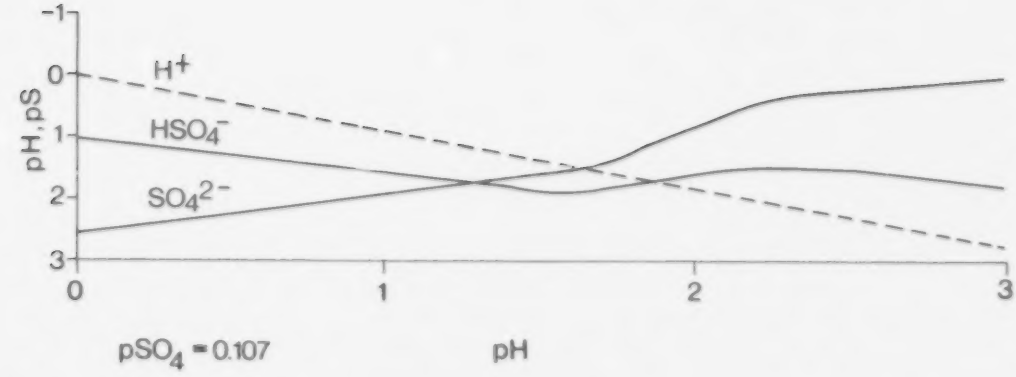

(g) Sulphate

FIGURE A.9 BJERRUM DIAGRAM FOR WATER 1 (ACTUAL pH = 0.7) (Cont'd)

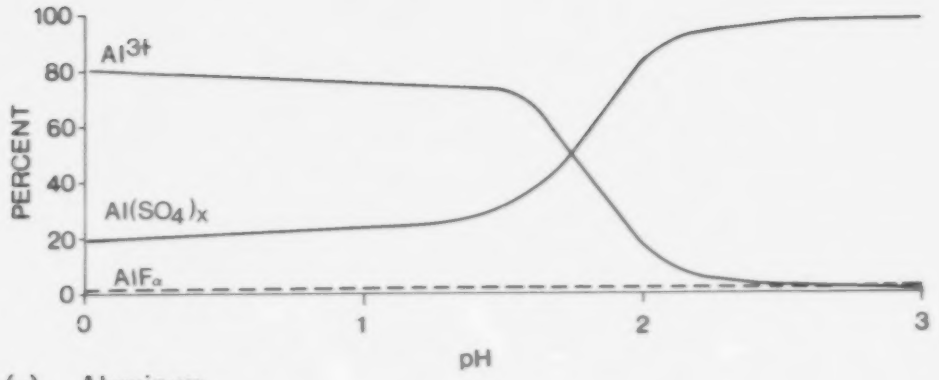

(a) Aluminum

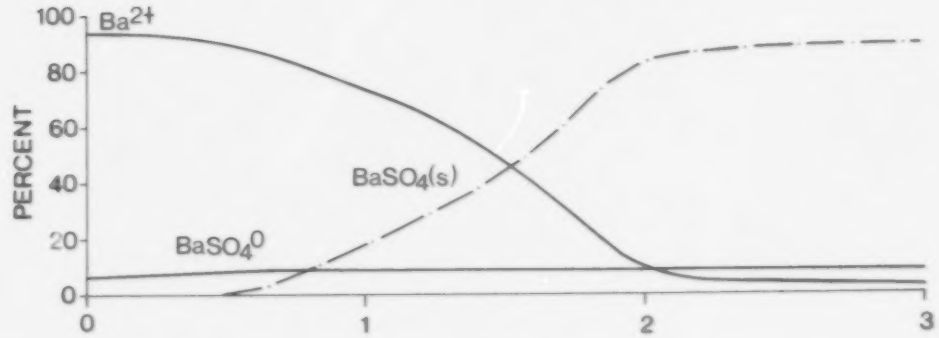

(b) Barium

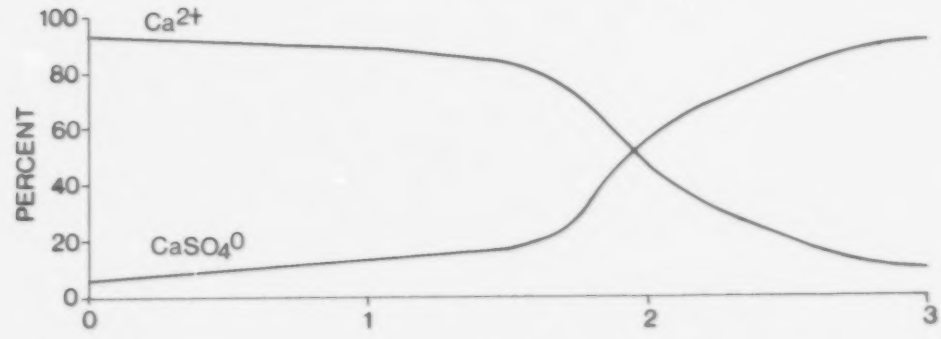

(c) Iron

FIGURE A.10 PERCENTAGE COMPOSITION OF VARIOUS METAL-LIGAND FORMS IN WATER 1 (ACTUAL pH = 0.7)

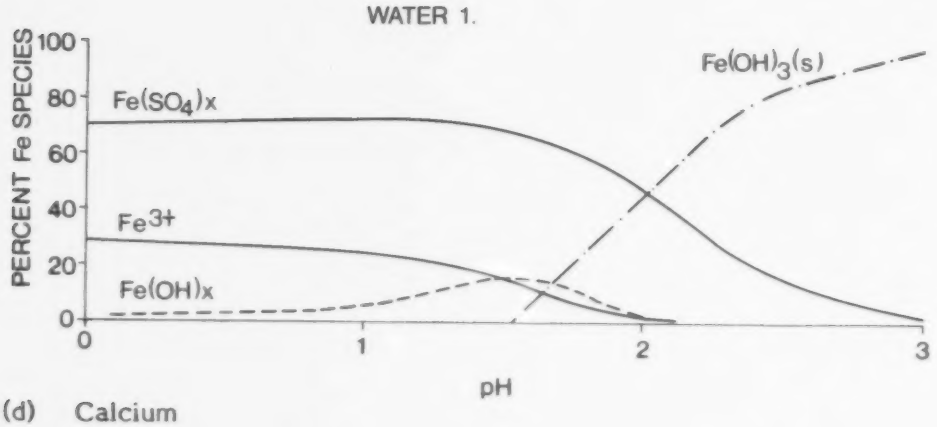

(d) Calcium

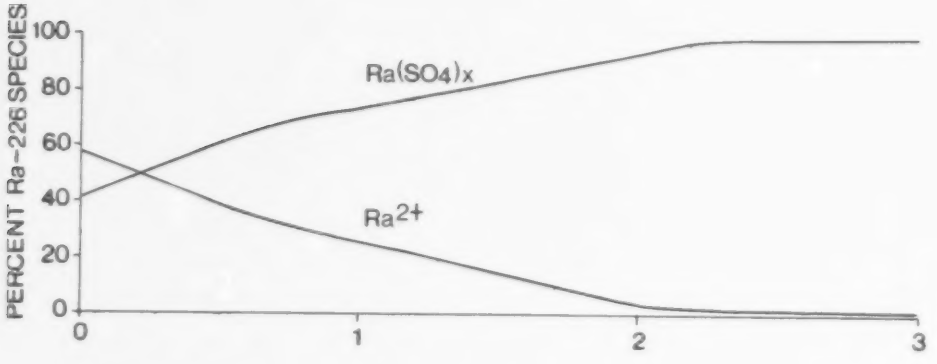

(e) Thorium

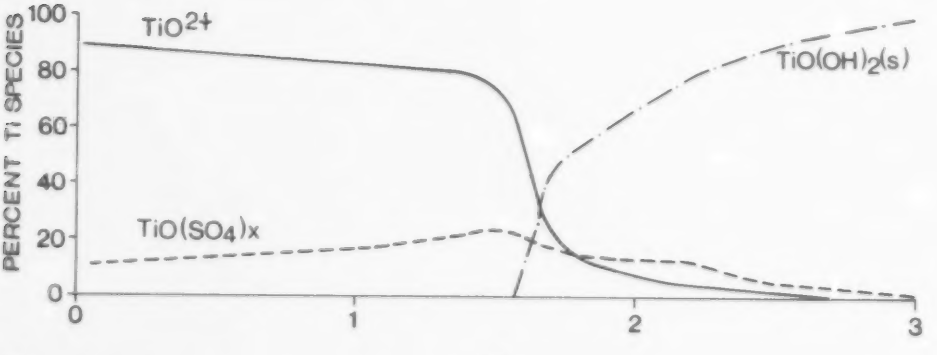

(f) Radium

FIGURE A.10 PERCENTAGE COMPOSITION OF VARIOUS METAL-LIGAND FORMS IN WATER 1 (ACTUAL pH = 0.7) (Cont'd)

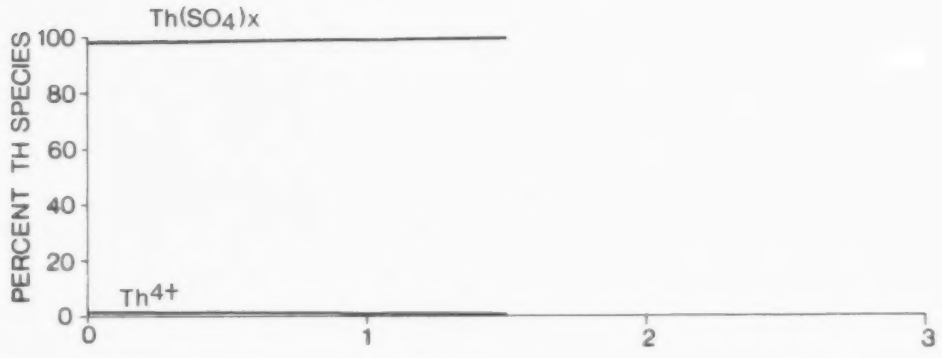

(g) Sulphate

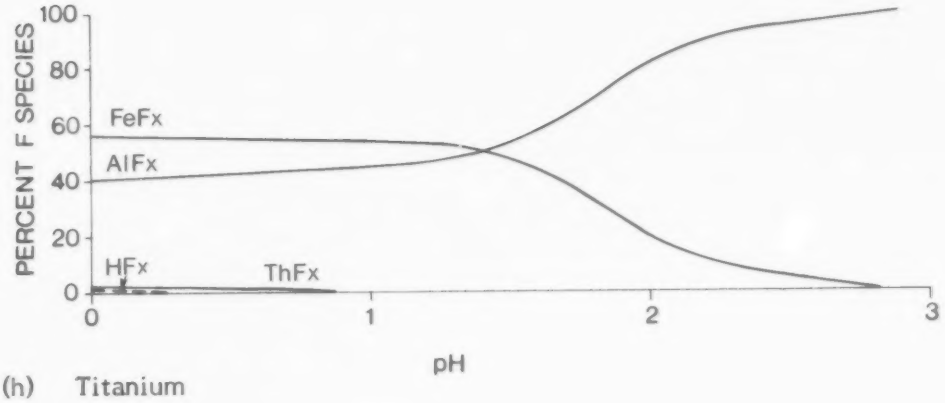

(h) Titanium

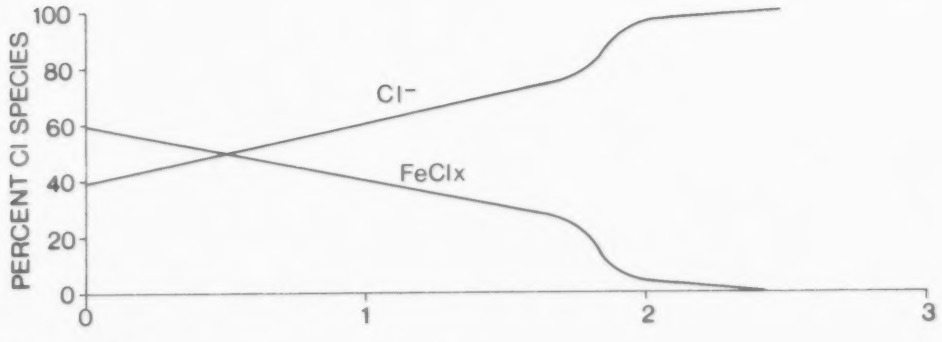

(i) Cobalt

FIGURE A.10 PERCENTAGE COMPOSITION OF VARIOUS METAL-LIGAND FORMS IN WATER ! (ACTUAL pH = 0.7) (Cont'd)

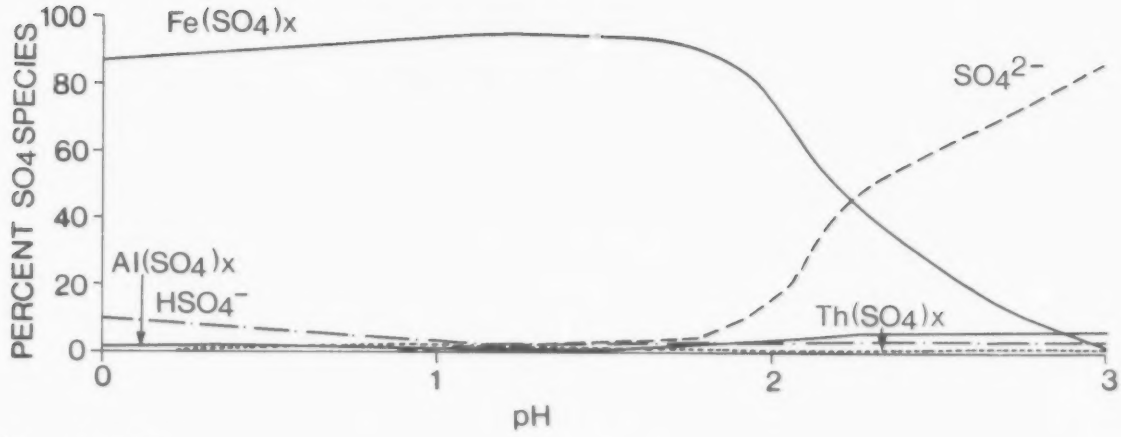

(j) Fluoride

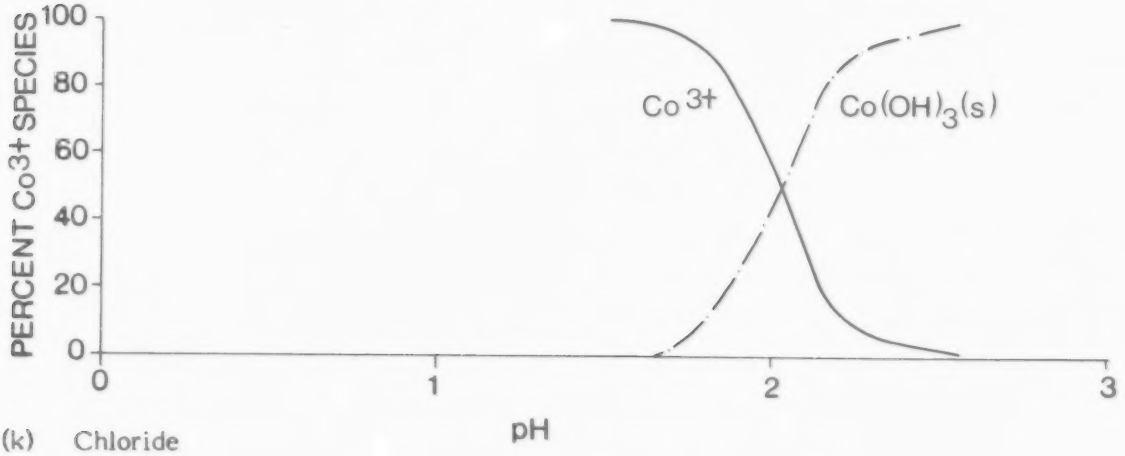

(k) Chloride

FIGURE A.10 PERCENTAGE COMPOSITION OF VARIOUS METAL-LIGAND FORMS IN WATER 1 (ACTUAL pH = 0.7) (Cont'd)

Cobalt	Co^{3+} (the assumed oxidation state of Co) precipitates as the hydroxide at pH 2 (Figure A.10i).
Fluoride	Fluoride is tied up mainly with aluminum and iron, despite the much lower concentrations of aluminum (Figure A.10j).
Chloride	Iron chloride complexes are important below pH 0.5 (Figure A.10k).

For Water 6 (the high-rate lysimeter; actual pH = 2.3 at time of sampling), several changes in speciation are noted (Figures A.11 and A.12). Some of the shifts occur because a wider pH range (0-6) is used in the diagrams.

Aluminum	AlF_3 complexes are much more important (Figures A.11a, A.12a), whereas aluminum hydroxide is predicted to precipitate at pH 5 whereas it does not precipitate in the Water 1 analysis.
Barium	$BaSO_{4(s)}$ precipitates at a slightly higher pH (Figures A.11b, A.12b).
Iron	$Fe(OH)_{3(s)}$ precipitates at a higher pH while $Fe(SO_4)$ complexes are less important over the pH range of 0 to 2 and Fe(OH) complexes and free Fe^{3+} increase in importance (Figures A.11c, A.12c).
Sulphate	Water 6 also has sufficiently less sulphate than in Water 1 so that the concentration of $CaSO_4^0$ is much less important than in Water 1 (Figures A.11d, A.12d). Sulphate species remain the dominant form of thorium (Figures A.11e, A.12e), although fluoride species assume some importance in the pH 3 to 6 range.
Radium	Ra^{2+} and $RaSO_4^0$ are of equal importance in Water 6 (Figures A.11f, A.12f), but the proportion of radium as $RaSO_4^0$ decreases from Water 1 to Water 6 because of the lower sulphate concentration in Water 6. Similarly the proportion of sulphate complexed with Fe^{3+} is substantially less in Water 6 (Figures A.11g, A.12g).
Titanium and Cobalt	TiO^{2+} and Co^{3+} precipitate at a higher pH in Water 6 than in Water 1 (see Figures A.12h and A.12i, respectively).
Fluoride	Thorium fluoride complexes are of importance in fluoride chemistry (Figure A.12j).
Chloride	Iron complexes of chloride are essentially unimportant (Figure A.12k).

The total concentrations measured in each model water are given in Table A.3 as pC (i.e., pC = the negative log, base 10, of the concentration in moles/L). The major forms of metal and ligand speciation for Waters 1 to 10 at their measured pH are given in Table A.4. If the percent of a complex is less than 0.5 percent, it is not included.

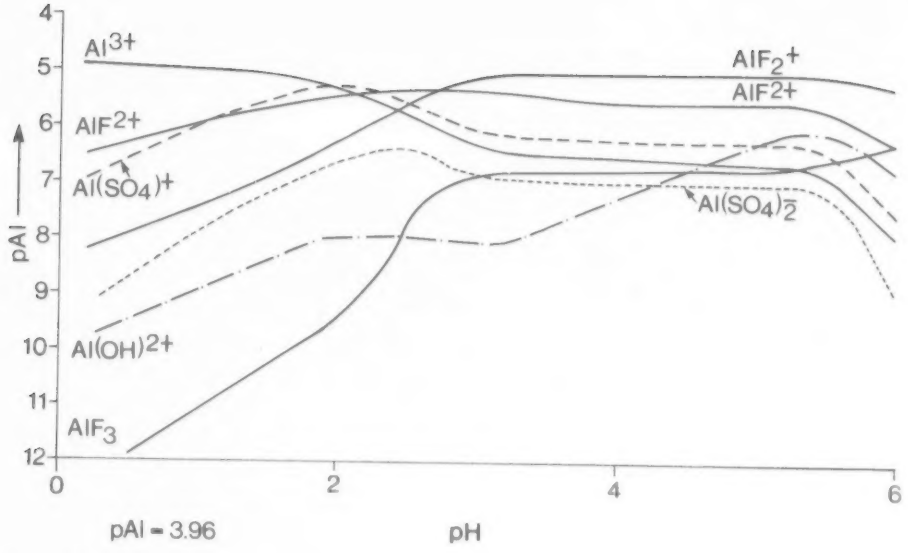

(a) Aluminum

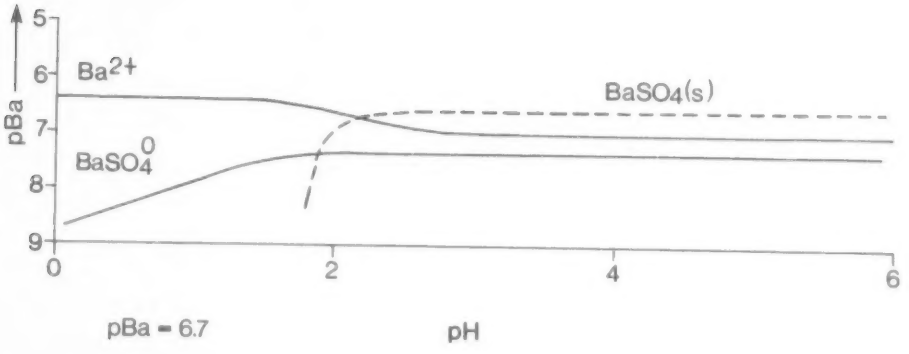

(b) Barium

FIGURE A.11 BJERRUM DIAGRAM FOR WATER 6 (ACTUAL pH = 2.3)

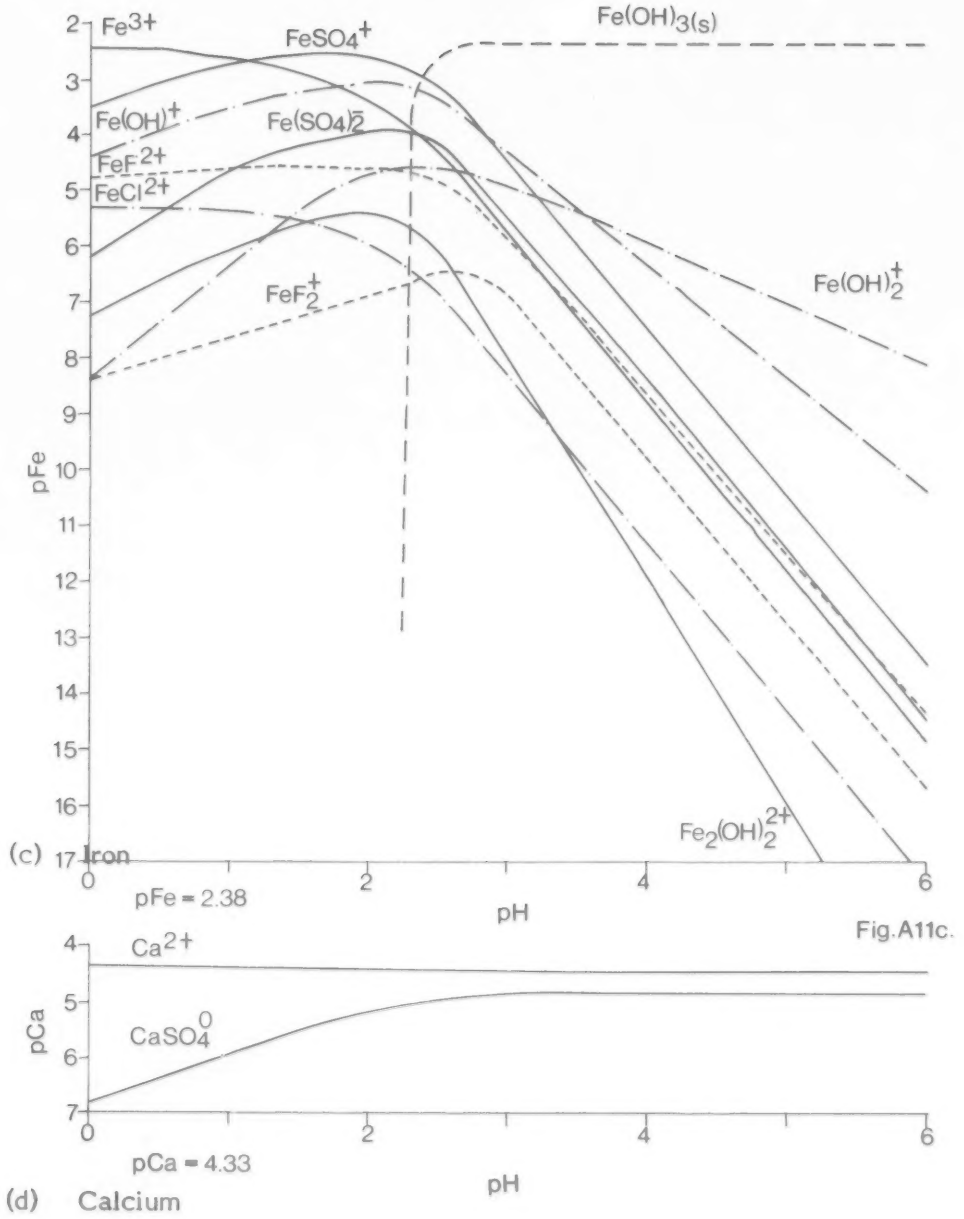

FIGURE A.11 BJERRUM DIAGRAM FOR WATER 6 (ACTUAL pH = 2.3) (Cont'd)

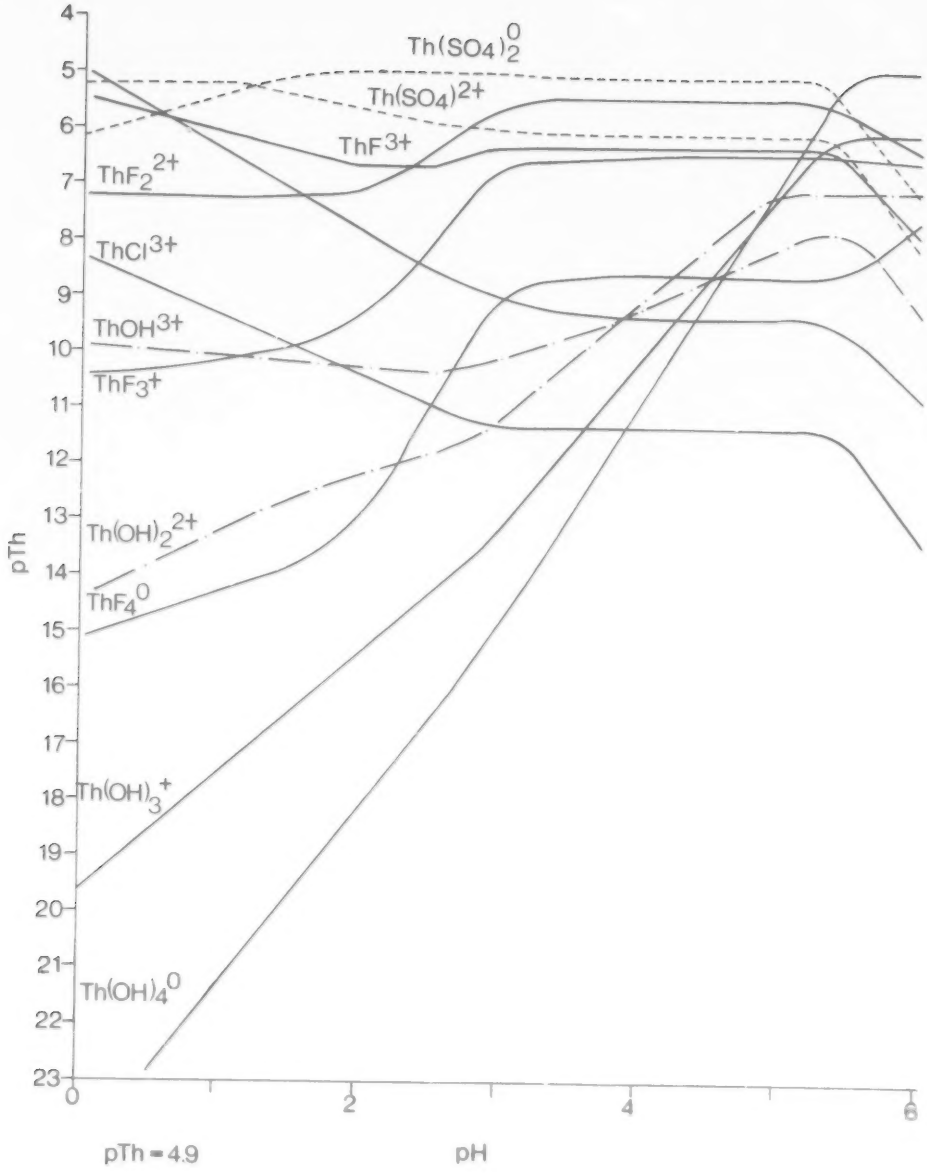

(e) Thorium

FIGURE A.11 BJERRUM DIAGRAM FOR WATER 6 (ACTUAL pH = 2.3) (Cont'd)

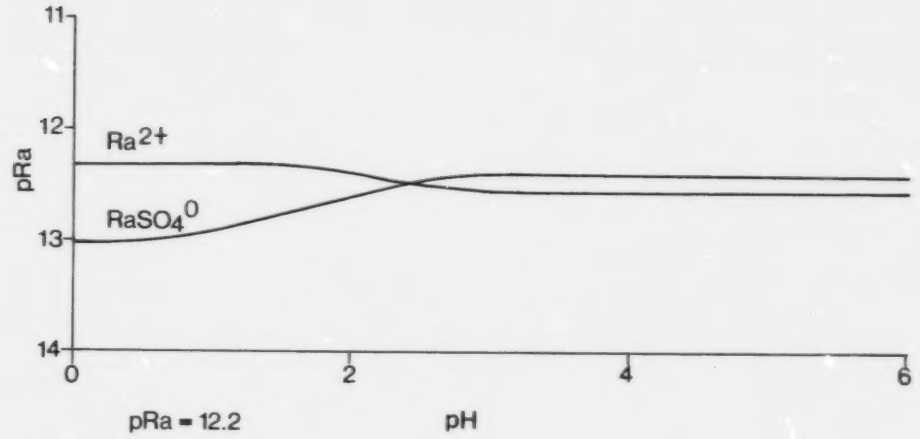

(f) Radium

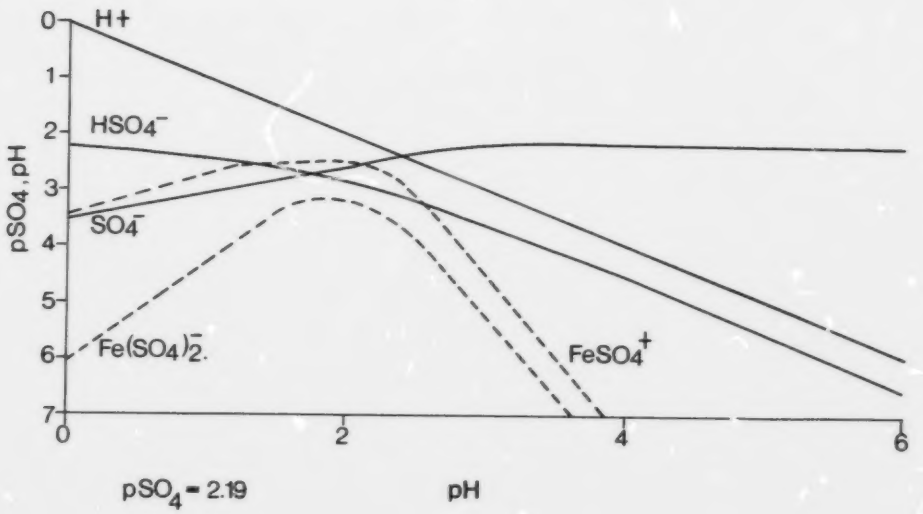

(g) Sulphate

FIGURE A.11 BJERRUM DIAGRAM FOR WATER 6 (ACTUAL pH = 2.3) (Cont'd)

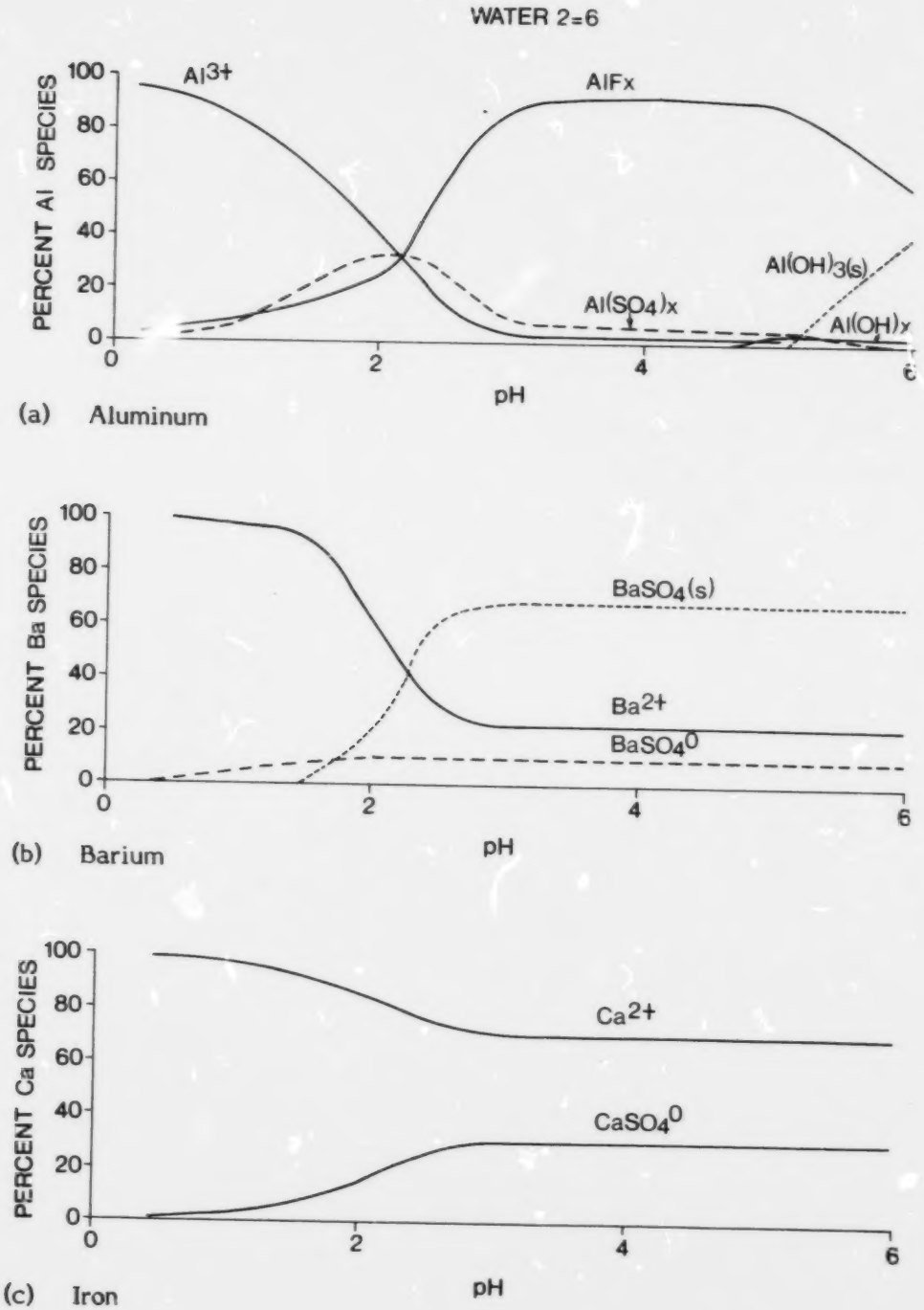

FIGURE A.12 PERCENTAGE COMPOSITION OF VARIOUS METAL-LIQUID FORMS IN WATER 6 (ACTUAL pH = 2.3)

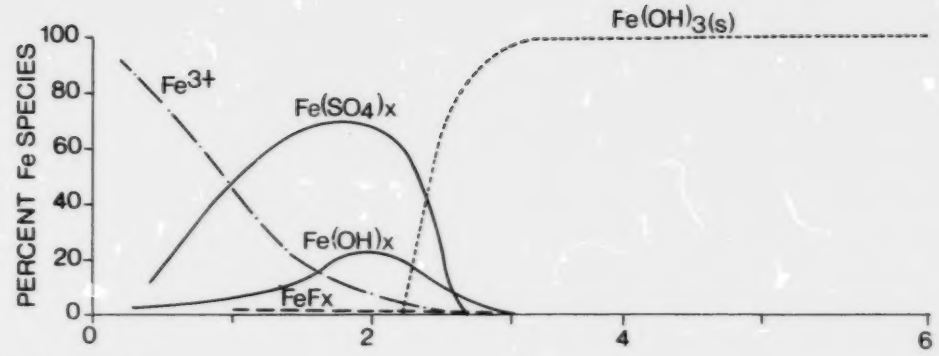

(d) Cadmium

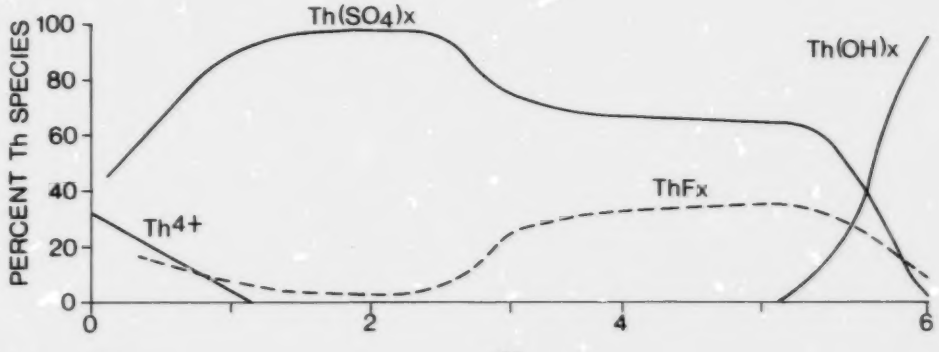

(e) Thorium

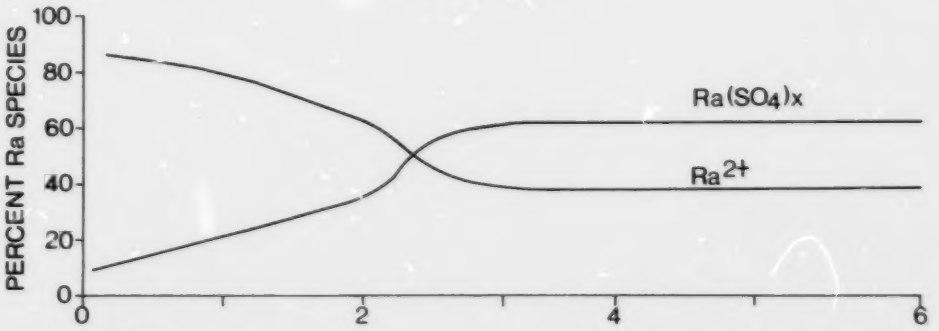

(f) Radium

FIGURE A.12 PERCENTAGE COMPOSITION OF VARIOUS METAL-LIQUID FORMS IN WATER 6 (ACTUAL pH = 2.3) (Cont'd)

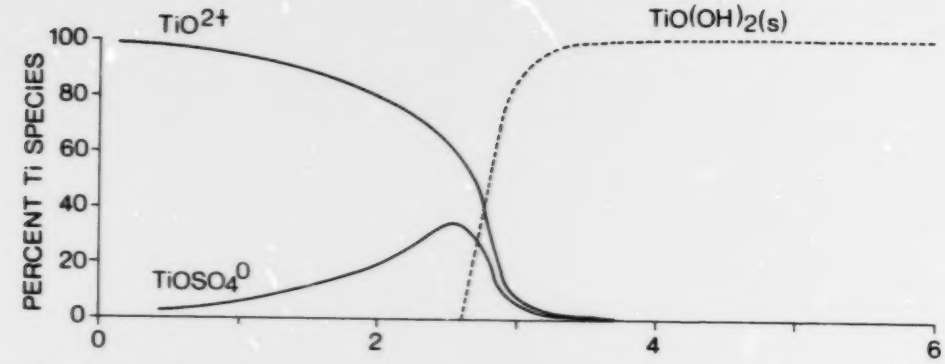

(g) Sulphate

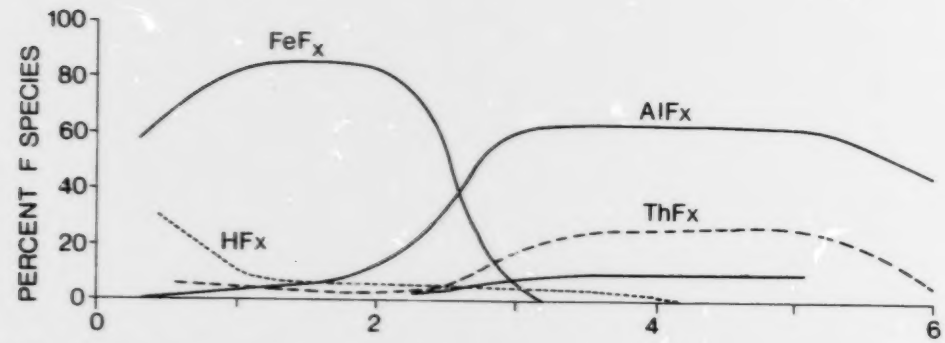

(h) Titanium

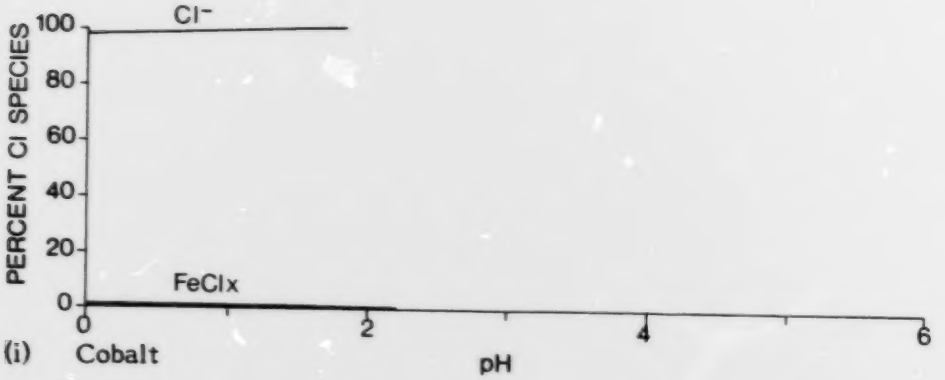

(i) Cobalt

FIGURE A.12 PERCENTAGE COMPOSITION OF VARIOUS METAL-LIQUID FORMS IN WATER 6 (ACTUAL pH = 2.3) (Cont'd)

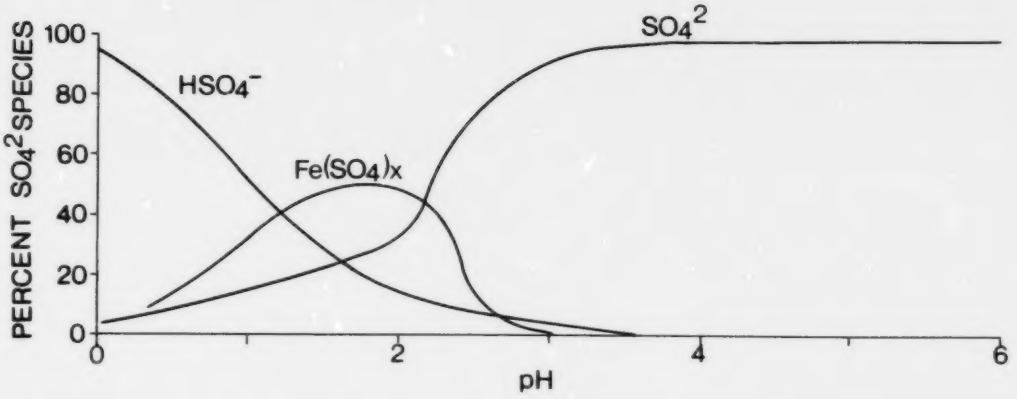

(j) Fluoride

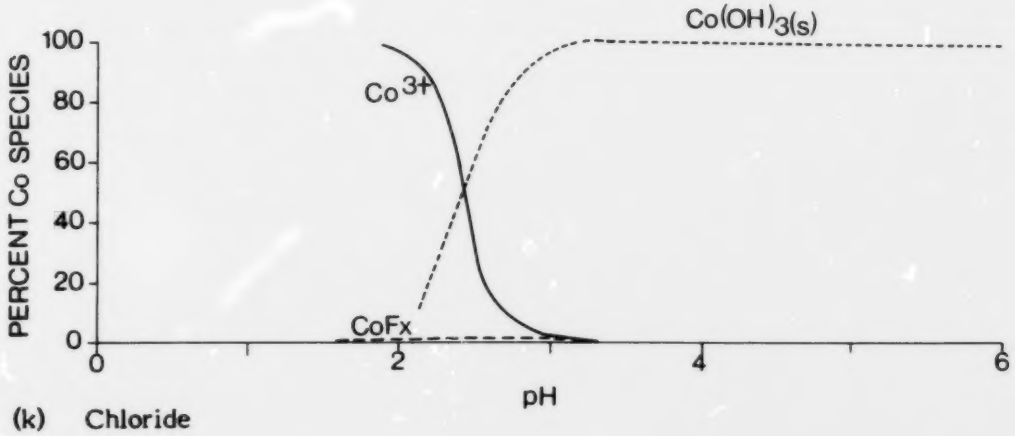

(k) Chloride

FIGURE A.12 PERCENTAGE COMPOSITION OF VARIOUS METAL-LIQUID FORMS IN WATER 6 (ACTUAL pH = 2.3) (Cont'd)

TABLE A.4 PERCENTAGE OF METAL/LIGAND CALCULATED TO BE IN FREE, BOUND AND SOLID FORMS

Metal-Ligand	Form	Water Number										
		Low-Rate Lysimeter					High-Rate Lysimeter					
		1	2	3	4	5	6	7	8	9	10	4*
Al	Free	77.4	34.0	55.7	47.7	23.0	36.2	28.1	21.9	35.2	25.4	98.5
	with F	0.6	1.2	0.7	1.8	0.9	17.4	40.4	67.9	22.0	53.0	0.7
	with SO_4	22.0	64.8	43.6	50.5	76.1	46.3	31.3	9.0	42.5	20.8	0.8
	with OH	-	-	-	-	-	-	-	1.2	-	0.8	-
Ba	Free	83.3	67.3	31.0	31.9	50.7	81.6	84.6	94.4	83.0	79.8	99.7
	with SO_4	9.5	32.7	10.2	13.2	39.8	18.4	15.4	5.6	17.0	10.0	-
	as $BaSO_{4(s)}$	7.2	-	58.8	54.9	9.5	-	-	-	-	10.2	-
Ca	Free	89.7	67.3	75.2	70.8	56.0	81.6	84.6	94.4	83.0	88.9	99.7
	with SO_4	10.3	32.7	24.8	29.2	44.0	18.4	15.4	5.6	17.0	11.1	-
Cd	Free	89.4	63.5	66.8	62.7	51.1	79.1	81.9	93.3	80.9	87.3	93.9
	with Cl	-	3.1	7.1	6.7	0.7	2.7	3.0	1.1	2.2	1.7	5.8
	with SO_4	10.6	33.4	26.1	30.6	48.1	18.1	15.7	5.6	16.9	11.0	-
Co^{3+}	Free	100.0	99.8	99.9	99.9	99.7	99.0	53.7	0.9	66.1	2.3	100.0
	with F	-	-	-	-	-	0.9	1.2	-	0.7	-	-
	as $Co(OH)_{3(s)}$	-	-	-	-	-	-	45.0	99.1	33.1	97.6	-
Ca^{2+}	Free	89.7	67.2	75.0	70.6	56.0	81.6	84.5	94.3	82.9	88.8	99.5
	with SO_4	10.3	32.7	24.8	29.2	44.0	18.4	15.4	5.6	17.0	11.1	-
Fe^{3+}	Free	26.0	5.2	12.2	9.3	3.3	4.3	4.0	-	2.6	1.7	72.1
	with F	-	-	-	-	-	-	0.6	-	-	-	-
	with SO_4	72.0	92.1	86.3	89.6	95.2	53.6	43.7	1.9	30.3	13.4	5.9
	with OH	1.9	2.6	0.8	1.0	1.5	27.1	51.7	41.6	22.6	84.6	21.5
	as $Fe(OH)_{3(s)}$	-	-	-	-	-	14.6	-	55.9	44.3	-	-
K	Free	98.8	96.2	95.5	94.9	93.0	98.9	99.2	99.8	98.9	99.5	100.0
	with SO_4	1.2	3.8	4.5	5.1	7.0	1.1	0.8	-	1.0	-	-
Mg	Free	91.7	72.1	79.2	75.3	61.6	84.8	87.4	95.5	86.0	90.9	99.8
	with SO_4	8.3	27.9	20.8	24.7	38.4	15.2	12.6	4.5	14.0	9.1	-
Mn	Free	89.7	67.1	74.7	70.3	56.0	81.4	84.4	94.3	82.8	88.7	99.2
	with Cl	-	-	0.6	0.6	-	-	-	-	-	-	-
	with SO_4	10.3	32.6	24.7	29.1	44.0	18.3	15.4	5.6	17.0	11.1	-
Na	Free	99.0	97.0	96.4	95.9	94.0	99.1	99.3	99.8	99.2	99.6	100.0
	with SO_4	1.0	3.0	3.6	4.1	5.6	0.9	0.7	-	0.8	-	-

TABLE A.4 PERCENTAGE OF METAL/LIGAND CALCULATED TO BE IN FREE, BOUND AND SOLID FORMS (Cont'd)

Metal-Ligand	Form	Water Number										
		Low-Rate Lysimeter					High-Rate Lysimeter					
		1	2	3	4	5	6	7	8	9	10	4*
Ni	Free	89.7	67.2	75.0	70.6	56.0	81.6	84.5	94.3	82.9	88.8	99.6
	with SO_4	10.3	32.7	24.8	29.2	44.0	18.4	15.4	5.6	17.0	11.1	-
Pb	Free	77.6	44.7	53.7	48.3	33.6	63.4	68.1	86.6	65.6	75.7	97.3
	with Cl	-	0.7	1.8	1.6	-	0.7	0.8	-	0.6	-	1.9
	with SO_4	22.4	54.6	44.5	50.1	66.3	35.9	31.1	13.0	33.8	23.8	0.7
Th	Free	1.0	-	-	-	-	-	-	-	-	-	43.3
	with F	-	-	-	-	-	0.7	3.4	33.4	1.0	9.4	-
	with SO_4	98.9	99.9	99.7	99.8	100.0	99.2	96.5	66.3	99.0	90.5	51.2
	with OH	-	-	-	-	-	-	-	-	-	-	-
TiO^{2+}	Free	84.6	56.3	65.6	60.4	44.5	73.7	77.6	4.4	75.5	75.9	99.5
	with SO_4	15.4	32.7	34.6	39.6	55.5	26.3	22.4	-	24.5	15.1	-
	as $TiO(OH)_{2(s)}$	-	-	-	-	-	-	-	95.2	-	9.1	-
Zn	Free	89.7	67.3	75.2	70.7	56.0	81.6	84.6	94.4	83.0	88.9	99.7
	with SO_4	10.3	32.7	24.8	29.2	44.0	18.4	15.4	5.6	17.0	11.1	-
Ra	Free	31.4	17.7	9.7	8.6	9.6	57.8	67.1	89.8	61.2	76.9	96.4
	with SO_4	68.6	82.3	90.3	91.4	90.4	42.2	32.9	10.2	38.8	23.1	3.6
F	Free	-	-	-	-	-	-	0.9	1.4	0.6	1.3	-
	with Al^{3+}	43.5	32.1	48.9	43.5	31.0	65.8	88.5	89.0	79.6	93.8	16.2
	with Fe^{3+}	55.6	66.0	50.4	55.7	66.0	31.8	6.9	-	18.0	0.7	79.1
	with Th	0.7	1.3	-	0.6	-	-	1.6	8.8	-	3.3	4.6
	with H	-	-	-	-	2.5	1.5	2.0	0.7	1.4	1.0	-
Cl	Free	51.9	97.4	81.8	88.3	98.7	99.8	99.4	100.0	99.9	100.0	40.0
	with Fe^{3+}	48.1	2.6	18.2	11.6	1.2	-	-	-	-	-	60.0
SO_4	Free	0.9	12.9	3.8	5.7	21.9	50.4	81.3	94.7	70.3	92.9	0.5
	with Al	1.0	0.5	1.2	0.9	-	0.8	0.7	-	0.8	0.6	-
	with Fe	92.7	72.6	83.0	80.8	59.3	36.3	6.0	-	18.5	0.6	97.3
	with Th	0.5	0.6	-	-	-	-	0.6	0.9	-	0.7	0.6
	with H	4.9	13.2	11.6	12.4	18.2	11.3	11.0	3.3	9.9	4.8	1.4

Note: Water 4* contains the actual pSO_4^{2-} measured analytically (i.e., the actual leachate sample). Other pC calculations are made using water 4, not 4* (see text).
Waters 1 to 5 are from the low-rate lysimeters; Waters 6 to 10 are from the high-rate lysimeters.

Model Water 4 has the same concentrations as those actually measured, except that the sulphate concentration is reduced from the actual value of $pSO_4 = 0.198$ to $pSO_4 = 1.53$. This model was used for most of the calculations; a few calculations are given for the actual leachate sample which is designated as Model Water 4* in Table A.4.

Aluminum (see Table A.4) is dominated by free and sulphate complex forms; fluoride complexes are of some importance in the low-rate lysimeters. Barium is predicted to precipitate in the low-rate lysimeters (Waters 1 to 5) but not in the high-rate lysimeters (Waters 6 to 10) except for one sample. Because the ICAP results for Ba have an accuracy of within 50 percent at these concentrations, these predictions are viewed as indicating that $BaSO_{4(s)}$ may form in the percolating waters of the low-rate lysimeters but not in those of the high-rate lysimeters. Ca^{2+}, Cd, Co^{3+}, Cu^{2+}, Mg, Mn, Ni, Pb, TiO^{2+}, and Zn are dominated by their free forms (Table A.4) but the sulphate complexes represent substantial portions of the total (10 to 30 percent). Na and K are primarily uncomplexed. Hydroxide precipitates of Co^{3+} and TiO^{2+} are predicted to occur in several leachate waters from the high-rate lysimeters but not the low-rate ones; this difference is essentially due to the higher solution pH in the high-rate lysimeter leachates.

Iron chemistry (Table A.4) is dominated by sulphate complexes in the low-rate lysimeter leachates and by sulphate and hydroxo complexes in the high-rate leachates. $Fe(OH)_{3(s)}$ is also predicted to occur in the high-rate leachates. The $RaSO_4^0$ complex dominates in the low-rate leachates while Ra^{2+} is the more significant species in the high-rate leachates.

For chloride (see Table A.4), the $FeCl^{2+}$ species occurs in substantial quantities in the low-rate leachate waters, but the free form, Cl^-, is dominant in all waters. Fluoride chemistry is controlled equally by Al^{3+} and Fe^{3+} complexes in the low-rate leachates but almost exclusively by Al^{3+} in the high-rate leachates. This reflects the higher affinity of F for Al^{3+}. Sulphate chemistry is dominated by $Fe(SO_4)_x$ complexes in the low-rate leachates but by the uncomplexed form (SO_4^{2-}) in the high-rate leachates.

The speciation calculations for Water 4* (Table A.4) show that if sulphate is substantially reduced without changing the metal concentrations (compare Water 4 with Water 4* whose pSO_4 is higher), the dominant form of all metals is free except for Fe and Th. For these two metals, sulphate complexes remain an important component of the total. The reduction of SO_4 also increases the proportion of Fe tied up with fluoride and chloride because less sulphate is available to compete for Fe.

As inferred in Section A.1, the exact redox potential for these waters is unknown. The calculations of Table A.4 assume that all anions and cations are in their

fully oxidized state. Speciation calculations for the various waters are given in Table A.5 for pE = 13, 12 and 10 assuming that iron (Fe^{3+}, Fe^{2+}) and sulphur (SO_4^{2-}, S^{2-}) participate in redox reactions. A redox potential of 13 has a small effect, allowing the formation of up to 5 percent Fe^{2+} (see Table A.5a). A redox potential of 12 increases the portion of Fe^{2+} to about 25 percent and prevents precipitation of $Fe(OH)_{3(s)}$ in Water 6 from the high-rate lysimeter. A pE equals to 10 increases Fe^{2+} to near 80 percent of the total; this liberates substantial SO_4 for complexing with other metals, because much less sulphate complexes with Fe^{2+} than with Fe^{3+}. As the pE decreases, the number of metal sulphate complexes increases to become the dominant complex for such metals as aluminum and lead. More $BaSO_{4(s)}$ precipitation is also induced (see Table A.5c). As the pE decreases, note that Water 4* does not fit the sequence of Water 3 to 5 because the pSO_4 is lower than the actual concentration measured in the leachate sample on which the chemistry of Water 4* is based.

Speciation calculations in which the sulphate and iron concentrations of Water 1 have been increased to pSO_4 = 0.89 and pFe = 0.08 are given in Table A.6. This represents a five-fold increase for Fe and a ten-fold increase for SO_4. These calculations describe the chemistry expected in interstitial waters and biofilms of the low-rate lysimeters, where the Fe, H^+, and SO_4 concentrations are higher. It is also expected that the concentrations of other metals would be higher in these local regions, but they were not increased to allow examination of the effects of Fe, H^+ and SO_4 upon the biofilm chemistry.

At these elevated concentrations for iron and sulphate, sulphate complexes (see Table A.6) of Al, Cu, Mg, Pb, Zn, and Ra over the pH range 0.1 to 1.5 are even more important than in the model water not containing the elevated sulphate concentrations; Ba is dominated by its solid form. However, the ionic strength does not change much, because most of the Fe and SO_4 are in single-charge complexes.

The calculations shown in Table A.6 also permit estimation of the solids which may form in the interstitial waters of the lysimeter biofilms. The main ones suggested are $TiO(OH)_{2(s)}$, $BaSO_{4(s)}$ and $Fe(OH)_{3(s)}$. $PbSO_{4(s)}$ is not expected to precipitate. Jarosite ($KFe_3(SO_4)_2(OH)_6(6H_2O)$) and silica ($Si(OH)_{4(s)}$) are not evaluated in the speciation calculations. The precipitation of jarosite can be evaluated by calculating its saturation index. The calculated concentrations of free metals and total metals are given in Table A.7 for Fe, K, and SO_4 together with the calculated ionic strengths of the ten waters. If precipitation is thermodynamically possible, the saturation index should be greater than unity. The calculations suggest that jarosite should form in the low-rate

TABLE A.5 PERCENTAGE OF METAL/LIGAND BOUND IN DIFFERENT COMPLEXES AS A FUNCTION OF REDOX POTENTIAL

(a) Iron/Sulphate Forms for pE = 13

Metal Ligand	Form	Water Number: Low-Rate Lysimeter 1	2	3	4*	5	High-Rate Lysimeter 6	7	8	9
Fe	Free Fe^{3+}	22.9	5.2	11.5	62.9	3.2	4.2	3.9	1.9	2.5
	Fe^{3+} with SO_4	70.3	90.0	85.4	5.8	94.0	52.6	42.1	42.1	31.1
	Fe^{3+} with OH	1.6	2.6	0.8	17.1	1.5	26.6	51.0	-	22.7
	Fe^{3+} as $(Fe(OH)_3(s)$	-	-	-	-	-	13.8	-	55.2	42.2
	Free Fe^{3+}	4.6	1.5	1.6	13.8	0.7	2.1	2.1	-	1.1
	Fe^{2+} with SO_4	0.6	0.7	0.6	-	0.6	-	-	-	-
SO_4	Free	1.1	13.5	3.9	0.6	21.7	50.5	81.2	94.6	68.8
	with Al	1.1	0.5	1.2	-	-	0.8	0.7	-	0.9
	with Fe^{3+}	91.0	71.2	81.4	95.9	58.9	36.1	5.8	-	19.1
	with Fe^{2+}	0.7	0.5	-	0.8	-	-	-	-	-
	with Th	0.5	0.6	-	0.6	-	-	0.6	0.9	-
	with H	5.5	13.5	12.1	1.7	18.5	11.6	11.2	3.4	10.7

(b) Iron/Sulphate Forms for pE = 10 and 12

Metal/ Ligand	Form	pE = 12 Water Number 1	2	3	4*	5	6	pE = 10 Water Number 1	2	3	4*	5
Fe	Free Fe^{3+}	12.4	4.6	8.1	31.7	3.3	4.2	-	0.9	0.6	1.4	0.9
	Fe^{3+} with SO_4	59.6	76.0	74.9	5.2	83.3	44.9	6.1	11.4	22.7	0.9	15.8
	Fe^{3+} with OH	0.7	2.0	0.5	5.8	1.5	27.1	-	-	-	-	-
	Fe^{3+} as $Fe(OH)_3(s)$	-	-	-	-	-	-	-	-	-	-	-
	Free Fe^{2+}	22.5	11.4	11.5	56.4	6.6	19.2	54.1	62.4	42.1	94.6	55.6
	Fe^{2+} with SO_4	4.8	5.9	4.9	-	5.3	4.3	39.5	25.0	34.5	-	27.5
SO_4	Free	2.0	17.3	4.9	1.9	24.2	52.9	6.3	54.8	16.5	19.3	58.8
	with Al	1.6	0.5	1.4	-	-	0.8	3.9	0.6	2.9	2.0	-
	with Fe^{3+}	80.1	61.1	73.8	85.2	52.9	30.9	9.5	10.5	28.1	15.5	11.1
	with Fe^{2+}	5.9	4.1	4.0	7.2	2.6	2.8	48.4	17.2	28.1	44.4	13.7
	with Th	0.5	0.6	-	0.8	-	-	0.6	0.6	-	1.6	-
	with H	9.7	16.2	15.4	4.4	19.7	.8	31.0	16.2	23.9	17.2	15.8

TABLE A.5 PERCENTAGE OF METAL/LIGAND BOUND IN DIFFERENT COMPLEXES AS A FUNCTION OF REDOX POTENTIAL (Cont'd)

(c) Metal/Ligand Forms of Al, Ba, Ca, Mg, Pb, Th, Zn and Ra for pE = 10 and 12

Metal/ Ligand	Form	pE = 12 Water Number					pE = 10 Water Number				
		1	2	3	4*	5	1	2	3	4*	5
Al	Free	65.7	35.3	48.7	97.2	24.9	28.3	37.7	16.9	90.6	29.9
	with F	0.8	1.3	0.8	1.2	1.0	1.2	2.6	1.1	3.4	1.9
	with SO_4	33.5	63.4	50.5	1.6	74.1	70.4	59.7	82.0	6.0	68.2
Ba	Free	44.7	63.9	23.8	99.2	50.2	13.1	71.4	12.5	97.2	66.9
	with SO_4	9.5	33.1	10.2	0.8	39.8	9.5	28.6	10.2	2.8	33.1
	$BaSO_4(s)$	45.7	3.0	66.0	-	9.9	77.4	-	77.3	-	-
Ca	Free	82.4	65.9	69.9	99.2	55.8	57.8	71.4	55.0	99.2	66.9
	with SO_4	17.6	34.1	30.1	0.8	44.2	42.2	28.6	45.0	2.8	33.1
Mg	Free	85.5	70.9	74.5	99.4	61.4	63.3	75.8	60.6	97.8	71.8
	with SO_4	14.5	29.1	25.5	0.6	38.6	36.7	24.2	39.4	2.2	28.2
Pb	Free	65.1	43.2	47.4	96.2	33.4	35.3	49.7	32.6	92.4	44.6
	with Cl	-	0.6	1.5	1.9	-	-	-	-	1.0	-
	with SO_4	34.9	56.2	51.1	1.9	66.5	64.7	50.1	67.0	6.6	55.4
Th	Free	-	-	-	35.4	-	-	-	-	-	-
	with SO_4	99.5	99.9	99.8	64.6	100.0	99.9	99.9	100.0	91.4	99.9
Zn	Free	82.4	65.9	69.9	99.2	55.8	57.8	71.4	55.0	97.2	66.9
	with SO_4	17.6	34.1	30.1	0.8	44.2	42.2	28.6	45.0	2.8	33.1
Ra	Free	17.9	14.4	7.8	88.4	9.3	6.4	10.6	5.3	61.6	8.1
	with SO_4	82.1	85.6	92.2	11.6	90.7	93.6	89.4	94.7	38.4	91.9

lysimeter and possibly in the high-rate lysimeter. The actual nucleation-crystal growth kinetics of jarosite precipitation is controlled by higher concentrations of Fe, H^+, and SO_4^{2-} in the biofilms about the pyritic particles and by the dilution of these films by higher pH water applied to the lysimeter. Such precipitation mechanisms require further evaluation than can be provided in this work.

The silica concentrations measured in four of the leachate samples are given in Table A.8. The saturation index is close to unity for most samples, suggesting that precipitation reactions may be occurring in the lysimeters.

TABLE A.6 SPECIATION CALCULATIONS FOR WATER 1 WHEN pFe = -0.68 AND pSO_4 = -0.98

Metal/ Ligand	Form	Percentage in Complex at pH					
		0.1	0.3	0.5	0.7	1.0	1.5
Fe^{3+}	Free	2.9	2.6	2.2	1.9	1.5	1.2
	with SO_4	97.0	97.3	97.7	98.0	98.3	98.0
	with OH	-	-	-	-	-	0.8
	with $Fe(OH)_{3(s)}$	-	-	-	-	-	-
SO_4	Free	1.0	1.4	1.8	2.1	2.6	3.0
	with Al	-	0.5	0.5	0.6	0.6	0.6
	with Fe^{3+}	80.2	84.3	87.4	89.9	92.4	94.7
	with Th	-	-	-	-	-	-
	with H	18.2	13.7	10.2	7.3	4.3	1.6
Al	Free	20.0	17.7	15.0	12.7	10.6	8.6
	with F	-	-	-	-	-	-
	with SO_4	79.7	82.0	84.7	86.9	89.1	91.1
Ba	Free	9.1	8.1	7.2	6.5	5.7	4.9
	with SO_4	9.5	9.6	9.6	9.6	9.6	9.6
	as $BaSO_{4(s)}$	81.4	82.3	83.2	83.9	84.7	85.5
Ca	Free	48.7	46.0	43.1	40.6	37.4	34.1
	with SO_4	51.3	54.0	56.9	59.4	62.6	65.9
Mg	Free	54.5	51.7	48.8	46.2	42.9	39.5
	with SO_4	45.5	48.3	51.2	53.8	57.1	60.5
Pb	Free	27.4	25.3	23.2	21.4	19.2	17.1
	with Cl	-	-	-	-	-	-
	with SO_4	72.6	74.7	76.8	78.6	80.8	82.9
Th	with SO_4	100.0	100.0	100.0	100.0	100.0	100.0
Zn	Free	48.7	46.0	43.1	40.6	37.4	34.1
	with SO_4	51.3	54.0	56.9	59.4	62.6	65.9
Ra	Free	4.4	3.7	3.1	2.8	2.5	2.2
	with SO_4	95.6	96.3	96.9	97.2	97.5	97.8
Ionic Strength		1.23	1.06	0.94	0.86	0.81	0.78

TABLE A.7 SATURATION INDEX FOR JAROSITE IN DIFFERENT WATERS

Water	Lysimeter[1]	pFe_T	pFe^{3+}	pK_T	pK^+	pSO_4T	pSO_4^{2-}	I (M)	SI*	$Fe(OH)_{3(s)}$ Present
1	L1 (low) before decline	0.0186	0.60	2.07	2.07	0.107	2.1	1.36	2	No
2	L1 (low) end of operation	1.05	2.3	3.9	3.9	0.885	1.8	0.074	4	No
3	L7 (low) before decline	0.114	1.0	2.3	2.3	0.025	1.4	0.637	5	No
4	L7 (low) middle of decline	0.314	1.3	2.6	2.6	0.198	1.4	0.353	8	No
5	L7 (low) end of operation	1.05	2.5	4.3	4.3	0.745	1.4	0.110	0.8	No
6	L2 (high) before decline	2.38	3.7	4.1	4.1	2.19	2.5	0.0105	30	pFe_s = 3.2; 15% of Fe_T
7	L2 (high) middle of decline	3.43	4.8	4.1	4.1	2.55	2.6	0.00652	0.002	No
8	L2 (high) end of operation	4.33	6.7	3.9	3.9	3.23	3.3	0.0017	0.006	pFe_s = 4.6; 56% of Fe_T
9	L8 (high) before decline	2.49	4.1	4.0	4.0	2.26	2.4	0.0108	4	pFe_s = 2.8; 44% of Fe_T
10	L8 (high) end of operation	4.35	6.5	4.3	4.3	2.97	3.0	0.00268	0.0005	No

[1] (low) or (high) describes rate of water application to lysimeter; before decline, middle of decline and end of operation refers to the start, middle or end of the decline in TDS concentrations during the last 1.5 years of lysimeter operation.

$$*SI = \frac{(K)(Fe^{3+})3(SO_4)2(H^+)-6}{10^{-9.4}}$$

TABLE A.8 SILICA CONCENTRATIONS IN FOUR SAMPLES

Sample*	Water	H_4SiO_4 (as Si, mg/L)	SI+
28	1	61.1	1.1
32	3	61.1	1.1
38	5	79.8	1.4
50	10	20.6	0.4

* See Table A.1(a)
+ $Si = pSi/pK_{SiO_2}$; $pK_{SiO_2} = 2.7$ for amorphorous SiO_2

Another method for examining silicon chemistry is to discern whether all silica possible is in the waters. Orthosilicic acid originates from proton attack upon quartz, K-feldspar, and other alumino-silicates, which compose the bulk of the tailings. Concentration ratios of elements in leachate can be used to assess the possible formation of secondary precipitation solids. The element in the denominator may be thought of as a normalizing agent. If the normalizing element is conservative (i.e., does not undergo reprecipitation), changes in the ratio of the element in the leachate to that in the parent mineral allows statements about whether the element in the numerator is also acting conservatively or whether it is being reprecipitated.

Concentration ratios of Si/Al, Fe/Al, F/Al, Ca/Al, and Mg/Al are presented in Table A.9 for the various leachate waters and for different minerals constituting the bulk solids. It would have been useful to have measured the actual ratios in the lysimeters solids to ascertain that they are similar to those of Zahary's et al. (1974) data, but that was not done. Thus Zahary's et al. data are assumed to be the best estimates for these lysimeter solids.

The Ca/Al molar ratios in the leachates (Table A.9a) are comparable to those in the tailings (Table A.9c). The variation in the Ca/Al leachate data (as indicated by the relatively large standard deviation) probably reflects residual calcium-sulphates formed in the mill whose resistance to dissolution is caused by the random occurrence, at depth, of surface coatings from precipitation reactions. The solids sulphate measurements (see Appendix A.2) indicate that sulphate is still present. The Mg/Al ratio is consistently higher (50 to 400 percent) in the leachates than in the bulk solids; but the solids ratio is much lower than that found in typical minerals. The K/Al ratio in leachate from the low-rate lysimeter is close to that of the bulk solids; the ratio in leachates from the high-rate lysimeter is quite variable but much higher (about four times) than that of the bulk solids.

TABLE A.9 RATIOS OF SEVERAL MAJOR ELEMENTS DERIVED FROM PROTON ATTACK UPON ALUMINO SILICATES

(a) F/Al, Ca/Al, Mg/Al, K/Al and K/Mg Molar Ratios

	Molar Ratios of Elements in Leachates				
Lysimeter	F/Al	Ca/Al	Mg/Al	K/Al	K/Mg
Low-Rate (L1, L7)	0.024±0.01 (n=8)*	0.10±0.13 (n=11)	0.033±0.005 (n=11)	0.23±0.04 (n=10)	7
Low-Rate (L7 only)	-	0.039±0.015 (n=7)	-	-	-
High-Rate (L2, L8)	-	0.33±0.2 (n=12)	0.078±0.036 (n=12)	1.5±0.89 (n=12)	15

* n = number of samples

(b) Silica/Aluminum Molar Ratios

Sample*	Water	Lysimeter	Description of Time of Sampling	Si/Al Molar Ratio
29	-	L1	Near start of decline of TDS in low-rate leachates	0.11
32	3	L2	Beginning of decline of TDS in low-rate leachates	0.11
38	5	L2	End of low-rate lysimeter operation	3.8
50	10	L8	End of high-rate lysimeter operation	18.0

* See Table A.1(a)

(c) Molar Ratios of Major Elements in Various Minerals

	Molar Ratios						
	F/Al	Ca/Al	Mg/Al	K/Al	K/Mg	Si/Al	Comments
1. Typical Characteristics of Nordic Lake Area Tailings (Zahary et al., 1974)							
Coarse Tailings	-	0.094	0.022	0.39	17	20	
Fine Tailings	-	0.268	0.022	0.36	17	16	

TABLE A.9 RATIOS OF SEVERAL MAJOR ELEMENTS DERIVED FROM PROTON ATTACK UPON ALUMINO SILICATES (Cont'd)

(c) Molar Ratios of Major Elements in Various Minerals

	Molar Ratios						
	F/Al	Ca/Al	Mg/Al	K/Al	K/Mg	Si/Al	Comments
2. Representative Minerals							
Plagioclase (andesine) ($Na_{0.5}Ca_{0.5}Al_{1.5}Si_{2.5}O_8$)							
Congruent Dissolution	0	0.33	0	0	-	1.7	Not probable:
Incongruent Dissolution	-	∞	-	-	-	∞	Na is too high
Kfeldspar (orthoclase) ($KAlSi_3O_8$)							
Congruent Dissolution	0	0	0	1	-	3	
Incongruent Dissolution	-	-	-	0	-		
Biotite ($KMg_3AlSi_3O_{10}(OH)_2$)							
Congruent Dissolution	0	0	3	1	0.33	3	
Incongruent Dissolution	-	-	∞	∞	-	∞	
Quartz($SiO_{2(s)}$)							
Congruent Dissolution	0	0	0	0	-	0	$Si(O)_4$ is
Incongruent Dissolution	-	-	-	-	-	-	dissolution product

The ratio in leachates from the high-rate lysimeter is much closer to that expected from the congruent dissolution of minerals such as K-feldspar and biotite than is the ratio in leachates from the low-rate lysimeters.

For silica characterization, the first question to decide is which of K, Mg, Ca, Al, or another metal in the tailings can be used as a normalizing element. Na is not a significant fraction, hence it does not warrant consideration. Other metal concentrations are sufficiently small in the leachates not to warrant consideration. Because it is possible that mill-formed calcium is present, Ca is not a useful tracer (normalizing element).

Al may be a useful tracer for Si, but one must determine whether Al acts conservatively. This can be done by examining various metal/Al ratios. The two ratios, Mg/Al and F/Al, are generally higher in the leachates than in the solids. However, the K/Al ratio is smaller in the low-rate leachates than in the solids. The data suggest that the low-rate lysimeters may be enriched in magnesium and that the high-rate lysimeters

are enriched in both magnesium and potassium, relative to aluminum. Enrichment would occur only by retention of aluminum in the solids.

Assuming that modest amounts of aluminum are retained in the low-rate lysimeter solids, either some K is also retained in the low-rate solids or the K value determined by Zahary et al. (1974) is somewhat high for these solids. This point awaits further resolution. The K/Mg ratio for the low-rate leachates is considerably lower than for the tailings solids, but the ratio in the high-rate leachates is similar to that of the high-rate lysimeter solids. K is probably retained in the low-rate lysimeters, but not in the high-rate lysimeters.

Accordingly, it can be concluded that:

(i) Mg is conservative (i.e., it leaches from the lysimeters as it dissolves),

(ii) K is conservative in the high-rate leachates, but some K is retained on the low-rate lysimeter solids, and

(iii) Al is retained in both low and high-rate lysimeters.

For silica, the Si/Al ratio is near 0.1 before the initiation of the decline of TDS concentrations in the low-rate leachates. Because it has been concluded that some Al is retained in the lysimeters and because the Si/Al ratio is much lower than typical ratios for alumino-silicate minerals (1:1 to 3:1), silica must be retained in the solids after dissolution of the alumino-silicate structure by proton attack. The Si/Al ratio of 0.1 would suggest that more than 90 percent of the Si from the alumino-silicate is retained. Furthermore, because the silica concentration is approximately the equilibrium concentration for orthosilicic acid-amorphorus silica ($SiO_{2(s)}$:$Ksp=10^{-2.7}$ at 25°C), the data suggest that silica solubility was maintained throughout the leaching history of the low-rate lysimeters. That is, alumino-silicate dissolution leads to precipitation of the Si as amorphorus $SiO_{2(s)}$ in the biofilms of the low-rate lysimeters.

The stoichiometry of low-rate lysimeter L2 (Si/Al=3.8) at the end of its operation is near that of 3:1 for congruent dissolution of typical alumino-silicates (see Table A.9c). Because some aluminum may be retained in the low-rate lysimeters, it is probable that some Si is also retained at the time of the end of its operation. This may occur by entrapment of Al^{3+} in the amorphorus hydrated $SiO_{2(s)}$ structure. In high-rate lysimeter L8, the Si/Al ratio approaches that of the parent solids; the leachate is not then saturated with respect to amorphorus $SiO_{2(s)}$, but it is saturated with respect to quartz ($SiO_{2(s)}$:$Ksp=10^{-3.7}$; SI = 4). The ratio data argue against dissolution of a quartz mineral. Hence, either both alumino-silicates and quartz are being attacked by the acid or only the

alumino-silicate minerals are being attacked at the end of the leaching period. With acid attack on alumino-silicate minerals, secondarily formed amorphorus silicates are dissolving near the end of the leaching history of the high-rate lysimeters and saturation with respect to amorphorus silica is not maintained because the flushing rate is faster than the dissolution rate. An acid attack on alumino-silicates only is more probable than an acid attack on alumino-silicates and quartz.

A.1.3 Biochemistry of Pyrite Oxidation Reactions. Oxidation of pyrite is the energy source for the pyrite-oxidizing bacteria *T. ferrooxidans*. Oxygen is the final electron acceptor for their respiration processes. Ammonia, organic nitrogen, organic carbon, and CO_2 are the main by-products; some phosphorus also exists in the leachates. The organic nitrogen and carbon originate from remains of the bacterial cells, whereas ammonia results from the release of amino and other -NH (amide) groups from cells. CO_2 originates from dissolved H_2CO_3* (carbonic acid) in the percolating water, air-water interchange in the lysimeters, and bacterial respiration.

The C/N ratio in the lysimeter leachates (see Table A.10, which is based on the TOC/NH ratio by weight) is considerably higher than that expected for typical cells (e.g., 5:1 for $C_5H_7O_2N$). Only in humic substances do C:N ratios approach 20:1 to 30:1. Accordingly, the total N contents of the leachate waters are lower than expected; measurements of Kjeldahl N are required, but were not carried out in the study.

TABLE A.10 METABOLISM OF LEACHATES OF EXPERIMENT 1

Molar Ratios	Low-Rate Lysimeters (L1,L7)		High-Rate Lysimeters (L2,L8)	
C/N	27±13	(n=10)*	14±11	(n=9)
With respect to S				
NH_3-N/S	0.51±0.36	(n=10)	12±8	(n=10)
C/S	2.7±0.71	(n=10)	50±76	(n=10)
With respect to Fe				
NH_3-N/Fe (mmol N/mol Fe)	0.71±0.47	(n=10)	28±19	(n=10)
TOC/Fe (mmol C/mol Fe)	14.3±3.6	(n=11)	170±69	(n=8)

*n = number of samples

Ratios of NH_3N/S, NH_3N/Fe, TOC/S and TOC/Fe in the leachates are also given in Table A.10. The TOC ratios are most relevant in this discussion because of the unknown quantity of organic N in the samples. There is a difference of over an order of magnitude between the ratios in leachates from the low-rate and the high-rate lysimeters. This infers that the overall biochemical metabolism of the two sets of lysimeters is significantly different. The samples were stored for 0.8 to 2.5 years before analysis for TOC and NH_3. A plot of the ratio data over time (not given in this report) shows that there is no trend in the TOC/Fe or TOC/S ratios over time. Accordingly, it is doubtful that the differences are due to metabolic activity in the bottles during storage. Because many of the bottles were full (i.e., no air space), aerobic metabolic activity would have ceased shortly after sample collection since bacterial metabolism would be limited by the dissolved oxygen concentration initially present. It is doubtful that a significant amount of S^{2-} would have formed from SO_4^{2-}, because the TDS measurements made by IEC-Beak in 1983 and those made by WTC in 1979-81 are about the same. In other bottles with head space gas, the large oxygen pool would have allowed for continued metabolism. In some bottles containing low-rate lysimeter leachates, microscopic examination showed that filamentous structures existed whose shape is consistent with that of *T. ferrooxidans*. Accordingly, some bacterial metabolism did occur in the sample bottles; the energy source for this metabolism is probably oxidation of sulphate which was incompletely oxidized in the low-rate lysimeters.

The TOC/Fe ratio differences could result from hydraulic or metabolic differences between the lysimeters. The same quantity of energy is available from the oxidation of pyrite in both sets of lysimeters, hence the same biomass of bacteria is expected. One can argue for hydraulic differences; a relatively high hydraulic flushing rate would be more effective in removing constituents from soil moisture and biofilms than a relatively low flushing rate by physically eroding more of the biofilm. But the TOC/Fe ratio should be the same in two lysimeters with different flushing rates; the only difference would be that the absolute concentrations of both TOC and Fe would be higher in the lysimeter with the lower flushing rate. Iron precipitation can be ruled out even though the chemistry of iron is dominated by complex formation with SO_4^{2-} in many of these waters. However, similar differences in the TOC/SO_4 ratio are observed for leachates from the low-rate and high-rate lysimeters. Thus the differences must be the result of metabolic differences between the lysimeters. The metabolic differences can be ascribed to oxidation of the cellular remains of the pyrite-oxidizers by hetecrotrophes capable of functioning in water of pH near unity. Their metabolism will convert the TOC

of cellular remains of pyrite-oxidizers to CO_2 and more TOC. Comparing the ratios of the low-rate and high-rate lysimeters suggests that at least 90 percent of the TOC formed is lost through this mechanism.

A similar loss from the biofilm occurs with nitrogen. While some errors exist with using the NH_3 data for estimating N, the amount of N in organic form should not change the N concentration more than four-fold. But the difference in N/Fe ratios between the low-rate and high-rate lysimeters is over an order of magnitude (20 to 40 times). Accordingly, a quantity of N similar in magnitude to that of C must be lost from the cellular remains in the low-rate lysimeters.

The mechanism for nitrogen loss is not clear. Volatilization of ammonia in significant quantities is possible, but ammonia volatilizes as NH_3, and the concentration of the non-ionized form is over eight orders of magnitude below 5 mg/L in these waters. Loss by N_2 formation is another possible mechanism, but it is difficult for denitrifying bacteria to function at low pH. Their presence is possible because the reactions involved for pyrite dissolution (attack on the FeS_2 structure by Fe^{3+} to release Fe^{2+}) provide for low Eh zones. However, ammonia oxidation is necessary to provide the NO_3 for denitrification. Nitrification at low pH is strongly inhibited (EPA, 1980).

The probable mechanism for nitrogen loss can be clarified by the following calculation. Assume that the ammonia concentration in the biofilm is 25 mg/L, the ammonia concentration in the percolating water leaving the lysimeter is 5 mg/L and that the biofilm is 10 μm thick. The rate of loss by volatilization is equal to the mass transfer coefficient of volatilization times the concentration of ammonia (non-ionized molecular concentration) divided by the mass of ammonia per unit surface area. For $NH_3 = 10^{-8} \times (NH_3 + NH_4^+)$, the loss rate of volatilization is 0.1 percent/day. For washout, the loss rate is equal to the outflow rate times the outflow concentration divided by the mass of ammonia present in the films. For the low-rate lysimeters, the outflow rate is about 0.1 L/day. The mass present in the films is equal to 25 mg/L times the volume of film water (the surface area of the particles times 10 μm). Assuming the tailings are essentially 90 kg of 70 μm spheres whose density is 2.65 g/cm^3, the surface area in one lysimeter is 1.46×10^3 m^2. This gives a loss rate by washout of 0.14 percent/day. Because volatilization is of the same order of magnitude as the loss rate by washout, volatilization of ammonia is the most probable mechanism for loss of nitrogen from the biofilm in the low-rate lysimeters. Its significance is considerably less in the high-rate lysimeters because washout is an order of magnitude higher and because more of the void spaces are more continuously occupied by percolating water.

The data suggest that the yield of cells from pyrite oxidation is at least as large as 170 mMol C/mol Fe and 50 mol C/mol S. Assuming that insignificant oxidation of TOC occurs in the high-rate lysimeters, these values would be the actual yield for the pyrite oxidation reactions. This yield compares with published yield values of 0.1 g TOC per Mol (or g) Fe.

A.2 Characterization of Lysimeter Solids

Cores were taken from lysimeters L1, L2, L7, and L8 and analyzed for bulk chemical parameters of sulphate, sulphide, and carbonate composition, and physical parameters of porosity, moisture content, and bulk density. Occasional samples were analyzed for the radioisotopes of Ra-226, Th-230, Th-232, Th-228, and Pb-210. The appearance of the cores as they were split and sectioned is given in Table A.11; available data for the chemical and physical composition of the tailings are given in Table A.12. The cumulative mass of radionuclides leached from the tailings is compared to the mass initially present in the lysimeters in Table A.13. The particle size distribution of the tailings is given in Figure A.13.

A.2.1 Physical and Chemical Characteristics. Of the physical parameters measured (see Table A.12), the bulk density and porosity are quite consistent; they are the same for all lysimeters. The average bulk density is 1.31; the average porosity of 0.52 is based upon an assumed density for the solids of 2.75 g/cc. A few density measurements were made to assure that this value for solids density was valid. The moisture content shows a gradation with depth. The moisture content of the two high-rate lysimeters is somewhat higher than that of the low-rate lysimeters with the exception of the bottom section of low-rate lysimeter L7. Because the lysimeters had been shut down for 1 year before analyses, the moisture contents reflect the result of drainage from the bottom and evaporation from the top of each column. The data suggest that, at the time of operation, bound soil water in the lysimeters constituted at least 0.2 percent of the tailings volume. It is probable that a higher moisture content existed during operation and that a higher moisture content existed in the high-rate lysimeters than in the low-rate lysimeters.

The importance of the moisture measurements is that it gives evidence for the maintenance of very limited thicknesses of biofilms during the period between cessation of water application and coring of the lysimeters. A moisture content of 0.05 percent corresponds to a biofilm thickness of less than 1 μm in a lysimeter, assuming a surface area of 1.5×10^3 m^2/lysimeter. Hence, the lysimeters at the time of coring (1 year after

TABLE A.11 PHYSICAL DESCRIPTION OF LYSIMETER SOLIDS IN CORE SAMPLES

Lysimeter L1 (low-rate; 7.6 cm ID Core)

1. General Comments: The entire core is a uniform, pale buff colour. There is no horizontal stratification observable. The total core length is 85 cm.

2. Particular Comments (depth given from top surface of tailings):
   (a) Section 4 (30 to 40 cm): a pyritic bleb found.
   (b) Sections 6 to 9 (50 to 82 cm): occasional pyritic lenses. One pyritic bleb of about 0.5 cm diameter is found at 69 cm.
   (c) Sections 8 to 9 (70 to 82 cm) is a little darker than upper material. This may be due to higher moisture or the pyrite lens.
   (d) Section 8 (70 to 80 cm) has about 1 cm lens of rounded quartz sand.
   (e) Section 9 (80 to 85 cm): In the top 2 cm are tailings; in the bottom 3 cm (82 to 85 cm) is silica sand assumed to be the bedding inserted into the lysimeter before addition of tailings.
   (f) Section 9: (82 cm): A thin, 0.2 cm thick orange oxide band is found at the top of the sand.

Lysimeter L2 (high-rate; 7.6 cm ID Core)

1. General Comments: The total core length is 85 cm.

2. Particular Comments:
   (a) Section 1 (0 to 5 cm) is uniform orange with rare pyritic blebs. There are pyrite nodules at about 1 cm depth with coatings.
   (b) Section 1 to 2 (5 to 10.5 cm) is a mottled orange colour with decreasing orange colour with depth.
   (c) Section 2 (10.5 to 12 cm) is the zone of fairly rapid transition from the orange colour to the uniform buff colour with occasional orange mottles (i.e., oranges covers 5 percent of surface).
   (d) Sections 2 to 6 (12 to 52 cm) is uniform buff colour; the orange mottles are occasional to rare.
   (e) Sections 6 to 8 (52 to 76.5 cm) is uniform buff colour with rare orange mottling.
   (f) Section 8 (at 76.5 cm): There is an approximately 0.3 cm thick band of orange "oxides" separating the "oxidized" buff coloured tailings from the reduced tailings below.
   (g) Sections 8 to 9 (76.8 to 82 cm) is a blotchy, medium gray colour with prominent pyrite-rich patches.
   (h) Section 9 (82 to 85 cm) contains silica sand placed before addition of tailings.

Lysimeter L7 (low-rate; 7.6 cm ID Core)

1. General Comments: Orange-brown mottled appearance on outer surface of core when tube was removed. This is more prominent below 40 cm. Core is very dark at 70 to 80 cm.

TABLE A.11 PHYSICAL DESCRIPTION OF LYSIMETER SOLIDS IN CORE SAMPLES (Cont'd)

Lysimeter L7 (low-rate; 7.6 cm ID Core) (Cont'd)

2. Particular Comments:
   (a) Section 4 (30 to 40 cm): Pyrite clusters are evident in this section, but not in above sections. The pyrite tends to occur in clusters of about 2 to 4 mm diameter. A dark cluster of pyrite grains is at 37 cm, showing this to be the oxidation zone.
   (b) Section 5 (40 to 50 cm): Prominent pyrite lens (3 mm thick) and mottled pyritic zones (2 to 4 mm thick) are observed, but no oxidized appearance. The major boundary between unmottled (above) and mottled orange-brown on the outer surface of the core material is at 48 cm.
   (c) Section 6 (50 to 60 cm) has a prominent mottled grey appearance due to pyritic grain clusters.
   (d) Section 7 (60 to 70 cm): Pyritic lenses are found up to 12 mm across and 15 to 20 mm long. The lens-shaped areas indicate substantial heterogeneity.
   (e) Section 8 to 9: At 78 cm, there is a sharp colour boundary. Below this boundary (between 78 and 84 cm) is a dark grey, pyritic layer. This zone is heavily mottled with orange-brown colour only on the outer rim of the core.

Lysimeter L8 (high-rate; 7.6 cm ID Core)

1. General Comments: The core is a pale yellow, but an orange colour is prominent.

2. Particular Comments:
   (a) Section 1 (0 to 10 cm): The top 8 cm is fairly dried out. The deep orange brown colour penetrates through the core but inner zones of grey pyrite are visible in clusters of 2 to 4 mm diameter. There is a 5 mm thick x 30 mm wide rose-coloured band at 3 cm depth. There is a discontinuous boundary at the 10 cm depth blending from the deep orange to mottled-orange yellow colour to yellow colour below.
   (b) Sections 2 to 3 (10 to 30 cm): Prominent horizontal bands, 10 mm thick, appear intercollating with the yellow, to a depth of 24 cm.
   (c) Section 6 (50 to 60 cm): At 55 cm, the orange mottled colour disappears; below, a pale yellow colour is observed almost exclusively.
   (d) Section 8 (70 to 80 cm): A wavy but distinct boundary occurs between the pale yellow above and the medium to dark grey pyritic colour below.
   (e) Section 9 (80 to 90 cm): The tailings layer from 80 to 86 cm is the dark grey pyritic colour. The bottom 3 cm (86 to 89 cm) contains silica sand. A thin abrupt zone of pale orange coloration is observed at the top of the silica sand (86 cm).

cessation of water application) had a bacterial population that would probably respond, if water application was reinitiated, by rapidly recommencing active growth.

The average porosity of 0.52 (Table A.12) is slightly less than that assumed (0.55) for the pore volume calculation and the graphs of radionuclide concentrations

TABLE A.12 PHYSICAL AND CHEMICAL COMPOSITION OF LYSIMETER SOLIDS

Section	Depth (cm)	Ra-226 (pCi/g)	Th-230 (pCi/g)	Th-232 (pCi/g)	Th-228 (pCi/g)	Pb-210 (pCi/g)	Sulphide (%)	Sulphate as Gypsum (%)	Carbonate (%)	Porosity	Moisture Content (%)	Bulk Density (g/cc)
(a) Lysimeter No. 1 (Low-Rate)												
1	0-10	160	15	<10	10	69	0.07	0.09	*	-	-	-
2	10-20	-	-	-	-	-	-	-	*	0.55	0.04	1.23
3	20-30	120	-	-	-	-	0.07	0.04	*	0.52	0.05	1.32
4	30-40	-	-	-	-	-	-	-	*	0.53	0.05	1.29
5	40-50	150	20	20	<10	95	0.09	0.15	*	0.50	0.05	1.38
6	50-60	-	-	-	-	-	-	-	*	0.52	0.06	1.31
7	60-70	160	-	-	-	-	0.54	0.16	*	0.51	0.07	1.36
8	70-80	150	-	-	-	-	0.19	0.20	*	0.52	0.07	1.33
9	80-90	80	<10	<10	10	51	0.81	0.21	*	0.50	0.10	1.38
(b) Lysimeter No. 2 (High-Rate)												
1	0-10	150	10	<10	<10	91	0.11	0.036	*	-	-	-
2	10-20	140	-	-	-	-	-	-	*	0.54	0.05	1.27
3	20-30	160	-	-	-	-	0.05	0.011	*	0.52	0.06	1.31
4	30-40	130	-	-	-	-	-	-	*	0.52	0.07	1.32
5	40-50	140	20	<10	<10	82	0.06	0.014	*	0.54	0.08	1.26
6	50-60	150	-	-	-	-	-	-	*	0.53	0.09	1.30
7	60-70	150	-	-	-	-	0.05	0.005	*	0.51	0.12	1.33
8	70-80	170	-	-	-	-	1.11	0.018	*	0.53	0.16	1.30
9	80-90	120	10	<10	<10	19	2.94	0.036	*	0.49	0.22	1.40
(c) Lysimeter No. 7 (Low-Rate)												
1	0-10	150	15.4	2.7	5.1	60	0.09	0.18	0.001	0.54	0.04	1.40
2	10-20	100	-	-	-	-	-	0.007	-	0.52	0.05	1.27
3	20-30	140	24.2	3.5	7.6	90	0.05	0.03	0.001	0.53	0.05	1.25
4	30-40	130	-	-	-	-	0.04	0.013	-	0.52	0.05	1.27
5	40-50	110	9.4	1.7	2.8	90	0.34	0.01	0.001	0.53	0.06	1.24
6	50-60	90	-	-	-	-	0.56	0.028	-	0.51	0.07	1.27
7	60-70	120	10.4	1.9	3.4	30	1.09	0.1	0.001	0.50	0.13	1.33
8	70-80	60	-	-	-	-	0.65	0.27	-	0.49	0.14	1.34
9	80-90	70	14.5	2.1	3.3	30	2.77	1.21	0.001	0.42	0.35	1.53
(d) Lysimeter No. 8 (High-Rate)												
1	0-10	30	15.3	3.1	1.8	80	0.66	0.01	<0.001	0.51	0.04	1.30
2	10-20	50	-	-	-	-	0.06	0.009	-	0.51	0.04	1.31
3	20-30	180	16.8	2.8	5.5	90	0.06	0.005	<0.001	0.52	0.04	1.26
4	30-40	120	-	-	-	-	0.00	0.005	-	0.53	0.05	1.24
5	40-50	150	16.1	2.4	4.7	80	0.06	0.03	<0.001	0.52	0.07	1.28
6	50-60	360	-	-	-	-	0.06	0.01	-	0.52	0.07	1.26
7	60-70	120	16.6	3.3	5.4	20	0.07	0.006	<0.001	0.51	0.09	1.29
8	70-80	80	-	-	-	-	0.39	0.11	-	0.50	0.12	1.33
9	80-90	130	12.0	2.2	4.2	30	0.40	0.53	<0.001	0.46	0.19	1.43
(e) Mill Samples												
Leaching Pachucas		230	180	180	40	210	1.17	-	<0.001			
Partial Neut. Tank		310	480	250	50	320	1.58	4.1	0.045			
Final Neut. Tank		300	250	480	90	320	1.74	4.3	0.020			

* Assumed as <0.001% based upon L7 and L8 results

TABLE A.13a LEACHING CHARACTERISTICS OF RADIOISOTOPES FROM LYSIMETER SOLIDS

	Typical Initial Mass from Mill+ (μ Ci/lysimeter)	Initial Mass in Lysimeter in 1974 (μ Ci)	Amount Leached 1974-1980	
			(μ Ci)	(%)
Low-Rate Controls				
Ra-226	29*	10.6	0.0024	0.02
Th-230	29	1.38	0.0839	6
Th-232	7.7	0.234	0.0139	6
Th-228	7.7	0.433	0.0328	8
High-Rate Controls				
Ra-226	29	11.1	0.0845	0.8
Th-230	29	1.55	0.147	9
Th-232	7.7	0.3	0.0188	6
Th-228	7.7	0.56	0.17	30

+ Calculations based upon typical tailings composition and 90 kg of tailings.
* If coarse tailings are used as model, typical mass would be 15 μ Ci per lysimeter.

TABLE A.13b AVERAGE CONCENTRATIONS OF RADIOISOTOPES IN LYSIMETER SOLIDS

	Low-Rate Controls	High-Rate Controls
Ra-226 (pCi/g)	118	122
Th-230 (pCi/g)	15	16
Th-232 (pCi/g)	2.4	3.1
Th-228 (pCi/g)	4.4	4.3

against pore volumes (e.g., as in Figure 13). However, a correction to the porosity of Table A.12 is required. Some degree of compaction occurred during the coring of the lysimeters. Lysimeter L1 contained 100 cm and L2 contained 97 cm of tailings, but only 85 cm existed in the core tubes. The difference is attributed to compaction. The porosity of the lysimeters after correction for compaction of the tailings is 0.59. The true bulk density is 1.14 g/cm^3. Hence, the number of pore volumes on the graphs are high by 7 percent.

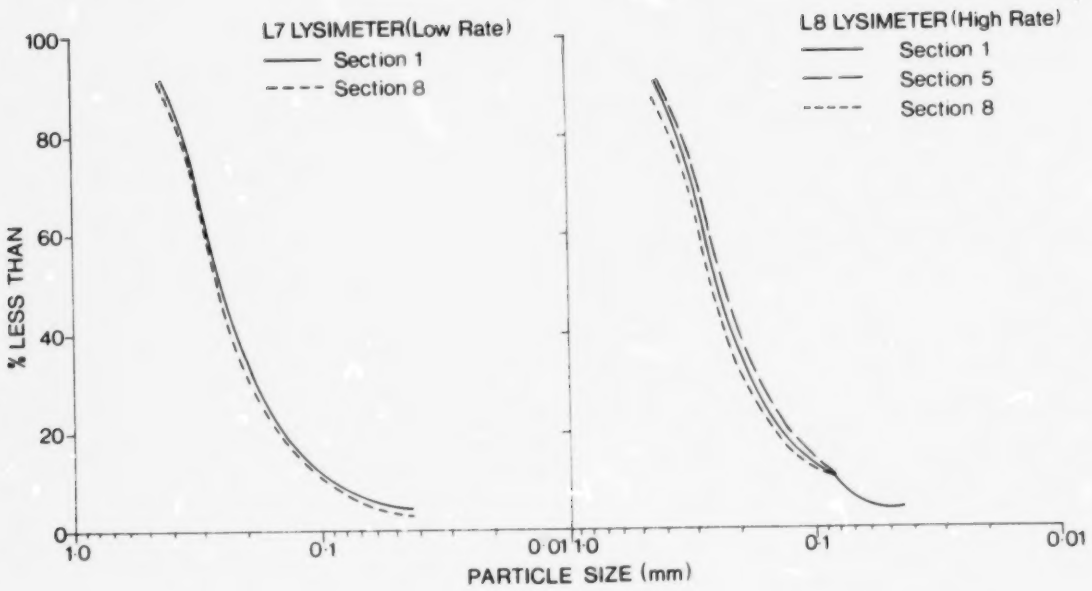

FIGURE A.13 PARTICLE SIZE DISTRIBUTION OF LYSIMETER SOLIDS

The coloration of the lysimeter solids correlates quite well with the chemical analyses for sulphide and sulphate. Most of the significant colour trends are probably due to pyrite oxidation and to precipitation coupled with the natural colour of the quartz solids rather than to the effects of gypsum.

In the low-rate lysimeters, significant pyrite reduction has occurred down to a depth of about 50 to 60 cm in lysimeter L1 and 40 cm in lysimeter L7 (see Table A.11). No sharp changes in colour are noted in lysimeter L1; rather it has a uniform buff colour throughout most of the core with occasional "pyritic" lenses observed below 50 cm and a darker colour observed below 70 cm. For lysimeter L7, large dark clusters of pyritic particles are observed at 37 cm, showing this to be the redox zone. Below this, increased numbers of pyrite lenses and a grey colour become more prominent. The high-rate lysimeters, L2 and L8, are both significantly leached of pyrite down to 70 cm. The grey pyrite zones start at 76.5 cm in lysimeter L2 and at 78 cm in lysimeter L8. This zone is delimited by an orange band ($Fe(OH)_{3(s)}$-$FeSO_{4(s)}$), 0.3 cm thick, separating the upper buff colour from the lower grey colour in lysimeter L2. Hence, the pyrite content in the 70 to 80 cm section of lysimeter L2 and L8 is concentrated in the bottom 3.5 cm of this section in lysimeter L2 and the bottom 2 cm of this section in lysimeter L8. This makes

the sulphide concentration in Section 8 of lysimeter L2 similar to that of its Section 9, but makes the concentration in Section 8 of lysimeter L8 five times that of its Section 9. The varying concentrations in Section 9 of each lysimeter reflect whether care was taken during initial lysimeter construction to avoid mixing the silica sand at the bottom of the lysimeters with the inserted tailings.

The pyrite particles are noted to occur in clusters (2 to 5 mm in diameter) and in lenses. Layering occurs in tailings piles because of the different settling rates of pyrite and quartz particles from the slurry of the mill's final neutralization tank. Accordingly, despite the attempts to homogenize the tailings before placement in the lysimeter, some stratification remained intact. The data for the bottom section suggest that pyrite concentrations in the lysimeters would have been at least 3 percent as sulphide by weight when the tailings were placed, if no significant movement of pyrite particles from above occurred. The pyrite content was not measured upon initiation of the experiment, but such a value is consistent with observations on other Nordic tailings. Calculation of mass balances for Fe and S, using TDS data as the master variable, would permit a check on this value.

Also of interest is the generally lower concentrations of sulphide throughout the bottom 40 cm of lysimeter L1 compared to the bottom sections of lysimeter L2 (see Table A.11). This comparison suggests that the lower flushing rate of lysimeter L1 allows for deeper oxygen penetration and hence more uniform oxidation of pyrite throughout depth. But higher concentrations in lysimeter L7 (low-rate) as opposed to the lower concentrations of lysimeter L8 complicate this argument. Some guidance is provided by the physical description (Table A.11). There are many areas of a dark orange-brown colour in addition to the dark-gray pyrite colour. It is possible that surface coatings have developed in lysimeter L7 on some of the pyrite particles, thus preventing their oxidation. The lower sulphide concentration throughout the bottom of lysimeter L8 compared to that of lysimeter L2 infers that pyrite oxidation is somewhat more complete in the lysimeter L8. This is confirmed by the slightly lower depth of the oxidizing layer in lysimeter L8 and the probable mixing of the pyritic layer with the silica sand layer in lysimeter L8 (see the subsequent discussion of Ra-226 concentrations).

The sulphate chemistry of the bottom layer (Table A.12) also complicates the picture. Some residual sulphate is left in all lysimeters where pyrite still exists. This could result from the downward movement of percolating waters whose large sulphate concentrations are sufficient to slow gypsum dissolution. But the actual timing of gypsum dissolution is not correlated with the oxidation of pyrite; gypsum is significantly dissolved

in lysimeters L1 and L2 relative to lysimeters L7 and L8. One could argue that complete dissolution would occur when local pyrite oxidation is nearly completed. The variance in the data does not allow one to confirm such an argument.

The radionuclide data (Table A.12) also permits substantial insight for modelling the geochemical behaviour of acidifying tailings. Snodgrass et al., 1982 suggest that radium is coprecipitated in the leaching pachucas; this coprecipitate, in turn, is covered by a gypsum precipitate formed in the partial neutralization and final neutralization tanks. Furthermore, thorium chemistry is thought to consist of transport through the mill until the final neutralization tank where the elevated pH forms a $TH(OH)_{4(s)}$ which is enmeshed in gypsum precipitate. Thorium may then remain intact on particles in the tailings pile during gypsum dissolution; however, when the pH becomes quite low, all thorium exposed to acidic pore waters may solubilize and travel with the acidic water. The thorium concentration on solids (see, for example, Table A.12) increase through the mill, which bears out this hypothesis. Furthermore, the concentrations on the lysimeter solids (see summary in Table A.13) are an order of magnitude lower in thorium, suggesting that thorium formed in the mill has been leached. No significant stratification is observed in the lysimeter data. These data do not absolutely confirm the hypothesis for thorium, but it provides evidence in support of it.

The vertical distribution of Ra-226 in lysimeter 7 is fairly uniform; the low value in Section 9 results from silica being mixed with tailings (Table A.12). The more uniform concentrations measured in the lowest section of lysimeter L8 suggests no mixing of the tailings with sand in Section 9. Significant quantities of Ra-226 have been lost from Sections 1 and 2 of lysimeter L8. Concentrations for lower layers suggest an enrichment immediately below the surface layer followed by a gradual decline. This suggests that some radium released from the surface layer is retained at lower depths, either by reversible adsorption or by coprecipitation. On the basis of the water chemistry speciation calculations of Section A.1.2, reprecipitation with a barium sulphate solid is probable. Accordingly, the mechanism suggested is one in which lysimeter L8 has reached the stage where pyrite oxidation reactions are sufficiently complete so that the sulphate minerals retaining the Ra-226 as a coprecipitate begin to dissolve. However, a higher sulphate environment occurs at a lower depth, causing some recoprecipitation.

This explanation is consistent with observations on Ra-226 and TDS in the leachate from lysimeter L8. A pulse of radium came through the high-rate lysimeter during the last year of lysimeter operation; during this time, TDS declined by an order of magnitude. The Ra-226 pattern had a history characteristic of a chromatographic

column. The surface layer (0 to 20 cm) of lysimeter L8 is the probable source for this pulse; the pulse, for some unknown reasons, ceased. Under normal conditions, it is expected that the solubility of the parent sulphate mineral containing the Ra-226 would be maintained in the pore water; hence a continual bleed of Ra-226 would be expected rather than the decline observed. Obviously, some local dynamics occur in the 10 to 20-cm layer which do not allow dissolution of more of the sulphate mineral. A possible explanation is the high sulphide concentration in Section 1 of lysimeter L8 (Table A.12). The reason that this layer is not oxidized completely before lower zones are oxidized lies probably with the formation of surface coatings on pyrite particles which have only recently dissolved. Upon dissolution of the coating, pyrite oxidation in the surface layer then provides sufficient pore water sulphate to prevent further dissolution of the sulphate mineral containing Ra-226 at lower depths.

The mass balance on radionuclides (Table A.13) suggests that little Ra-226 left the lysimeters during the leaching period. The mass balance is not closed, because the Ra-226 concentration in the solids, when leaching began, was not measured. An order of magnitude higher quantity of radium has left the high-rate lysimeters than the low-rate lysimeters. Approximately 6 to 8 percent of all thorium species have been leached, except for a 30-percent loss of Th-228 in the high-rate lysimeters. Because the final Th-228 concentrations in the low-rate and high-rate lysimeters are about the same, the larger flux of Th-228 may result from a greater isotopic partitioning of one of Th-228's parents in the high-rate lysimeters than in the low-rate lysimeters. If a substantial portion of Ra-228 (a parent of Th-228) is assumed to have been mobilized at the same time as Ra-226 in the high-rate lysimeters, then a possible source of this Th-228 is from liberation of ingrown Th-228 from Ra-228.

Correlations of radionuclide concentrations in the leachates (not given here) were made with pH and TDS. Of particular note is an inverse correlation between the pH of the solution and thorium activity (Th-228, Th-230, and Th-232); that is, the higher the proton concentration, the higher the thorium concentration. These results are interpreted to mean that most of the thorium remaining in the lysimeter solids are the original thorium species not mobilized in the mill, and that the attack on residual thorium minerals increases with increasing proton concentrations.

The particle size distributions of the solids in lysimeters L7 and L8 (Figure A.13) show no significant differences with depth or between lysimeters. The mean grain size is close to 0.25 mm; the portion of the size distribution between 2 mm and 50 mm is 95 percent, and is quite atypical of the solids examined by Murray and Moffett

(1977), who found 64 percent within this size range. These tailings may be described as very coarse tailings which have lost all fines of significance. This explains the low Ra-226 concentrations; average composite mill tailings contain 375 pCi/g of Ra-226, whereas coarse tailings characteristically contain approximately 165 pCi/g.

APPENDIX B
DESCRIPTION OF LYSIMETER SOLIDS USING SEM-XRE AND MOSSBAUER TECHNIQUES

B.1 Scanning Electron Microscope - X-ray Emission (SEM-XRE)

An exploratory analysis of the lysimeter solids was undertaken with a Scanning Electron Microscope - X-ray Emission (SEM-XRE) instrument, recently obtained by the Department of Civil Engineering at the University of Toronto. It is operated by Dr. R. Mills, Prof. of Civil Engineering. Most of the analyses were conducted on samples from the top and bottom section (Sections 1 and 8). Samples were also obtained from the leaching pachucas (LP), the partial neutralization (PN) tank and the final neutralization (FN) tank discharges of an operating mill (samples provided by A. Vivyurka). Samples of the solids were prepared for analysis by placing dried solids on a carbon stud and coating them with a gold/palladium layer. The photographs of the solids prepared in this manner are shown in Figures B.1 to B.10.

Preliminary SEM photographs of the lysimeter solids showed crystalline materials attached to the surface of the quartz grains. An effort was made to remove these crystals by ultrasonication techniques so that they could be more closely examined in the XRE without interference from the silica matrix of the quartz grains. Several samples were placed in iso-octane and ultrasonicated for 30 minutes; the solids were allowed to settle and the suspended particles and iso-octane were decanted. The solids from the LP and Sections 1, 4 and 8 of lysimeter 8 were ultrasonicated. Particles from the decant were removed with a Pasteur pipette and placed upon the carbon stud for analysis; the stud was left uncoated. The photographs of the solids prepared in this manner are shown in Figures B.11 to B.15.

In this appendix, emphasis is placed upon the results from the mill solids to give a qualitative indication of the nature and composition of the solids before their disposal. Selected SEM electromicrographs from lysimeter L8 are also presented to describe the characteristics of 25-year-old tailings. Micrographs given here have a few areas which show charging effects. This results from the use of a very small amount of gold/platinum coating. A small quantity was used to minimize the thickness of the coating and to allow detection of fine structures such as fibres and dendrites. Future work should use an alternate coating (e.g., carbon) or double-sided tape.

Figures B.1 and B.2 show solids from the LP; the host solids are coated to varying degrees with particles which appear to be precipitation products formed in the leaching pachucas. The XRE of Figure B.1 shows that the whole field is dominated by Si with significant amounts of Al, K, Fe, and Ca present; significant amounts of S are not present. Figure B.2 has small dendritic solids covering the parent silica particle and the 10-μm plate. The whole field is dominated by Si, with Al and K present. Analyses of the two plates (2 to 10 μm) in the centre of the picture indicated that they have the same composition; they are enriched in Al and K relative to Si compared to the whole field. The actual Si content of the small plates may be much smaller because the depth of field of the SEM beam (about 1 μm) picks up Si from the larger parent solid. These plates are the probable mineral which undergoes proton attack in the lysimeters and liberate Al and K. Analysis of other sectors of the electron micrograph (not given) shows similar behaviour, with Al, Si, K, Fe, Cu, Ca, and S present in significant amounts but in varying ratios. This suggests that crystals of uniform composition are not formed in the LP, but rather crystals of quite a variable composition.

ELEMENT	WHOLE FRAME
Al	150
Si	2283
K	173
Fe	91
Ca	206

FIGURE B.1(a) RELATIVE COMPOSITION OF ELECTROMICROGRAPH IN FIGURE B.1(b)

FIGURE B.1(b) ELECTROMICROGRAPH OF LEACHING PACHUCA SOLIDS

ELEMENT	WHOLE FRAME	LOCATION 1 & 2
Al	77	393
Si	1671	1459
S	-	-
K	122	278
Ca	-	-
Ti	-	-
Fe	-	-

FIGURE B.2(a) RELATIVE COMPOSITION OF ELECTROMICROGRAPH IN FIGURE B.2(b)

FIGURE B.2(b) ELECTROMICROGRAPH OF LEACHING PACHUCA SOLIDS

The surface of solids from the PN tank (see Figure B.3) appears to be covered to a larger extent than those of the LP; this may result from gypsum precipitation in the LP. The surface coatings appear to have a needle- and fibre-like structure at this large magnification with many small void spaces. The whole field of Figure B.3 is dominated by Si, but significant amounts of Al, K, Ca, Fe, and S are present, suggesting the presence of alumino-silicates, gypsum, and pyrite. The whole field of Figure B.4, also of PN tank solids, is dominated by Si with lesser quantities of Al, S, K, and Ca. Fe is not present in significant quantities. The center of the large particle (No. 1 in Figure B.4) is dominated by Al, Si, and K, whereas the linear structure to the lower left is enriched in Ca and S relative to Al and Si; no significant amount of K is present. The structure is consistent with a gypsum rod because the Al and Si would result from penetration of the electron beam.

ELEMENT	WHOLE FRAME
Al	201
Si	1622
S	191
K	229
Ca	274
Fe	109

FIGURE B.3(a) RELATIVE COMPOSITION OF ELECTROMICROGRAPH IN FIGURE B.3(b)

FIGURE B.3(b) ELECTROMICROGRAPH OF PARTIAL NEUTRALIZATION TANK SOLIDS

ELEMENT	WHOLE FRAME	LOCATION 1	LOCATION 2
Al	199	578	54
Si	1144	1209	893
S	98	-	350
K	245	381	-
Ca	114	-	455
Ti	-	-	-
Fe	-	-	-

FIGURE B.4(a) RELATIVE COMPOSITION OF ELECTROMICROGRAPH IN FIGURE B.4(b)

FIGURE B.4(b) ELECTROMICROGRAPH OF PARTIAL NEUTRALIZATION TANK SOLIDS

The tailings from the final neutralization tank (Figures B.5 and B.6) qualitatively show a similar density of cover on their surface as those from the PN tank. Of note are certain distinct structures. The whole frame of Figure B.5 has Al, Si, K, Ca, Fe, and S present in significant amounts. The 20-μm particle in the middle is an iron-sulphur particle with some Al, Si, and Ca. The whole field of Figure B.6 is dominated by Si, Ca, and S; Al and K are also present in large quantities with minor amounts of Fe. The rod in the middle is enriched in Ca and S but also contains significant quantities of Al, Si, and K. The morphology of the rod is consistent with ettringite (calcium sulphate aluminate hydrate).

ELEMENT	WHOLE FRAME	LARGE CRYSTAL IN CENTRE
Al	153	103
Si	988	302
S	580	3962
K	173	-
Ca	427	156
Ti	-	-
Fe	203	1908

FIGURE B.5(a) RELATIVE COMPOSITION OF ELECTROMICROGRAPH IN FIGURE B.5(b)

FIGURE B.5(b) ELECTROMICROGRAPH OF FINAL NEUTRALIZATION TANK SOLIDS

ELEMENT	WHOLE FRAME	LOCATION 1
Al	779	340
Si	4291	1686
S	1174	1369
K	813	323
Ca	1114	1367
Fe	140	86

FIGURE B.6(a) RELATIVE COMPOSITION OF ELECTROMICROGRAPH IN FIGURE B.6(b)

FIGURE B.6(b) ELECTROMICROGRAPH OF FINAL NEUTRALIZATION TANK SOLIDS

The degree of covering of tailings solids from lysimeter L8 (Figures B.7 through B.10) by surface precipitates is much less than that for solids from the final neutralization tank, which can be seen by comparing Figures B.3 and B.7. The quantity of Ca and S is routinely much less or non-existent in lysimeter L8 solids (Figure B.7). The whole frame of Figure B.7, which was collected from the top section of the high-rate lysimeter L8, is dominated by Si and Fe; no S of significance is noted. This suggests silica and iron hydroxides as the dominant forms. This is consistent with the physical description of the core (Table A.11) involving a deep orange colour throughout the section and a rose coloured band 5 mm thick at a depth of 3 cm (i.e., $Fe(OH)_{3(s)}$ covering silica particles). Figure B.8 centers on a flaky structure cemented to the edge of a host solid. The whole frame is dominated by Si; some Al, K, and Fe are present. The relative enrichment of the flaky structure by Al and K suggests that it is a Al-Si-K structure which has reprecipitated.

ELEMENT	WHOLE FRAME
Si	379
Fe	97

FIGURE B.7(a) RELATIVE COMPOSITION OF ELECTROMICROGRAPH IN FIGURE B.7(b)

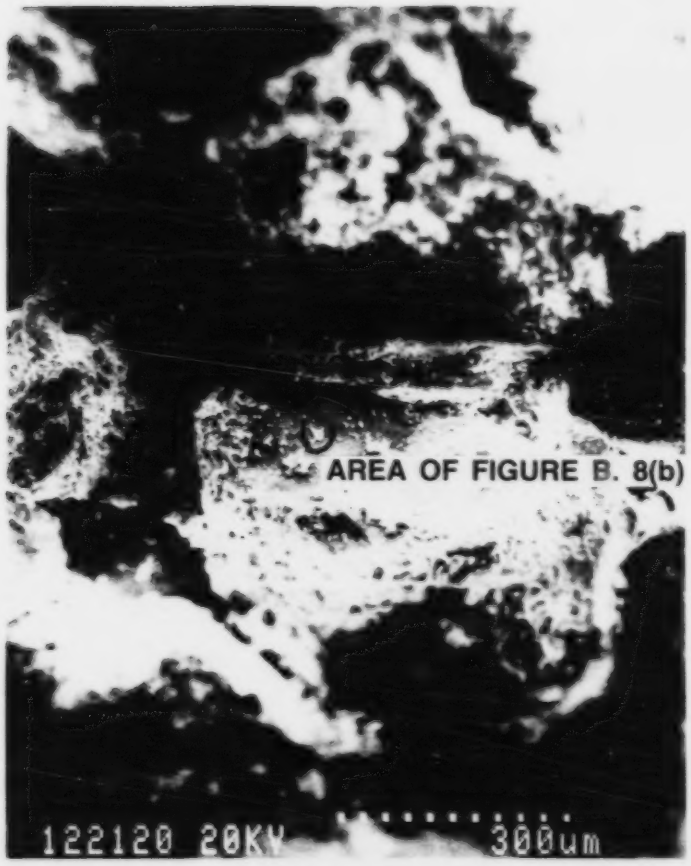

FIGURE B.7(b) ELECTROMICROGRAPH OF SOLIDS FROM SECTION 1 OF LYSIMETER 8

ELEMENT	WHOLE FRAME	LOCATION 1
Al	51	149
Si	2565	753
K	77	152
Fe	167	141

FIGURE B.8(a) RELATIVE COMPOSITION OF ELECTROMICROGRAPH IN FIGURE B.8(b)

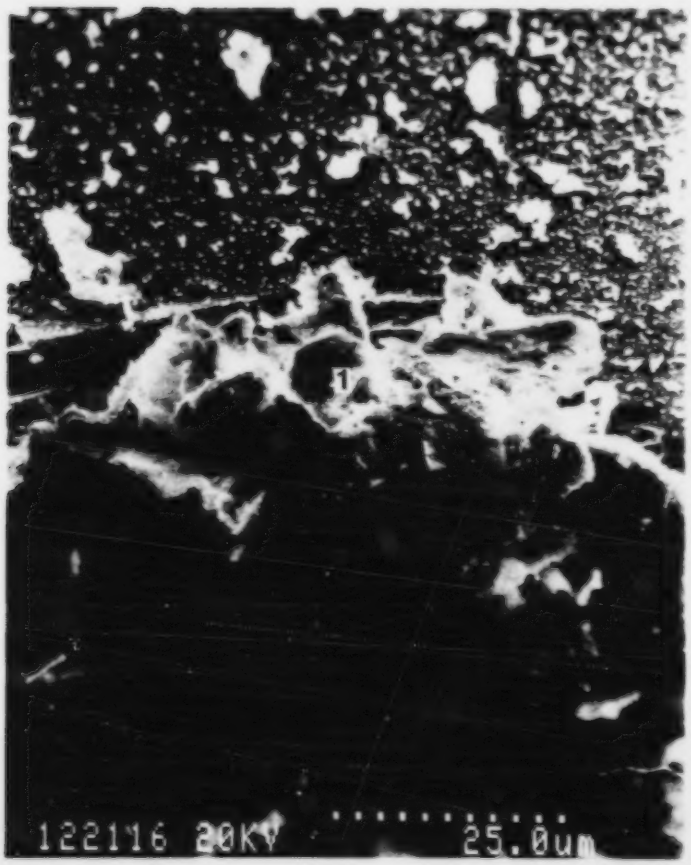

FIGURE B.8(b) ELECTROMICROGRAPH OF SOLIDS FROM SECTION 1 OF LYSIMETER 8 (AREA SHOWN IN FIGURE B.7(a))

The surface of particles from Section 8 (at depth 70 to 80 cm) of lysimeter 8 (Figure B.9) is more densely covered with small precipitates than those from the top section; some charging effects are evident on the small precipitates. Figure B.9 contains Al, Si, and K with small amounts of Fe and S; the rod in the middle qualitatively contains approximately the same portions of Al-Si-K as the whole field but without significant quantities of Fe and S. This section was physically described (Table A.11) as one in which the pale-yellow from above was replaced by a dark-grey pyrite colour. The iron is probably pyrite, whereas the rod may be a mill-formed or a precipitated alumino-silicate (see Appendix A.2). The composition of Figure B.10 (Section 8, lysimeter L8) illustrates the care required with use of SEM-XRE technology. The whole field has significant quantities of Mo and Ca. The small (10 μm) particle in the middle of the large particle is characterized as being dominated by Mo and by what has been mistakenly identified as Ar, and slightly enriched in Cu relative to the whole field. No Al, Si, or Ca is present. Ar is not probable; hence the peak from a nearby metal on the spectrum of the XRE is being misinterpreted by the XRE computer program. Because the Th peak is near the Ar peak on the energy-dispersive spectra, the small (10 μm) particle is probably monazite containing thorium. Therefore the large particle is dominated by Mo and probably Th.

ELEMENT	WHOLE FRAME	LOCATION 1
Al	402	206
Si	2628	1527
K	603	153
S	136	-
Fe	126	-

FIGURE B.9(a) RELATIVE COMPOSITION OF ELECTROMICROGRAPH IN FIGURE B.9(b)

FIGURE B.9(b) ELECTROMICROGRAPH OF SOLIDS FROM SECTION 8 OF LYSIMETER 8

ELEMENT	WHOLE FRAME	LOCATION 1
Al	138	-
Si	485	-
Mo	352	1991
Ar	-	4361
Ca	658	-
Fe	182	199
Cu	178	222

FIGURE B.10(a) RELATIVE COMPOSITION OF ELECTROMICROGRAPH IN FIGURE B.10(b)

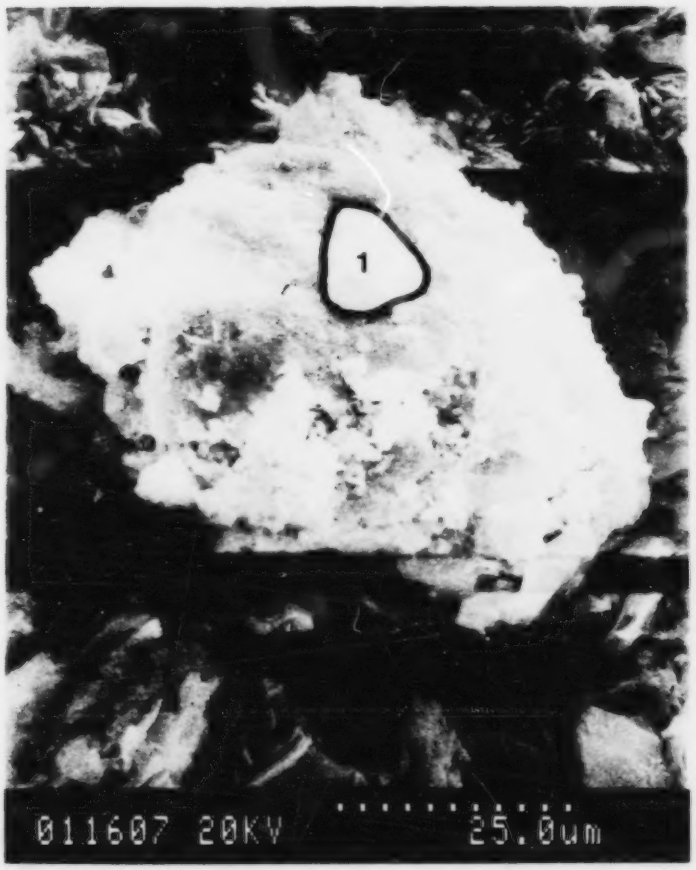

FIGURE B.10(b) ELECTROMICROGRAPH OF SOLIDS FROM SECTION 8 OF LYSIMETER 8

The last four electromicrographs present a few results from the ultrasonicated experiments using uncoated samples. A flaky shell-like structure (Figure B.11), isolated from the leaching pachucas, resulted from charged particles moving during the taking of the micrograph. The structure is mainly Si and S with lesser amounts of Al, K, Ca, and Fe. Figure B.12 was isolated from the surface section of the high-rate lysimeter. The amorphorus-appearing particle at the middle of the picture is mainly Al and S.

ELEMENT	WHOLE FRAME
Al	435
Si	1080
S	1082
K	320
Ca	304
Fe	228

FIGURE B.11(a) RELATIVE COMPOSITION OF ELECTROMICROGRAPH IN FIGURE B.11(b)

FIGURE B.11(b) ELECTROMICROGRAPH OF SOLID ULTRASONICALLY ISOLATED FROM LEACHING PACHUCA SOLIDS

ELEMENT	WHOLE FRAME
Al	245
S	998

FIGURE B.12(a) RELATIVE COMPOSITION OF ELECTROMICROGRAPH IN FIGURE B.12(b)

FIGURE B.12(b) ELECTROMICROGRAPH OF SOLID ULTRASONICALLY ISOLATED FROM SECTION 1 OF LYSIMETER 8

Figure B.13 shows the distinct morphology of jarosite crystals from Section 5 of lysimeter L8. There are large amounts of Fe, Si, K, and Ti in the center of the field. Figure B.14 (from the 70 to 80-cm depth of lysimeter L8) shows a wide spectrum of particles removed by ultrasonic vibration. Si dominates the picture with significant amounts of Al, K, Fe, and S present. Other fields of view show that fields with many Fe-S crystals (which have the morphology of jarosite) are dominated by Si with lesser amounts of Fe and S, and even smaller amounts of Al and K.

ELEMENT	WHOLE FRAME
Al	802
Si	4655
S	3664
K	1852
Fe	3798
Ti	206

FIGURE B.13(a) RELATIVE COMPOSITION OF ELECTROMICROGRAPH IN FIGURE B.13(b)

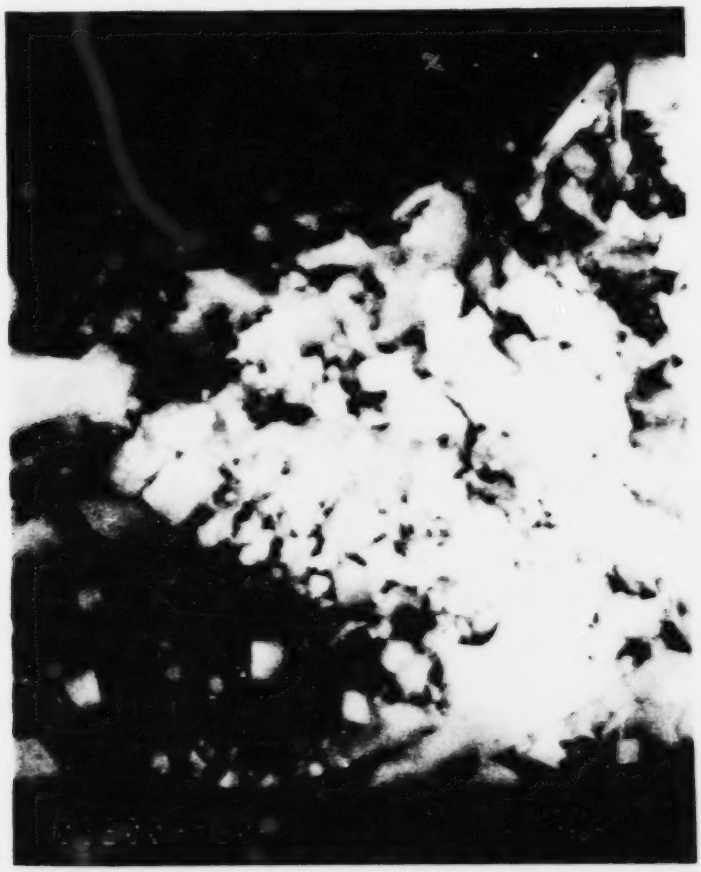

FIGURE B.13(b) ELECTROMICROGRAPH OF SOLID ULTRASONICALLY ISOLATED FROM SECTION 5 OF LYSIMETER 8

ELEMENT	WHOLE FRAME
Al	387
Si	5116
S	412
K	500
Fe	265

FIGURE B.14(a) RELATIVE COMPOSITION OF ELECTROMICROGRAPH IN FIGURE B.14(b)

FIGURE B.14(b) ELECTROMICROGRAPH OF SOLID ULTRASONICALLY ISOLATED FROM SECTION 8 OF LYSIMETER 8

That such fields may be dominated by Si shows that further work with ultrasonic techniques are required to examine the morphology of the $SiO_{2(s)}$ particles and to isolate it to allow identification of other spectra (Figure B.15). The silica may originate as part of the original ore, broken down to these small sizes in the mill. It may also result from acid attack on silica sand in the tailings, leading to the development of cleavage sites. This is possible because similar dominance by Si was not observed in the ultrasonicated mill samples. The amorphorus-appearing forms may be secondary (amorphous) silica or alumino-silicates, as suggested by the analyses of metal ratios in the lysimeter leachates. During reprecipitation, migrating radioisotopes may be coprecipitated in significant quantities. Hence these structures cannot be neglected.

To examine other structures, the SiO_2 structures might be removed by differential centrifugation or timed gravity separation. Thus SEM-XRE technology requires more work and creative sample preparation techniques to attain its full potential.

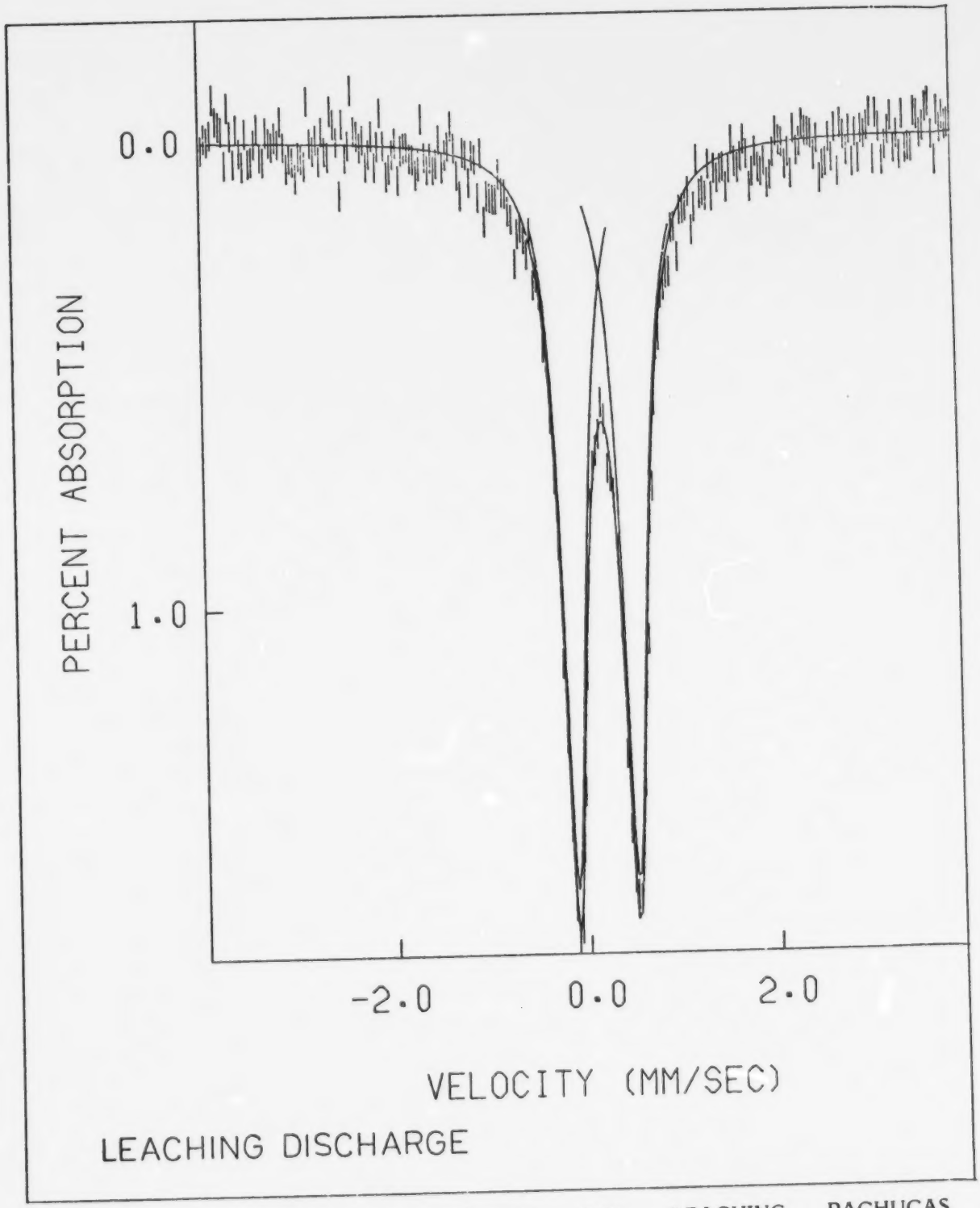

FIGURE B.15 MOSSBAUER SPECTRA FOR LEACHING PACHUCAS DISCHARGE

The use of the SEM-XRE in this project shows a few points of interest and a few areas which require more work to allow it to fulfill its potential capabilities. This study provides evidence for the formation of precipitates in the leaching pachucas, the formation of dense coatings in the PN and FN tanks and a dramatic decrease in the surface area of host solids covered by these coatings in the leached tailings samples. The denser degrees of coverage by coatings on host solids at the bottom of lysimeter L8 compared to its top section is correlated with:

(i) the leaching behaviour,
(ii) the occurrence of probable iron hydroxide bands and the complete oxidation of pyrite in the surface layers, and
(iii) chemical measurements of sulphides and sulphates.

The coatings are not uniformly thick, but rather quite porous. The coatings provide a large surface area for adsorption but cause difficulties for selecting "model" structures for use in mathematical modelling of the geochemical evolution of tailings piles.

The following recommendations concerning use of SEM-XRE for future tailings work arise from this study.

1. The work at present has shown SEM-XRE to be capable of rapidly resolving different structures in a semi-quantitative manner. Evaluation of standard structures are required to allow quantitative determination of masses of elements present in the field of view.
2. A set of standard structures are required for incorporation into the SEM-XRE library. The structures would include the name of the mineral and quantities of different elements in each mineral. Sample analysis would then be followed by the SEM-XRE microprocessor searching the library to give estimates about the most probable minerals present and their respective masses. A library particularly tailored to uranium ores, mill-formed precipitates, and secondary precipitates formed during weathering reactions would be particularly valuable. Development of such a library is quite analogous to the libraries of morphology and X-ray spectra developed for XRD instrumentation.
3. Identification of Fe minerals, particularly secondary minerals formed by weathering reactions (e.g., jarosite), presents some difficulties because of the occurrence of Fe and S as pyrite and $Fe(SO_4)_x$ in jarosites. Techniques for separating pyrite from the tailings would be useful for mineral identification. Similar developments would be useful for application of Mossbauer techniques (see below).

4. This work has identified the possible existence of an ettringite mineral. Such minerals are important in cement reactions. They are described as a calcium sulphate aluminate hydrate. The chemical concentrations of Ca, SO_4, and Al in mill waters in the PN and FN tanks and in the lysimeter pore waters provide for its formation. If present in significant quantities, dissolution kinetics for this precipitate will be required for modelling the geochemical evolution of tailings piles. A useful starting point would be more work to identify its existence and an assessment of the differences between gypsum and ettringite formation and dissolution kinetics.
5. The chemical leachate analysis (Appendix A.1.2) suggest that secondary alumino-silicates and amorphorus $SiO_{2(s)}$ are forming on the tailings due to dissolution of primary minerals and to solubility controls on orthosilicic acid in percolating waters. The opaque structures observed in lysimeter 8 are possible candidates for this amorphorus silica. Because $SiO_{2(s)}$ is X-ray amorphorus, SEM-XRE provides a technique for its identification. Such structures may entrap soluble radioisotopes by coprecipitation reactions. Upon separation of these structures from the parent solids, analysis of these structures for radioisotopes using SEM-XRE, chemical methods, and chemical speciation calculations should be carried out to permit some conclusions concerning the ability of these structures to entrap migrating radionuclides.
6. The Al-Si-K ratios vary from sample to sample and even within the same sample. This can result both from varying beam angles and from formation of solids of differing composition. Different nucleation crystallization reactions are possible because of local concentration differences. Whether the nucleation and crystal growth of such particles would be controlled by transport of cations from solution or more as a corrosion reaction at the alumino-silicate surface awaits further work.
7. There is a resolution problem with SEM-XRE technology when one is attempting to identify elements in precipitates on the host solids because the quartz peak can dominate and even mask the spectra of the other elements. The pointer on the SEM provides an advantage by allowing one to isolate upon the centre of one particular particle (e.g., a rod) and to assay its elemental composition. Its elemental composition and morphology allow rapid mineral identification. However, the depth of field used by the electron beam (e.g., 1 μm) often picks up some of the Si from the host solid. Further development of ultrasonic techniques and separation of the

precipitates by centrifugation is one possible method for removing some of the masking effect of the $SiO_{2(s)}$.

8. A gold-palladium coating on the tailings placed upon the carbon stub is required to obtain XRE spectra of most specimens. The long time required to take a photograph on the SEM (near 100s) produces a blurry picture of uncoated specimens because of the charging effects and associated motion of small particles. Use of a videotape presents one possible approach for attempting to capture visual detail of the small dendrites due to its ability to obtain a picture of a changing electron micrograph.

B.2 SEM-XRE Analysis of Wash Waters from Gypsum Chemical Analyses

It was observed that several waters used for washing lysimeter solids for gypsum analysis developed a light- to dark-orange colouration within a few hours after the washing was completed and after the solids had been filtered from the wash water. The colour appeared to be due to the presence of an orange, fluffy precipitate formed in a previously clear wash water. These coloured precipitates were filtered off for further analysis. The colours of the filter papers are listed in Table B.1. Wash waters from lysimeter 2 (high-rate) were generally clear, although some precipitates developed in the wash waters from sections near the bottom of the lysimeters. Wash waters from lysimeter 8 (high-rate) appeared to behave similarly, but more precipitate development was observed in L8 wash waters. Large amounts of precipitates formed in wash waters from all depths of lysimeters L1 and L7 (the two low-rate lysimeters) except for the surface sections. Some precipitates formed in the mill washings.

The filtered precipitates from Section 3 of lysimeter 1 (L1-3), Section 8 of lysimeter 7 (L7-8) and Section 8 of lysimeter 8 (L8-8) were analyzed by SEM-XRE. The precipitate from the middle of one low-rate lysimeter (L1-3) was dominated by an Fe-S solid; small amounts of Al and Cu were also present. Because the sample should be oxygenic, the Fe-S solid should be an iron sulphate; the unit cell formula might be $CuFe_x(SO_4)\cdot Al(OH)_3$, a formula which approximates jarosite. Debate exists over whether a basic metal sulphate of aluminum actually forms by precipitation; the evidence of DeHek et al. (1978) argues against it although substitution of Al into the structure of $FeSO_4$ is possible.

A SEM-XRE search of the filter paper from the bottom of the low-rate lysimeter (L7-8) shows variable chemical composition. One location has Zn as the dominant element with some Fe, Ca, and Al and a little S; other locations are dominated by Al, Si, K, and Fe, but without S. Such characteristics suggest the presence of an

TABLE B.1 COLOURS OF FILTERS USED TO REMOVE PRECIPITATE FORMED AFTER SULPHATE LEACH

	Lysimeter			
Section	1 (Core 2)	2 (Core 2)	7 (Core 1)	8 (Core 1)
1	Moderate Orange	Very Light Buff to Orange		
2			Clear	Very Light Buff
3	Moderate Orange	Clear		
4			Light Yellow Buff	
5	Heavy Orange	Clear		
6			Heavy Orange	Clear
7	Heavy Orange	Very Light Buff		
8	Light Orange	Clear	Heavy Orange	Heavy Orange
9	Heavy Orange	Very Light Orange		

Leaching Pachucas - Very light buff
Partial Neutralization Tank - Very light orange
Final Neutralization Tank - Very light orange to buff

alumino-silicate, a reprecipitated quartz entrapping Al, an iron sulphate or an iron hydroxide. The heavy-orange colour is typical of $Fe(OH)_{3(s)}$.

The third filter paper from the high-rate lysimeter (L8-8) is dominated by Si and Fe with a small quantity of Al. K is present in one location; Ti is strongly present in another location. No S is present. These data suggest that amorphous silica and iron hydroxide have formed and dominate the spectra. The presence of Ti as $TiO(OH)_{2(s)}$ is most probable, particularly because the speciation calculations given in Appendix A.1.2

suggest that it should precipitate. It is possible that Al and K are incorporated into an amorphous $SiO_{2(s)}$. $Al(OH)_{3(s)}$ could not be significant due to the low pH.

These phenomena provide some evidence to suggest that the kinetics of the precipitation of iron sulphate as well as iron hydroxide are fairly rapid. The rapid kinetics for iron sulphate and its formation in these solutions are possible because of low pH; the pH of the waters of L1-3 was 3.1, whereas those of L7-8 were 2.9 and of L8-8 2.7. But $Fe(OH)_3$ is more stable than $Fe(SO_4)_x$ at pH greater than 2 (Brown, 1971). Hence, the formation of $Fe(SO_4)_x$ on the L1-3 filter paper awaits explanation. Assuming that some of the iron washed from the solids is in a +2 oxidation state (i.e., Fe^{2+}), these phenomena suggest that iron-oxidizing bacteria were still active in the tailings, 1 year after cessation of operation of the lysimeters. Another possible explanation is that the bacteria created a large concentration of Fe^{2+} in the biofilm after cessation of lysimeter operations and before they became sessile, and that the oxidation kinetics of Fe^{2+} are sufficiently slow at pH 1 that a large pool of Fe^{2+} had still remained when these solids were washed for gypsum analysis.

B.3 Mossbauer Spectra of Uranium Tailings Samples

(M. Bancroft, University of Western Ontario)

Mossbauer spectra were obtained by Dr. Michael Bancroft's laboratory, Dept. of Chemistry, University of Western Ontario, for six samples: L8-1-8, L8-1-1, L7-1-1, L7-1-8, L7-1-10 and "Leaching Pachaca Discharge". L8-1-1, L8-1-8, L7-1-1, and L7-1-8 are respectively the top (0 to 10 cm) and eighth (70 to 80 cm) sections from core 1 of lysimeter L8 (the high-rate lysimeter) and lysimeter L7 (the low-rate lysimeter). L7-1-10 is a section of yellowish silica sand from the bottom of lysimeter L7 (Section 9; depth 84 cm). It is thought to be a redox boundary where jarosite, iron hydroxide, or a similar crystallite has reprecipitated. All samples contained sufficient iron to yield satisfactory spectra. Samples L7-1-1 and L7-1-10 required large counting times, and spectra were only run long enough to establish that they were consistent with the other spectra.

The spectra obtained (see Figures B.15 to B.17) were essentially identical, with a well resolved ferric doublet and narrow line widths indicating a unique iron-containing environment (within instrumental resolution). Four of the spectra were statistically analyzed using a conventional chi-squared minimization program assuming Lorentzian peak shapes. The results are shown in Table B.2.

The parameters shown for Quadrupole splittings and Isomer shifts are consistent with those of pyrite (FeS_2): IS = 0.31 mms^{-1}, QS = 0.61 mms^{-1}. The narrow

TABLE B.2 MOSSBAUER CHARACTERISTICS FROM VARIOUS SAMPLES

	Isomer Shift (mm/s)*	Quadrupole Splitting (mm/s)
Leaching Pachucas Discharge	0.338 ± 0.009	0.600 ± 0.008
L8-1-1	0.35 ± 0.01	0.62 ± 0.01
L7-1-8	0.34 ± 0.02	0.626 ± 0.0
L7-1-10	0.35 ± 0.03	0.65 ± 0.03
FeS_2	0.31	0.61
Jarosite	0.43	1.20

* Relative to natural iron

line widths observed (0.3 mms^{-1}) make it unlikely that a second iron-containing species is making any significant contribution to the spectrum. A possible exception is Spectrum L7-1-10, where there is evidence of a second ferric resonance, possibly jarosite defined as $MFe_3(OH)_6(SO_4)_2$, where M is Na^+, K^+, etc. (IS = 0.43 mms^{-1}, QS = 1.2 mms^{-1}). However, the low levels of iron in this sample make it impossible to resolve such a contribution from the instrumental sinusoidal baseline. In the well resolved spectra (Leaching Discharge, L8-1-1, L8-1-8, L7-1-8), a significant jarosite contribution (e.g., greater than 5 percent) would cause visible shoulders, particularly on the high-velocity peak. Although in all spectra the higher velocity peak is the larger of the two, the difference in all but Spectrum L7-1-10 is not statistically significant.

Pyrite is the dominant iron-containing species in all the samples examined, with a possible contribution from a second ferric iron species in sample L7-1. This could be jarosite. The low total iron level in this sample, however, makes it impossible to resolve a second resonance.

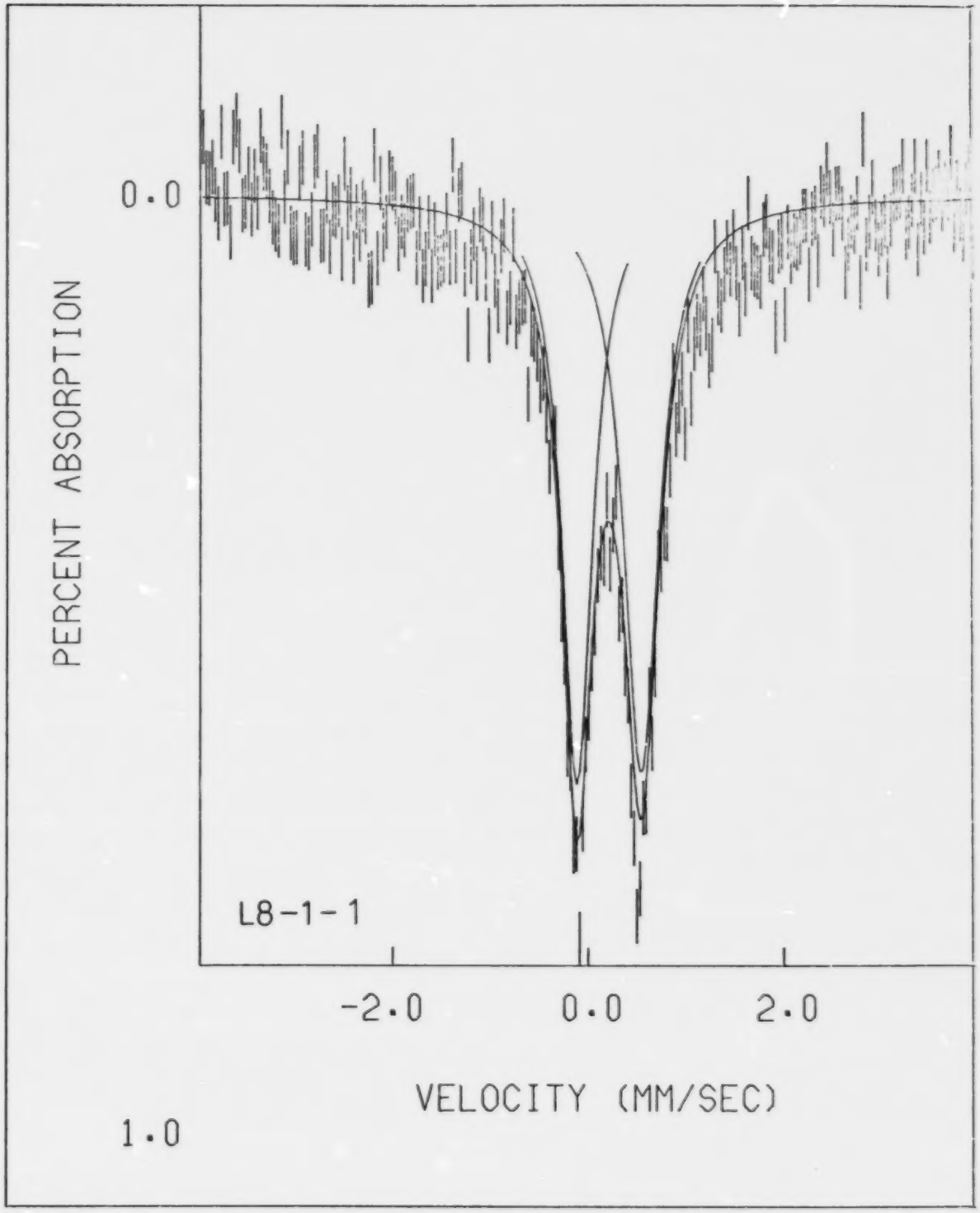

FIGURE B.16 MOSSBAUER SPECTRA FOR SECTION 1 OF LYSIMETER 8

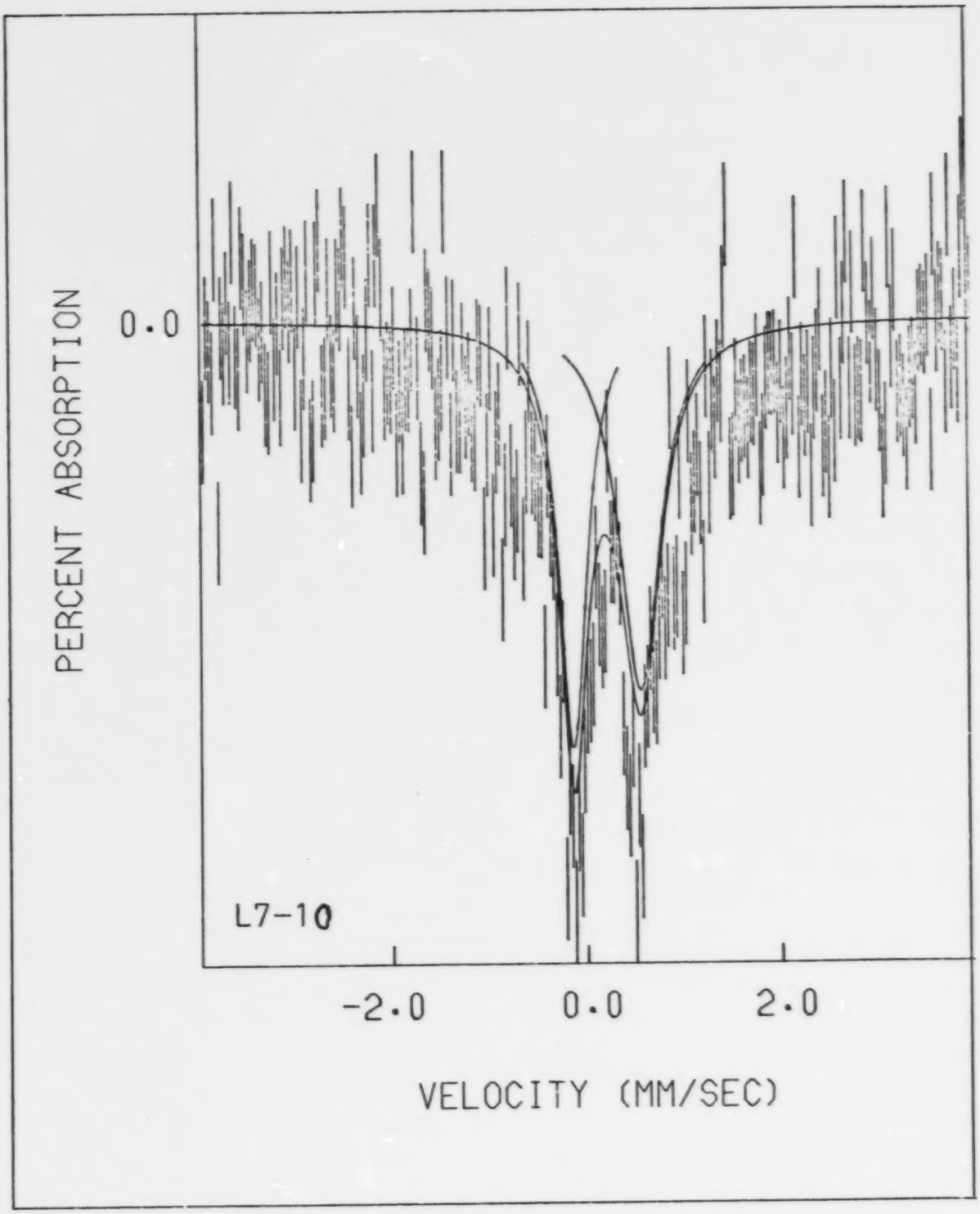

FIGURE B.17 MOSSBAUER SPECTRA FOR SECTION 10 OF LYSIMETER 7